Title
Prescribed Time Stabilization and Estimation for Linear Systems with Applications in Tactical Missile Guidance

Author
Holloway, John Charles

Publication Date
2018

UNIVERSITY OF CALIFORNIA SAN DIEGO

Prescribed-Time Stabilization and Estimation for Linear Systems with Applications in Tactical Missile Guidance

A dissertation submitted in partial satisfaction of the requirements for the degree Doctor of Philosophy

in

Engineering Sciences (Mechanical Engineering)

by

John Charles Holloway

Committee in charge:

Professor Miroslav Krstic, Chair
Professor Thomas Bewley
Professor Mauricio de Oliveira
Professor Stefan Llewellyn Smith
Professor Jose Restrepo

2018

The Dissertation of John Charles Holloway is approved, and it is acceptable in quality and form for publication on microfilm and electronically:

Chair

University of California San Diego

2018

DEDICATION

In loving memory, I dedicate this dissertation to my mother,

Evelyn Reynolds Holloway,

who met her Lord and Savior

on July 4, 2014.

Her love and spirit will always be with me.

EPIGRAPH

Never forget the "3 Rules for PhD Students":

1. Something is better than nothing.
2. Done is better than good.
3. Your advisor is always right.

Fr. Edwin L. Lisson, SJ, SThD, 1938-2014

TABLE OF CONTENTS

LIST OF FIGURES

ACKNOWLEDGEMENTS

The theorem, corollaries, and proofs pertaining to Proportional Navigation in Chapter 3 first appeared in a paper by Prof. Krstic and myself, which was published as "Predictor observers for Proportional Navigation systems subjected to seeker delay," *IEEE Transactions on Control Systems Technology*, 24(6), 2002–2015, 2016.

Most of the material in Chapter 4 first appeared in a paper by Prof. Yongduan (David) Song, his student, Dr. Yujuan Wang, Prof. Krstic, and myself, which was published as "Time-varying feedback for regulation of normal-form nonlinear systems in prescribed finite time," *Automatica*, 83, 243–251, 2017. Thank you, Prof. Song and Yujuan, for allowing me to work with you on this project, and thank you for allowing me to include the material in my dissertation.

Most of the material in Chapter 5 may appear in a paper by Prof. Krstic and myself entitled "Prescribed-time observers for linear systems in observer canonical form," which is under review for possible publication in *IEEE Transactions on Automatic Control*.

Most of the material in Chapter 6 may appear in a paper by Prof. Krstic and myself entitled "Prescribed-time output feedback for linear systems in controllable canonical form," which has been provisionally accepted to appear in *Automatica*.

Most of the material in Chapter 7 was accepted for inclusion in the AIAA SciTech 2017 conference in a paper by Prof. Krstic and myself entitled "Finite-time terminal guidance laws based on robust time-varying feedback for uncertain normal form systems." We later withdrew the paper because I was unable to attend the conference to present it. However, we may submit this material elsewhere for possible publication in the future.

I now wish to express my sincere thanks and gratitude to the many people who have aided and guided me along the way, the key people who made the achievement of this life goal possible.

To my mentors during my undergraduate studies:

Thank you, Capp, for your avuncular guidance and friendship while I attended Morehead State University. You introduced me to the Research Experiences for Undergraduates (REU) program, and without your encouragement and guidance, I probably wouldn't have considered pursuing a graduate degree, or sought adventures outside of Kentucky.

Thank you, Dr. McDonough, for being my mentor while I attended the University of Kentucky. Thank you for taking me under your wing as an undergraduate researcher, and for leading me into the one scientific field I always looked forward to working on for fun: the modeling of turbulence for computational fluid dynamics (CFD). Your command of applied mathematics truly inspired me, and you helped steer me towards the University of California system to pursue my PhD. Without your guidance, your urging me to be co-author on some of your conference proceedings, and your help with networking and recommendations for graduate schools, I would not have been competitive for admission into the University of California San Diego (UCSD).

Thank you, Prof. Cosby, Prof. Morrison, Prof. Bording, Prof. Wai Sun Don, and Profs. Hung Tao and Hayley Shen for being my advisors and guides during my undergraduate summer research programs: REU at Ball State University, 2000; REU at University of Louisville, 2001; NASA Goddard Space Flight Center (GSFC) Visiting Student Enrichment Program (VSEP), 2002; University of California Los Angeles (UCLA) Research in Industrial Projects for Students (RIPS), 2003; REU in China, 2004. Thank you for accepting me into your programs, and for providing references that greatly increased my chances of gaining admission into UCSD.

To my supervisors, managers, mentors, and friends in industry:

Thank you, Alex, Mike, Gary W., Gary S., Joe, and Ron, who supported me in every way you could to maintain the continuous funding I needed to complete my protracted academic programs at Stanford University (Graduate Certificate in Guidance and Control) and UCSD (PhD) while I worked for you at Northrop Grumman, TASC, and Engility. Thank you also for your patience and flexibility with my work schedule as I struggled to balance work, family, and school all at the same time.

Thank you, John D., for mentoring me on how to navigate through life as a PhD student while also being an engineer in industry and a family man at the same time. Thank you for your guidance and suggestions on my research project early on. But most importantly, thank you for sharing your *3 Rules for PhD Students*, without which I would never have survived this program.

Thank you, Kyu, for our many chats about our PhD student experiences, and for all your encouragement since I began my PhD program so many years ago. Thank you for helping me realize that when all of this is over, it isn't actually going to change my value as a person.

Thank you, Eric L., for encouraging me and providing me guidance during the terminal stage of my PhD program. Thank you also for those two very thoughtful graduation presents.

I also sincerely thank my many good friends at the San Bernardino Engineering Center for their support and encouragement which I so desperately needed over the last six years. In particular, thank you Gary S., Andy, Janis, Jesus, Keith, and Chuck for always trying to perk me up when I was tired or discouraged, and for repeatedly reminding me that all of this hard work and pain will pay off someday.

To my doctoral commmittee:

Thank you, Prof. Bewley, for mentoring me during my first two years at UCSD, for finding funding for my tuition for a while, for encouraging me when I struggled through academic probation, and for chairing and guiding the committee that allowed me to obtain my Master of Science (MS) degree. Thank you also for your guidance and service on my doctoral committee.

Thank you, Prof. de Oliveira, for giving me that MAE 143A teaching assistantship during my second year at UCSD, and for not being upset when I failed in my duties in that position. Thank you also for your guidance and service on my doctoral committees.

Thank you, Prof. Llewellyn Smith, for serving on my MS committee, and for allowing me to pass my oral Departmental Qualifying Exam (DQE) with a lackluster performance. Thank you also for your guidance and service on my doctoral committee.

Thank you, Prof. Restrepo, for your guidance and service on my doctoral committee. Without your kind offer to be on my committee despite not knowing who I was, I would have been in a real dilemma to finish forming my committee on time.

Thank you, Prof. Krstic, my research advisor and mentor, for your guidance, patience, and special accommodations throughout my graduate studies at UCSD. Thank you for accepting my late homeworks for full credit, and for being more than generous in grading my exams. Thank you for giving me a second chance at the PhD as a part-time student, and for having patience with my primary responsibilities to my family and my employer. Thank you for redirecting my research path to this new approach to prescribed-time stabilization and estimation, which through your brilliant ideas and inspiring scholarship, gave me the opportunity to contribute something of potential significance in my research.

To my closest friends:

Thank you, Leslie, for your friendship and encouragement throughout our lives. You were one of the few people I could turn to for the encouragement I desperately needed to help get me through some of the toughest times in the early stages of my PhD program.

Thank you, Justin, my childhood friend, confidant, and advocate throughout this challenging time, who provided unique perspective and support that helped keep me going. Insight into your experiences as a PhD student and researcher helped me keep things in a healthier perspective as I trudged on for six years as a thirty-something, part-time PhD student.

And finally, to my family:

Thank you, Linda, my dear wife, for not giving up on me while I was terribly difficult to live with during these last six years. Thank you for your love, your patience, and your encouragement during this challenging and formative time in our lives. Thank you, Ethan, for being such a wonderful boy, and for giving me the main reason to continue this program to its fruition long after I realized that it wasn't something I needed anymore to be happy in life. Thank you, Bethany, for your support and friendship throughout our lives as siblings. Although I never felt that I had accomplished anything special in life, you always loved me, encouraged me, were proud of me, and even introduced me to your friends as if I were some kind of *rock star*. And most importantly, thank you, Mom and Dad, who sacrificed so much of your own happiness for that of your children's, and always encouraged me and guided me throughout the toughest times in my life. To my family, I love you all more than anything in the world.

VITA

2004	Bachelor of Science, Morehead State University
2004	Bachelor of Science, University of Kentucky
2006	Master of Science, University of California San Diego
2006–2009	Northrop Grumman Corporation
2009–2015	TASC (divesture from Northrop Grumman Corporation)
2010	Graduate Certificate in Guidance and Control, Stanford University
2015–Present	Engility Corporation (merger with TASC)
2018	Doctor of Philosophy, University of California San Diego

PUBLICATIONS

J. Holloway and M. Krstic, "Predictor Observers for Proportional Navigation Systems Subjected to Seeker Delay," *IEEE Transactions on Control Systems Technology*, 24(6), 2002–2015, 2016.

Y. Song, Y. Wang, J. Holloway, and M. Krstic, "Time-varying feedback for regulation of normal-form nonlinear systems in prescribed finite time," *Automatica*, 83, 243–251, 2017.

J. Holloway and M. Krstic, "Prescribed-time observers for linear systems in observable canonical form," under review with *IEEE Transactions on Automatic Control*.

J. Holloway and M. Krstic, "Prescribed-time output feedback for linear systems in controllable canonical form," provisionally accepted to appear in *Automatica*.

ABSTRACT OF THE DISSERTATION

Prescribed-Time Stabilization and Estimation for Linear Systems

with Applications in Tactical Missile Guidance

by

John Charles Holloway

Doctor of Philosophy in Engineering Sciences (Mechanical Engineering)

University of California San Diego, 2018

Professor Miroslav Krstic, Chair

Motivated by tactical missile guidance, in which there exists a short, finite amount of time to intercept a moving target, we introduce a new approach to stabilization and estimation in finite time which allows the user to prescribe the time by which the estimation and control objectives will be achieved. We accomplish this by employing time-varying feedback gains which tend to infinity as time approaches the prescribed time. Remarkably, despite the gains going to infinity, the overall control inputs and output estimation error injections remain finite, thereby allowing for potential use in real-world finite-time control applications such as tactical missile guidance. The first step in the design process involves extending existing stability concepts for nonlinear systems by introducing new definitions for finite-time stability using class $\mathscr{K}$ and class $\mathscr{K}\mathscr{L}$ functions. This is done by compressing the usual infinite time interval to a finite one through the use of a time-varying, monotonic scaling function which tends to infinity as time approaches the prescribed time. Then, time-varying state coordinate transformations are used to design two feedback controllers for nonlinear systems in the normal form which stabilize the state in a finite time that is independent of initial conditions and freely prescribed by the user. The first controller is appropriate for systems having no uncertainties, while the second is intended for systems having matched uncertainties and possibly unknown control input coefficient. Prescribed-time observers for linear systems in the observer canonical form are then introduced using a similar time-varying state coordinate transformation design, resulting in observers akin to the Luenberger observer but with time-varying gains that tend to infinity as time approaches the prescribed time. Then, the prescribed-time uncertainty-free controller and prescribed-time observer are combined, and it is shown that a finite-time separation principle exists between the controller and the observer. The presentation is concluded with a series of examples in which the new prescribed-time controllers and observers are applied to provide new solutions to canonical problems in tactical missile guidance.

Part I

Introduction

Chapter 1

Preface

1.1 Motivation

The results of this dissertation are motivated by tactical missile guidance and other applications in which there exists a short, finite amount of time remaining to achieve state estimation and control objectives, and that time is known to within some small uncertainty. In finite-time applications such as these, observers and controllers that allow the user to *prescribe* the convergence time of the state observer and controller *a priori* (i.e., without knowledge of initial conditions) offer a clear advantage over finite-time approaches that do not allow for prescription of the convergence time, let alone those that exhibit asymptotic convergence to nonzero values. The majority of estimation and control solutions achieve asymptotic performance in general, and only approach finite-time performance with high gains. Existing finite-time solutions are dominated by sliding mode control (SMC) approaches, which are known to exhibit *chattering* when the state trajectories approach the origin. The results presented in this dissertation offer an alternative approach to finite-time control for linear systems which exhibits new advantages and challenges in practice.

Most tactical missile guidance laws in use today are extensions of a classical missile guidance law called *Proportional Navigation (PN)*. Essentially, PN is a missile steering policy for short-range missiles that is based on nulling the rate of the missile-to-target line-of-sight (LOS) relative to an inertial reference, for doing so achieves *collision course* kinematic conditions that lead to eventual intercept under constant velocities. In the *near-collision course (NCC)*, the PN guidance law exhibits time-varying gains that go to infinity as the time remaining to reach the target, the so-called *time-to-go*, decreases linearly to zero. It turns out that in this formulation, the PN guidance law achieves a perfect intercept, or zero *miss distance*, but sometimes at the cost of infinite control authority. Furthermore, although the miss distance is made zero, the rate of the miss distance is not stabilized, and results in a nonzero value dependent on the initial conditions of the engagement.

Is it possible to design similar guidance laws with gains that go to infinity, but which stabilize the entire state to the origin? And if so, can one design an observer counterpart to such a control law? In this dissertation, we present viable solutions to these challenges, and further show that there exists a separation principle between the controller and the observer. At the end, we show how the new guidance law and state observer may be used with a linearized target engagement model which may have utility in some realistic tactical missile guidance applications.

1.2 My nonlinear trajectory

Like many PhD students, once I had finished my graduate coursework, and my research objectives had my full attention, I initially struggled to find an appropriate research topic that would not only be suitable for a PhD, but would also be interesting enough to keep me focused until I met whatever requirements there would be to graduate. With my full-time job in industry, part-time student status, a wife, a mortgage, and a son on the way, the probability of failure loomed in my mind, and guided me towards an area that would educate me on topics on the periphery of my job in industry. That way, if I failed to graduate, at least I might be better qualified for a different job in industry if ever needed. Having several years of experience performing Guidance, Navigation, and Controls (GN&C) independent validation and verification (IV&V) for the Northrop Grumman Rocket Systems Launch Program (RSLP), I had great interest in missile defense, but knew nothing of how interceptor systems operated. So, tactical missile guidance seemed like a perfect research area for this early stage in my career. A challenge remained, however, and that was to capture the interest of Prof. Krstic, so that we could form some type of bond and I could start actually making progress.

Initially, following the footsteps of several of Prof. Krstic's previous students, I searched for a way to apply his existing contributions to general control theory to my application of interest. After purchasing a small library of books on tactical missile guidance, and performing a substantive literature review of the state-of-the-art in missile guidance, I learned that Prof. Krstic's then-recent book, *Delay Compensation for Nonlinear, Adaptive, and PDE Systems* [44], provided for an interesting way to compensate for measurement delays in tactical missile interceptors, and that idea hadn't been published yet. We had finally found some common ground, and then after way longer than I had hoped or planned, we submitted my first paper, *Predictor Observers for Proportional Navigation Systems Subjected to Seeker Delay* [32], to IEEE Transactions on Control Systems Technology for review. It was during that review process that we finally began to take stride, after a reviewer requested a proof of the stability of our predictor observer. On the way towards our proof that the classical predictor observer is input-to-state stable (ISS) with respect to bounded measurement disturbances, we learned that under our idealized target engagement model, the Proportional Navigation (PN) guidance law only stabilizes part of the state to zero, while allowing the rest to go wherever the dynamics take it. But what was even more interesting to Prof. Krstic was that PN is a type of control law that achieves stabilization in finite time by employing control gains that go to infinity, while somehow keeping the overall control feedback finite. These observations intrigued Prof. Krstic and, just by chance, resonated with his concurrent work with Prof. Yongduan (David) Song and his student, Dr. Yujuan Wang. Ultimately, this engendered the ideas and results we developed as a team, which now form most of the content in Chapter 4 of this dissertation.

And so, with some new ideas, Prof. Krstic guided me by sketching out what he wanted and leaving me to figure out as many of the details as I could on my own. A year-and-a-half later, by building on our collaborative effort with Prof. Song and Yujuan, not only had we developed a new prescribed-time observer to complement the controllers we designed, but we were also able to demonstrate that a separation principle holds between them as well. In the end, by following Prof. Krstic's instructions, and the *3 Rules for PhD Students* (see the Epigraph!), I was able to accomplish much more than I originally thought was possible.

1.3 Chapter roadmap

Part I of this dissertation continues with Chapter 2, which provides the reader with the mathematical preliminaries required to understand the theoretical contributions of this work. In Chapter 3, the reader is given a high-level overview of tactical missile guidance before developing the near-collision course (NCC) model for the missile homing loop that will be used in Chapter 7 and Chapter 8.

Part II presents our new approach to prescribed-time stabilization and estimation. First, in Chapter 4, we assume perfect knowledge of the state, and develop prescribed-time full-state feedback controllers for nonlinear systems in the normal form. Next, in Chapter 5, we develop a new prescribed-time observer for linear systems in the observable canonical form. Then, having both a prescribed-time controller and a prescribed-time observer, we combine them in Chapter 6 and demonstrate that a separation principle holds between them.

Part III shows how the prescribed-time controllers and prescribed-time observer can be used to design simple tactical missile guidance laws in the context of the missile homing loop model developed in Chapter 3. We first provide examples of new prescribed-time full-state feedback guidance laws in Chapter 7, and then introduce new prescribed-time output feedback guidance laws in Chapter 8.

Part IV concludes this dissertation with a summary of the contributions of this work in Chapter 9, which highlights the strengths and limitations of the methods presented here and suggests ideas for future work.

Chapter 2

Mathematical Preliminaries

In order to understand the new results presented in this work, the reader requires a basic understanding of the language and terminology that is typically used to study the stability of continuous-time dynamical systems. The definitions and concepts presented in this chapter will be used heavily throughout the remainder of this dissertation. Most of the background material in this chapter was borrowed and paraphrased from Hassan Khalil's popular textbook, *Nonlinear Systems* [42], and will be cited throughout to emphasize this. But also in this chapter, we introduce new concepts of *fixed-time stability* which form the basis of our designs in Part II, as well as *fixed-time scaling functions* which are used to implement the designs.

2.1 State equation models for continuous-time dynamical systems

In this work, we restrict our study to continuous-time dynamical systems. With the intent that the new concepts and designs presented will be used in applications such as missile guidance, which require implementation in discrete-time (digital) or hybrid systems, the stability analysis of such systems involves additional layers of complexity that should only be added after a solid foundation is laid for the simpler, underlying continuous-time system model. This is the usual approach not only for the study of missile guidance, but for dynamical systems in general.

2.1.1 Nonlinear systems

The discussion in this section is paraphrased material from Chapter 1 of Khalil's *Nonlinear Systems* [42].

Many continuous-time dynamical systems are modeled by a finite number of coupled first-order differential equations

$$
\begin{aligned}
\dot{x}_1 &= f_1(t, x_1, \ldots, x_n, u_1, \ldots, u_p) \\
\dot{x}_2 &= f_2(t, x_1, \ldots, x_n, u_1, \ldots, u_p) \\
\vdots \quad & \quad \vdots \\
\dot{x}_n &= f_n(t, x_1, \ldots, x_n, u_1, \ldots, u_p)
\end{aligned}
$$

where the x_i are called the *state variables*, $\dot{x}_i$ denotes the derivative of x_i with respect to the time variable t, and u_i are called *input variables*. The above system is usually rewritten as a single n-dimensional first-order vector differential equation

$$\dot{x} = f(t, x, u) \tag{2.1}$$

where x is called the *state* and u is called the *input*. Absent of an input u, or when $u = \gamma(x)$ can be rewritten in terms of the state, (2.1) can be written as

$$\dot{x} = f(t, x) \tag{2.2}$$

which is called the *unforced state equation*. When the function f does not depend explicitly on t, i.e.,

$$\dot{x} = f(x) \tag{2.3}$$

the system is said to be *autonomous* or *time-invariant*. If f does explicitly depend on t, then the system is said to be *nonautonomous* or *time-varying*.

2.1.2 Linear systems

Most dynamical systems in nature are nonlinear. However, most of the results presented in this work pertain to linear systems, in which many of the complexities of nonlinear dynamics are absent.

The system (2.1) is said to be a *linear time-varying (LTV)* system if it can be written in the form

$$\dot{x}(t) = A(t)x(t) + B(t)u(t), \tag{2.4}$$

$$y(t) = C(t)x(t) + D(t)u(t), \tag{2.5}$$

where $x(t) \in \mathbb{R}^n$ is the state, $y(t) \in \mathbb{R}^m$ is the output, $u(t) \in \mathbb{R}^p$ is the input, and the elements of the matrices $A(t)$, $B(t)$, $C(t)$, and $D(t)$ are independent of the state $x(t)$. If the elements of the matrices are also independent of time, then the system (2.1) is called a *linear time-invariant (LTI)* system.

In the majority of this work, we restrict our analysis to LTI *single-input single-output (SISO)* systems in which $m = p = 1$. Such systems are often written in the frequency domain *transfer function* form

$$y(s) = \frac{B(s)}{A(s)} = \frac{b_{n-1}s^{n-1} + b_{n-2}s^{n-2} + \ldots + b_1 s + b_0}{s^n + a_{n-1}s^{n-1} + a_{n-2}s^{n-2} + \ldots + a_1 s + a_0} u(s), \tag{2.6}$$

where s is the *frequency variable* or *Laplace variable* and the a_is and b_is are constants.

2.1.3 Canonical forms

The nth-order system (2.1) can be rewritten in a variety of forms to exhibit characteristics that are particularly convenient for achieving certain stabilization or estimation objectives. In this work, we use the following forms of the state equations, which are so often used that they are referred to as *canonical forms* in the literature.

To design controllers in Chapter 4, we employ a canonical form for nonlinear systems which are *full-state linearizable* by a diffeomorphic transformation, i.e., the so-called *normal form*,

$$\begin{aligned} \dot{x}_q(t) &= x_{q+1}(t), \quad q = 1,\ldots,n-1 \\ \dot{x}_n(t) &= f(x,t) + b(x,t)u(t). \end{aligned} \tag{2.7}$$

Here, $x(t) = [x_1(t), \cdots, x_n(t)]^T$ is the state, $u(t) \in \mathbb{R}$ is the control input, $b(x,t) : \mathbb{R}^{n+1} \times \mathbb{R} \to \mathbb{R}$ is the input coefficient, and $f(x,t) : \mathbb{R}^{n+1} \times \mathbb{R} \to \mathbb{R}$ denotes the system nonlinearity which could include parametric uncertainties and external disturbances.

When no nonlinearities or uncertainties are present, the normal form reduces to the *controllable canonical form*,

$$\dot{x}_i(t) = x_{i+1}(t), \quad i = 1, \ldots, n-1 \tag{2.8}$$

$$\dot{x}_n(t) = -a_0 x_1(t) - a_1 x_2(t) - \ldots - a_{n-1} x_n(t) + u(t) \tag{2.9}$$

$$y(t) = b_0 x_1(t) + b_1 x_2(t) + \ldots + b_{n-2} x_{n-1}(t) + b_{n-1} x_n(t), \tag{2.10}$$

which is written more compactly as

$$\dot{x}(t) = Ax(t) + Bu(t) \tag{2.11}$$

$$y(t) = Cx(t), \tag{2.12}$$

where

$$A = \begin{bmatrix} 0 & I_{n-1} & & \\ \vdots & & & \\ -a_0 & -a_1 & \ldots & -a_{n-1} \end{bmatrix}, \quad B = \begin{bmatrix} 0 \\ \vdots \\ 1 \end{bmatrix}, \quad C = \begin{bmatrix} b_0 & b_1 & \ldots & b_{n-1} \end{bmatrix}. \tag{2.13}$$

To design observers in Chapter 5, we rewrite the system in the *observer canonical form*,

$$\dot{x}_1(t) = x_2(t) - a_{n-1}y(t) \tag{2.14}$$

$$\vdots$$

$$\dot{x}_{r-1}(t) = x_r(t) - a_{\rho+1}y(t) \tag{2.15}$$

$$\dot{x}_r(t) = x_{r+1}(t) - a_\rho y(t) + b_\rho u(t) \tag{2.16}$$

$$\vdots$$

$$\dot{x}_{n-1}(t) = x_n(t) - a_1 y(t) + b_1 u(t) \tag{2.17}$$

$$\dot{x}_n(t) = -a_0 y(t) + b_0 u(t) \tag{2.18}$$

$$y(t) = x_1(t), \tag{2.19}$$

where $n > \rho \geq 0$, and $r = n - \rho$ is the relative degree of the system. This is written more compactly as

$$\dot{x}(t) = Ax(t) - ay(t) + \begin{bmatrix} 0_{(r-1)\times 1} \\ b \end{bmatrix} u(t) \tag{2.20}$$

$$y(t) = \mathrm{e}_1^T x(t), \tag{2.21}$$

and

$$A = \begin{bmatrix} 0 & I_{n-1} \\ \vdots & \\ 0 & \ldots 0 \end{bmatrix}, \quad a = \begin{bmatrix} a_{n-1} \\ \vdots \\ a_0 \end{bmatrix}, \quad b = \begin{bmatrix} b_\rho \\ \vdots \\ b_0 \end{bmatrix}. \tag{2.22}$$

2.2 Stability notions

The main contributions of this work consist of results pertaining to the stability of linear systems whose solutions are only required to exist for a finite time. In the following, we briefly review several stability concepts from Khalil's *Nonlinear Systems* [42], but then introduce new stability notions for finite-time systems. Sections 2.2.1–2.2.3 are paraphrased from [42], while Section 2.3 introduces new concepts for stability analyses of finite-time systems.

2.2.1 Equilibrium points

Consider the nonautonomous system

$$\dot{x} = f(t,x) \tag{2.23}$$

where $f : [0,\infty) \times D \to \mathbb{R}^n$ is piecewise continuous in t and locally Lipschitz in x on $[0,\infty) \times D$, and $D \subset \mathbb{R}^n$ is a domain that contains the origin $x = 0$. The origin is an equilibrium point for (2.23) at $t = 0$ if

$$f(t,0) = 0, \quad \forall t \geq 0. \tag{2.24}$$

In this work, we study equilibria at the origin, since any nonzero equilibrium to the system can be translated to the origin by a change of coordinates [42].

2.2.2 Stability concepts for general nonlinear systems

The following definitions are excerpts from Chapter 4 of Khalil's *Nonlinear Systems* [42] and are generally accepted as standard definitions for studying the stability of continuous-time dynamical systems.

Definition 2.1. *The equilibrium point $x = 0$ of (2.23) is*

- *stable if, for each $\varepsilon > 0$, there exists $\delta = \delta(\varepsilon, t_0) > 0$ such that*

$$|x(t_0)| < \delta \quad \Rightarrow |x(t)| < \varepsilon, \quad \forall\, t \geq t_0 \geq 0 \tag{2.25}$$

- *uniformly stable if, for each $\varepsilon > 0$, there exists $\delta = \delta(\varepsilon) > 0$, independent of t_0, such that (2.25) is satisfied.*

- *unstable if it is not stable.*

- *asymptotically stable if it is stable and there exists a positive constant $c = c(t_0)$ such that $x(t) \to 0$ as $t \to \infty$, for all $|x(t_0)| < c$.*

- *uniformly asymptotically stable if it is uniformly stable and there exists a positive constant c, independent of t_0, such that for all $|x(t_0)| < c$, $x(t) \to 0$ as $t \to \infty$, uniformly in t_0; that is, for each $\eta > 0$, there exists $T = T(\eta) > 0$ such that*

$$|x(t)| < \eta, \quad \forall\, t \geq t_0 + T(\eta), \quad |x(t_0)| < c \tag{2.26}$$

- *globally uniformly asymptotically stable if it is uniformly stable, $\delta(\varepsilon)$ can be chosen to satisfy $\lim_{\varepsilon\to\infty} \delta(\varepsilon) = \infty$, and, for each pair of positive numbers η and c, there exists $T = T(\eta, c) > 0$ such that*

$$|x(t)| < \eta, \quad \forall\, t \geq t_0 + T(\eta, c), \quad |x(t_0)| < c \tag{2.27}$$

Comparison functions

The fundamental stability properties introduced in the previous section can simplified conceptually through the use of the following *comparison functions*.

Definition 2.2. ***(Class $\mathscr{K}$ Function)*** *A continuous function $\gamma : [0,a) \to \mathbb{R}^+$ is said to belong to class $\mathscr{K}$ if it is strictly increasing and $\gamma(0) = 0$. It is said to belong to class $\mathscr{K}_\infty$ if $a = \infty$ and $\gamma(r) \to \infty$ as $r \to \infty$.*

Definition 2.3. ***(Class $\mathscr{KL}$ Function)*** *A continuous function $\beta : [0,a) \times \mathbb{R}^+ \to \mathbb{R}^+$ is said to belong to class $\mathscr{KL}$ if for each fixed s the mapping $\beta(r,s)$ belongs to class $\mathscr{K}$ with respect to r, and for each fixed r the mapping $\beta(r,s)$ is decreasing with respect to s and $\beta(r,s) \to 0$ as $s \to \infty$. It is said to belong to class $\mathscr{KL}_\infty$ if, in addition, for each fixed s the mapping $\beta(r,s,)$ belongs to class $\mathscr{K}_\infty$ with respect to r.*

Stability based on comparison functions

Using these comparison functions, we introduce stability concepts that begin to form the framework for the more-complex stability notions to follow.

Lemma 2.1. *The equilibrium point $x = 0$ of (2.23) is*

- *uniformly stable if and only if there exist a class $\mathscr{K}$ function α and a positive constant c, independent of t_0, such that*

$$|x(t)| \leq \alpha(|x(t_0)|), \quad \forall\ t \geq t_0 \geq 0, \quad \forall\ |x(t_0)| < c \tag{2.28}$$

- *uniformly asymptotically stable if and only if there exist a class $\mathscr{KL}$ function β and a positive constant c, independent of t_0, such that*

$$|x(t)| \leq \beta(|x(t_0)|, t - t_0), \quad \forall\ t \geq t_0 \geq 0, \quad \forall\ |x(t_0)| < c \tag{2.29}$$

- *globally uniformly asymptotically stable if and only if (2.29) is satisfied for any initial state $x(t_0)$.*

The proof of Lemma 2.1 is provided in an appendix of [42]. The next definition provides a notion for stability that is often used for linear systems.

Definition 2.4. *The equilibrium point $x = 0$ of (2.23) is exponentially stable if there exist positive constants c, k, and λ such that*

$$|x(t)| \leq k|x(t_0)|\mathrm{e}^{-\lambda(t-t_0)}, \quad \forall\ |x(t_0)| < c \tag{2.30}$$

and globally exponentially stable if (2.30) is satisfied for any initial state $x(t_0)$.

The previous notions of stability are applicable for unforced systems. But when an input is present, the following stability notion is more useful.

Definition 2.5. *The system (2.1) where f is piecewise continuous in t and locally Lipschitz in x and u, is said to be input-to-state stable (ISS) if there exist a class $\mathscr{K}\mathscr{L}$ function β and a class $\mathscr{K}$ function γ, such that for any initial state $x(t_0)$, and for any bounded input $u(t)$, the solution $x(t)$ exists for all $t \geq t_0$ and satisfies*

$$|x(t)| \leq \beta(|x(t_0)|, t-t_0) + \gamma\left(\sup_{t_0 \leq \tau \leq t} |u(\tau)|\right) \tag{2.31}$$

for all t_0 and t such that $0 \leq t_0 \leq t$.

Note that for $u(t) = 0$, (2.31) implies that the origin of the unforced system (2.1) is globally uniformly asymptotically stable.

2.2.3 Lyapunov stability

The discussion in this section is paraphrased from Chapter 4 of Khalil's *Nonlinear Systems* [42]. In several of the proofs of our main results in Part II, we employ *Lyapunov's method*. The first fundamental result from Lypaunov's method we often use is referred to as *Lyapunov's stability theorem*.

Theorem 2.1. *Let $x = 0$ be an equilbrium point for (2.3) and $D \subset R^n$ be a domain containing $x = 0$. Let $V : D \to R$ be a continuously differentiable function such that*

$$V(0) = 0 \quad \text{and} \quad V(x) > 0 \quad \text{in} \quad D - \{0\} \tag{2.32}$$

$$\dot{V}(x) \leq 0 \quad \text{in} \quad D. \tag{2.33}$$

Then, $x = 0$ is stable. Moreover, if

$$\dot{V}(x) < 0 \quad \text{in} \quad D - \{0\}, \tag{2.34}$$

then $x = 0$ is asymptotically stable.

A continuously differentiable function $V(x)$ satisfying (2.32) and (2.33) is called a *Lyapunov function*.

In this dissertation, we deal with a number of LTI systems (see Section 2.1.2). Consider the unforced LTI system

$$\dot{x} = Ax, \tag{2.35}$$

which has an equilibrium at the origin. The next important theorem relates the stability properties of the origin in system (2.35) to the eigenvalues of the matrix A.

Theorem 2.2. *The equilibrium point $x = 0$ of $\dot{x} = Ax$ is stable if and only if all eigenvalues of A satisfy $Re\lambda_i \leq 0$ and for every eigenvalue with $Re\lambda_i = 0$ and algebraic multiplicity $q_i \geq 2$, rank$(A - \lambda_i I) = n - q_i$, where n is the dimension of x. The equilibrium point $x = 0$ is globally asymptotically stable if and only if all eigenvalues of A satisfy $Re\lambda_i < 0$.*

When all eigenvalues of A satisfy $\mathrm{Re}\lambda_i < 0$, the matrix A is said to be *Hurwitz*. Asymptotic stability of the origin of (2.35) can be investigated using Lyapunov's method by employing the *Lyapunov function candidate*,

$$V(x) = x^T P x, \tag{2.36}$$

where P is a real symmetric positive definite matrix. The derivative of V along the trajectories of (2.35) is

$$\begin{aligned} \dot{V}(x) &= x^T P \dot{x} + \dot{x}^T P x \\ &= x^T \left(PA + A^T P \right) x \\ &= -x^T Q x \end{aligned} \tag{2.37}$$

where Q is a symmetric matrix defined by the *Lyapunov equation*,

$$PA + A^T P = -Q. \tag{2.38}$$

So, if Q is positive definite, then by Theorem 2.1, the origin is asymptotically stable. The following related result is also useful for linear systems.

Theorem 2.3. *A matrix A is Hurwitz; that is* $\mathrm{Re}\lambda_i < 0$ *for all eigenvalues of A, if and only if for any positive definite symmetric matrix Q there exists a positive definite symmetric matrix P that satisfies the Lyapunov equation (2.38). Moreover, if A is Hurwitz, then P is the unique solution of (2.38).*

2.3 Extensions for finite-time systems

In this section we introduce several new definitions of stability that are finite-time extensions to the classical stability definitions introduced in the previous section.

2.3.1 Notions of "fixed time" and "prescribed time"

The notions of stability introduced earlier exhibit *asymptotic convergence*, i.e., where the state trajectories do not actually reach the equilibrium, but instead only approach it in the limit as the time t goes to infinity. But in finite-time applications, one may instead require the trajectory to actually reach the equilibrium in finite time. There now exist a variety of different frameworks with which to approach the problems of finite-time stabilization and estimation, with the most popular ones employing sliding mode control (SMC) and/or concepts of homogeneity. Recent works have introduced a number of formal definitions of not only finite-time convergence and stability, but also *fixed-time* convergence and stability [6,19,21,48,50,68]. But since we disagree on the terminology used in some of these works (particularly the use of "settling time" and "settling time function"), and since in this dissertation we do not use these definitions, we do not state them here. Instead, we introduce some intuitive definitions before stating the formal ones we will use for the remainder of this dissertation.

Suppose a state trajectory $x(t) \in \mathbb{R}^n$ is stable and convergent to an equilibrium in some finite time $T^*(x(t_0)) > 0$ which depends upon the initial condition of the state, $x(t_0)$. If in addition there exists a $T > 0$ such that, for all $x(t_0) \in \mathbb{R}^n$, it is true that $T^*(x(t_0)) \leq T$, then the trajectory is said to be *fixed-time convergent in time T*. When the trajectory is fixed-time convergent to the origin in time T, the trajectory is said to be *fixed-time stable in time T*. When this fixed time T can be arbitrarily selected by the user as a design parameter, then we say the trajectory is *prescribed-time* *convergent in time T* or *prescribed-time stable in time T* as applicable. Formal definitions for some of these stability notions are provided later in Section 2.3.4.

2.3.2 Fixed-time coordinate transformations

In this section we introduce a key concept upon which many of our designs are based in Part II. Define $T > 0$ as a constant which is arbitrarily selected by the user. Now consider the change of coordinates of a scalar dynamical system ($n = 1$) defined for $t \in [t_0, t_0 + T)$,

$$w(t) := \mu(t - t_0, T)x(t) \tag{2.39}$$

where for $t \in [t_0, t_0 + T)$, $\mu(t - t_0, T) : [t_0, t_0 + T) \mapsto \mathbb{R}^+$ is a monotonically-increasing function (to be defined) having the property that $\mu(t - t_0, T)$ *tends to infinity* as $t \to t_0 + T$. Clearly, (2.39) also gives the inverse mapping from $w(t)$ to $x(t)$,

$$x(t) = \mu(t - t_0, T)^{-1} w(t). \tag{2.40}$$

Since $\mu(t - t_0, T)$ grows monotonically to infinity, then $\mu(t - t_0, T)^{-1}$ *decreases monotonically to zero*. So from (2.40), if the state $w(t)$ remain finite, then clearly $x(t) \to 0$ as $t \to t_0 + T$. Therefore, if $w(t)$ is stable for $t \in [t_0, t_0 + T)$, then by nature of the special relationship between $w(t)$ and $x(t)$ in (2.40), we simultaneously enforce the condition that $x(t) \to 0$ as $t \to t_0 + T$.

Note that in general, the change of coordinates (2.39) may result in a transformed system that is much more complicated than the original one, and finding its inverse may not be trivial. However, it offers the advantage of providing a means of achieving fixed-time convergence in the prescribed time T.

Later in Part II, we extend this concept for prescribed-time coordinate transformations to nth-order linear systems.

2.3.3 Fixed-time scaling functions

Fix $T > 0$. We define the function $\mu_1(t-t_0,T) : [t_0, t_0+T) \mapsto \mathbb{R}^+$ as

$$\mu_1(t-t_0,T) := \frac{T}{T+t_0-t}, \tag{2.41}$$

which starts from 1 at $t = t_0$ and increases monotonically to infinity as $t \longrightarrow t_0+T$, as shown in Figure 2.1 for $T = 10$ and sample values of t_0. We also define the function $\nu(t-t_0,T) : [t_0, t_0+T) \mapsto \mathbb{R}^+$ as

$$\nu(t-t_0,T) := \mu_1(t-t_0,T)^{-1} = \frac{T+t_0-t}{T}, \tag{2.42}$$

which starts from 1 at $t = t_0$ and *decreases monotonically to zero* as $t \longrightarrow t_0+T$. Then also using (2.41), we define the function $\mu(t-t_0,T) : [t_0, t_0+T) \mapsto \mathbb{R}^+$ as

$$\mu(t-t_0,T) := \mu_1(t-t_0,T)^{n+m} = \frac{T^{n+m}}{(T+t_0-t)^{n+m}}, \tag{2.43}$$

which also starts from 1 at $t = t_0$ and increases monotonically to infinity as $t \longrightarrow t_0+T$, but can be tuned to do so more quickly than $\mu_1(t-t_0,T)$ through the positive integers $n \geq 1$ (the order of the system) and $m \geq 1$, a design parameter selected by the user. Finally, we introduce the monotonically decreasing function

$$\zeta(t-t_0,T) = \exp^{\frac{T}{m}\left(1-\mu_1(t-t_0,T)^m\right)}, \quad t \in [t_0, t_0+T), \tag{2.44}$$

where again $m \geq 1$ is an integer design parameter, and $\zeta(t-t_0,T)$ is the smooth, "bump-like" function (Fry & McManus [24]) having the properties that $\zeta(0,T) = 1$ and $\zeta(T,T) = 0$. The function $\zeta(t-t_0,T)$ is plotted in Figure 2.4 for $t_0 = 0$, $T = 10$ and several values of m.

In the remainder of this dissertation, the integer design parameter m and the functions that employ it (i.e., μ, ζ) will be subscripted with "C" and "O" to denote *"controller"* and *"observer"* parameters and functions, respectively.

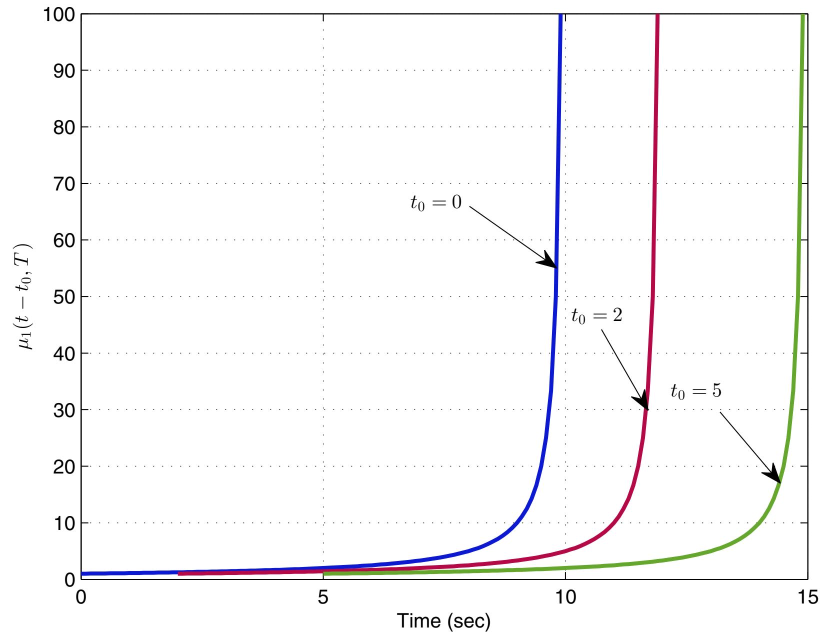

Figure 2.1: Scaling function $\mu_1(t - t_0, T)$ for $T = 10$, $m = 1$, and different values of t_0.

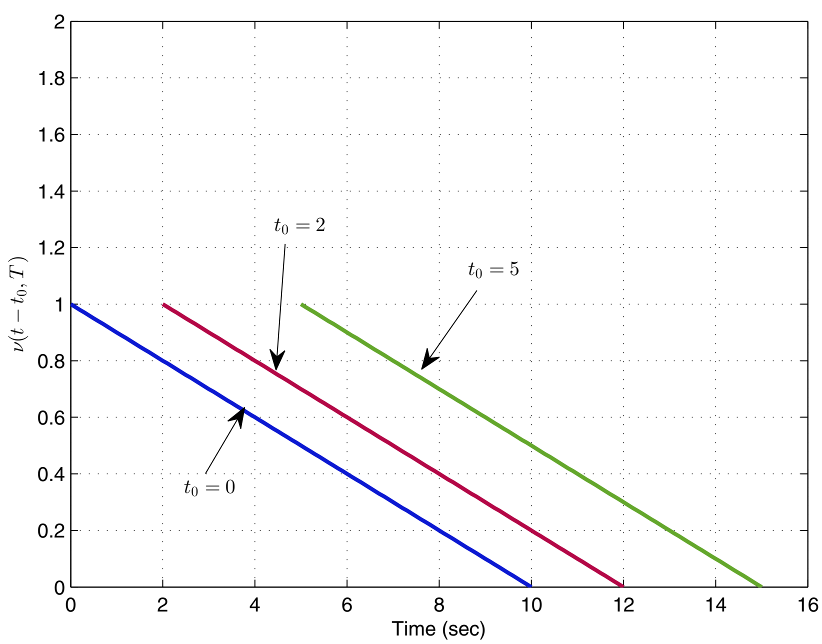

Figure 2.2: Scaling function $\nu(t - t_0, T)$ for $T = 10$, $m = 1$, and different values of t_0.

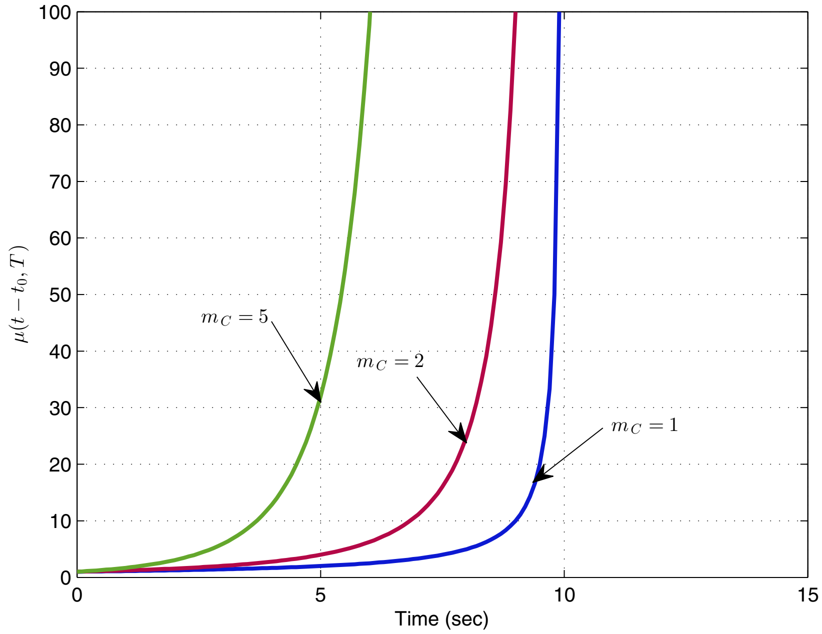

Figure 2.3: Scaling function $\mu(t-t_0,T)$ for $t_0 = 0$, $T = 10$, and different values of m.

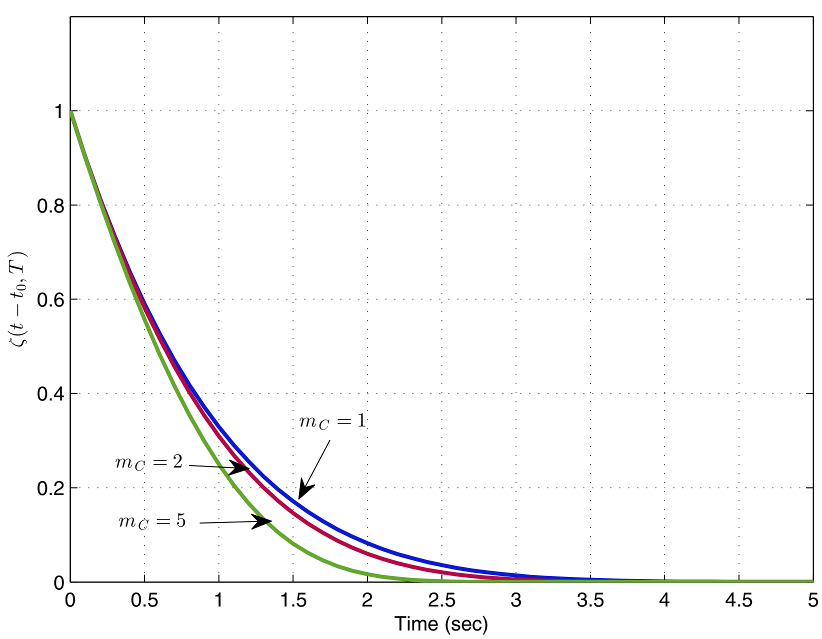

Figure 2.4: Scaling function $\zeta(t-t_0,T)$ for $t_0 = 0$, $T = 10$, and different values of m.

2.3.4 Fixed-time stability

We now introduce new definitions of stability for finite-time continuous dynamical systems. Although in this work we limit our study to linear systems, the following definitions are general enough that they can be used to study the stability of nonlinear systems as well. Note that in all of these, T is a constant that is independent of initial conditions.

Definition 2.6. ***(FT-GUAS)*** *The system $\dot{x} = f(x,t)$ (of arbitrary dimension of x) is said to be fixed-time globally uniformly asymptotically stable (FT-GUAS) in time T if there exists a class $\mathscr{K}\mathscr{L}$ function β such that for all $t \in [t_0, t_0 + T)$,*

$$|x(t)| \leq \beta(|x(t_0)|, \mu_1(t - t_0, T) - 1), \tag{2.45}$$

where the function $\mu_1(t - t_0, T)$ is defined in (2.41).

Notice that the function $\mu_1(t - t_0, T) - 1 = (t - t_0)/(T + t_0 - t)$ starts from zero at $t = t_0$ and increases monotonically to infinity as $t \to t_0 + T$. Therefore, the function $\beta(|x(t_0)|, \mu_1(t - t_0, T) - 1)$ decays to zero as $t \to t_0 + T$, i.e., at a time that is prescribed by T.

Definition 2.7. ***(FT-ISS)*** *The system $\dot{x} = f(x,t,d)$ (of arbitrary dimensions of x and d) is said to be fixed-time input-to-state stable (FT-ISS) with respect to d in time T if there exists a class $\mathscr{K}\mathscr{L}$ function β and a class $\mathscr{K}$ function γ, such that for all $t \in [t_0, t_0 + T)$,*

$$|x(t)| \leq \beta(|x(t_0)|, \mu_1(t - t_0, T) - 1) + \gamma(||d||_{[t_0,t]}), \tag{2.46}$$

where the function $\mu_1(t - t_0, T)$ is defined in (2.41).

Notice that a system that is FT-ISS is, in particular, ISS, with the additional property that, in the absence of the disturbance $d(t)$, it is FT-GUAS in time T.

Definition 2.8. ***(FT-ISS+C)*** *The system $\dot{x} = f(x,t,d)$ (of arbitrary dimensions of x and d) is said to be fixed-time input-to-state stable and convergent to zero (FT-ISS+C) in time T if there exist class $\mathcal{KL}$ functions β and β_f, and a class $\mathcal{K}$ function γ, such that for all $t \in [t_0, t_0 + T)$,*

$$|x(t)| \leq \beta_f \left(\beta(|x(t_0)|, t - t_0) + \gamma(||d||_{[t_0,t]}), \mu_1(t - t_0, T) - 1 \right), \tag{2.47}$$

where the function $\mu_1(t - t_0, T)$ is defined in (2.41).

So, a system that is FT-ISS+C is also FT-ISS, with the additional property that its state converges to zero in the time T despite the presence of a disturbance.

For the remainder of this dissertation, the parameter T is not only a constant that is independent of initial conditions, but it is furthermore a design parameter that is freely prescribed by the user. Therefore, our designs can be said to exhibit *prescribed-time convergence*, and *prescribed-time stability* properties.

Chapter 3

Missile Guidance: A Brief Primer

Having been studied for more than 70 years, missile guidance is a very broad and well-established field. There exist many hundreds of technical journal articles devoted to it, as well as numerous textbooks and research monographs to which the student of missile guidance can turn to. In the interests of the purpose of this dissertation, we do not provide an in-depth introduction to the field here. Our objectives in this chapter are instead to: *1)* provide the minimal background on missile guidance neccessary to appreciate and use the contributions of this dissertation, and *2)* introduce the reader to the interesting and challenging field of missile guidance, which hopefully will encourage further study in the field beyond this dissertation. In this chapter, we highly leverage the pedagogical presentations of tactical missile guidance provided by N. A. Shneydor in *Missile Guidance and Pursuit: Kinematics, Dynamics and Control* [80], by Paul Zarchan in *Tactical and Strategic Missile Guidance* [108], and by George Siouris in *Missile Guidance and Control Systems* [84].

3.1 Introduction

For more than seventy years, missile guidance has remained a challenging application of feedback control theory which has enormous real-world consequences. In general, missile guidance is a complex, multi-disciplinary engineering endeavor, with the ultimate objective being no less than to destroy or save human life. From the perspective of a controls engineer, in which the majority of designs have focused on achieving asymptotic performance as time goes to infinity, missile guidance presents an intriguing challenge: not only do its problems demand extremely high accuracy and precision, but they require it in a short, *finite* amount of time.

Guided missile technology as we understand it today originated during World War II in Germany [84, 108]. According to Siouris [84] and Zarchan [108], the German *V-1* and *V-2* were the first experimental surface-to-surface missiles and were developed by scientists and engineers at Peenemunde. Zarchan [108] states that the first tactical missiles were the Hs 298, an air-to-air missile developed by the Henscehel Company, and the first U.S. tactical missile successfully implemented in combat was the Lark missile. Readers interested in additional history and anecdotes on the origins of missile guidance are referred to Chapter 1 of [84] and Chapter 2 of [108].

3.2 Missile guidance classifications

The expression "missile guidance" is quite general, and in fact encompasses a multitude of military applications in which a missile is guided (either autonomously or with external aiding) to strike or *intercept* a target, which may be moving or stationary. There are many ways to classify missiles and their guidance systems, and preferences vary widely among engineers and authors. For the purposes of this dissertation, however, it is sufficient to classify guided missiles into two broad categories which are based on the distance the missile must travel in application.

Tactical missile guidance deals with the guidance of *tactical missiles* which typically operate over “short” ranges (less than a mile up to a few hundreds of miles) [84], and can be used to strike both stationary and moving targets. Tactical missiles include air-to-air missiles (AAMs) fired from aircraft and helicoptors, shoulder-fired surface-to-air missiles (SAMs), surface-to-air interceptors fired from mobile launchers, and exo-atmospheric kill vehicles (EKVs) deployed from ground-based interceptors (GBIs). Tactical missiles are usually mobile so that they can be easily transported to locations where they are needed for combat [84]. As discussed by Shneydor [80] and Siouris [84], tactical missile guidance can be further classified into *command-to-line-of-sight (CLOS) guidance* and *homing missile guidance*. In CLOS guidance, the missile is steered by commands sent remotely from aircraft or ground stations. In homing missile guidance, the missile tracks its target with an onboard seeker and steers itself autonomously to intercept the target.

Strategic missile guidance deals with the guidance of *strategic missiles*, which operate over very long ranges (many hundreds to several thousand miles) and are used to strike stationary targets. Strategic missiles can be further divided into *ballistic missiles* and *cruise missiles*. Strategic ballistic missiles are launched from ground-based or submarine-based launch facilities and guided to points in outer space from which they deploy reentry vehicles (RVs) which then follow ballistic trajectories to deliver nuclear warheads to their targets [84, 108]. Strategic ballistic missiles include both ground-based and mobile inter-continental ballistic missiles (ICBMs) as well as submarine-launched ballistic missiles (SLBMs). On the other hand, strategic cruise missiles are pilotless, self-guided, subsonic air-breathing vehicles that use onboard sensors to fly like airplanes over surface terrain for very long ranges to deliver either conventional or nuclear warheads to their targets [84]. Strategic cruise missiles include ground-launched cruise missiles (GLCMs), sea-launched cruise missiles (SLCMs), and air-launched cruise missiles (ALCMs) [84].

From the above discussion, it is clear that the missions of guided missiles span a very broad spectrum. Therefore, the designs of these missiles involve a broad range of navigation, guidance, and control problems that must be approached in different ways. For the remainder of this dissertation, we focus only on applications of tactical missile guidance, and more specifically, homing missile guidance.

3.2.1 Homing missile guidance

Shneydor defines *homing missile guidance* as guidance in which the missile guidance system detects and tracks the target using energy emitted by the target [80]. Both Shneydor [80] and Siouris [84] explain that homing missiles are often classified into three groups which are based on how energy is emitted and received by the guidance system: *1) active*, *2) semi-active*, and *3) passive*. In active homing, the guidance system uses an onboard energy source and receiver to illuminate the target and absorb the energy reflected off of the target to detect its whereabouts. In semi-active homing, the guidance system receives energy reflected off of the target which was originally provided by an external source, such as a ground-based tracking radar. In passive homing, the guidance system absorbs and tracks energy naturally emitted by the target itself. According to Siouris [84], electromagnetic radiation is the most widely used source of energy in homing guidance systems.

3.3 Mission and design objectives

In simple terms, the mission of the homing missile is “to seek and destroy” the target. Such seek-and-destroy missiles encompass a variety of tactical missiles, ranging from shoulder-fired anti-aircraft missiles such as the *Stinger*, to heat-seeking missiles employed by tactical aircraft such as the *Sidewinder*, to ballistic missile interceptors such as the *PATRIOT*, *THAAD*, and *Ground Based*

Interceptor (GBI) exo-atmospheric kill vehicles (EKVs) [84]. The mission of seek-and-destroy can only be accomplished with regularity by achieving specific missile guidance design objectives. In the following subsections, we state the mission design objectives with specificity in terms of kinematics and a geometrical rule, which then leads to explicit mathematical equations that pave the way for missile guidance feedback control solutions.

3.3.1 Three levels of guidance

In Chapter 1 of *Missile Guidance and Pursuit: Kinematics, Dynamics, and Control* [80], Shneydor frames the guidance of an object (whether a missile or otherwise) as the following three-tiered hierarchical process. (In the following, note that all of Section 3.3.1 is paraphrased from [80]).

The highest or most basic level of guidance is a *geometrical rule* that involves the *line-of-sight (LOS)* from the guided object to the target. The shape of the trajectories of the guided object and the target, the kinematic conditions required for the guided object to hit the target, and the *time-of-flight* of the guided object, t_f, are all examined at this level [80].

The middle level of guidance involves the construction of a *guidance law*, which is an algorithm or policy that implements the guidance geometrical rule. All such guidance laws are feedback control problems, in which the input is the deviation or "error" in the states of the guided object and target relative to that required by the guidance geometrical rule, and the output is a *steering command* that implements the guidance geometrical rule. In missile guidance, the steering command is typically in the form of a desired or "commanded" *lateral acceleration* for the missile (sometimes called *latax*) , denoted $a_{M_c}(t)$ [80].

The lowest level of guidance involves the finer details of how the guided object or "body" is able to implement the guidance steering command. This is referred to as the *control loop*, which in general consists of one or more "inner loop" feedbacks within the guidance law "outer loop" feedback. It is here that the control forces and moments acting on the body are considered, which consist of actuator dynamics and disturbances external to the body [80]. In missile guidance, the input of the control loop is the commanded lateral acceleration, $a_{M_c}(t)$, and the output is the actual or achieved missile lateral acceleration, $a_M(t)$.

3.3.2 Parallel navigation

The majority of tactical missile guidance laws are based on a geometrical rule that Shneydor refers to as *parallel navigation*, which received an entire chapter of treatment (Chapter 4) in [80]. According to Shneydor, parallel navigation has been known to mariners since antiquity, and is also referred to as the *constant bearing rule* [80]. Referring to Figure 3.1, the rule of parallel navigation states that the direction of the missile-to-target line-of-sight (LOS), having *LOS angle*, denoted $\lambda(t)$, must be kept constant relative to inertial space. In other words, the LOS must be kept *parallel* to its initial orientation at the beginning of the engagement [80]. Equivalently, the rate of rotation of the LOS, i.e., the *LOS rate*, denoted $\dot{\lambda}(t)$, must be kept zero. The rule of parallel navigation can also be stated as saying the relative range, $r(t)$, and relative range rate, $\dot{r}(t)$, must be colinear, with the caveat that the $\dot{r}(t)$ is negative (otherwise the missile would be receding from the target) [80].

When the parallel navigation rule is followed, $\dot{\lambda}(t) = 0$, and the so-called *collision course (CC)* conditions prevail. In the planar case, under constant velocities, and for a non-maneuvering target, the engagement can be characterized as shown in Figure 3.1, and the CC conditions reduce to

$$v_M \sin\delta = v_T \sin\theta \tag{3.1}$$

$$v_M \cos\delta > v_T \cos\theta. \tag{3.2}$$

Shneydor [80] shows that these CC conditions can be illustrated by a *collision triangle* having sides defined by v_T, v_M, and the *closing velocity*, $v_c := -\dot{r} = v_M - v_T$. When $\dot{\lambda}(t)$=0, thereby enforcing (3.1) and (3.2), the missile will coast to intercept the target without the need for further maneuvering. In this dissertation, we leverage this fact and aim to implement guidance laws that achieve CC conditions by stabilizing $\dot{\lambda}(t)$ to zero.

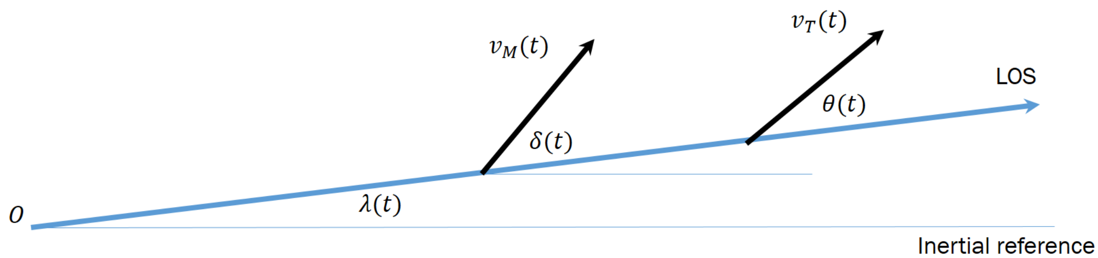

Figure 3.1: Illustration of geometry referenced in the rule of parallel navigation. (Figure concept borrowed from Shneydor [80].)

3.4 A model for the missile homing loop

As stated earlier, every homing missile guidance law algorithm is by definition a solution to a feedback control problem [80]. Viewed at the most basic, single-input single-output (SISO) level, this feedback control problem takes the form depicted in Figure 3.2. In Figure 3.2, the plant is the missile-target engagement kinematics, the input is the control feedback from the missile guidance and control system, denoted $a_M(t)$, and the output is the relative lateral displacement in physical space between the missile and the target, denoted $y(t)$. At the end of the engagement, when the relative range $r(t)$ reaches zero, the remaining relative lateral displacement is called the *miss distance*.

A more-detailed signal-flow model of the homing loop is shown in Figure 3.3, which, although still greatly simplified relative to models used in the design of real homing missiles, is sufficient for guidance law design at an intermediate level. In Figure 3.3, the engagement kinematics are shown with the aggregate of missile guidance and control system dynamics replaced by various models of missile guidance subsystems which are helpful in guidance law design. The following subsections provide brief overviews of these key elements of the missile homing loop.

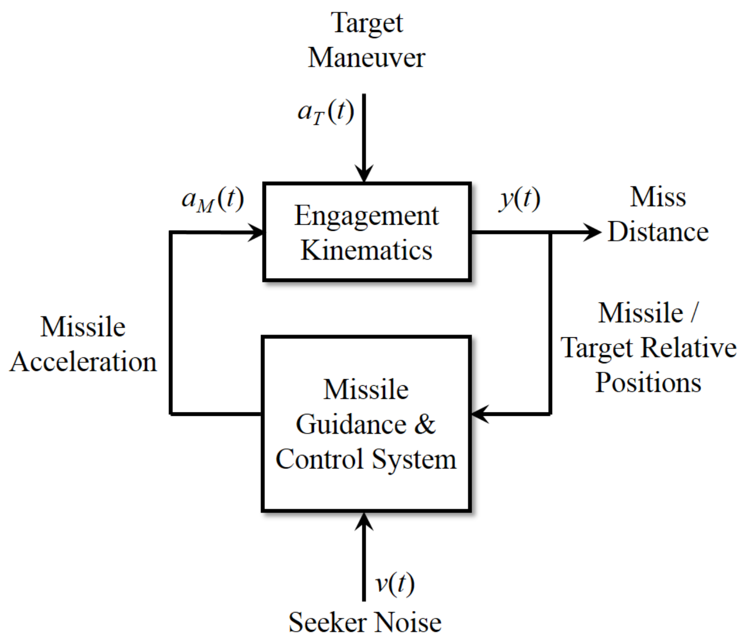

Figure 3.2: Basic SISO model for the missile homing loop.

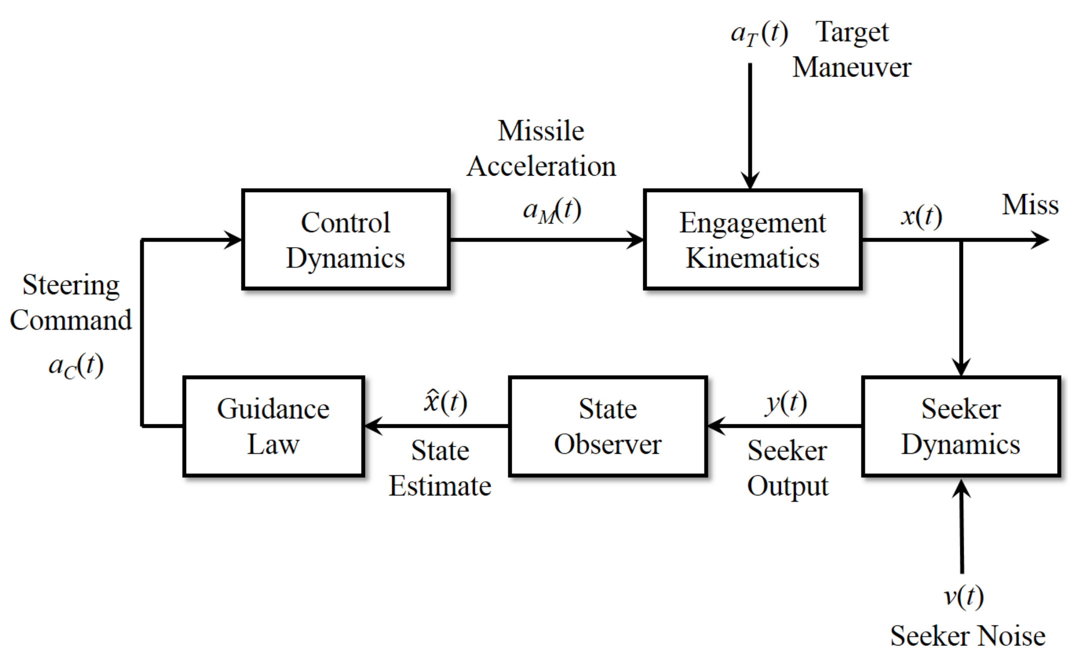

Figure 3.3: Signal flow model of the missile homing loop.

3.4.1 Engagement kinematics

The most fundamental element of any missile homing loop model is the model assumed for the kinematic differential equations which govern how the missile and target move relative to one another in physical space. In general, missile-target engagements occur in three-dimensional (3D) space, and in practice, homing missile guidance laws may employ a number of coordinate reference frames accelerating relative to one another in order to accurately model the kinematics of the engagement. However, by appropriate choices of coordinate reference frames, and invoking assumptions regarding the target and missile accelerations, the engagement becomes constrained to a two-dimensional (2D) plane. For initial studies and development of guidance laws, such planar engagement models are typically assumed, because they can reduce the mathematical complexity of the guidance problem dramatically while still capturing the key physics required to implement a successful guidance law.

A planar kinematic model for a general homing missile target engagement is shown in Figure 3.4. Without loss of generality, X and Y denote local horizontal and vertical coordinates, respectively, of a 2D plane selected to model the engagement. The vectors $\mathbf{r}_T(t)$ and $\mathbf{r}_M(t)$ denote the position vectors of the target and missile relative to the origin of the frame, and $\mathbf{v}_T(t)$ and $\mathbf{v}_M(t)$ denote the corresponding velocities. The angles $\gamma_T(t)$ and $\gamma_M(t)$ denote the target and missile *flight path angles*, where flight path angle is defined as the angle the velocity vector makes relative to the local horizontal plane. The relative horizontal displacement between the target and missile is denoted $x(t)$, and the relative vertical displacement is denoted $y(t)$. Then, as introduced earlier, $\lambda(t)$ denotes the missile-to-target LOS angle relative to the local horizontal.

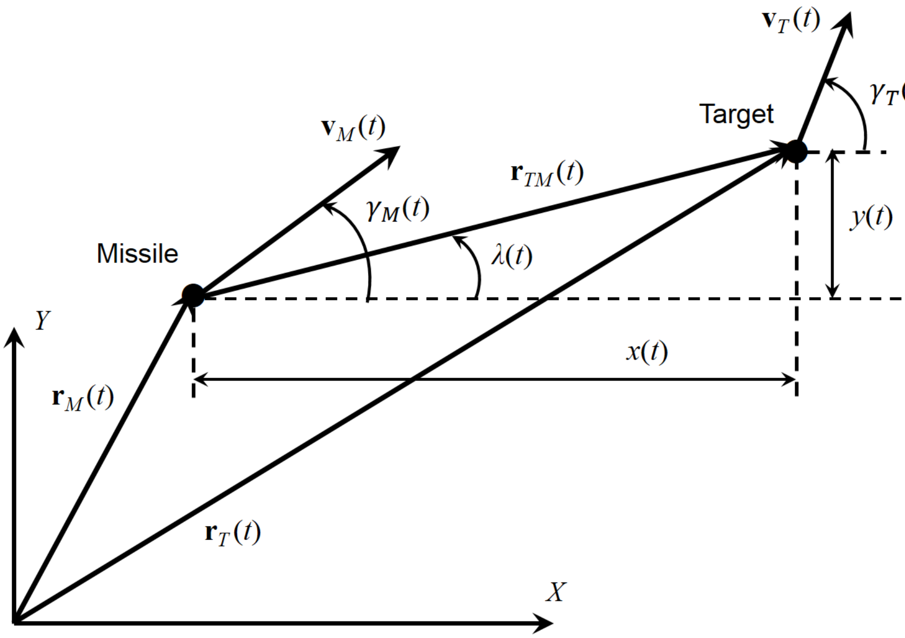

Figure 3.4: Planar kinematic model for a general missile-target engagement.

In many homing missile guidance applications, additional approximations can be made that further reduce the complexity of the kinematic equations without substantially sacrificing performance of the homing loop. In this work, in order to focus on new guidance law and state observer development, we invoke the so-called *near-collision course (NCC)* approximations [80], and thereby obtain a low-order linear kinematic model that is sufficient for homing missile guidance law design in some applications. We introduce the NCC assumptions and equations in Section 3.5.

3.4.2 Seeker dynamics

Homing guidance systems employ one or more sensors called *seekers* to observe and track the location and movement of the target relative to the missile. In general, the purpose of the seeker is to provide the measurements of target motion that are required to implement the guidance law [84]. This typically involves measuring the LOS angle, $\lambda(t)$, the LOS rate, $\dot{\lambda}(t)$, and/or the relative range rate, $\dot{r}$(t), by absorbing energy emitted by the target [80,84]. According to Siouris [84], homing missile seekers are sometimes categorized based on the type of electromagnetic energy they absorb for homing:

- Radio/radar frequency (RF)
- Infrared (IR)
- Visible (Optical)

RF seekers are widely used in active and semi-active homing guidance, while both IR and optical seekers are used in passive homing guidance. Readers interested in detailed descriptions and examples of seekers used in homing guidance systems are referred to Sections 3.4.1, 4.1, and 4.2 of [84].

3.4.3 State observer ("filter")

In practice, homing missile seekers do not provide perfect measurements, so it is necessary for the homing missile guidance system to employ some form of state observer or estimator to estimate the states needed by the guidance law. Homing missile guidance systems usually employ some type of Kalman filter to estimate the required states, which, with proper tuning, can be effective in the presence of both seeker measurement noise and plant model uncertainties. Perhaps for this reason, in tactical missile guidance, the state observer used in the homing missile guidance system is often referred to as *the filter*. For additional introductory discussions and derivations of equations pertaining to missile guidance state observers, the interested reader is referred to Chapter 9 of [108], Chapter 4 of [84], and Chapter 8 of Shneydor [80].

3.4.4 Guidance law

The purpose of the guidance law is to generate steering commands which result in missile accelerations that will eventually enforce the geometric rule (see Section 3.3.1) that results in target intercept. For most homing missiles, this means enforcement of the parallel navigation rule, which is equivalent to the CC kinematic conditions introduced in Section 3.3.2. To be effective, the guidance law must take into account the available knowledge of the control loop dynamics, and, if appplicable, the maneuvering capability of the target.

3.4.5 Control loop dynamics ("autopilot")

The purpose of the guidance system control loop is to employ actuators onboard the missile to impart specific forces that achieve a desired acceleration, $a_M(t)$, which will effect the steering command provided by the guidance law, $a_{M_c}(t)$. For endo-atmospheric homing missiles, these "divert" forces are provided by moving aerodynamic surfaces to impart lift forces. For exo-atmospheric interceptors, such divert forces are provided by propulsive forces from hot-gas thrusters. Homing missiles that may be required to operate in both regimes may employ a combination of these actuators [91].

As mentioned in Section 3.3.1, control dynamics in homing missiles typically consist of one or more "inner loop" feedbacks which must be designed to achieve regulation of the steering command. The loop closure includes the dynamics of both the control and external disturbance forces and moments acting on the missile. In tactical missile guidance literature, these control loop dynamics are often referred to as *the autopilot*, and in practice, may require very complex and sophisticated design solutions to achieve satisfactory tracking of the guidance steering commands. However, in the early stages of guidance law design, such complex control dynamics are often approximated as SISO linear systems. The simplest such model for homing missile autopilot dynamics, which has been widely used in the development of classical tactical missile guidance laws, is the first-order, so-called *single-lag* transfer function [80, 108],

$$G_A(s) := \frac{a_M(s)}{a_{M_c}(s)} = \frac{1}{1+sT_A}, \tag{3.3}$$

which has the equivalent representation in the time domain,

$$\dot{a}_M(t) = -\frac{1}{T_A}a_M(t) + \frac{1}{T_A}a_{M_c}(t), \tag{3.4}$$

such that

$$a_M(t) = \frac{1}{T_A}\int_{t_0}^{t} \mathrm{e}^{-\frac{1}{T_A}(\xi - t)} a_{M,c}(\xi)d\xi. \tag{3.5}$$

Generally speaking, as the autopilot time constant T_A becomes large relative to the homing time-of-flight, t_f, the performance of the homing guidance law will deteriorate if the lag is not accounted for in the design [80]. Higher-order transfer functions (second-order and higher) are also employed in guidance law design, although less frequently than the single-lag model [80, 108]. Again speaking in general, the higher the order of the autopilot dynamics, the lower the performance of the guidance law if it is not accounted for in the design [80].

3.4.6 Target dynamics ("maneuver")

In some applications of tactical missile guidance, the target may exhibit dynamics or *maneuver* in ways that act as external disturbances to the homing loop. Examples include aircraft performing evasive maneuvers to escape air-to-air missiles (AAMs) or surface-to-air missiles (SAMs), and ballistic missile RVs maneuvering to evade EKVs. Simple models for target maneuvers consist of unit steps and sinusoids, however more complex models are often used in guidance law design.

In general, missile guidance engineers have limited knowledge of the target dynamics prior to an engagement. Therefore, in some applications, it is assumed that the target manuever is random but has some known structure. Two target maneuver models often used in guidance law design are the *random step maneuver* [64, 108] and the *randomly-reversing Poisson square wave maneuver* (or *random telegraph maneuver*) [83, 84]. Both of these are based on the concept of the *shaping filter*, whereby to simplify modeling and simulations, a system with a random input is replaced by the original system without the random input, but augmented with a shaping filter equivalent, which is some function of white noise. It can be shown on a case-by-case basis that, although the original random input and its shaping filter equivalent do not have the same time histories, their time histories do have the same means and standard deviations [84, 108]. Then by using a shaping filter equivalent of a random input, one implicitly assumes that the shaping filter input will have the same effect on the system as the original random input, at least in some statistical sense.

According to missile guidance literature, shaping filters appear to be used often in missile guidance law design. However, in this dissertation we will use simpler models of target maneuvers, such as step and sinusoidal maneuvers. Readers interested in learning more about the shaping filter approach to modeling target maneuvers are referred to Chapter 4 of [108], Chapter 4 of [84], and the articles by Nesline and Zarchan [64] and Singer [83].

3.5 Kinematic model for the near-collision course (NCC)

In tactical missile guidance, the flight of the missile can be viewed as having three distinct phases. The first phase is the *launch* of the missile from some type of launcher or platform, in which the guidance objective is egress, i.e., to simply steer the missile away from the launching platform without contacting the platform itself or surrounding structures. The second phase, called *midcourse*, is the longest phase of the missile flight, in which the missile is guided to within a neighborhood of its target and the kinematic conditions required to make intercept possible are nearly achieved. The final phase of flight is called the *terminal* phase, and lasts only a few seconds in most applications. The objective of terminal guidance is to remove any residual heading and velocity errors and enforce the kinematic conditions required to coast to the target and achieve intercept. For homing missiles, this is also called the *homing* phase of flight.

In this dissertation, we focus our study only on the homing phase of missile guidance, in which the missile has nearly achieved CC conditions (see Section 3.3.2) and requires only minimal velocity corrections to hit the target. In this *near-collision course (NCC)*, the LOS angle $\lambda(t)$ and LOS rate $\dot{\lambda}(t)$ have already been made "small" relative to their initial values, and the nonlinear engagement kinematics are adequately modeled by linear perturbational equations [80]. We invoke the following assumptions to obtain our model:

Assumption 3.1. *The missile-target engagement is confined to a two-dimensional plane.*

Assumption 3.2. *The missile and target are modeled as point masses.*

Assumption 3.3. *The flight path angles of the missile and the target are approximately equal, and the missile pursues the target from behind.*

Assumption 3.4. *The longitudinal missile velocity V_M and longitudinal target velocity V_T are ap-*

proximately constant, and $V_M > V_T$.

Assumption 3.5. *The LOS angle $\lambda(t)$ and LOS rate $\dot{\lambda}(t)$ remain small relative to their initial values.*

Assumption 3.6. *The differential gravitational, aerodynamic, and longitudinal propulsive forces between the target and missile are small relative to the missile divert forces resulting from guidance and control.*

Figure 3.5 illustrates the geometry of the engagement. We define a local inertial frame XY in Cartesian coordinates such that X lies along the LOS of the target relative to the missile at the commencement of homing guidance, denoted t_0, and Y is perpendicular to X. By Assumption 3.1, the engagement remains confined to the XY plane, so the distance $y(t)$ can be viewed as either a vertical or lateral distance perpendicular to the LOS. By Assumptions 3.1–3.4, the missile-to-target relative longitudinal distance along the LOS, denoted $r(t)$, is decreasing linearly according to

$$r(t) = r_0 - V_{cl}(t - t_0), \tag{3.6}$$

where r_0 is the initial distance of the target relative to the missile at time t_0, and $V_{cl} := V_M - V_T$ is the missile *closing velocity*, which is constant. We define the parameter $t_f := \frac{r_0}{V_{cl}} > 0$ as the *time-of-flight*. Notice that when $t = t_0 + t_f$, $r(t) = 0$, so then $r(t)$ can also be written as

$$\begin{aligned} r(t) &= r_0 - V_{cl}(t - t_0) \\ &= V_{cl}(t_0 + t_f - t) \\ &= V_{cl} t_{go}(t), \end{aligned} \tag{3.7}$$

where $t_{go}(t) := t_0 + t_f - t$ is called the *time-to-go*. Invoking further Assumptions 3.5–3.6, the distance of the target relative to the missile perpendicular to the LOS, denoted $y(t)$, is governed by

$$\ddot{y}(t) = a_T(t) - a_M(t), \tag{3.8}$$

where $a_T(t)$ and $a_M(t)$ are the target and missile accelerations perpendicular to the LOS, respectively. We also assume a linear model for the missile seeker output according to

$$z(t) = y(t) + v(t), \tag{3.9}$$

where $v(t)$ is some bounded disturbance to be defined later.

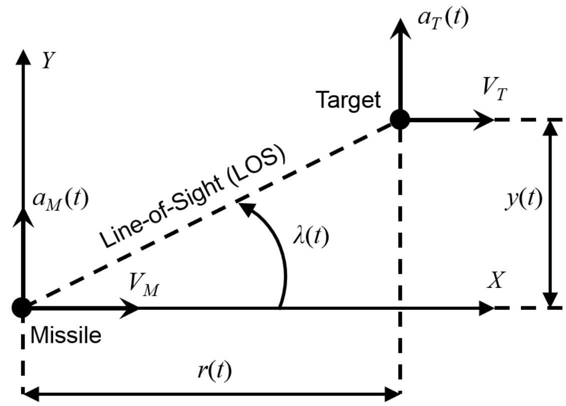

Figure 3.5: Missile-target engagement geometry for the near-collision course.

By defining the state as $x(t) = \begin{bmatrix} y(t) & \dot{y}(t) \end{bmatrix}^T$, the above equations for the kinematics perpendicular to the LOS are written in state space form as

$$\dot{x}(t) = Ax(t) + B_M a_M(t) + B_T a_T(t), \tag{3.10}$$

$$z(t) = Cx(t) + v(t), \tag{3.11}$$

where

$$A := \begin{bmatrix} 0 & 1 \\ 0 & 0 \end{bmatrix}, \quad B_M := \begin{bmatrix} 0 \\ -1 \end{bmatrix}, \quad B_T := \begin{bmatrix} 0 \\ 1 \end{bmatrix}, \quad C := \begin{bmatrix} 1 & 0 \end{bmatrix}. \tag{3.12}$$

The purpose of the missile guidance law and flight control system are to effect maneuvers through $a_M(t)$ that result in target intercept, i.e., make $y(t) \to 0$ at $t = t_0 + t_f$, since at that time, $r(t) = 0$. The target maneuver $a_T(t)$ acts as a disturbance against this objective. When $t = t_0 + t_f$, any remaining displacement $M := y(t_0 + t_f)$ is called the *miss distance*. We emphasize that homing missile guidance as presented here is a finite-time control problem, with solutions $y(t)$, $\dot{y}(t)$ defined only for $t \in [t_0, t_0 + t_f)$, since at $t = t_0 + t_f$, the missile either achieves intercept or misses the target. Note that in many applications, a nonzero miss distance may be acceptable, as long as the miss is smaller than the missile warhead's radius of effectiveness, i.e., the so-called *lethality radius*.

3.6 Proportional Navigation (PN) guidance

The most widely-studied guidance law for homing missiles is Proportional Navigation (PN) [80, 108], which probably derives its name from the fact that it implements a simple controller feedback that is proportional to the LOS rate, $\dot{\lambda}(t)$. Once the missile is in the NCC (see Section 3.5), if $\dot{\lambda}(t)$ is stabilized to zero, then the missile trajectory will converge to a collision course with the target (see Section 3.3.2). In its usual form, PN guidance is written as

$$a_M(t) = N' V_{cl} \dot{\lambda}(t), \tag{3.13}$$

where $N' > 2$ is the *effective navigation ratio*, a design parameter that missile guidance engineers must tune in order to optimize performance [108]. Experience has shown that N' between 3 and 5 often works well in practice [108]. PN guidance is known to perform well against non-maneuvering and stationary targets, but its performance degrades in the presence of target maneuvering [108].

3.6.1 Some history of PN

PN was developed in the 1940s and 1950s [80] and proven to be effective in practice up through the 1960s and early 1970s [7]. In particular, Shneydor [80] noted that PN was used by the Raytheon Lark missile in late 1950s. Most popular textbooks on missile guidance [84, 108] and recent journal articles that discuss PN say it has been widely used in practice and has been successful in many applications. A number of variations of PN were developed over the years, to include Pure Proportional Navigation (PPN) [3, 65, 66], True Proportional Navigation (TPN) [25, 26, 28, 82, 98], Augmented Proportional Navigation (APN) [80, 84, 108], Ideal Proportional Navigation (IPN) [105], Generalized Proportional Navigation (GPN) [103], Realistic True Proportional Navigation (RTPN) [17], and others. Researchers have also developed generalized or unified frameworks for studying and implementing PN guidance [25, 36, 92, 99, 100].

Several authors have stated that PN is likely the most widely-used form of guidance for homing missiles due to its simplicity, ease in implementation, and effectiveness against stationary and non-maneuvering targets [84, 93, 102, 108]. According to [7, 63], most modern guidance laws can be shown to be modified forms of PN, and according to Siouris [84], *all* missile homing systems in use today employ some form of PN.

PN in its basic form is simple to implement in practice [84, 108]. PN only requires measurement of the LOS angle, $\lambda(t)$, or more specifically, it does *not* require an additional measurement of the relative range, $r(t)$. In the hypothetical case of having ideal autopilot dynamics (perfect control with unbounded capability), PN assures intercept from almost any initial state [63]. Further, assuming ideal autopilot dynamics and a non-maneuvering target, PN is also the optimal guidance law in terms of a cost function that is quadratic in miss distance and control effort [80]. On the other hand, it is virtually impossible to achieve zero miss distance in real systems with PN [93]. When autopilot dynamics (e.g., lags) are considered, the LOS rate diverges in the end game, which has a detrimental effect on miss distance [63]. PN's performance also degrades when implemented against maneuvering targets and when measurement noise is present [80, 84, 93].

The reader interested in further study of PN is referred to the missile guidance textbooks that cover PN in depth [80, 84, 102, 108], and some of the most highly-cited journal articles pertaining to PN [1, 3, 27, 28, 46, 62, 74, 82, 105, 107].

3.6.2 Stability of PN in the NCC

In this section we obtain an interesting result that helps motivate Part II of this work. Under the NCC target engagement model of Section 3.5, and the implementation of PN guidance with ideal autopilot dynamics ($a_M(t) = a_{M_c}(t)$), not all of the state is stabilized to zero. In the context of traditional stability analyses of nonlinear systems, this result is unusual, since in most nominal feedback designs the entire state is stabilized to the origin.

By Assumption 3.5 in Section 3.5, $\lambda(t)$ remains small such that with $\tan\lambda(t) = y(t)/r(t)$, we obtain $\lambda(t) \approx \tan\lambda(t) = y(t)/r(t)$, or

$$\lambda(t) = \frac{y(t)}{r(t)}. \tag{3.14}$$

Substituting (3.14) into (3.13) gives

$$\begin{aligned}
a_M(t) &= N'V_{cl}\frac{d}{dt}\left(\frac{y(t)}{r(t)}\right) \\
&= N'V_{cl}\left(-\frac{\dot{r}(t)y(t)}{r(t)^2} + \frac{\dot{y}(t)}{r(t)}\right) \\
&= N'V_{cl}\left(\frac{V_{cl}y(t)}{r(t)^2} + \frac{\dot{y}(t)}{r(t)}\right) \\
&= \frac{N'V_{cl}^2}{r(t)^2}y(t) + \frac{N'V_{cl}}{r(t)}\dot{y}(t) \\
&= \begin{bmatrix} \frac{N'V_{cl}^2}{r(t)^2} & \frac{N'V_{cl}}{r(t)} \end{bmatrix} \begin{bmatrix} y(t) \\ \dot{y}(t) \end{bmatrix} \qquad (3.15) \\
&= K(t)x(t), \qquad (3.16)
\end{aligned}$$

where we have used $\dot{r}(t) = -V_{cl}$, and defined

$$\begin{aligned}
K(t) &:= \begin{bmatrix} K_1(t) & K_2(t) \end{bmatrix} \\
&= \begin{bmatrix} \frac{N'V_{cl}^2}{r(t)^2} & \frac{N'V_{cl}}{r(t)} \end{bmatrix}. \qquad (3.17)
\end{aligned}$$

Notice that as $t \to t_0 + t_f$, $r(t) \to 0$, so the gains $K_1(t)$, $K_2(t) \to \infty$ as $t \to t_0 + t_f$. It is therefore natural to inquire whether PN guidance in this form is a stable guidance law. In the ideal case, which assumes perfect state information, ideal autopilot dynamics, and a non-maneuvering target, the feedbacks $K_1(t)y(t)$ and $K_2(t)\dot{y}(t)$ remain in a delicate balance that keeps the quantity $K(t)x(t)$ finite as $t \to t_0 + t_f$. Several notions of stability for PN systems are found in the literature, to include *frozen-time stability* [80], *short-time stability* [90], and *finite-time stability* [40]. The specific definitions of PN stability and the sufficient criteria to demonstrate them are strongly dependent upon the engagement model assumed. It turns out that the special structure of our NCC model makes it possible to obtain solutions for the state evolution $x(t)$ directly. Then with expressions for $x(t)$, some basic notions of stability can be deduced. The proofs of these results are provided later in Section 3.8.

Ideal case

Suppose that the missile guidance system has perfect knowledge of the state, ideal flight control dynamics, and the target is non-manuevering. By substituting (3.16) and $a_T(t) = 0$ into (3.10) and using (3.17), the NCC engagement kinematics reduce to

$$\begin{aligned} \dot{x}(t) &= (A + B_M K(t))x(t) \\ &= \mathscr{A}(t)x(t), \end{aligned} \tag{3.18}$$

where $\mathscr{A}(t) := A + B_M K(t)$, and

$$\mathscr{A}(t) = \begin{bmatrix} 0 & 1 \\ -\frac{N' V_{cl}^2}{r(t)^2} & -\frac{N' V_{cl}}{r(t)} \end{bmatrix}. \tag{3.19}$$

The solution to (3.18) is significant enough that we state it as a theorem.

Theorem 3.1. *If in the NCC engagement characterized by (3.10), the missile guidance system has perfect knowledge of the state and implements PN guidance with ideal flight control dynamics as* $a_M(t) = K(t)x(t) = \begin{bmatrix} \frac{N'V_{cl}^2}{r(t)^2} & \frac{N'V_{cl}}{r(t)} \end{bmatrix} x(t)$*, and the target is non-maneuvering, then the state* $x(t)$ *evolves for* $t \in [t_0, t_0 + t_f)$ *according to*

$$x(t) = \frac{1}{1-N'}\Psi(t,t_0)x(t_0), \tag{3.20}$$

where $\Psi(t,t_0)$ *is the state transition matrix, defined as the matrix that satisfies*

$$\frac{d}{dt}\Psi(t,t_0) = \mathscr{A}(t)\Psi(t,t_0), \tag{3.21a}$$

$$\Psi(t_0,t_0) = (1-N')I, \tag{3.21b}$$

where $N' > 2$*, and*

$$\Psi_{11}(t,t_0) = \frac{r(t)}{r_0}\left[\left(\frac{r(t)}{r_0}\right)^{N'-1} - N'\right], \tag{3.22}$$

$$\Psi_{12}(t,t_0) = \frac{r(t)}{V_{cl}}\left[\left(\frac{r(t)}{r_0}\right)^{N'-1} - 1\right], \tag{3.23}$$

$$\Psi_{21}(t,t_0) = \frac{N'V_{cl}}{r_0}\left[1 - \left(\frac{r(t)}{r_0}\right)^{N'-1}\right], \tag{3.24}$$

$$\Psi_{22}(t,t_0) = 1 - N'\left(\frac{r(t)}{r_0}\right)^{N'-1}. \tag{3.25}$$

An important consequence of Theorem 3.1 is that with perfect knowledge of the state, ideal flight control, and a non-maneuvering target, PN guidance in the NCC achieves zero miss distance in finite time.

Corollary 3.1. *If the hypotheses of Theorem 3.1 are met, then at* $t = t_0 + t_f$*,* $y(t_0 + t_f) = 0$*, and* $\dot{y}(t_0 + t_f) = \frac{1}{1-N'}\left(\frac{N'V_{cl}y_0}{r_0} + \dot{y}_0\right)$.

Note also, however, that in the NCC, PN guidance exhibits a somewhat peculiar result: the miss distance is regulated to zero, but the rate of the missile perpendicular to the LOS is not regulated to anything, and ends up converging to some finite value that depends on N', the initial conditions, and the time-of-flight, $t_f = r_0/V_{cl}$. Since even with perfect state information, perfect flight contol, and a non-maneuvering target, not all of the state is regulated to $x(t) = 0$, once we relax one or more of these assumptions, we do not expect the desirable, traditional stability concepts (see Section 2.2.2) like input-to-state stability (ISS) to hold. Despite this inconvenience, we can still demonstrate the following stability property.

Corollary 3.2. *The origin $x = 0$ of (3.20) is globally uniformly stable for $t \in [t_0, t_0 + t_f)$.*

The next example illustrates the performance of PN in this ideal case for a sample set of initial conditions.

Example 3.1. In this example, we show the results of simulating PN for an engagement having a non-maneuvering target and ideal flight control dynamics, where $t_0 = 0$, $t_f = 10$, the initial conditions are $(y(t_0), \dot{y}(t_0)) = (1, 0.5)$, and the effective navigation ratio is selected as $N' = 5$. Figure 3.6 shows time histories of the states, and Figure 3.7 shows time histories of the control gains and the overall control input $u(t) = a_M(t)$. In Figure 3.6, we see that $y(t_f) = 0$ and $\dot{y}(t_f) = -0.25$, which corroborates the final values stated by Corollary 3.1. In Figure 3.7, we see that as $t \to t_0 + t_f$, the gains go to infinity, but the overall control input $u(t) = a_M(t)$ goes to zero smoothly.

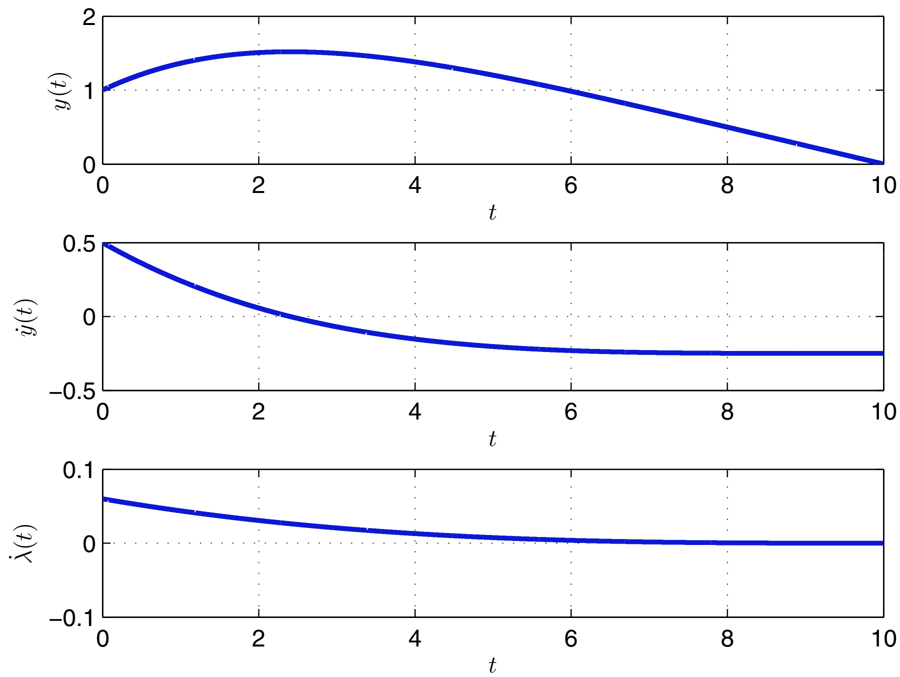

Figure 3.6: Time histories of states resulting from application of PN with a non-maneuvering target, ideal flight control dynamics, $t_0 = 0$, $t_f = 10$, and $N' = 5$.

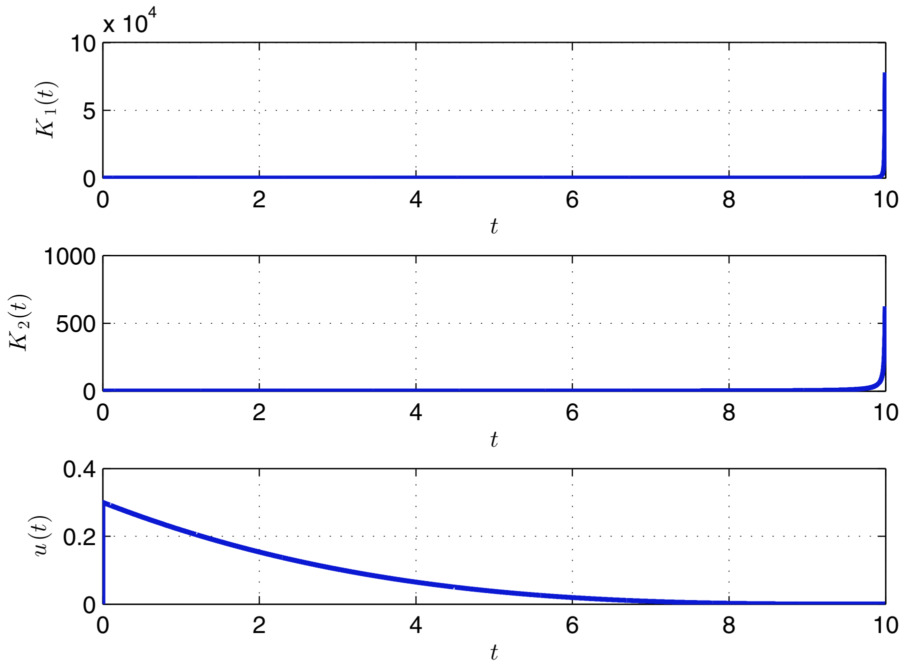

Figure 3.7: Time histories of control gains and overall control input resulting from application of PN with a non-maneuvering target, ideal flight control dynamics, $t_0 = 0$, $t_f = 10$, and $N' = 5$.

General case

For the general case where the state must be estimated using the seeker measurement (3.9), and the target is maneuvering, we define the estimate of the state as $\hat{x}(t) := \begin{bmatrix} \hat{y}(t) & \hat{\dot{y}}(t) \end{bmatrix}^T$, and assume that $r(t)$ is still known perfectly according to (3.6). The PN guidance law then becomes

$$a_M(t) = K(t)\hat{x}(t). \tag{3.26}$$

Then defining the state estimation error as $\tilde{x}(t) := x(t) - \hat{x}(t)$, we have

$$a_M(t) = K(t)x(t) - K(t)\tilde{x}(t), \tag{3.27}$$

and the engagement kinematics become

$$\begin{aligned} \dot{x}(t) &= Ax(t) + B_M a_M(t) + B_T a_T(t) \\ &= (A + B_M K(t))x(t) - B_M K(t)\tilde{x}(t) + B_T a_T(t) \\ &= \mathscr{A}(t)x(t) - B_M K(t)\tilde{x}(t) + B_T a_T(t). \end{aligned} \tag{3.28}$$

The solution to (3.28) provides another noteworthy consequence of Theorem 3.1.

Corollary 3.3. *For the NCC engagement characterized by (3.10), in which the missile implements PN guidance with ideal control in the form* $a_M(t) = K(t)\hat{x}(t) = \begin{bmatrix} \frac{N'V_{cl}^2}{r(t)^2} & \frac{N'V_{cl}}{r(t)} \end{bmatrix}\hat{x}(t)$*, where* $\hat{x}(t) = \begin{bmatrix} \hat{y}(t) & \hat{\dot{y}}(t) \end{bmatrix}^T$ *is the state estimate provided by an observer, and* $\tilde{x}(t)$ *is the state estimation error, the state evolves for* $t \in [t_0, t_0 + t_f)$ *and* $N' > 2$ *according to*

$$x(t) = \frac{1}{1-N'}\Psi(t,t_0)x(t_0) - \frac{1}{1-N'}\int_{t_0}^{t}\Psi(t,\theta)B_M K(\theta)\tilde{x}(\theta)d\theta + \frac{1}{1-N'}\int_{t_0}^{t}\Psi(t,\theta)B_T a_T(\theta)d\theta. \tag{3.29}$$

Since by (3.20) not all of the state is stabilized to zero even without the disturbances $\tilde{x}(t)$ and $a_T(t)$, ISS cannot be established. Furthermore, the finite-time nature of PN guidance in the

NCC makes it difficult to obtain meaningful bounds on the trajectories $x(t)$ once the disturbances $\tilde{x}(t)$ and $a_T(t)$ are added to the problem. For these reasons, we consider a rigorous, finite-time stability analysis of (3.29) to be an open problem. In practice, missile guidance engineers typically rely on numerical simulations to verify the stability of guidance laws in the closed loop.

3.6.3 Gains that tend to infinity

It is a remarkable fact that in the NCC formulation of PN, which has been explored extensively in the literature (see, e.g., [80, 84, 108]), the control feedback gains (3.17) go to infinity, yet the state remains bounded, and in fact part of the state, $y(t)$, is stabilized to zero. This is possible because as $t \to t_0 + t_f$, not only do the feedback gains go to infinity, but the state simultaneously decreases towards the origin. And, this takes place in a delicate way such that the overall feedback quantity, $a_M(t)$, which is a linear combination of products of things that get very big and things that get very small, remains finite. It is important to understand that this does not occur with the implementation of PN in its original form, (3.13), which feeds back a function of the *true* LOS rate, $\dot{\lambda}(t)$, rather than a linearized approximation to it.

We have shown that despite using gains that tend to infinity in finite time, the implementation of PN in the NCC with ideal control dynamics and no target maneuver yields a closed-loop system that is globally uniformly stable (GUS), meaning the state remains bounded independent of the initial time and initial conditions. Note that this version of PN is *not* globally uniformly asymptotically stable (GUAS), because not all of the state (i.e., $\dot{y}(t)$) goes to zero as $t \to [t_0, t_0 + t_f)$. Inspired by these results, in Part II of this dissertation, we develop controllers and observers whose gains go to infinity in finite time, yet the overal feedbacks remain finite, and yield closed-loop systems exhibiting some of the fixed-time stability properties introduced in Section 2.3.4.

3.7 The “state of the art” in tactical missile guidance

Although it is not necessary to understand the remainder of this dissertation, this section summarizes the current “state of the art” in tactical missile guidance design. Hopefully, it will interest readers and inspire further study in this important engineering discipline.

3.7.1 Optimal guidance laws

According to [7], most modern tactical missile guidance laws are obtained using optimal control theory. These *optimal guidance laws* are usually based on linear quadratic regulator (LQR) theory for a linear constant coefficient missile [7, 63], and assume the enforcement of zero miss, the availability of target maneuver information, and knowledge of the missile autopilot/response [7, 63, 88]. Optimal guidance laws are often combined with optimal estimation techniques such as Kalman filtering [11, 80, 86, 87], and many are formulated using pursuit-evasion differential game theory [2, 8, 9, 79, 84, 88]. Interestingly, most optimal missile guidance laws can be shown to be modified forms of PN [7, 63].

The development of optimal guidance laws began in the late 1960s, and their use became practical in the 1970s [7,63,80,84]. According to [7,91], optimal guidance laws are still prevalent in applications today. They offer the advantages of being able to achieve small miss distances [63, 93], having smaller energy requirements [63], and the ability to impose final constraints on mission objectives (e.g., impact angle) [13, 63]. On the other hand, optimal guidance laws require precise model knowledge, are very sensitive to modeling errors, and increase measurement requirements for estimation [63, 80]. Further, they require knowledge of future target behavior, and could even perform worse than simple PN if a bad estimate of target acceleration is used [7, 63]. Lastly, many optimal guidance laws also require an accurate estimate of time-to-go [7, 84].

Readers who are interested in further study of optimal missile guidance now have volumes of excellent resources to turn to. Most textbooks on missile guidance in general discuss optimal guidance laws and emphasize their continued use in practice. For examples, see the pedagogical works by Shneydor [80], Zarchan [108], and Siouris, [84], the book on theater ballistic missile defense by Naveh and Lorber [63], and the book on recent advances in missile guidance, control, and estimation by Balakrishnan, Tsourdos, and White [91]. The classical reference for the game-theoretical approach to missile guidance is the widely-used optimal control textbook by Bryson and Ho [8]. The book cited most in works pertaining to optimal missile guidance is the one by Ben-Asher and Yaesh [4]. In addition to textbooks, there exist dozens (if not hundreds) of journal articles on the subject of optimal missile guidance. The 1968 article by Willems [97] appears to the oldest article on the subject one can find in the open literature, and some of the most-cited journal articles for optimal missile guidance are [2, 13–15, 29, 64].

3.7.2 Recent advances

The survey article by Vathsal and Sarkar [93] provides an excellent summary of recent contributions to missile guidance theory and the directions missile guidance researchers may be headed in. The recent book by Balakrishnan, Tsourdos, and White [91] also summarizes several major advances in tactical missile guidance, control, and estimation in topical chapter form. Reviews of the AIAA and IEEE journal archives also show active research in various approaches to tactical missile guidance. The topics that receive the most attention in tactical missile guidance research today appear to be the following:

- **Design of integrated/combined guidance law and autopilot**, which exploit synergy between subsystems (guidance, control, estimation) and reduce the iterations needed in the design of subsystems [91].

- **Constraints on impact time and/or angle** [91]. By including this design objective, the effectiveness of the missile warhead can be maximized by attacking the weakest part of a target, or by achieving maximum penetration of a target.

- **Guidance laws based on sliding mode control (SMC)** [39, 61, 81, 91] can mitigate the disturbances of target maneuvering. High-order SMC has been shown to reduce chattering, and high-order robust exact differentiators (HOREDs) are capable of estimating the state without an accurate plant model.

- **Guidance as a pursuit-evasion game** was introduced in [8] and remains a popular way to formulate guidance laws [4, 9, 10, 63, 79, 88]. This approach makes no assumption on future target maneuvers, but does require knowledge of the target's maximal maneuvering capability.

- **Finite-time guidance laws**. In addition to classical PN, SMC guidance laws [61,89] are capable of achieving intercept in finite time, but only a few in *prescribed time* [89]. Furthermore, it appears that none of the existing SMC guidance laws can prescribe the convergence time without utilizing the initial conditions in the implementation, which in practice are not known perfectly. Some of the most-cited journal articles on SMC missile guidance are [39, 61, 81].

3.7.3 Current challenges

According to the survey text of recent advances in missile guidance, control, and estimation by Balakrishnan, Tsourdos, and White [91], some of the current major challenges in tactical missile guidance design are the following:

1. Intercepting highly-maneuverable targets moving at high speeds (i.e., for theater ballistic missile defense)

2. Robustness to missile plant model uncertainties due to an increasing flight domain

3. Incorporating the knowledge of maneuvering capabilities of particular threats into the guidance law

4. Designing missile autopilots that use more than one type of divert mechanism (e.g., aerodynamic surfaces and hot-gas thrusters) to work in different flight regimes, since they can exert disturbances against one another

3.8 Proofs of results

Some of the proofs in this section require additional notation. We denote the Euclidean 2-norm of an n element vector of real elements x as $|x| = \left(x^T x\right)^{1/2}$, the induced 2-norm of an $m \times n$ matrix of real elements A by $|A| = [\overline{\lambda}(A^T A)]^{1/2}$, where $\overline{\lambda}(\cdot)$ denotes the maximum eigenvalue of a matrix, and the induced ∞-norm of A by $|A|_\infty = \max_i \sum_{j=1}^{n} |a_{ij}|$, where a_{ij} is the element of A in the i^{th} row and j^{th} column.

3.8.1 Proof of Theorem 3.1

In the NCC, PN guidance can be expressed as

$$a_M(t) = N' V_{cl} \frac{d}{dt} \left(\frac{y(t)}{r(t)} \right). \tag{3.30}$$

Assuming a non-maneuvering target, the engagement kinematics (3.8) reduce to

$$\ddot{y}(t) = -N' V_{cl} \frac{d}{dt} \left(\frac{y(t)}{r(t)} \right). \tag{3.31}$$

Integration of (3.31) gives

$$\begin{aligned} \dot{y}(t) + \left(\frac{N' V_{cl}}{r(t)} \right) y(t) &= \dot{y}_0 + N' V_{cl} \frac{y_0}{r_0} \\ &=: C, \end{aligned} \tag{3.32}$$

which is a first-order linear, ordinary differential equation (ODE) for $y(t)$. We solve it by multiplying both sides by an integrating factor and then integrating. The integrating factor is

$$\begin{aligned} I(t) &= \mathrm{e}^{\int_{t_0}^{t} \frac{N' V_{cl}}{r(\tau)} d\tau} \\ &= \mathrm{e}^{\int_{t_0}^{t} \frac{N' V_{cl}}{r_0 - V_{cl}(\tau - t_0)} d\tau} \\ &= \mathrm{e}^{\ln \left(\frac{r_0}{r_0 - V_{cl}(t - t_0)} \right)^{N'}} \\ &= \left(\frac{r_0}{r_0 - V_{cl}(t - t_0)} \right)^{N'}. \end{aligned} \tag{3.33}$$

Multiplying (3.32) by $I(t)$ gives

$$\frac{d}{dt}\left[I(t)y(t)\right] = \left(\frac{r_0}{r_0 - V_{cl}(t-t_0)}\right)^{N'} C, \tag{3.34}$$

and then integration results in

$$y(t) = y_0 \left(\frac{r_0 - V_{cl}(t-t_0)}{r_0}\right)^{N'} + \left(\frac{r_0 - V_{cl}(t-t_0)}{r_0}\right)^{N'} \int_{t_0}^{t} \left(\frac{r_0}{r_0 - V_{cl}(\theta - t_0)}\right)^{N'} C d\theta. \tag{3.35}$$

For any constant C, integration by substitution shows that

$$\int_{t_0}^{t} \left(\frac{r_0}{r_0 - V_{cl}(\theta - t_0)}\right)^{N'} C d\theta = -\frac{C}{V_{cl}(1-N')} \left(\frac{r_0}{r(t)}\right)^{N'} r(t) + \frac{C r_0}{V_{cl}(1-N')}, \tag{3.36}$$

where the integration requires $N' \neq 1$. Using this fact, after substituting in $C = \dot{y}_0 + N' V_{cl} \frac{y_0}{r_0}$ from (3.32) and reducing through algebra, we find the solution to $y(t)$ is

$$y(t) = \frac{1}{1-N'} \left(\frac{r(t)}{r_0}\right) \left(\left[y_0 + \frac{r_0}{V_{cl}} \dot{y}_0 \right] \left(\frac{r(t)}{r_0}\right)^{N'-1} - N' y_0 - \frac{r_0}{V_{cl}} \dot{y}_0 \right). \tag{3.37}$$

The solution is verified by first differentiating to find $\dot{y}(t)$

$$\dot{y}(t) = \frac{1}{1-N'} \left(\left[-\frac{N' V_{cl}}{r_0} y_0 - N' \dot{y}_0 \right] \left(\frac{r(t)}{r_0}\right)^{N'-1} + \frac{N' V_{cl}}{r_0} y_0 + \dot{y}_0 \right), \tag{3.38}$$

and then substituting $y(t)$ and $\dot{y}(t)$ back into (3.32).

It is more convenient to express the solutions for $y(t)$, $\dot{y}(t)$ in matrix form. For a general linear time varying system with state $x(t)$ and input $u(t)$,

$$\dot{x}(t) = \mathscr{A}(t)x(t) + \mathscr{B}(t)u(t), \tag{3.39}$$

the general solution is provided by the *variation of parameters* formula,

$$x(t) = \Phi(t,t_0)x(t_0) + \int_{t_0}^{t} \Phi(t,\theta)\mathscr{B}(\theta)u(\theta)d\theta, \tag{3.40}$$

where $x(t_0)$ is the initial condition of the state, and $\Phi(t,t_0)$ is the *state transition matrix*, which is defined as the matrix that satisfies

$$\frac{d}{dt}\Phi(t,t_0) = \mathscr{A}(t)\Phi(t,t_0), \tag{3.41a}$$

$$\Phi(t_0,t_0) = I. \tag{3.41b}$$

For the state $x(t) = \begin{bmatrix} y(t) & \dot{y}(t) \end{bmatrix}^T$, we have already found $\Phi(t,t_0)$ by solving the first-order ODE (3.32). For notational convenience, we factor out the $\frac{1}{1-N'}$ and rewrite the state transition matrix as

$$\Phi(t,t_0) = \frac{1}{1-N'}\Psi(t,t_0), \tag{3.42}$$

where $\Psi(t,t_0)$ is the state transition matrix that satisfies

$$\frac{d}{dt}\Psi(t,t_0) = \mathscr{A}(t)\Psi(t,t_0), \tag{3.43a}$$

$$\Psi(t_0,t_0) = (1-N')I. \tag{3.43b}$$

Then by inspection of (3.37) for $y(t)$ and (3.38) for $\dot{y}(t)$, the elements of $\Psi(t,t_0)$ are obtained, and the theorem is proved. ■

3.8.2 Proof of Corollary 3.1

The proof follows by inspection of the solution of $x(t)$. As $t \to t_0 + t_f$, $r(t) \to 0$. Then for any integer M, $(r(t)/r_0)^M \to 0$. So as $t \to t_0 + t_f$, $y(t) \to 0$, and $\dot{y}(t) \to \frac{1}{1-N'}\left(\frac{N'V_{cl}y_0}{r_0} + \dot{y}_0\right)$. ■

3.8.3 Proof of Corollary 3.2

From (3.20) we have

$$\begin{aligned} |x(t)| &\leq \left|\frac{1}{1-N'}\right| |\Psi(t,t_0)||x(t_0)| \\ &\leq \frac{\sqrt{2}}{|1-N'|}|\Psi(t,t_0)|_\infty |x(t_0)|. \end{aligned} \tag{3.44}$$

Using (3.22)–(3.25), we obtain

$$|\Psi(t,t_0)|_\infty \leq \max\left\{N'\left(\frac{1}{t_f}+1\right)-1, N'+t_f\right\}, \tag{3.45}$$

which is always bounded for finite N' and t_f. Since $|\Psi(t,t_0)|_\infty$ is bounded for all $t \in [t_0, t_0+t_f)$, $x(t)$ remains bounded, so $x = 0$ is stable for all $t \in [t_0, t_0+t_f)$. Since the bound (3.44) is true for any initial state, the stability is global, and since (3.45) is independent of t_0, the stability is also uniform.

■

3.8.4 Proof of Corollary 3.3

The proof follows from (3.20) and (3.28) by simple application of the variation of parameters formula. ■

3.9 Acknowledgement

The theorem, corollaries, and proofs pertaining to Proportional Navigation in Chapter 3 first appeared in a paper by Prof. Krstic and myself, which was published as “Predictor observers for Proportional Navigation systems subjected to seeker delay,” *IEEE Transactions on Control Systems Technology*, 24(6), 2002–2015, 2016.

Part II

Prescribed-Time Stabilization and Estimation for Linear Systems

Chapter 4

Prescribed-Time Stabilization

We introduce two prescribed-time controllers for nonlinear systems in the normal form which employ time-varying gains that go to infinity as time approaches a fixed time prescribed by the user. When the uncertain nonlinearity is absent, the normal form reduces to the controllable canonical form, and the "nominal" controller we develop exhibits the FT-GUAS property. When the uncertain nonlinearity is present, the "robust" controller we develop exhibits the FT-ISS+C property. For both controllers, despite the gains going to infinity, the magnitude of the overall control input remains finite.

The results of this chapter were obtained through a collaborative effort with Prof. Yongduan (David) Song, his student, Dr. Yujuan Wang, and Prof. Krstic in 2016, and were first published as "Time-varying feedback for regulation of normal-form nonlinear systems in prescribed finite time," *Automatica*, 83, 243–251, 2017 [33].

4.1 Introduction

4.1.1 Existing approaches to finite-time stabilization

For high-order nonlinear systems exhibiting non-parametric uncertainties and unknown time-varying control gains, the goal of achieving asymptotic stabilization imposes daunting technical challenges. Therefore, it may seem ambitious to pursue stabilization for such systems in finite time. In fact, the problem of global and continuous finite-time, full-state stabilization for high-order uncertain systems has so far remained "uncharted territory."

Due to the appealing features associated with finite-time convergence, such as stronger robustness and faster disturbance rejection [31], finite-time control has received increasing attention from the control community during the past decades, and there now exists a rich collection of finite-time stabilization results published in the literature [6], [5], [37], [34], [35], [96], [72], [30], [55], [70], [104], [75], [19].

Almost all of the existing finite-time control results available in the literature are derived from what is referred to as the "Lyapunov differential inequality" established in [6]. For instance, by using this inequality, together with other conditions, C^0 finite time stabilizing state feedback control is derived for the double integrator in [5]. In [37] a finite time output feedback controller for the double integrator was proposed, and also by output feedback the global finite-time stabilization for a class of planar systems was addressed in [72], again based on this inequality. Continuous state feedback finite time control for the triangular systems and certain class of nonlinear systems was also developed in [30], [34], [35], [96] by combining the inequality with the homogeneous systems theory. All these results are local because of the use of the homogeneous approximation. In the work [55] global finite-time stabilization of the strict feedback systems by continuous state feedback is proposed; in [70] a Lyapunov function design providing a finite-time convergence was discussed, in which a sign function based (discontinuous) controller was developed; in [104] a non-singular terminal sliding mode finite time controller was employed for the robot systems; a global finite-time observer was established in [75] for nonlinear systems that are uniformly observable and globally Lipschitzian; based on Implicit Lyapunov Functions (ILF) approach, finite-time and fixed-time stability analysis for a chain of integrators were presented in [19]; and in [95], [18], [53], the idea of finite control has been extended to address finite-time consensus or containment of multiple agent systems governed by single or double integrators, where the Lyapunov differential inequality plays a crucial role in control development and stability analysis.

Another technique used in most existing finite time control results is the inclusion of "adding a power integrator" [55], [18], [53], [94], [45] in the Lyapunov function candidate. This addition, however, is both a blessing and a curse; it allows for finite-time control to be developed for high-order systems; but at the same time, adding a power itegrator is demanding both in terms of designing and implementing the control schemes.

Furthermore, in most existing finite time control algorithms, the fractional power state feedback of the form $x^{\frac{l}{p}}$ (with x being system state and p and l being some positive odd integers) has been commonly used [6], [5], [37], [34], [35], [96], [72], [30], [55], [104], [75], [95], [18], [53], [94], [45], which, unfortunately, not only makes control design and stability analysis complicated, but also renders the control action non-smooth due to $0 < l/p < 1$, yet such type of control can only address the case of unknown but constant gains in second-order mechanical systems [94] or high-order systems with known (unit) control gains [34], [35], [96], [55], [75], [19]. Thus far, all the finite time control methods are based on the principle of fractional power state feedback, and the territory of smooth finite time control for high-order nonlinear systems with unknown and time-varying control gains remains underexplored.

4.1.2 Problem statement

In this chapter, we consider nonlinear systems which are *full-state linearizable* by a diffeomorphic transformation, i.e., the *normal form* (see Section 2.1.3),

$$\begin{aligned} \dot{x}_q(t) &= x_{q+1}(t), \quad q = 1, \ldots, n-1 \\ \dot{x}_n(t) &= f(x,t) + b(x,t)u(t). \end{aligned} \tag{4.1}$$

Here, $x(t) = [x_1(t), \cdots, x_n(t)]^T$ is the state, $u(t) \in \mathbb{R}$ is the control input, $b(x,t) : \mathbb{R}^{n+1} \times \mathbb{R} \to \mathbb{R}$ is the input coefficient, which is possibly uncertain, and $f(x,t) : \mathbb{R}^{n+1} \times \mathbb{R} \to \mathbb{R}$ denotes the system nonlinearity which could include parametric uncertainties and external disturbances.

We invoke the following assumptions for the analysis of this chapter.

Assumption 4.1 (Global controllability). *There exists a known* $\underline{b} \neq 0$ *(and, without loss of generality,* $\underline{b} > 0$*) such that* $\underline{b} \leq |b(x,t)| < \infty$ *for all* $x \in \mathbb{R}^n, t \in \mathbb{R}_+$.

Assumption 4.2. (Bound on matched but possibly nonvanishing uncertainty) *The nonlinearity* f *obeys*

$$|f(x,t)| \leq d(t)\psi(x), \tag{4.2}$$

where $d(t)$ *is a disturbance with an unknown bound*

$$\|d\|_{[t_0,t]} := \sup_{\tau \in [t_0,t]} |d(\tau)|, \tag{4.3}$$

and $\psi(x) \geq 0$ *is a known scalar-valued continuous function.*

4.1.3 Design approach (a scalar example)

To illustrate our design approach, we first consider the following first-order system,

$$\dot{x}(t) = b(x,t)u(t) + f(x,t), \quad x_0 = x(t_0) \tag{4.4}$$

where $x(t) \in \mathbb{R}$ and $u(t) \in \mathbb{R}$ are the system state and control input, respectively. We assume that there exists a known constant $\underline{b}$ such that $0 < \underline{b} \leq b(\cdot)$ for all $t \geq 0$ and $x \in \mathbb{R}$ and that the system nonlinearity obeys

$$|f(x,t)| \leq d(t)\psi(x), \tag{4.5}$$

where $d(t)$ is a disturbance with an unknown bound and $\psi(x) \geq 0$ is a known continuous function.

Our prescribed-time controller design is based on using $\mu_C(t-t_0,T)$ to implement the prescribed-time scaling transformation

$$w(t) = \mu_C(t-t_0,T)x(t), \tag{4.6}$$

which has the trivial inverse

$$x(t) = \frac{1}{\mu_C(t-t_0,T)}w(t) \tag{4.7}$$

Notice that if the dynamics of $w(t)$ can be stabilized (i.e., at least kept finite), then since $\mu_C(t-t_0,T) \to \infty$ as $t \to t_0+T$, we will obtain $x(t) \to 0$ as $t \to t_0+T$, i.e., in a time T that is prescribed by the user. With this transformation, the original dynamic model (4.4) is converted into

$$\begin{aligned} \dot{w} &= \mu_C\dot{x} + \dot{\mu}_C x \\ &= \mu_C\left(bu + f + \frac{\dot{\mu}_C}{\mu_C}x\right). \end{aligned} \tag{4.8}$$

A feedback law for the scalar case is captured in the following theorem, which guarantees both the stabilization of this w-system and of the original x-system.

Theorem 4.1. *The system (4.4) with the controller*

$$u = -\frac{1}{\underline{b}}\left(k + \lambda\psi(x)^2 + \frac{1+m_C}{T}\right)\mu_C(t-t_0,T)x, \tag{4.9}$$

where $k,\lambda > 0$, is FT-ISS+C and

$$|x(t)| \leq \nu(t-t_0,T)^{1+m_C}\left(\zeta_C(t-t_0,T)^k|x(t_0)| + \frac{\|d\|_{[t_0,t]}}{2\sqrt{k\lambda}}\right) \tag{4.10}$$

for all $t \in [t_0, t_0+T)$, which means, in particular, that stabilization is achieved within the prescribed time T. Furthermore, the control input remains uniformly bounded over $[t_0, t_0+T)$.

Since the control gains go to infinity, it is a remarkable fact that the magnitude of the overal control feedback remains finite. In the next section, we extend these design ideas to achieve similar results for higher-order systems.

4.2 Results

This section summarizes our main results pertaining to our prescribed-time controllers. For easier readability, the proofs are provided later in Section 4.5.

We denote by $\mu_C^{(k)}$ $(k = 0,\ldots,n)$ the kth derivative of $\mu_C(t-t_0,T)$, with $\mu_C^{(0)} = \mu_C$, and denote by μ_C^l the lth power of $\mu_C(t-t_0,T)$. By taking the derivatives of $\mu_C(t-t_0,T)$ successively, we get

$$\mu_C^{(k)} = \frac{(n+m_C+k-1)!}{T^k(n+m_C-1)!}\mu_1^{n+m_C+k}, \quad k = 1,\ldots,n, \tag{4.11}$$

where μ_1 is as defined in (2.41). The integral of $\mu_C(t-t_0,T)$, to be used later, is

$$\int_{t_0}^{t}\mu_C(\tau-t_0,T)d\tau = \frac{T}{n+m_C-1}(\mu_1(t-t_0,T)^{n+m_C-1} - 1). \tag{4.12}$$

4.2.1 Finite-time Lyapunov inequality

Our first main result for prescribed-time stabilization is a lemma originally obtained to aid in the design of stabilizing controllers, which as it turns out, is applicable for many problems considering the Lyapunov-like stability of systems in finite time. This result was obtained by Yujuan Wang and David Song [33].

Lemma 4.1. *Consider the function $\mu_C(t-t_0,T)$ defined by (2.43), with positive integers m_C, n. If a continuously differentiable function $V:[t_0,t_0+T)\to[0,+\infty)$ satisfies*

$$\dot{V}(t) \leq -2k\mu_C(t-t_0,T)V(t) + \frac{\mu_C(t-t_0,T)}{4\lambda}d(t)^2 \tag{4.13}$$

for positive constants k and λ, then

$$V(t) \leq \zeta_C(t-t_0,T)^{2k}V(t_0) + \frac{||d||^2_{[t_0,t]}}{8k\lambda}, \quad \forall t \in [t_0,t_0+T), \tag{4.14}$$

where $\zeta_C(t-t_0,T)$ is the monotonically decreasing, smooth "bump-like" (Fry & McManus [24]) function.

Corollary 4.1. *Under the conditions of Lemma 4.1, if $d(t)=0$, then $\lim_{t\to t_0+T}V(t)=0$.*

Corollary 4.1 is a time-varying, fixed-time counterpart of the basic non-smooth finite-time result of Theorem 4.2 by Bhat and Bernstein [6], whereas Lemma 4.1 is a time-varying finite-time counterpart of the robustness result in Theorem 5.2 by Bhat and Bernstein [6].

4.2.2 Prescribed-time coordinate transformations

In order to stabilize the system (4.1) in prescribed time, we employ a higher-order version of the transformation (4.6) by using the scaling function $\mu_C(t-t_0,T)$ defined in (2.43) as follows,

$$\begin{aligned} w_1(t) &= \mu_C(t-t_0,T)x_1(t), \\ w_q(t) &= dw_{q-1}(t)/dt, \quad q=2,\cdots,n+1. \end{aligned} \tag{4.15}$$

We denote $w_{n+1} = \dot{w}_n$ and $x_{n+1} = \dot{x}_n$, with which we present the following two lemmas, whose proofs are provided later in Section 4.5.

Lemma 4.2. *Given integers $n \geq 1$ (the order of the system) and $m_C \geq 1$ (a design parameter), the transformation $x(t) \mapsto w(t)$ given by*

$$w(t) = \mu_1^{m_C+1} P_C(\mu_1) x(t), \tag{4.16}$$

where the matrix $P_C(\mu_1)$ is a lower triangular matrix having elements $\{p_{C_{ij}}\}$ given, for $i = 1, 2, \ldots, n$, and $j = 1, 2, \ldots, i$, as

$$p_{C_{ij}}(\mu_1) = \bar{p}_{C_{ij}} \mu_1^{n+i-j-1} \tag{4.17}$$

$$\bar{p}_{C_{ij}} = \begin{pmatrix} i-1 \\ i-j \end{pmatrix} \frac{(n+m_C+i-j-1)!}{T^{i-j}(n+m_C-1)!}, \tag{4.18}$$

yields the system (4.15).

Lemma 4.3. *Given integers $n \geq 1$ (the order of the system) and $m_C \geq 1$ (a design parameter), the inverse of the transformation (4.16) is given by*

$$x(t) = \nu^{m_C+1} Q_C(\nu) w(t), \tag{4.19}$$

where the inverse matrix $Q_C(\nu) := P_C(\mu_1)^{-1}$ is a lower triangular matrix having elements $\{q_{C_{ij}}\}$ given, for $i = 1, 2, \ldots, n$, and $j = 1, 2, \ldots, i$, as

$$q_{C_{ij}}(\nu) = \bar{q}_{C_{ij}} \nu^{n+j-i-1} \tag{4.20}$$

$$\bar{q}_{C_{ij}} = \begin{pmatrix} i-1 \\ i-j \end{pmatrix} \frac{(-1)^{i-j}(n+m_C)!}{T^{i-j}(n+m_C+j-i)!}. \tag{4.21}$$

Furthermore, $\bar{q}_C = \sup_{\nu \in (0,1]} |Q_C(\nu)|$ is finite.

4.2.3 Synthesis

Define $r_1(t), r_2(t) \in \mathbb{R}^{n-1}$ such that

$$\begin{aligned} r_1(t) &= [w_1(t), \cdots, w_{n-1}(t)]^T \\ &= J_1 w(t) \end{aligned} \tag{4.22}$$

$$\begin{aligned} r_2(t) &= \dot{r}_1(t) \\ &= [w_2(t), \cdots, w_n(t)]^T \\ &= J_2 w(t), \end{aligned} \tag{4.23}$$

where

$$J_1 = \left[I_{n-1},\, 0_{(n-1)\times 1}\right], \quad J_2 = \left[0_{(n-1)\times 1},\, I_{n-1}\right], \tag{4.24}$$

and $K_{n-1} = [k_1, \cdots, k_{n-1}]^T \in \mathbb{R}^{n-1}$, where K_{n-1} is an appropriately chosen coefficient vector so that the polynomial $s^{n-1} + k_{n-1}s^{n-2} + \cdots + k_1$ and the matrix

$$\Lambda_C = \begin{bmatrix} 0 & & I_{n-2} & \\ -k_1 & -k_2 & \cdots & -k_{n-1} \end{bmatrix} \tag{4.25}$$

are both Hurwitz. Now we replace the state $w_n(t)$ by the new variable $z(t)$ as

$$z(t) = w_n(t) + K_{n-1}^T r_1(t), \tag{4.26}$$

This then results in

$$\dot{r}_1(t) = \Lambda_C r_1(t) + \mathrm{e}_{n-1} z(t), \tag{4.27}$$

where $\mathrm{e}_{n-1} = [0, \cdots, 0, 1]^T \in \mathbb{R}^{n-1}$. Before proceeding, note that the linear system (4.27) is ISS, i.e., there exist positive constants M_1, δ_1, γ_1 such that

$$|r_1(t)| \le M_1 \mathrm{e}^{-\delta_1(t-t_0)} |r_1(t_0)| + \gamma_1 \|z\|_{[t_0, t_0+T)}, \quad t \in [t_0, t_0+T), \tag{4.28}$$

because we will use this later.

The derivative of the new state (4.26) is

$$\dot{z}(t) = \dot{w}_n(t) + K_{n-1}^T J_2 w(t), \tag{4.29}$$

which, by substitution of $\dot{w}_n(t) = w_{n+1}(t)$, $\dot{x}_n(t) = x_{n+1}(t)$ and then (4.48), and writing out the $k = 0$ term from the sum, yields

$$\begin{aligned}\dot{z}(t) &= \mu_C(t-t_0,T)(\dot{x}_n(t) + L_0(t) + L_1(t)) \\ &= \mu_C(t-t_0,T)(b(x,t)u(t) + f(x,t) + L_0(t) + L_1(t))\end{aligned} \tag{4.30}$$

with

$$L_0(t) := \sum_{k=1}^{n} \begin{pmatrix} n \\ k \end{pmatrix} \frac{\mu_C^{(k)}(t-t_0,T)}{\mu_C(t-t_0,T)} x_{n+1-k}(t), \tag{4.31}$$

$$L_1(t) := \nu^{n+m_C} K_{n-1}^T J_2 w(t). \tag{4.32}$$

To aid in the stability analysis, we express the quantity $L_0(t)$ in terms of $w(t)$, as captured in the next lemma.

Lemma 4.4 ($L_0(t)$ in terms of $w(t)$). *Given integers $n \geq 1$ (the order of the system) and $m_C \geq 1$ (a design parameter), the quantity L_0 is expressed as*

$$L_0(t) = \nu^{m_C} l_0(\nu) w(t), \tag{4.33}$$

where $l_0(\nu) = [l_{0,1}, l_{0,2}, \ldots, l_{0,n}]$, and for $j = 1, 2, ..., n$,

$$l_{0,j}(\nu) = \bar{l}_{0,j} \nu^{j-1} \tag{4.34}$$

with

$$\bar{l}_{0,j} = \frac{n+m_C}{T^{n+1-j}} \sum_{i=0}^{n-j} \begin{pmatrix} n \\ n-i-j+1 \end{pmatrix} \begin{pmatrix} i+j-1 \\ i \end{pmatrix} \frac{(-1)^i (2n+m_C-i-j)!}{(n+m_C-i)!}. \tag{4.35}$$

Furthermore, $l_0(\nu)$ is bounded.

4.2.4 Prescribed-time (nominal) stabilization for uncertainty-free systems

We consider the normal-form system (4.1), and first present a simpler, "nominal" contoller design for the case where the functions $b(x,t)$ and $f(x,t)$ are known.

Theorem 4.2. *The system (4.1) with the controller*

$$u(t) = -\frac{1}{b(x,t)}\big(f(x,t)+L_0(t)+L_1(t)+kz(t)\big), \tag{4.36}$$

has a FT-GUAS equilibrium at the origin, with a prescribed convergence time T, and there exist $\tilde{M}, \tilde{\delta} > 0$ such that

$$|x(t)| \leq \nu(t-t_0,T)^{m_C+1}\tilde{M}\mathrm{e}^{-\tilde{\delta}(t-t_0)}\,|x(t_0)| \tag{4.37}$$

for all $t \in [t_0, t_0+T)$. Furthermore, the control $u(t)$ remains uniformly bounded over $[t_0, t_0+T)$ and, if $f(x,t)$ is vanishing at $x=0$, $u(t)$ also converges to zero as $t \to t_0+T$.

4.2.5 Prescribed-time (robust) stabilization for uncertain systems

In most applications, the ideal dynamical behavior characterized by system (4.1) when $b(x,t)$ and $f(x,t)$ are known perfectly is too restrictive, for there exist either unknown nonlinearities, or, at a minimum, matched uncertainties in the nonlinearities of the system. For such systems, the following controller may be more suitable than the one provided by Theorem 4.2.

Theorem 4.3. *Under Assumptions 4.1 and 4.2, consider the system (4.1) with the controller*

$$u(t) = -\frac{1}{\underline{b}}\left(k+\theta+\lambda\,\psi(x)^2\right)z(t), \tag{4.38}$$

where $z(t)$ is defined via (4.26), (4.22), and Lemma 4.4 as

$$\begin{aligned} z(t) &= \mu_1(t-t_0,T)^{m_C+1}K_+^T P(\mu_1(t-t_0,T))x(t) && (4.39)\\ K_+^T &= [k_1,\ldots,k_{n-1},1]^T. && (4.40)\end{aligned}$$

If the control gains are chosen such that $\rho, k, \lambda > 0$,

$$\rho k > \gamma_1/4, \tag{4.41}$$

where γ_1, defined in (4.76), depends on the choice of the gain vector K_{n-1} in (4.25) and (4.27), and where $\theta \geq \theta_*$ and

$$\theta_* = k_{n-1} + \bar{l}_{0,n} + \rho \max_{\nu\in[0,1]}\left|\left(\nu^n K_{n-1}^T J_2 + l_0(\nu)\right)\left(J_1^T - \mathrm{e}_n K_{n-1}^T\right)\right|^2, \tag{4.42}$$

then the closed-loop system (4.1) with (4.38) is FT-ISS-C, and there exist $\check{M}, \check{\delta}, \check{\gamma}$ such that

$$|x(t)| \leq \nu(t-t_0,T)^{m_C+1}\left(\check{M}\mathrm{e}^{-\check{\delta}(t-t_0)}\,|x(t_0)| + \check{\gamma}\|d\|_{[t_0,t]}\right) \tag{4.43}$$

for all $\forall t \in [t_0, t_0+T)$. Furthermore, the control $u(t)$ remains uniformly bounded over $[t_0, t_0+T)$.

4.3 Discussion

4.3.1 Merits of the design approach

We emphasize three aspects of the design approach presented: *1)* its finite-time stabilization capability, *2)* its robustness to both non-vanishing disturbances and to the uncertain input coefficient, and *3)* the implications of employing a gain that grows unbounded.

1) Finite-time stabilization: We have shown that the finite-time stabilization demonstrated here is the result of employing the gain $\mu_C(t-t_0,T)$, defined in (2.43) and growing to infinity, inside the control law (4.9). The design is based on the scaling transformation (4.16), followed by a stabilizing control design for the scaled system, (4.8). Employing a gain that goes to infinity seems counterintuitive—are we achieving finite-time regulation by employing control inputs that go to infinity? Are we achieving a strong result at an exorbitant price? The answer is no. As illustrated by (4.9) and (4.47), the product $\mu_C(t-t_0,T)x(t)$ in the control law is the scaled state $w(t)$, which is kept bounded. As $\mu_C(t-t_0,T)$ goes to infinity, $x(t)$ goes to zero, resulting in the boundedness of $w(t)$ and hence of $u(t)$. In the absence of uncertainty, the result achieved in (4.10) yields even more insight. Suppose, for simplicity of explanation, that the nonlinearities b and f in (4.4) are known, in which case the control would be chosen as $u(t) = -(1/b)\left[f + \left(k + \frac{1+m_C}{T}\nu(t-t_0,T)\right)\mu_C(t-t_0,T)x(t)\right]$ to result in the simple closed-loop system $\dot{w}(t) = -k\mu_C(t-t_0,T)w(t)$. The scaled state $w(t)$ is not only bounded, and not only convergent to zero in infinite time (exponentially), but in finite time T. This results in x going to zero in finite time T at a rate that is *not* (merely) polynomially fast, namely, at a rate dictated by $\nu(t-t_0,T)^{1+m_C}$, but at a rate that is *finite-time exponential* and governed by the function $\zeta_C(t-t_0,T) = \exp^{\frac{T}{m_C}\left(1-1/\nu(t-t_0,T)^{m_C}\right)}$, which is a function with a property that not only its value goes to zero in time T, but all of the function's derivatives are zero at the final time T. This means that $x(t)$ approaches zero not only at a fast rate but it "lands smoothly" at time T. This is captured in the theorem's estimate (4.10), which, when $d=0$, gives $|x(t)| \leq \nu(t-t_0,T)^{(1+m_C)}\zeta_C(t-t_0,T)^k|x(t_0)|$, which ensures global finite-time asymptotic stability with a smooth approach to zero as $t \to t_0+T$.

2) Robustness (to uncertainty in b and f): The control presented has not only the ability to maintain boundedness in the presence of a non-vanishing uncertainty, which would be captured by the property FT-ISS. This controller achieves the stronger property FT-ISS+C, guaranteeing that $x(t) \to 0$ in the presence of any non-vanishing uncertainty, even when its size $\|d\|_{[t_0,t]}$ is unknown. To see things more clearly, consider the special situation where $x_0 = 0$. In that case (4.10) would yield $|x(t)| \leq \nu(t-t_0,T)^{1+m_C}\frac{\|d\|_{[t_0,t]}}{2\sqrt{k\lambda}}$, ensuring that x is regulated to zero in T in the presence of a non-vanishing disturbance. This may be reminiscent of the capability of sliding mode control (which also employs a gain that goes to infinity as x reaches zero), but the result here is stronger. In standard sliding mode control a bound on $\|d\|_{[t_0,t]}$ would need to be known, whereas here it doesn't need to be known. The need to know such a bound is eliminated by employing the nonlinear damping component $\psi(x)^2\mu_C(t-t_0,T)x(t)$ in the controller (4.9). (A similar capability in sliding mode control would be achievable by feedback with a term $\psi(x)^2\mathrm{sgn}(x)$.)

3) The consequences of employing a gain that grows unbounded and its necessity for stabilization in prescribed finite time: There are possible concerns about the implementation of feedback that contains a gain that goes to infinity. Even though, ideally, the product $\mu_C(t-t_0,T)x(t)$ of two signals, the latter of which goes to zero, while the former goes to infinity, is bounded, problems may arise either when there is noise in the measurement of $x(t)$, resulting in a product of a gain $\mu_C(t-t_0,T)$ that grows unbounded, while $x(t)$ doesn't decay fully to zero, or in the computation of the feedback $\mu_C(t-t_0,T)x(t)$, where a multiplication of very large and very small values creates numerical problems.

Such problems can be addressed in multiple ways. One way is employing a deadzone on $x(t)$. This approach would somewhat sacrifice the asymptotic performance—the stabilization would not be to zero but to a small set near zero. Another way is by setting T in the gain $\mu_C(t-t_0,T)$ to a larger value than the desired finite time of stabilization, which would prevent the gain from becoming infinite over the desired stabilization time but, again, with some sacrifice on the stabilization accuracy ($x(t)$ would only be stabilizated *near* zero). Estimates of the residual sets for $x(t)$ could be provided for both of these "compromise" solutions to the potential problems arising from employing a gain that grows large near the terminal time T.

The "high-gain challenge" in this time-varying approach should be contrasted with the challenge of employing discontinuous feedback in the standard sliding mode setting or non-smooth feedback in related approaches. In such approaches the gain similarly becomes infinite near $x = 0$ and the problem manifests itself through chattering in "long-time" applications. The approach that we present here is specifically intended for finite-time feedback problems, which arise in a number of applications, and the concern arises only at the terminal time, with viable ways to address it discussed above.

It should be understood that any approach that is geared towards regulation in *prescribed* finite time, including finite-horizon optimal control with a *terminal constraint*, inevitably yields gains that go to infinity. So, the "high-gain challenge" is not particular to the approach presented here. The advantage of the present approach is its simplicity, transparency, and explicitness, both in terms of the feedback that needs to be implemented, and in terms of the convergence estimates provided.

4.3.2 Comparison with other finite-time designs

Our time-varying finite-time design is another option in the control designer's toolbox and we do not claim its superiority with respect to the existing designs. What is more important is to understand the conceptual tradeoffs.

Most existing results on finite-time regulation employ non-smooth feedback and are often based on first order systems [95], [30]. The guaranteed finite time of regulation, $T^* \leq \frac{V(x(t_0))^{1-\alpha}}{c(1-\alpha)}$, grows with the size of the initial condition. Furthermore, for high order systems, most existing results, including, in particular, [55], [18], [53], [94], [45], use the "adding a power integrator" approach of the form $W_j(x_1,\cdots,x_j) = \int_{x_j^*}^{x_j}\left(\tau^{\frac{1}{q_j}} - x_j^{*\frac{1}{q_j}}\right)^{1+h-q_j} d\tau$, where $j = 2,\cdots,n$ and $h = (2n-1)/(2n+1)$. In these non-smooth approaches, if a specific T is required, one has to seek the required values of α, c, and other design parameters, which are hard to find because they are coupled implicitly through various bounds.

The proposed time-varying method does not involve those difficulties and achieves stabilization in prescribed time T using feedback that explicitly depends on T.

4.4 Examples

We provide two examples to illustrate our proposed approach to prescribed-time stabilization through numerical simulation.

Example 4.1. Consider the double integrator with no disturbance,

$$\dot{x}_1(t) = x_2(t),$$

$$\dot{x}_2(t) = u(t).$$

Since $b(x,t) = 1$ and $f(x,t) = 0$, we employ the nominal controller of Theorem 4.2. Using (4.26), (4.31), (4.32), and Lemmas 4.3 and 4.4, we find the state feedback controller (4.36) to be

$$u(t) = -\kappa(t-t_0,T)^T x(t)$$

where $\kappa(t-t_0,T) := [\kappa_1(t-t_0,T), \kappa_2(t-t_0,T)]^T$, and

$$\kappa_1(t-t_0,T) = k_1\frac{m_C+2}{T}\mu_1 + \frac{(m_C+3)(m_C+2)}{T^2}\mu_1^2 + k_1k_2\mu_1^{m_C+2} + k_2\frac{m_C+2}{T}\mu_1^{m_C+3}$$
$$\kappa_2(t-t_0,T) = k_1 + 2\frac{m_C+2}{T}\mu_1 + k_2\mu_1^{m_C+2}.$$

Simulation of the system for three sets of initial conditions is shown in Figures 4.1 and 4.2. Figure 4.1 shows time histories for the state variables, and Figure 4.2 shows time histories of the control gains $\kappa_1(t-t_0,T)$, $\kappa_2(t-t_0,T)$, and overall control input $u(t)$. For these simulations, we set $t_0=0$, $T=11$, $k_1=k_2=1$, and $m_C=1$. We see that for all three sets of initial conditions, the states are stabilized to zero by the prescribed time $T=11$, and despite the time-varying control gains going to infinity, the overall control input remains bounded and even goes to zero smoothly as $t \to t_0+T$.

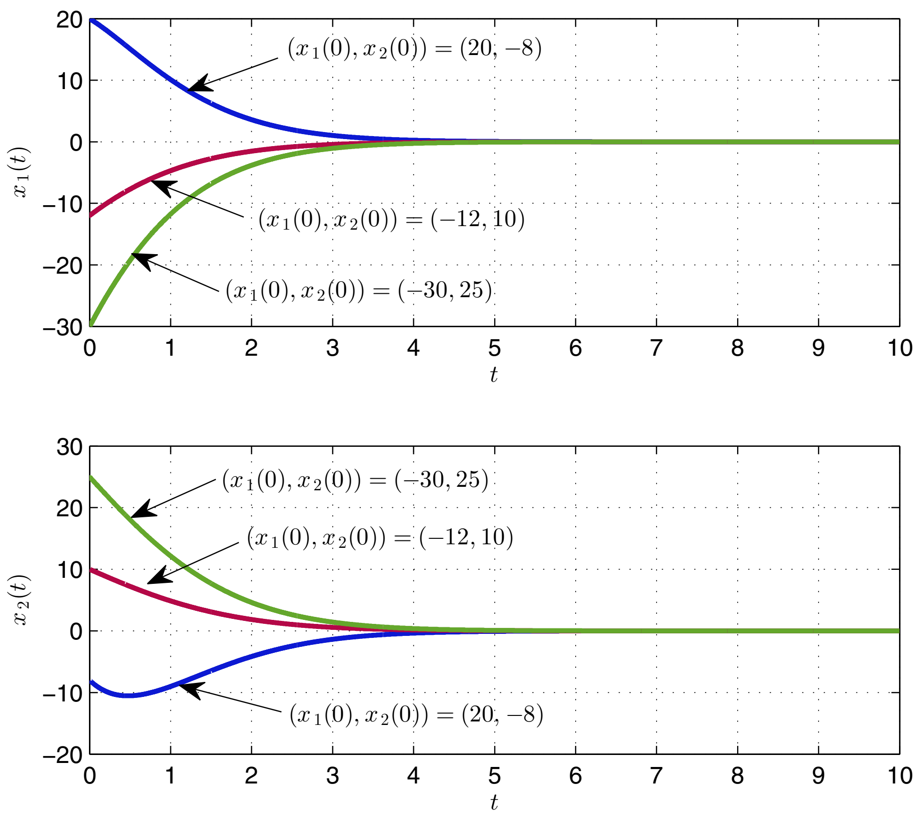

Figure 4.1: Time histories of states resulting from application of the nominal controller in Example 4.1, for three sets of initial conditions.

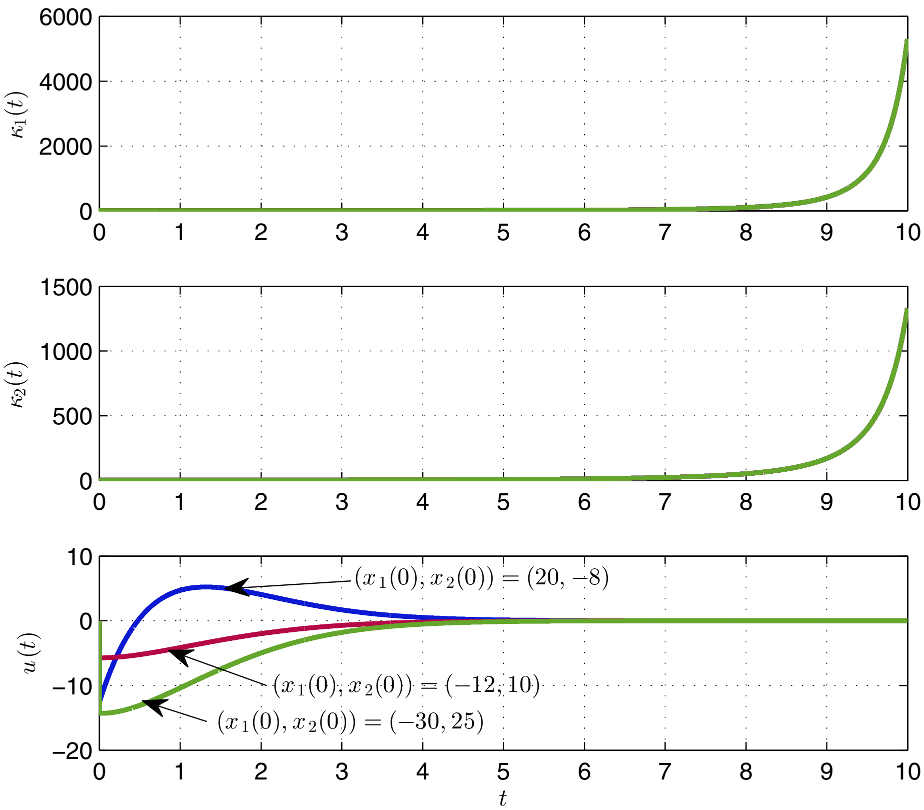

Figure 4.2: Time histories of control gains and overall control input resulting from application of the nominal controller in Example 4.1, for three sets of initial conditions.

Example 4.2. Consider the system

$$\dot{x}_1 = x_2,$$

$$\dot{x}_2 = b(x,t)u + f(x,t),$$

which describes wing-rock motion involving time-varying non-parametric and non-vanishing uncertain terms [57]. The nonlinear function is of the form $f(x,t) = a_0 + a_1(t)x_1 + a_2(t)x_2 + a_3|x_1|x_2 + a_4|x_2|x_2 + a_5x_1^3$ with $a_0 = 1$, $c_1 = 1$, $c_2 = 2$, $a_3 = 2$, $a_4 = 3$, and $a_5 = 1$, where $a_1(t) = c_1\cos(\omega_1 t)$ and $a_2(t) = c_2\sin(\omega_2 t)$, with ω_1 and ω_2 being two non-parametric constants. The time-varying uncertain control input coefficient is of the form $b(x,t) = 2 + 0.4\sin(t)$.

We employ the robust controller of Theorem 4.3 to stabilize the system within a desired time $t_f = 1$ for three sets of initial conditions. For these simulations, we selected $t_0 = 0$, $T = 1.2$, $m_C = 2$, $k_1 = 0.1$, $k = 2$, $\underline{b} = 1.6$, $\theta = 2$, and $\lambda_1 = 0.1$. Notice that in this example, we selected T to be slightly larger than the desired stabilization time of t_f in order to mitigate numerical instability near the terminal time of the simulation. The results are shown in Figure 4.3–Figure 4.5. We see in Figure 4.3 that for all three sets of initial conditions, the states are stabilized to the origin within the prescribed time $T = 1.2$, despite the presence of the time-varying disturbance shown in Figure 4.4 and the uncertain control input coefficient. The time-varying control gains and overal control input are shown in Figure 4.5. The latter remains uniformly bounded as proven in Theorem 4.3.

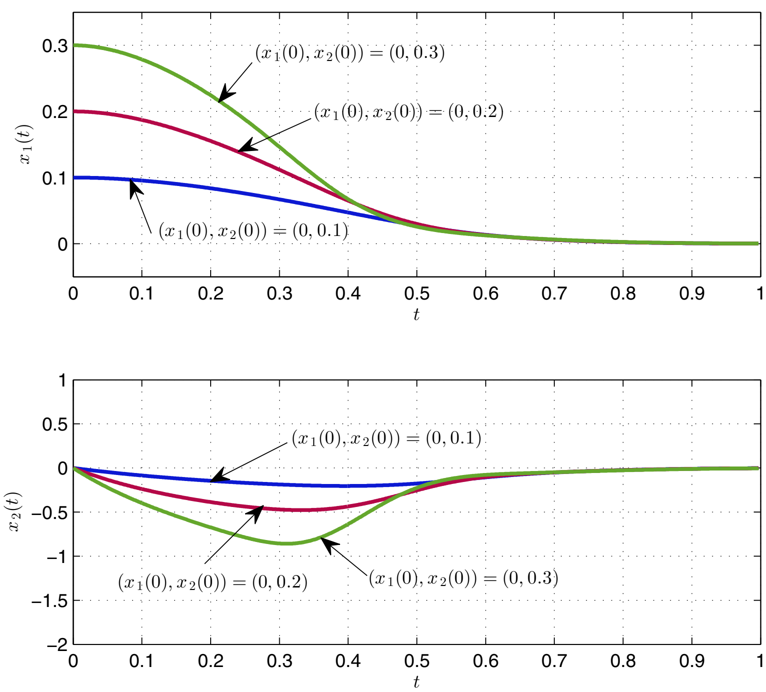

Figure 4.3: Time histories of states resulting from application of the robust controller in Example 4.2, for three sets of initial conditions.

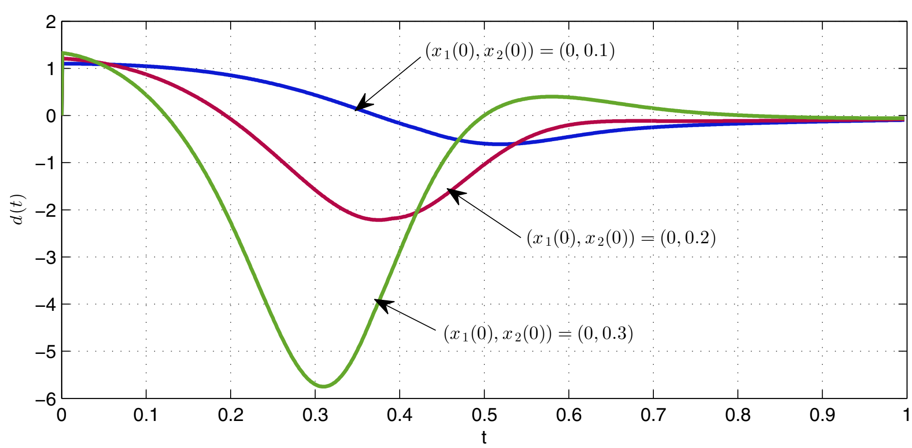

Figure 4.4: Time histories of the wing-rock disturbance in Example 4.2, for three sets of initial conditions.

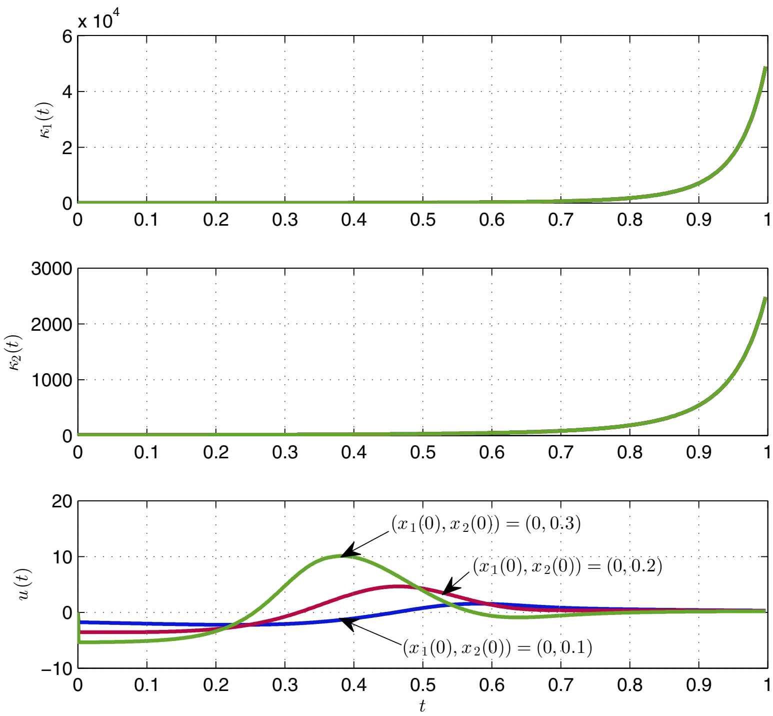

Figure 4.5: Time histories of control gains and overall control input resulting from application of the robust controller in Example 4.2, for three sets of initial conditions.

4.5 Proofs of results

4.5.1 Proof of Lemma 4.1

Solving the differential inequality (4.70) gives

$$V(t) \leq \exp^{-2k\int_{t_0}^{t}\mu_C(\tau-t_0,T)d\tau}V(t_0)+\frac{1}{4\lambda}\int_{t_0}^{t}\exp^{-2k\int_{\tau}^{t}\mu_C(s-t_0,T)ds}d(\tau)^2\mu_C(\tau-t_0)d\tau. \tag{4.44}$$

We then compute the second term in the right hand of (4.44) to obtain

$$\begin{aligned}
&\int_{t_0}^{t}\exp^{-2k\int_{\tau}^{t}\mu_C(s-t_0,T)ds}d(\tau)^2\mu_C(\tau-t_0,T)d\tau\\
&\leq \|d\|_{[t_0,t]}^2\int_{t_0}^{t}\exp^{2k\left(-\int_{t_0}^{t}\mu_C(s-t_0,T)ds+\int_{t_0}^{\tau}\mu_C(s-t_0,T)ds\right)}\mu_C(\tau-t_0,T)d\tau\\
&=\|d\|_{[t_0,t]}^2\exp^{-2k\int_{t_0}^{t}\mu_C(s-t_0,T)ds}\int_{t_0}^{t}\exp^{2k\int_{t_0}^{\tau}\mu_C(s-t_0,T)ds}d\left(\int_{t_0}^{\tau}\mu_C(s-t_0,T)ds\right)\\
&=\|d\|_{[t_0,t]}^2\exp^{-2k\int_{t_0}^{t}\mu_C(s-t_0,T)ds}\frac{1}{2k}\exp^{2k\int_{t_0}^{\tau}\mu_C(s-t_0,T)ds}\bigg|_{t_0}^{t}\\
&=\|d\|_{[t_0,t]}^2\exp^{-2k\int_{t_0}^{t}\mu_C(s-t_0,T)ds}\frac{1}{2k}\left(\exp^{2k\int_{t_0}^{t}\mu_C(s-t_0,T)ds}-1\right)\\
&=\|d\|_{[t_0,t]}^2\frac{1}{2k}\left(1-\exp^{-2k\int_{t_0}^{t}\mu_C(s-t_0,T)ds}\right)\\
&\leq\frac{\|d\|_{[t_0,t]}^2}{2k}.
\end{aligned}\tag{4.45}$$

According to

$$\int_{t_0}^{t}\mu_C(\tau-t_0,T)d\tau=\frac{T}{n+m_C-1}\left(\mu_1(t-t_0,T)^{n+m_C-1}-1\right), \tag{4.46}$$

with (4.65) and (4.45), we obtain

$$\begin{aligned}
V(t) &\leq \exp^{-2k\frac{T}{m_C+n-1}(\mu_1(t-t_0,T)^{m_C+n-1}-1)}V(t_0)+\frac{\|d\|_{[t_0,t]}^2}{8k\lambda}\\
&=\zeta_C(t-t_0,T)^{2k}V(t_0)+\frac{\|d\|_{[t_0,t]}^2}{8k\lambda}.
\end{aligned}\tag{4.47}$$

■

4.5.2 Proof of Lemma 4.2

Since $w_1 := \mu_C x_1$, the generalized Leibniz rule gives

$$\begin{aligned} w_{i+1} &= (\mu_C x_1)^{(i)} \\ &= \sum_{k=0}^{i} \begin{pmatrix} i \\ \\ k \end{pmatrix} \mu_C^{(k)} x_1^{(i-k)} \\ &= \sum_{k=0}^{i} \begin{pmatrix} i \\ \\ k \end{pmatrix} \mu_C^{(k)} x_{i+1-k}, \qquad i = 0, \ldots, n-1, n \end{aligned} \tag{4.48}$$

Shifting the i index gives

$$w_i = \sum_{k=0}^{i-1} \begin{pmatrix} i-1 \\ \\ k \end{pmatrix} \mu_C^{(k)} x_{i-k}, \quad i = 1, \ldots, n, n+1. \tag{4.49}$$

We next rewrite the summation using the substitution $j := i-k$, where $j = 1, 2, ...i$, and arrive at

$$w_i = \sum_{j=1}^{i} \begin{pmatrix} i-1 \\ \\ i-j \end{pmatrix} \mu_C^{(i-j)} x_j, \quad i = 1, \ldots, n, n+1. \tag{4.50}$$

Substituting in the expression for $\mu_C^{(i-j)}$ in (4.11) then results in

$$w_i = \mu_1^{n+m_C} \sum_{j=1}^{i} \begin{pmatrix} i-1 \\ \\ i-j \end{pmatrix} \frac{(n+m_C+i-j-1)!}{T^{i-j}(n+m_C-1)!} \mu_1^{i-j} x_j, \tag{4.51}$$

from which we find the elements $\{p_{C_{ij}}\}$ by inspection. ■

4.5.3 Proof of Lemma 4.3

Since $x_1 = \frac{1}{\mu_C} w_1$, the generalized Leibniz rule gives

$$\begin{aligned} x_{i+1} &= x_1^{(i)} \\ &= \left(\frac{1}{\mu_C} w_1 \right)^{(i)} \\ &= \sum_{k=0}^{i} \begin{pmatrix} i \\ k \end{pmatrix} \left(\frac{1}{\mu_C} \right)^{(k)} w_1^{(i-k)} \\ &= \sum_{k=0}^{i} \begin{pmatrix} i \\ k \end{pmatrix} \left(\frac{1}{\mu_C} \right)^{(k)} w_{i+1-k},\ i = 0, \ldots, n-1, n. \end{aligned} \tag{4.52}$$

Taking the k-th derivative of $1/\mu_C$, we have

$$\left(\frac{1}{\mu_C} \right)^{(k)} = \frac{(-1)^k (n+m_C)!}{T^k (n+m_C-k)!} \nu^{n+m_C-k}. \tag{4.53}$$

Substituting (4.53) into (4.52), we obtain

$$x_{i+1} = \nu^{n+m_C} \sum_{k=0}^{i} \begin{pmatrix} i \\ k \end{pmatrix} \frac{(-1)^k (n+m_C)!}{T^k (n+m_C-k)!} \nu^{-k} w_{i+1-k}, \quad i = 0, \ldots, n-1, n, \tag{4.54}$$

which after shifting the i index can be written as

$$x_i = \nu^{n+m_C} \sum_{k=0}^{i-1} \begin{pmatrix} i-1 \\ k \end{pmatrix} \frac{(-1)^k (n+m_C)!}{T^k (n+m_C-k)!} \nu^{-k} w_{i-k}. \tag{4.55}$$

We next rewrite the summation using the substitution $j := i-k$, where $j = 1, 2, ..., i$ to arrive at

$$x_i = \nu^{n+m_C} \sum_{j=1}^{i} \begin{pmatrix} i-1 \\ i-j \end{pmatrix} \frac{(-1)^{i-j} (n+m_C)!}{T^{i-j} (n+m_C+j-i)!} \nu^{j-i} w_j, \tag{4.56}$$

from which we find the elements $\{q_{C_{ij}}\}$ by inspection.

The finiteness of $\bar{q}_C$ follows from the fact that $|Q_C(\nu)|$ is a continuous function of a bounded argument $\nu \in (0, 1]$. ■

4.5.4 Proof of Lemma 4.4

By substituting in (4.52) for x_{n+1-k} in (4.31), we obtain

$$L_0 = \sum_{k=1}^{n} \begin{pmatrix} n \\ k \end{pmatrix} \frac{\mu_C^{(k)}}{\mu_C} \left[\sum_{i=0}^{n-k} \begin{pmatrix} n-k \\ i \end{pmatrix} \left(\frac{1}{\mu_C}\right)^{(i)} w_{n-k+1-i} \right]$$

$$= \sum_{k=1}^{n} \sum_{i=0}^{n-k} \begin{pmatrix} n \\ k \end{pmatrix} \begin{pmatrix} n-k \\ i \end{pmatrix} \frac{\mu_C^{(k)}}{\mu_C} \left(\frac{1}{\mu_C}\right)^{(i)} w_{n-k+1-i}. \tag{4.57}$$

The double sum can be viewed as the sum of function evaluations $f_{ki}(n)$ defined on a triangle in (k,i) space. Viewed this way, the terms in the double sum can be reordered according to

$$\sum_{k=1}^{n} \sum_{i=0}^{n-k} f_{ki}(n) = \sum_{i=0}^{n-1} \sum_{k=1}^{n-i} f_{ki}(n). \tag{4.58}$$

This allows us to write (4.57) as

$$L_0 = \sum_{i=0}^{n-1} \sum_{k=1}^{n-i} \begin{pmatrix} n \\ k \end{pmatrix} \begin{pmatrix} n-k \\ i \end{pmatrix} \frac{\mu_C^{(k)}}{\mu_C} \left(\frac{1}{\mu_C}\right)^{(i)} w_{n-k+1-i}. \tag{4.59}$$

Next define $j := n-k+1-i$, where $j = n-i, n-i-1, ..., 1$. Rewriting (4.59) in terms of j rather than k results in

$$L_0 = \sum_{i=0}^{n-1} \sum_{j=1}^{n-i} \begin{pmatrix} n \\ n-i-j+1 \end{pmatrix} \begin{pmatrix} i+j-1 \\ i \end{pmatrix} \frac{\mu_C^{(n-i-j+1)}}{\mu_C} \left(\frac{1}{\mu_C}\right)^{(i)} w_j. \tag{4.60}$$

We now reorder the double sum in (4.60) using (4.58) in reverse order to obtain

$$L_0 = \sum_{j=1}^{n} \sum_{i=0}^{n-j} \begin{pmatrix} n \\ n-i-j+1 \end{pmatrix} \begin{pmatrix} i+j-1 \\ i \end{pmatrix} \frac{\mu_C^{(n-i-j+1)}}{\mu_C} \left(\frac{1}{\mu_C}\right)^{(i)} w_j. \tag{4.61}$$

Then after substituting in (4.11) for $\mu_C^{(n-i-j+1)}$, (4.53) for $(1/\mu_C)^{(i)}$, and $1/\mu_C = \nu^{n+m_C}$, we arrive at

$$L_0 = \sum_{j=1}^{n}\sum_{i=0}^{n-j}\begin{pmatrix} n \\ n-i-j+1 \end{pmatrix}\begin{pmatrix} i+j-1 \\ i \end{pmatrix}\nu^{n+m_C}\left[\frac{(2n+m_C-i-j)!}{T^{n-i-j+1}(n+m_C-1)!}\mu_1^{2n+m_C-i-j+1}\right]$$
$$\times\left[\frac{(-1)^i(n+m_C)!}{T^i(n+m_C-i)!}\nu^{n+m_C-i}\right]w_j, \tag{4.62}$$

which reduces to

$$L_0 = \sum_{j=1}^{n}\frac{n+m_C}{T^{n-j+1}}\sum_{i=0}^{n-j}\begin{pmatrix} n \\ n-i-j+1 \end{pmatrix}\begin{pmatrix} i+j-1 \\ i \end{pmatrix}\frac{(-1)^i(2n+m_C-i-j)!}{(n+m_C-i)!}\nu^{m_C+j-1}w_j, \tag{4.63}$$

which proves the first part of the lemma.

The boundedness of the $l_{0,j}(\nu)$ follows by inspection, since $\nu(t-t_0,T)\leq 1$ for $t\in[t_0,t_0+T)$, and the $\bar{l}_{0,j}$ are bounded since they are finite sums of real numbers. ■

4.5.5 Proof of Theorem 4.1

We begin by noting that the derivative and integral of μ_C satisfy the properties that

$$\dot{\mu}_C = \frac{(1+m_C)T^{1+m_C}}{(T+t_0-t)^{1+m_C+1}} = \frac{1+m_C}{T}\mu_1^{2+m_C}, \tag{4.64}$$

and

$$\int_{t_0}^{t}\mu_C(\tau-t_0,T)d\tau = \frac{T}{m_C}(\mu_1(t-t_0,T)^{m_C}-1). \tag{4.65}$$

We then choose the Lyapunov function candidate $V = w^2/2$, whose derivative is

$$\dot{V} = w\mu_C bu + w\mu_C f + w\dot{\mu}_C x. \tag{4.66}$$

The first two of the three terms in this expression are uncertain and we compute bounds on them.

First,

$$\begin{aligned} w\dot{\mu}_C x &= w\frac{1+m_C}{T}\mu_1^{2+m_C}x \\ &= w\mu_C\frac{1+m_C}{T}\mu_1 x \\ &= w\mu_C\frac{1+m_C}{T}\nu^{m_C}\mu x \\ &\leq w\mu_C b\frac{1}{\underline{b}}\frac{1+m_C}{T}\mu_C x. \end{aligned} \tag{4.67}$$

Second, by applying Young's inequality with $\lambda > 0$,

$$\begin{aligned} w\mu_C f &\leq \mu_C|w|d\psi \\ &\leq \mu_C\lambda w^2\psi^2 + \frac{\mu_C}{4\lambda}d^2 \\ &\leq w\mu_C b\frac{1}{\underline{b}}\lambda\psi^2\mu_C x + \frac{\mu_C}{4\lambda}d^2. \end{aligned} \tag{4.68}$$

Inserting (4.67) and (4.68) into (4.66) yields

$$\dot{V} \leq w\mu_C b\left(u + \frac{1}{\underline{b}}\mu_C\lambda\psi^2 x + \frac{1}{\underline{b}}\frac{1+m_C}{T}\mu x\right) + \frac{\mu_C}{4\lambda}d^2. \tag{4.69}$$

Upon applying the control law given in (4.9), we get from (4.69) that

$$\begin{aligned} \dot{V} &\leq -\frac{b}{\underline{b}}k\mu_C w^2 + \frac{\mu_C}{4\lambda}d^2 \\ &\leq -k\mu_C w^2 + \frac{\mu_C}{4\lambda}d^2 \\ &\leq -2k\mu_C V(t) + \frac{\mu_C}{4\lambda}d^2. \end{aligned} \tag{4.70}$$

Further,

$$\begin{aligned} x(t)^2 &= \frac{1}{\mu_C(t-t_0,T)^2}w(t)^2 \\ &= \nu(t-t_0,T)^{2(1+m_C)}2V(t) \\ &\leq \nu(t-t_0,T)^{2(1+m_C)}\left(\zeta_C(t-t_0,T)^{2k}x(t_0)^2 + \frac{\|d\|^2_{[t_0,t]}}{4k\lambda}\right) \end{aligned} \tag{4.71}$$

for all $t \in [t_0, t_0 + T)$, which yields (4.10).

The claimed properties of the control law follow from the fact that (4.9) can be written as

$$u = -\frac{1}{\underline{b}}\left(k + \lambda\,\psi(x)^2 + \frac{1+m_C}{T}\right)w, \tag{4.72}$$

with the boundedness of w following from (4.47) and the boundedness of x established in (4.71). ■

4.5.6 Proof of Theorem 4.2

By substituting (4.36) into (4.30), we get

$$\dot{z} = -k\mu_C z, \tag{4.73}$$

which, following a calculation similar to (4.70)–(4.47), and employing (4.12), yields

$$|z(t)| \leq \zeta_C(t-t_0,T)^k |z_0|, \qquad \forall t \in [t_0, t_0+T), \tag{4.74}$$

where $\zeta_C(t-t_0,T)$ is a monotonically decreasing function defined as

$$\zeta_C(t-t_0,T) = \exp^{\frac{T}{n+m_C-1}\left(1-\mu_1(t-t_0,T)^{n+m_C-1}\right)}, \tag{4.75}$$

and whose value, as well as all of this function's derivatives, are zero at $t-t_0 = T$. At the same time, as indicated earlier, (4.27) is a linear system that is ISS with respect to z, which means that there exist positive constants M_1, δ_1, γ_1 such that

$$|r_1(t)| \leq M_1 \mathrm{e}^{-\delta_1(t-t_0)}|r_1(t_0)| + \gamma_1 \|z\|_{[t_0,t]}, \qquad \forall t \in [t_0, t_0+T). \tag{4.76}$$

Applying the standard cascade stability theorem to the system (4.27), (4.73), from (4.74), (4.75), (4.76) it follows that there exist positive constants $\bar{M}, \bar{\delta}$ such that

$$|\bar{w}(t)| \leq \bar{M}\mathrm{e}^{-\bar{\delta}(t-t_0)}\,|\bar{w}(t_0)|, \quad \forall t \in [t_0, t_0+T), \tag{4.77}$$

where

$$\bar{w} = \begin{bmatrix} r_1 \\ \\ z \end{bmatrix} = \left(J_1^T + \mathrm{e}_n K_{n-1}^T \right) r_1 + \mathrm{e}_n w_n =: Rw, \tag{4.78}$$

which follows from (4.22), (4.24), and (4.26), with the lower-triangular matrix R and its inverse defined as

$$R = I + \mathrm{e}_n K_{n-1}^T J_1, \qquad R^{-1} = I - \mathrm{e}_n K_{n-1}^T J_1. \tag{4.79}$$

From (4.19) and (4.78) it follows that

$$x = \nu^{m_C+1} Q_C(\nu) R^{-1} \bar{w}, \tag{4.80}$$

whereas from (4.16) and (4.78) it follows that

$$\bar{w}_0 = RP(0)x_0. \tag{4.81}$$

Invoking the last statement in Lemma 4.3, (4.80), (4.81), and (4.77), we get, for all $t \in [t_0, t_0 + T)$,

$$|x(t)| \leq \nu(t - t_0, T)^{m_C+1} \bar{q}_C \left| R^{-1} \right| \; |RP(0)| \bar{M} \mathrm{e}^{-\bar{\delta}(t-t_0)} |x(t_0)| \tag{4.82}$$

and arrive at (4.37) with $\tilde{M} = \bar{q}_C \left| R^{-1} \right| \; |RP(0)| \bar{M}$ and $\tilde{\delta} = \bar{\delta}$.

Now we turn our attention to proving the claims regarding the input u given in (4.36). From (4.31), (4.32) and (4.33) we get

$$L_0 + L_1 = \nu^{m_C} \left(l_0(\nu) + \nu^n K_{n-1}^T J_2 \right) w, \tag{4.83}$$

which is bounded and converges to zero as $t \to t_0 + T$. From (4.74), the term kz in (4.36) is also bounded and converges to zero. Finally, f is bounded and, if $f(0,t) \equiv 0$, then $f(x(t),t)$ also converges to zero as $t \to t_0 + T$, establishing the same properties for $u(t)$. ■

4.5.7 Proof of Theorem 4.3

Consider (4.30). The derivative of $V = z^2/2$ is

$$\dot{V} = \mu_C zbu + \mu_C zf + \mu_C z(L_0 + L_1). \tag{4.84}$$

By using Young's inequality, we have

$$\begin{aligned} z\mu_C f &\leq \mu_C |z| d\psi \\ &\leq \mu_C \lambda z^2 \psi^2 + \frac{\mu_C}{4\lambda} d^2 \\ &\leq z\mu_C b \frac{1}{\underline{b}} \lambda \psi^2 z + \frac{\mu_C}{4\lambda} d^2. \end{aligned} \tag{4.85}$$

From (4.78) it follows that

$$w = \left(J_1^T - \mathrm{e}_n K_{n-1}^T\right) r_1 + \mathrm{e}_n z. \tag{4.86}$$

Substituting (4.86) into (4.83), we obtain

$$L_0 + L_1 = \nu^{m_C} \left[\nu^{n-1} \left(k_{n-1}\nu + \bar{l}_{0,n}\right) z + \left(\nu^n K_{n-1}^T J_2 + l_0(\nu)\right) \left(J_1^T - \mathrm{e}_n K_{n-1}^T\right) r_1 \right], \tag{4.87}$$

where, from (4.35), we note that

$$\bar{l}_{0,n} = \frac{n(n+m_C)}{T} > 0. \tag{4.88}$$

Then, using (4.87) and Young's inequality, we get

$$\begin{aligned} \mu_C z(L_0 + L_1) \leq & \mu_C \nu^{m_C+n-1} \left|k_{n-1}\nu + \bar{l}_{0,n}\right| z^2 + \mu_C \rho \nu^{2m_C} \left| \left(\nu^n K_{n-1}^T J_2 + l_0(\nu)\right) \left(J_1^T - \mathrm{e}_n K_{n-1}^T\right) \right|^2 z^2 \\ & + \mu_C \frac{|r_1|^2}{4\rho}, \qquad \rho > 0. \end{aligned} \tag{4.89}$$

Denote

$$\rho_1(\rho) = \rho \max_{\nu \in [0,1]} \left| \left(\nu^n K_{n-1}^T J_2 + l_0(\nu)\right) \left(J_1^T - \mathrm{e}_n K_{n-1}^T\right) \right|^2. \tag{4.90}$$

Since $k_{n-1} > 0$ and, from (4.88), $\bar{l}_{0,n} > 0$, with (4.90) it follows from (4.89) that

$$\mu_C z(L_0 + L_1) \leq \mu_C \left[\left(k_{n-1} + \bar{l}_{0,n} + \rho_1(\rho)\right) z^2 + \frac{|r_1|^2}{4\rho} \right]. \tag{4.91}$$

From (4.84), (4.85), and (4.91) we get

$$\dot{V} \leq \mu_C z b \left[u + \frac{1}{\underline{b}} \left(k_{n-1} + \bar{l}_{0,n} + \rho_1(\rho) + \lambda \psi^2 \right) z \right] + \frac{\mu_C}{4} \left(\frac{|r_1|^2}{\rho} + \frac{d^2}{\lambda} \right). \tag{4.92}$$

Following a calculation similar to (4.70)–(4.47), and employing (4.12), from (4.92) we obtain, for $t \in [t_0, t_0 + T)$, that

$$|z(t)| \leq \zeta_C(t - t_0, T)^k |z_0| + \frac{1}{2\sqrt{k}} \left(\frac{\|r_1\|_{[t_0,t]}}{\sqrt{\rho}} + \frac{\|d\|_{[t_0,t]}}{\sqrt{\lambda}} \right). \tag{4.93}$$

Hence, the z-system is FT-ISS w.r.t. the r_1-input with a gain of $\frac{1}{2\sqrt{k\rho}}$, and is, additionally, FT-ISS w.r.t. the d-input. By being FT-ISS, the z-system is, in particular, ISS, w.r.t. the same inputs (r_1, d). From (4.76) we recall that the r_1-system is ISS (though not FT-ISS) w.r.t. the z-input with a gain of γ_1. Hence, if $\frac{\gamma_1}{2\sqrt{k\rho}} < 1$, namely, if $\rho k > \gamma_1/4$, the (r_1, z)-system is ISS w.r.t. d. Note that we cannot conclude the FT-ISS property for the overall (r_1, z)-system w.r.t. d, but only the ISS property, because the r_1-subsystem is merely ISS. Now, since, from (4.78), $(r_1, z) = \bar{w}$, from the small-gain and ISS argument that we have just completed it follows that there exist positive constants $\hat{M}, \hat{\delta}, \hat{\gamma}$ such that

$$|\bar{w}(t)| \leq \hat{M} \mathrm{e}^{-\hat{\delta}(t-t_0)} |\bar{w}(t_0)| + \hat{\gamma} \|d\|_{[t_0,t]}, \quad \forall t \in [t_0, t_0 + T). \tag{4.94}$$

Following the same argument as in (4.80)–(4.81), we obtain

$$|x(t)| \leq \nu(t - t_0, T)^{m_C+1} \bar{q}_C \left| R^{-1} \right| \left(|RP(0)| \hat{M} \mathrm{e}^{-\hat{\delta}(t-t_0)} |x(t_0)| + \hat{\gamma} \|d\|_{[t_0,t]} \right) \tag{4.95}$$

and arrive at (4.43) with $\check{M} = \bar{q}_C \left| R^{-1} \right| |RP(0)| \hat{M}$, $\check{\gamma} = \bar{q}_C \left| R^{-1} \right| \hat{\gamma}$, $\check{\delta} = \hat{\delta}$, establishing also that the x-system is FT-ISS-C w.r.t. input d. The boundedness of u is proved as at the end of the proof of Theorem 4.2. ∎

4.6 Acknowledgement

Most of the material in Chapter 4 first appeared in a paper by Prof. Yongduan (David) Song, his student, Dr. Yujuan Wang, Prof. Krstic, and myself, which was published as "Time-varying feedback for regulation of normal-form nonlinear systems in prescribed finite time," *Automatica*, 83, 243–251, 2017. Thank you, Prof. Song and Yujuan, for allowing me to work with you on this project, and thank you for allowing me to include the material in my dissertation.

Chapter 5

Prescribed-Time Estimation

For linear systems in the observer canonical form, we introduce a prescribed-time state observer with time-varying gains that tend to infinity as time approaches the prescribed convergence time. The observer is shown to exhibit the FT-GUAS property with convergence time prescribed by the user and independent of initial conditions. In addition, despite the observer gains going to infinity, the output estimation error injection terms are shown to remain uniformly bounded and converge to zero at the prescribed convergence time.

5.1 Introduction

In the previous chapter, we studied the problem of robust prescribed-time stabilization of nonlinear systems in normal form using an alternative approach to finite-time stabilization that employs feedback with time-varying gains that tend to infinity as time approaches the prescribed convergence time. In this chapter, we explore this alternative approach to finite-time stabilization further in the context of prescribed-time estimation, which involves time-varying observer gains that tend to infinity as time approaches the prescribed convergence time. We demonstrate the feasibility of the approach for linear systems in the observer canonical form, with the goal that it be a stepping-stone to extending the approach to more complicated systems.

In this chapter, as with the previous, we present the results first and then provide the proofs in a later section to improve chapter flow and readability.

5.1.1 Existing approaches to finite-time estimation

The general problem of state estimation in finite time has been studied for some time, with the most prevalent approaches being ones based on sliding mode control (SMC) [47–50, 58, 59], concepts of homogeneity [21, 23, 38, 49, 59, 60, 71, 75, 77, 101], or the use of multiple observers [22, 54, 67, 73]. In general, these approaches achieve convergence of estimation errors to zero within *some* finite time, which in most cases depends on initial conditions, and is often unknown. When this time can be shown to be bounded for all initial conditions, the approach is said to achieve *fixed-time* stabilization [68].

Depending on the approach employed, and how the controller or observer parameters are linked to the convergence time, fixed-time convergence in a *prescribed* time, whereby the user can prescribe the convergence time a priori and independently of initial conditions, is in some cases possible, but in general is not guaranteed, and with most methods is difficult to implement in practice. Sliding mode differentiators [47–50, 58, 59] provide for it in theory, but with these observers the convergence times are functions of the initial observer estimation errors, and gain scheduling becomes difficult for higher-order systems. Observers based on concepts of homogeneity [23, 38, 60, 71, 75, 101] also provide for prescribed convergence time, but with these observers the methods for selecting the observer gains are very complicated, again particularly so for higher-order systems. The approach of using multiple observers to prescribe convergence time for linear feedback systems was introduced by Engel and Kreisselmeier [22], and their basic idea was extended in a hybrid-systems framework by Raff and Allgower [73], Zheng, Orlov, Perruquetti and Richard [67], and Li and Sanfelice [54]. With these observers, the convergence time can be prescribed by selecting it and observer gains to simultaneously make two matrices Hurwitz and satisfy an invertibility condition, which can be done offline for almost any desired convergence time. Most recently, Lopez-Ramirez, Polyakov, Efimov, and Perruquetti [21] established a different framework to design finite-time and fixed-time observers for multiple-input multiple-output (MIMO) feedback systems using the Implicit Lyapunov Function (ILF) approach. To select the observer parameters, these methods require offline iteration over a grid until a set of linear matrix inequalities (LMI) are satisfied. Although existing approaches make it possible to prescribe estimation error converge time, a simpler framework for doing so is desirable.

5.1.2 Problem statement

As in the previous chapter for the prescribed-time controllers, we now study systems whose solutions are only required to exist on a finite-time interval, $t \in [t_0, t_0 + t_f)$, where $t_0 \geq 0$ is the initial time, and $t_f > t_0$ is the final or terminal time by which to meet the estimation and control objectives. In particular, we restrict our analysis to linear single-input single-output (SISO) systems in the observer canonical form,

$$\begin{aligned}
\dot{x}_1(t) &= x_2(t) - a_{n-1}y(t) \\
&\vdots \\
\dot{x}_{r-1}(t) &= x_r(t) - a_{\rho+1}y(t) \\
\dot{x}_r(t) &= x_{r+1}(t) - a_\rho y(t) + b_\rho u(t) \\
&\vdots \\
\dot{x}_{n-1}(t) &= x_n(t) - a_1 y(t) + b_1 u(t) \\
\dot{x}_n(t) &= -a_0 y(t) + b_0 u(t) \\
y(t) &= x_1(t),
\end{aligned}$$

which is written more compactly as

$$\dot{x}(t) = Ax(t) - ay(t) + \begin{bmatrix} 0_{(r-1)\times 1} \\ b \end{bmatrix} u(t) \tag{5.1}$$

$$y(t) = \mathrm{e}_1^T x(t), \tag{5.2}$$

where

$$A = \begin{bmatrix} 0 & I_{n-1} \\ \vdots & \\ 0 & \ldots 0 \end{bmatrix}, \quad a = \begin{bmatrix} a_{n-1} \\ \vdots \\ a_0 \end{bmatrix}, \quad b = \begin{bmatrix} b_\rho \\ \vdots \\ b_0 \end{bmatrix}. \tag{5.3}$$

Here, $x(t) \in \mathbb{R}^n$ is the state, $u(t) \in \mathbb{R}$ is a known and bounded control input, $y(t) \in \mathbb{R}$ is the measured output, $n > \rho \geq 0$, $r = n - \rho$ is the relative degree of the system, and the constant coefficients a_i's and b_i's are known. Our goal is to obtain perfect estimation of the state within a finite time $T : 0 < T \leq t_f$, in a manner in which T is fixed (independent of initial conditions) and easily prescribed a priori.

We accomplish this with a dynamic state observer of the form

$$\dot{\hat{x}}(t) = A\hat{x}(t) - ay(t) + \begin{bmatrix} 0_{(r-1)\times 1} \\ b \end{bmatrix} u(t) + \begin{bmatrix} g_1(t-t_0,T) \\ \vdots \\ g_n(t-t_0,T) \end{bmatrix} (y(t) - \hat{x}_1(t)), \tag{5.4}$$

where the time-varying observer gains $\{g_i(t-t_0,T)\}_{i=1}^n$ are functions of the prescribed convergence time T and must be designed. Defining the observer estimation error as $\tilde{x}_i(t) := x_i(t) - \hat{x}_i(t), i = 1,\ldots,n$, yields the error dynamics

$$\dot{\tilde{x}}_i(t) = \tilde{x}_{i+1}(t) - g_i(t-t_0,T)\tilde{x}_1(t), \quad i = 1,\ldots,n-1 \tag{5.5}$$

$$\dot{\tilde{x}}_n(t) = -g_n(t-t_0,T)\tilde{x}_1(t). \tag{5.6}$$

5.1.3 Design approach

We show that by using a particular time-varying change of coordinates of the observer error states, and selecting the time-varying observer gains $\{g_i(t-t_0,T)\}_{i=1}^n$ in a particular way, we achieve a form of *fixed-time stability* for (5.5), (5.6) in a convergence time $T > 0$, which we prescribe a priori and independently of initial conditions. To motivate our approach, consider the change of coordinates

$$\tilde{\zeta}_i(t) := \mu_O(t-t_0,T)\tilde{x}_i(t), \quad i = 1,\ldots,n, \tag{5.7}$$

where for $t \in [t_0, t_0+T)$, $\mu_O(t-t_0,T) : [t_0,t_0+T) \mapsto \mathbb{R}^+$ is a monotonically-increasing function (to be defined) having the property that $\mu_O(t-t_0,T)$ *tends to infinity* as $t \to t_0 + T$, where T is prescribed by the user. Equation (5.7) also gives the inverse mapping from $\tilde{\zeta}_i(t)$ to $\tilde{x}_i(t)$,

$$\tilde{x}_i(t) = \mu_O(t-t_0,T)^{-1}\tilde{\zeta}_i(t), \quad i = 1,\ldots,n. \tag{5.8}$$

Since $\mu_O(t-t_0,T)$ grows monotonically to infinity, then $\mu_O(t-t_0,T)^{-1}$ *decreases monotonically to zero*. So from (5.8), if the error states $\tilde{\zeta}_i(t)$ remain finite, then clearly $\tilde{x}_i(t) \to 0$ as $t \to t_0 + T$. Therefore, if after transforming the $\tilde{x}_i(t)$ system into the $\tilde{\zeta}_i(t)$ coordinates we can select the observer gains $\{g_i(t-t_0,T)\}_{i=1}^n$ in a way that *stabilizes* the $\tilde{\zeta}_i(t)$ system, then by nature of the special relationship between $\tilde{\zeta}_i(t)$ and $\tilde{x}_i(t)$ in (5.8), we simultaneously enforce the condition that $\tilde{x}_i(t) \to 0$ as $t \to t_0 + T$.

Note that in general, the change of coordinates (5.7) may result in a transformed version of (5.5), (5.6) that is much more complicated than the original one, and finding its inverse may not be trivial. However, it offers the advantage of providing a means of achieving fixed-time convergence in the prescribed time T. Using this approach, the convergence is global (with respect to initial conditions), uniform (with respect to t_0), and the convergence time T is fixed (independent of initial conditions). In application, we calculate the state estimate online using (5.4) and the time-varying observer gains $\{g_i(t-t_0,T)\}_{i=1}^n$. The latter will be shown to have a special structure and are easy to calculate.

5.2 Results

Using the functions defined in (2.41)–(2.42), it is possible to transform the error system (5.5), (5.6) in a way that retains the attractive property of (5.8), but also results in a transformed system that is easy to stabilize asymptotically. This then provides for fixed-time stabilization of (5.5), (5.6) in the sense of Definition 2.6.

5.2.1 Prescribed-time coordinate transformations

As captured by the next lemma, our prescribed-time coordinate transformation for the observer is different than the one employed to design the prescribed-time controllers in the previous chapter.

Lemma 5.1. *Consider the transformation $\tilde{x}_i(t) \mapsto \tilde{\zeta}_i(t)$ defined by*

$$\tilde{\zeta}_i(t) = \mu_O(t-t_0,T)\tilde{x}_i(t), \quad i = 1,\dots,n, \tag{5.9}$$

and the transformation $\tilde{\zeta}_i(t) \mapsto \tilde{z}_i(t)$ defined by

$$\tilde{z}_i(t) = \sum_{j=1}^{n} p^*_{O_{i,j}}(\mu_1)\tilde{\zeta}_j(t), \quad i = 1,\dots,n, \tag{5.10}$$

where the functions $\{p^*_{O_{i,j}}(\mu_1)\}$ are defined by

$$p^*_{O_{i,j}}(\mu_1) := \bar{p}_{O_{i,j}}\mu_1^{i-j}, \quad 1 \le j \le i \le n, \tag{5.11}$$

and the coefficients $\{\bar{p}_{O_{i,j}}\}$ are constants to be determined. By selecting the $\{\bar{p}_{O_{i,j}}\}$ according to

$$\bar{p}_{O_{i,i}} = 1, \tag{5.12}$$

$$\bar{p}_{O_{i,j}} = 0, \quad j > i, \tag{5.13}$$

for $\{\bar{p}_{O_{i,j}}\}$ with $j \ge i$, the recursion relations

$$\bar{p}_{O_{i,j-1}} = -\frac{n+m_O+i-j}{T}\bar{p}_{O_{i,j}} + \bar{p}_{O_{i+1,j}}, \quad n-1 \ge i \ge j \ge 2, \tag{5.14}$$

$$\bar{p}_{O_{n,j-1}} = -\frac{2n+m_O-j}{T}\bar{p}_{O_{n,j}}, \quad j = n, n-1, \dots, 2, \tag{5.15}$$

for $\{\bar{p}_{O_{i,j}}\}$ with $j < i$, and the observer gains $\{g_i(t-t_0,T)\}_{i=1}^{n-1}$ according to

$$g_i(t-t_0,T) = l_i + \left(\frac{n+m_O+i-1}{T}\bar{p}_{O_{i,1}} - \bar{p}_{O_{i+1,1}}\right)\mu_1^i - \sum_{j=1}^{i-1} g_j(t-t_0,T)\bar{p}_{O_{i,j}}\mu_1^{i-j}, \tag{5.16}$$

and $g_n(t-t_0,T)$ *according to*

$$g_n(t-t_0,T) = l_n + \frac{2n+m_O-1}{T}\bar{p}_{O_{n,1}}\mu_1^n - \sum_{j=1}^{n-1} g_j(t-t_0,T)\bar{p}_{O_{n,j}}\mu_1^{n-j}, \tag{5.17}$$

where the $\{l_i\}_{i=1}^n$ *are constants to be selected, the observer error system (5.5), (5.6) is transformed into*

$$\dot{\tilde{z}}_i(t) = \tilde{z}_{i+1}(t) - l_i\tilde{z}_1(t), \quad i = 1,\ldots,n-1, \tag{5.18}$$

$$\dot{\tilde{z}}_n(t) = -l_n\tilde{z}_1(t). \tag{5.19}$$

As shown in Lemma 5.1 and its proof, the change of coordinates of the observer error system (5.5), (5.6) consists of two parts: *1)* transformation (5.9) to scale the error dynamics in a way that facilitates fixed-time stabilization through the approach outlined in Section 5.1.3, and *2)* transformation (5.10) to rewrite the scaled error dynamics into a form that is easily stabilized asymptotically. This two-step change of coordinates can be expressed as a single transformation, and the resuling transformation is invertible. These results are captured in the following lemmas, whose proofs are provided later.

Lemma 5.2. *Given integers* $n \geq 1$ *(the order of the system) and* $m_O \geq 1$ *(a design parameter), the transformation* $\tilde{x}_i(t) \mapsto \tilde{z}_i(t)$ *is expressed as*

$$\tilde{z}(t) = \mu_1^{m_O+1} P_O(\mu_1)\tilde{x}(t), \tag{5.20}$$

where $P_O(\mu_1)$ *is a lower triangular matrix having elements* $\{p_{O_{i,j}}(\mu_1)\}$ *given by*

$$p_{O_{i,j}}(\mu_1) = \bar{p}_{O_{i,j}}\mu_1^{n+i-j-1}, \quad 1 \leq j \leq i \leq n, \tag{5.21}$$

where the constant coefficients $\{\bar{p}_{O_{i,j}}\}$ *are defined by (5.12)–(5.15).*

Lemma 5.3. *Given integers $n \geq 1$ (the order of the system) and $m_O \geq 1$ (a design parameter), the inverse of the transformation (5.20) is expressed as*

$$\tilde{x}(t) = \nu^{m_O+1} Q_O(\nu)\tilde{z}(t), \tag{5.22}$$

where $Q_O(\nu) := P_O(\mu_1)^{-1}$ is a lower triangular matrix having elements $\{q_{O_{i,j}}(\nu)\}$ given by

$$q_{O_{i,j}}(\nu) = \bar{q}_{O_{i,j}} \nu^{n+j-i-1}, \quad 1 \leq j \leq i \leq n, \tag{5.23}$$

where the constant coefficients $\{\bar{q}_{O_{i,j}}\}$ can be explicitly obtained from the constant coefficients $\{\bar{p}_{O_{i,j}}\}$ defined by (5.12)–(5.15). Furthermore, $\bar{q}_O := \sup_{\nu \in (0,1]} |Q_O(\nu)|$ is finite.

5.2.2 Time-varying observer gains

The time-varying observer gains $\{g_i(t-t_0,T)\}_{i=1}^n$ provided by (5.16) and (5.17) are calculated recursively as follows. Observe from (5.16) and (5.17) that if we proceed in the order $i = 1,2,..,n$, then explicit expressions for each $g_i(t-t_0,T)$ are obtained in terms of $\{g_j(t-t_0,T)\}_{j=1}^{i-1}$ and the constants $\{l_j\}_{j=1}^{i}$, regardless of the values of the latter. Thus after determining the $\{\bar{p}_{O_{i,j}}\}$ according to (5.12)–(5.15), and selecting $\{l_i\}_{i=1}^n$ as desired, we calculate the $\{g_i(t-t_0,T)\}_{i=1}^n$ using (5.16) and (5.17) by proceeding in the order $i = 1,2,..,n$.

It turns out that the observer gains $\{g_i(t-t_0,T)\}_{i=1}^n$ are polynomials in μ_1. This fact is captured in the following lemma, which is needed for our stability proof later.

Lemma 5.4. *The time-varying observer gains* $\{g_i(t-t_0,T)\}_{i=1}^n$ *given by (5.16) and (5.17) are ith-order polynomials in* μ_1*, which we denote as*

$$\begin{aligned} g_i(t-t_0,T) &= h_i(\mu_1) \\ &:= \sum_{k=0}^{i} \bar{h}_{i,k}\mu_1^k, \quad i=1,2,...,n, \end{aligned} \tag{5.24}$$

where the coefficients $\{\bar{h}_{i,k}\}$ *for* $i=1,2,...,n$ *and* $k=0,1,...,i$ *are constants.*

5.2.3 Stability analysis

The system (5.18), (5.19) is stabilized by selecting the constants $\{l_i\}_{i=1}^n$ to make the polynomial $s^n + l_1 s^{n-1} + \ldots + l_n$ and the companion matrix Λ_O Hurwitz, where Λ_O is defined from (5.18), (5.19) as

$$\Lambda_O := \begin{bmatrix} -l_1 & I_{n-1} \\ \vdots & \\ -l_n & 0 \end{bmatrix}. \tag{5.25}$$

Then by nature of the transformations used in Lemma 5.1, we obtain fixed-time stability of the system (5.5), (5.6) in the sense of Definition 2.6, as stated in the following theorem. Its proof is provided later in Section 5.5.

Theorem 5.1. *For the dynamic system (5.1)–(5.3) defined on the finite-time interval $t \in [t_0, t_0 + t_f)$, consider the observer (5.4) having error dynamics (5.5), (5.6) and observer gains $\{g_i(t - t_0, T)\}_{i=1}^{n}$ given by (5.16), (5.17) where the $\{l_i\}_{i=1}^{n}$ are constants to be selected. If the constants $\{l_i\}_{i=1}^{n}$ are selected such that the polynomial $s^n + l_1 s^{n-1} + \ldots + l_n$ and the companion matrix (5.25) are both Hurwitz, then the system (5.5), (5.6) has a FT-GUAS equilibrium at the origin, with a prescribed convergence time T, and there exist positive constants $\tilde{M}$, $\tilde{\delta} > 0$ such that*

$$|\tilde{x}(t)| \leq \nu(t - t_0, T)^{m_O + 1} \tilde{M} \mathrm{e}^{-\tilde{\delta}(t - t_0)} |\tilde{x}(t_0)|, \tag{5.26}$$

for all $t \in [t_0, t_0 + T)$, where $\nu(t - t_0, T)$ is defined in (2.42), and $m_O \geq 1$ is an integer and a design parameter. Furthermore, the output estimation error injection terms $\gamma_i(t - t_0, T) := g_i(t - t_0, T)\tilde{x}_1(t)$ for $i = 1, \ldots, n$ remain uniformly bounded over $[t_0, t_0 + T)$, and also converge to zero as $t \to t_0 + T$.

5.2.4 Explicit solutions for the $\{\bar{p}_{O_{i,j}}\}$

The coefficients $\{\bar{p}_{O_{i,j}}\}$ for $j < i$ defined by the recursion relations (5.14), (5.15) are easily calculated offline using the following algorithm. Beginning with (5.15), since $\bar{p}_{O_{n,n}} = 1$ is known from (5.12), we first obtain the set $\{\bar{p}_{O_{n,j-1}}\}$ by working backwards for $j = n, n-1, \ldots, 2$. Next, we proceed to solve (5.14), beginning with $i = n-1$ and $j = i = n-1$ for the set $\{\bar{p}_{O_{n-1,j-1}}\}$ with $j = n-1, n-2, \ldots, 2$. Since $\bar{p}_{O_{n-1,n-1}} = 1$ is known from (5.12), and $\bar{p}_{O_{n,n-1}}$ is known from the previous $i = n$ step, we can again work backwards to obtain the remaining $\{\bar{p}_{O_{n-1,j-1}}\}$. We continue this process for $i = n-2, \ldots, 2$ by working backwards from $j = i, i-1, \ldots 2$ to obtain the remaining $\{\bar{p}_{O_{i,j}}\}$.

In practice, we obtain the constants $\{\bar{p}_{O_{i,j}}\}$ for $j < i$ defined by the recursion relations (5.14), (5.15) as described above. However, it is possible to obtain explicit solutions for them as shown in the following proposition. The proof is provided in the next section. The solution, however, requires the following lemma.

Lemma 5.5. *Consider a linear discrete-time dynamic system that steps backward in time,*

$$x(j-1) = a(j)x(j) + u(j), \tag{5.27}$$

where j plays the role of time, $x(j)$ is the state, $u(j)$ is an input, $a(j)$ is a time-varying coefficient, and $x(i)$ is the initial condition. For integers i,k,l, define the function

$$\Gamma(i-k, i-l) := \begin{cases} \prod_{s=l}^{k-1} a(i-s), & 0 \leq l < k, \\ 1, & k = l. \end{cases} \tag{5.28}$$

Then the solution to (5.27) for k steps backward from the initial condition $x(i)$ is given by

$$x(i-k) = \Gamma(i-k,i)x(i) + \sum_{l=0}^{k-1} \Gamma(i-k, i-(l+1))u(i-l). \tag{5.29}$$

Proposition 5.1. *For $\{\bar{p}_{O_{i,j}}\}$ with $1 \leq j < i < n$, the solution to (5.14) is expressed as*

$$\bar{p}_{O_{i,j}} = \frac{(-1)^{i-j}(n+m_O+i-j-1)!}{T^{i-j}(n+m_O-1)!} + \sum_{l=0}^{i-j-1} \frac{(-1)^{i-j-(l+1)}(n+m_O+i-j-1)!}{T^{i-j-(l+1)}(n+m_O+l)!}\bar{p}_{O_{i+1,i-l}}, \tag{5.30}$$

and for $\{\bar{p}_{O_{n,j}}\}$ with $1 \leq j \leq n-1$, the solution to (5.15) is expressed as

$$\bar{p}_{O_{n,j}} = \frac{(-1)^{n-j}(2n+m_O-j-1)!}{T^{n-j}(n+m_O-1)!}. \tag{5.31}$$

5.3 Discussion

Some remarks on the observer (5.4) and how it compares to existing finite-time observers are in order.

5.3.1 Implementation

The observer (5.4) is conceptually easy to understand and implement. Indeed, for system (5.1), (5.2) of any given order n, its construction consists of simply selecting the constants $\{l_i\}_{i=1}^n$ to make the companion matrix Λ Hurwitz, and then (independently) selecting the prescribed convergence time T and the design parameter $m_O \geq 1$. These are the only "tuning parameters" of the observer, since we have explicit formulas for the $\{\bar{p}_{O_{i,j}}\}$ in (5.12)–(5.15), which are set by n, m_O, and T, and the time-varying gains $\{g_i(t-t_0,T)\}_{i=1}^n$ in (5.16), (5.17), which are functions of the $\{\bar{p}_{O_{i,j}}\}$ and the function $\mu_1(t-t_0,T)$, where the latter is defined by (2.41) based on T and $t-t_0$.

Although the output estimation error injection terms $\{\gamma_i(t-t_0,T)\}_{i=1}^n$ remain finite (see Theorem 5.1), in practice the observer (5.4) will exhibit numerical precision limitations as time tends to t_0+T, because the gains $\{g_i(t-t_0,T)\}_{i=1}^n$ go to infinity. This can be mitigated by either: *1)* extending the prescribed convergence time T to some time larger than t_f, or by *2)* "turning off" the injections $\{\gamma_i(t-t_0,T)\}_{i=1}^n$ (zero them out) at some time $t_{stop} < t_0+T$. Doing either will achieve convergence of the estimation error to within some neighborhood of the origin that could be tuned by the user if desired. For the latter option, one can, in principle, determine such a t_{stop} a priori as follows. First, set each of the $\{g_i(t-t_0,T)\}_{i=1}^n$ in (5.16), (5.17) to some maximum value selected by the user, say $g_{max} = 10^{10}$. Next, solve each expression for $t-t_0$. Finally, define t_{stop} as the minimum of those times. Clearly, for high-order systems, this method becomes difficult, and may not be worth the trouble in practice. A simpler solution is to instead monitor the magnitude of the $\{g_i(t-t_0,T)\}_{i=1}^n$ in real time during estimation until any of them approach g_{max}, and then at that time, turn off the injections. Once the injections are turned off, the estimation errors will grow again. But if desired, the observer could be reset to begin anew from that time, treating the current time t_{stop} as a new t_0, and the current estimation error $\tilde{x}(t_{stop})$ as a new initial condition.

5.3.2 Existing methods

In theory, higher-order sliding mode differentiators [48–50, 58, 59] and observers based on concepts of homogeneity [23, 38, 60, 71, 75, 77, 101] can achieve convergence in finite time. However, with both of these approaches, simple, constructive procedures for selecting observer parameters that guarantee convergence in a fixed, *prescribed* time appear to be unavailable for higher-order systems, and parameter tuning must usually be done through trial and error in numerical simulation. Approaches that use multiple observers [22, 54, 67, 73] provide for prescription of the convergence time, but by requiring either delays or a hybrid-systems framework, their implementation is relatively complicated. The ILF approach [21] also provides for prescribed convergence time, by iterating parameters over a grid until a set of LMI are satisfied, and this can be done offline for linear MIMO systems. However, implementation of this method is also complicated, and ultimately still requires trial and error to tune the parameters through numerical simulation. The attractive features of (5.4) are the simplicity of its design and implementation, and the ease by which the user can prescribe the convergence time T and constructively calculate the observer gains.

5.4 Examples

We illustrate the performance of the observer (5.4) through several examples.

Example 5.1. Consider the double integrator with single output,

$$\dot{x}_1(t) = x_2(t),$$

$$\dot{x}_2(t) = u(t),$$

$$y(t) = x_1(t).$$

The observer (5.4) becomes

$$\dot{\hat{x}}_1(t) = \hat{x}_2(t) + g_1(t-t_0,T)\left(y(t) - \hat{x}_1(t)\right),$$

$$\dot{\hat{x}}_2(t) = u(t) + g_2(t-t_0,T)\left(y(t) - \hat{x}_1(t)\right),$$

which has the error dynamics

$$\dot{\tilde{x}}_1(t) = \tilde{x}_2(t) - g_1(t-t_0,T)\tilde{x}_1(t),$$

$$\dot{\tilde{x}}_2(t) = -g_2(t-t_0,T)\tilde{x}_1(t).$$

Using (5.12)–(5.15) and the algorithm provided in Section 5.2.4, we find the constants $\{\bar{p}_{O_{i,j}}\}$ to be $\bar{p}_{O_{1,1}} = \bar{p}_{O_{2,2}} = 1$, $\bar{p}_{O_{1,2}} = 0$, and $\bar{p}_{O_{2,1}} = -\frac{m_O+2}{T}$. Then from (5.16) and (5.17), $g_1(t-t_0,T)$ and $g_2(t-t_0,T)$ are found to be

$$g_1(t-t_0,T) = l_1 + 2\frac{m_O+2}{T}\mu_1,$$
$$g_2(t-t_0,T) = l_2 + l_1\frac{m_O+2}{T}\mu_1 + \frac{(m_O+1)(m_O+2)}{T^2}\mu_1^2.$$

Figure 5.1 illustrates simulation of Example 5.1 with control input $u(t) = \sin(10t) + \cos(t)$ for three sets of initial conditions: $(x_1(0), x_2(0)) = (0,1)$, $(x_1(0), x_2(0)) = (0,5)$, and $(x_1(0), x_2(0)) = (0,10)$. In all cases, the observer was initialized to $(\hat{x}_1(0), \hat{x}_2(0)) = (0,0)$. The initial time is $t_0 = 0$, and the terminal time is $t_f = 5$. For observer parameters, we selected $l_1 = l_2 = 1$, $m_O = 1$, and $T = 5$. In Figure 5.1, solid lines denote the states, and dashed lines denote the estimates. Figure 5.2 shows the corresponding estimation error states versus time. Figure 5.1 and Figure 5.2 show that convergence of the estimation errors to zero is achieved at the prescribed time $T = 5$, regardless of the initial conditions, demonstrating the fixed-time property of the observer. Figure 5.3 shows the corresponding output estimation error injection terms versus time. As proven in Theorem 5.1, they remain uniformly bounded and converge to zero as $t \to t_0 + T$.

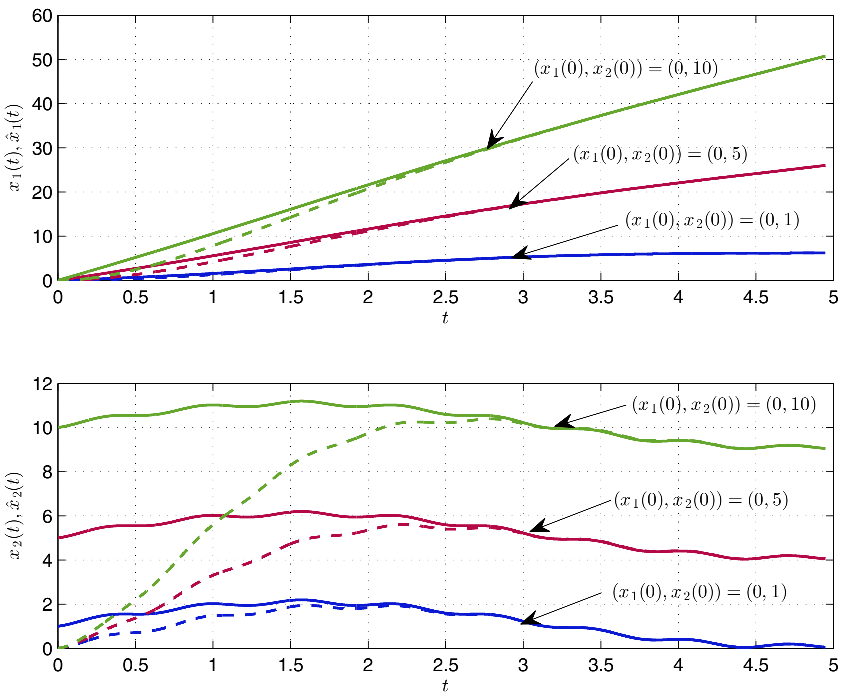

Figure 5.1: Time histories of states and state estimates for Example 5.1, for three sets of initial conditions.

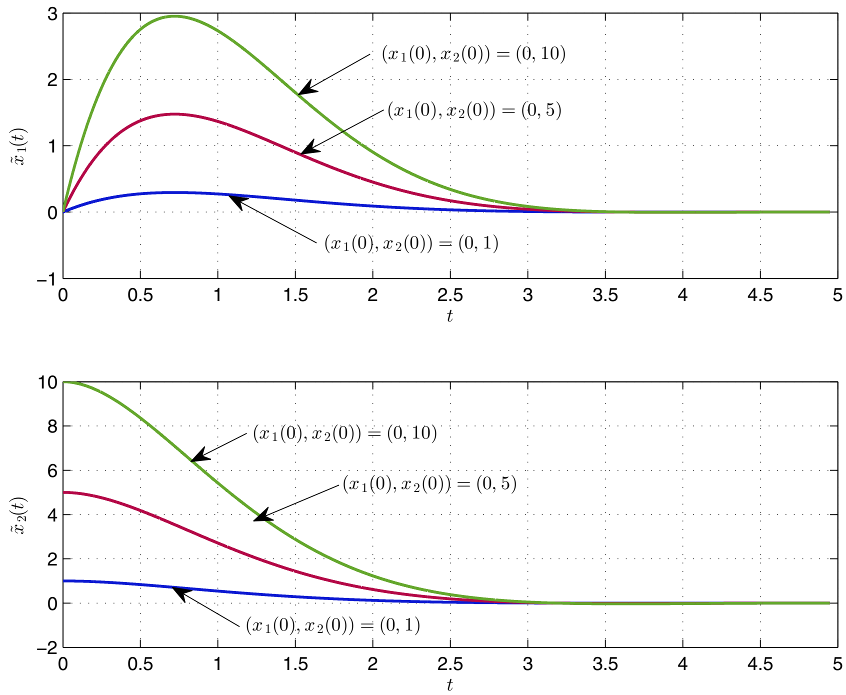

Figure 5.2: Time histories of state estimation errors for the simulations shown in Figure 5.1.

Figure 5.4–Figure 5.6 again illustrate simulation of Example 5.1 with control input $u(t) = \sin(10t) + \cos(t)$, but with initial conditions $(x_1(0), x_2(0)) = (20, 1)$, $(\hat{x}_1(0), \hat{x}_2(0)) = (0, 0)$, observer parameters $l_1 = l_2 = 1$ and $T = 5$, and the observer parameter $m_O \geq 1$ is varied. In Figure 5.4, solid lines denote the states, and dashed lines denote the estimates. Figure 5.5 and Figure 5.6 show the corresponding estimation error states and output estimation error injection terms. Figure 5.4–Figure 5.6 show that varying the parameter m_O tunes the transient responses of the estimation error states, but for all m_O used, the estimation error states converge to zero at the prescribed time $T = 5$.

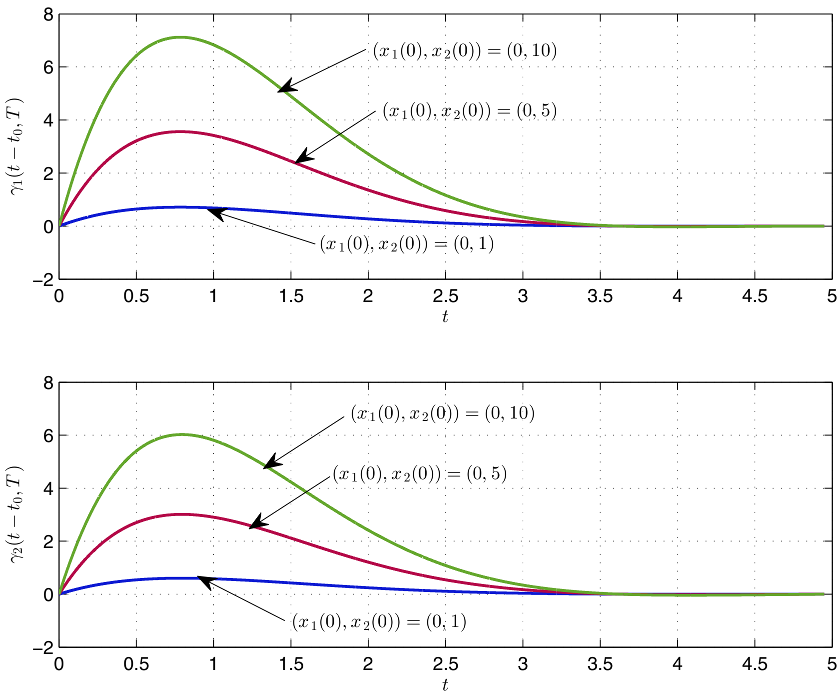

Figure 5.3: Time histories of output estimation error injection terms for the simulations shown in Figure 5.1.

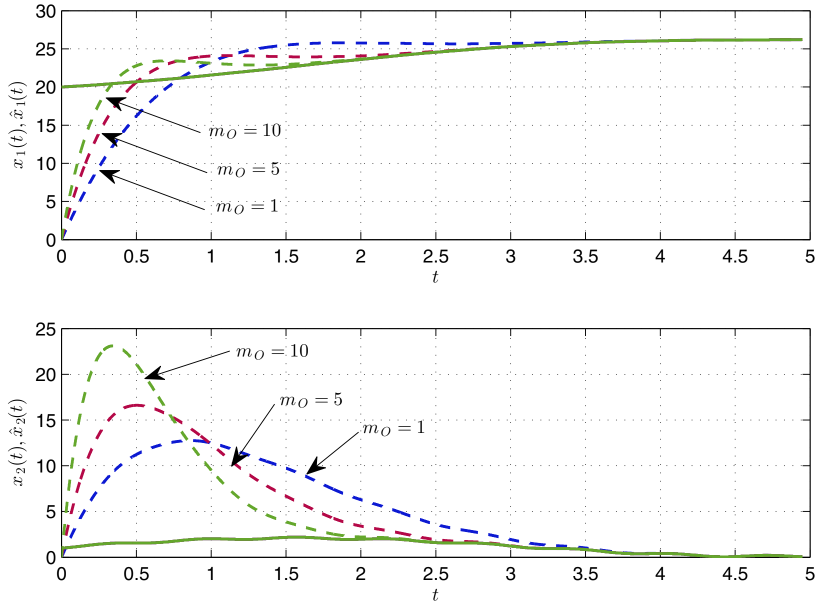

Figure 5.4: Time histories of states and state estimates for Example 5.1, for three values of the observer parameter m_O.

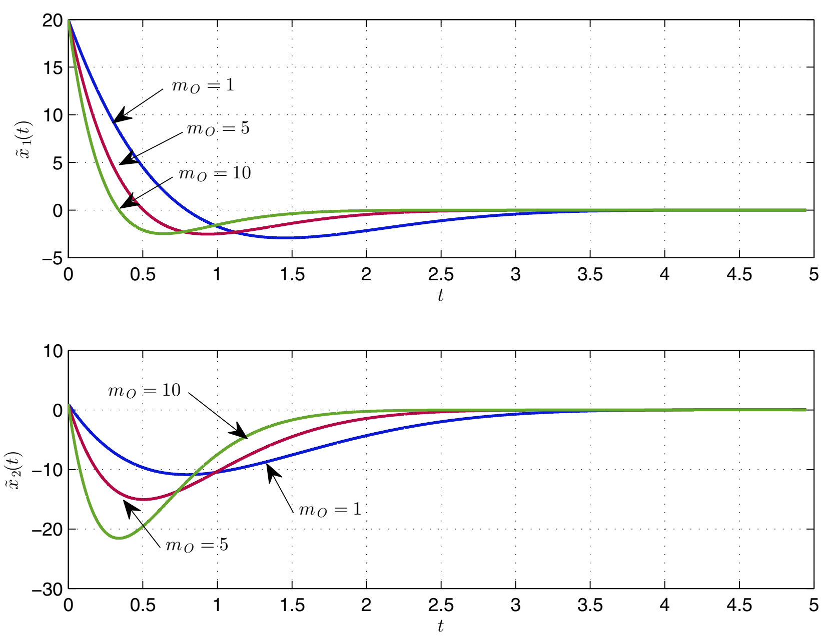

Figure 5.5: Time histories of state estimation errors for the simulations shown in Figure 5.4.

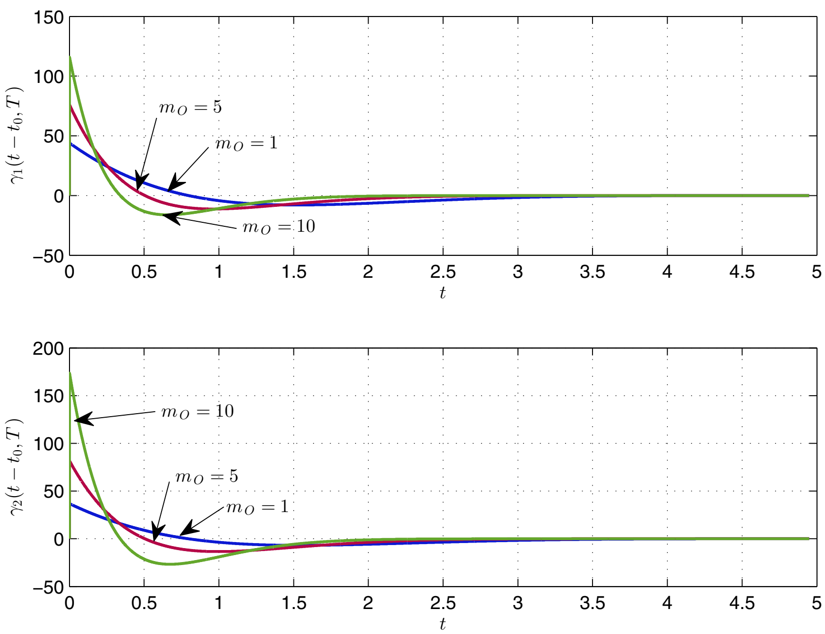

Figure 5.6: Time histories of output estimation error injection terms for the simulations shown in Figure 5.4.

Example 5.2. Consider the open-loop unstable system

$$Y(s) = \frac{1}{s^4 - 3s^3 + 4s^2 - 2s} U(s)$$

expressed in the observer canonical form,

$$\dot{x}_1(t) = x_2(t) + 3x_1(t)$$

$$\dot{x}_2(t) = x_3(t) - 4x_1(t)$$

$$\dot{x}_3(t) = x_4(t) + 2x_1(t)$$

$$\dot{x}_4(t) = u(t).$$

The observer for this system is

$$\dot{\hat{x}}_1(t) = \hat{x}_2(t) + 3x_1(t) + g_1(t - t_0, T)(y(t) - \hat{x}_1(t))$$

$$\dot{\hat{x}}_2(t) = \hat{x}_3(t) - 4x_1(t) + g_2(t - t_0, T)(y(t) - \hat{x}_1(t))$$

$$\dot{\hat{x}}_3(t) = \hat{x}_4(t) + 2x_1(t) + g_3(t - t_0, T)(y(t) - \hat{x}_1(t))$$

$$\dot{\hat{x}}_4(t) = u(t) + g_4(t - t_0, T)(y(t) - \hat{x}_1(t)),$$

which yields the error system

$$\dot{\tilde{x}}_1(t) = \tilde{x}_2(t) - g_1(t - t_0, T)\tilde{x}_1(t)$$

$$\dot{\tilde{x}}_2(t) = \tilde{x}_3(t) - g_2(t - t_0, T)\tilde{x}_1(t)$$

$$\dot{\tilde{x}}_3(t) = \tilde{x}_4(t) - g_3(t - t_0, T)\tilde{x}_1(t)$$

$$\dot{\tilde{x}}_4(t) = u(t) - g_4(t - t_0, T)\tilde{x}_1(t).$$

We simulated this system in MATLAB using a classical RK4 algorithm, and a time step of 0.001. We selected $T = 15$ as the prescribed time for convergence of the estimation error, $m_O = 1$, and $l = [\,929.59, 627.44, 166.77, 20.60\,]^T$. For all simulations, the state estimates were initialized

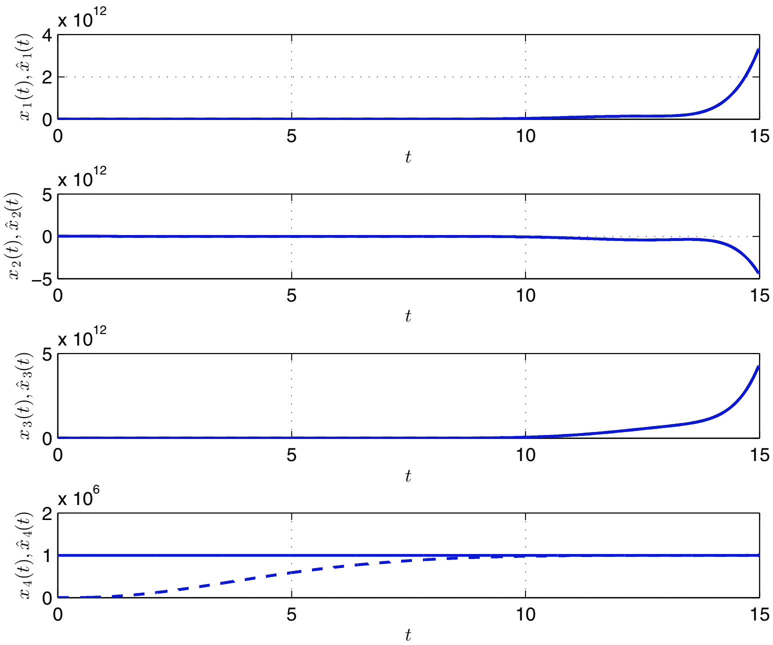

Figure 5.7: Time histories of states for Example 5.2 with initial condition $\tilde{x}_4(0) = 10^6$.

to zero, while we varied the initial condition of the state x_4 from 10^{-2} to 10^{10}. The simulation was stopped when any one of the gains reached a value of $g_{max} = 10^{10}$.

Simulations showed that the time t_{stop} is independent of initial conditions (see (5.16) and (5.17)), however it is dependent upon g_{max}, in addition to the numerical method and time step employed. For the large range of initial conditions simulated, when the simulation is stopped at t_{stop}, convergence is obtained to within a neighborhood of the origin that is orders of magnitude smaller than the initial condition. If the user desires a smaller neighborhood, then he can achieve it by increasing the magnitude of g_{max} used to stop the simulation, up to the limit of the computer real number representation.

To illustrate the temporal behavior of the solutions, we provide some results of the case of $\tilde{x}_4(0) = 10^6$ in Figure 5.7—Figure 5.9.

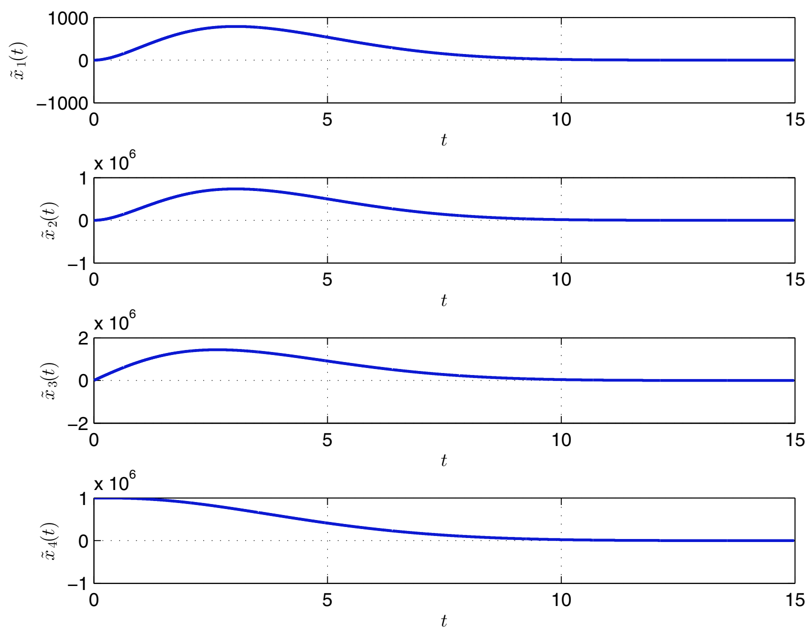

Figure 5.8: Time histories of state estimation errors for Example 5.2 with initial condition $\tilde{x}_4(0) = 10^6$.

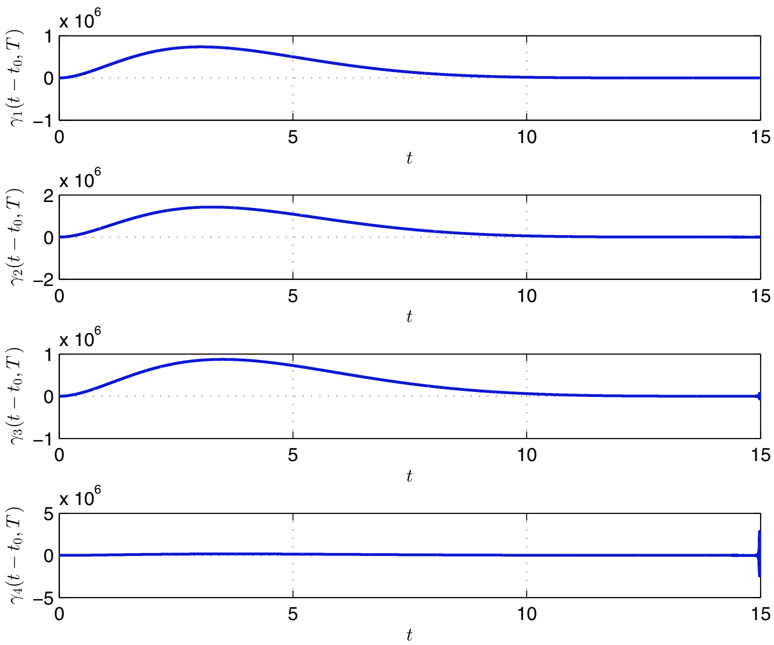

Figure 5.9: Time histories of output estimation error injections for Example 5.2 with initial condition $\tilde{x}_4(0) = 10^6$.

While developing the observer of this chapter, we assumed no nonlinearities or disturbances to the plant, and perhaps more importantly, no disturbances to the measured output. Although we have not yet explored with any mathematical rigor how such disturbances would affect the performance of our observer, we provide the following results from simulations which provide some practical evidence of the effects of disturbances. We consider only measurement disturbances in the examples, and look forward to exploring the problems rigorously in the future.

For the next examples, we replace the measured output (5.2) with

$$y(t) = x_1(t) + v(t), \tag{5.32}$$

where the disturbance $v(t) \in \mathbb{R}$ takes several forms.

Example 5.3. For this example, we simulate the double integrator (Example 5.1) with zero control input, but subjected to pseudo-random white Gaussian measurement noise, which we model as

$$v(t) = \bar{v} + r(t)\sigma_v, \tag{5.33}$$

where $r(t)$ is a normally distributed pseudo-random variable having zero mean ($\bar{v} = 0$) and standard deviation of one ($\sigma_v = 1$). For simulation, we selected $t_0 = 0$, $T = 10$, $m_O = 1$, and $l_1 = l_2 = 1$. The initial conditions were varied as $(x_1(0), x_2(0)) = (0, 1)$, $(x_1(0), x_2(0)) = (0, 25)$, and $(x_1(0), x_2(0)) = (0, 100)$. Results are shown in Figure 5.10–Figure 5.14.

In Figure 5.13 and Figure 5.14, the measurement disturbance is evident in the dynamics of the output estimation error injection terms. But in Figure 5.11 and Figure 5.12, we see that for the "larger" initial conditions, ($x_2(0) = 25, x_2(0) = 100$), this level of pseudo-random measurement noise doesn't prohibit the observer from converging the estimation errors to within a tiny neighborhood of the origin relative to their initial conditions. And, even for the smaller initial condition ($x_2(0) = 1$), this disturbance doesn't seem to exacerbate the numerical instability of the method until the final few fractions of the prescribed convergence time.

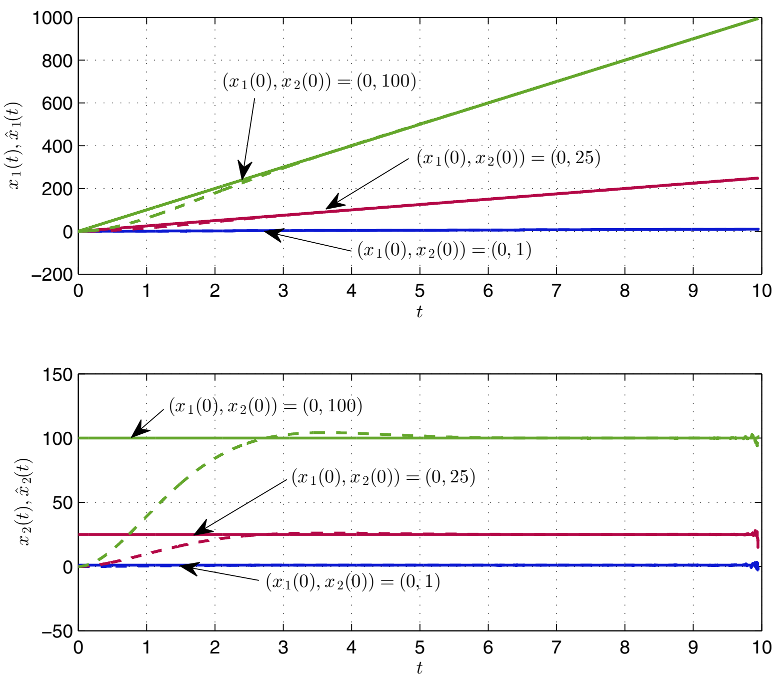

Figure 5.10: Time histories of states for Example 5.3 with $\bar{v} = 0$ and $\sigma_v = 1$.

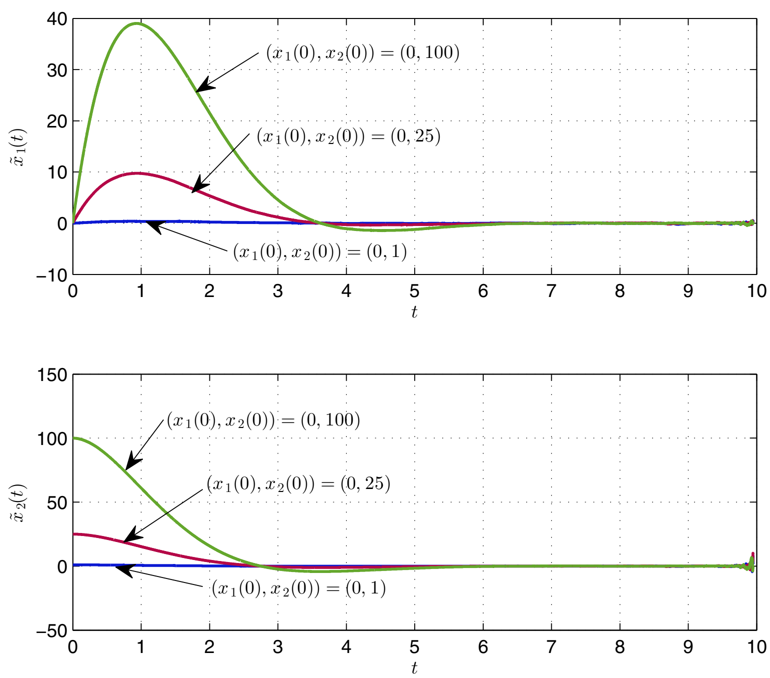

Figure 5.11: Time histories of state estimation errors for Example 5.3 with $\bar{v} = 0$ and $\sigma_v = 1$.

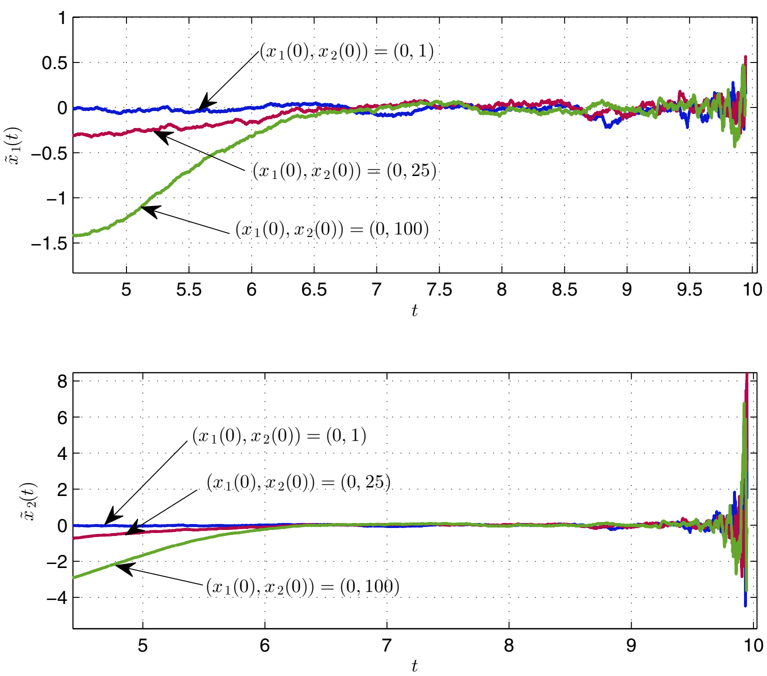

Figure 5.12: Zoom-in of time histories of state estimation errors for Example 5.3 with $\bar{v} = 0$ and $\sigma_v = 1$.

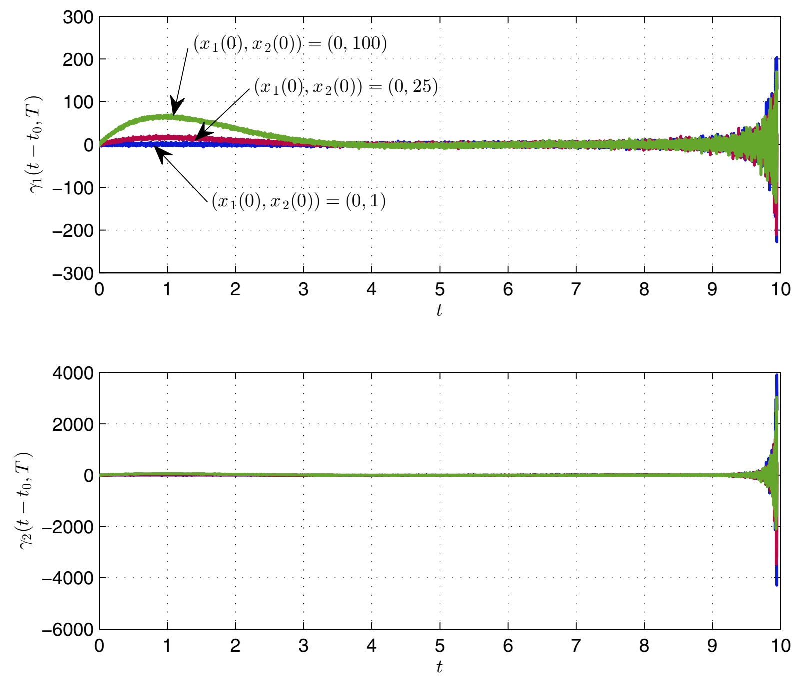

Figure 5.13: Time histories of output estimation error injections for Example 5.3 with $\bar{v} = 0$ and $\sigma_v = 1$.

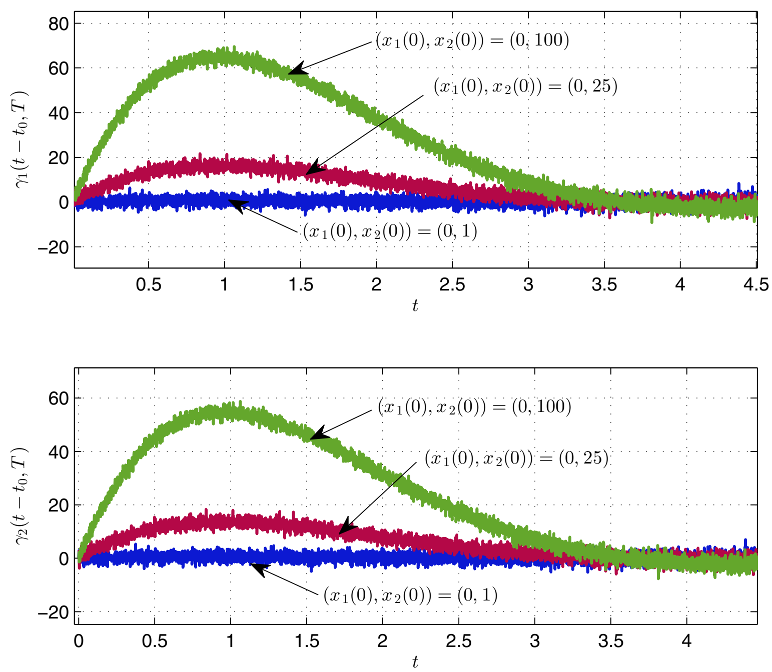

Figure 5.14: Zoom-in of time histories of output estimation error injections for Example 5.3 with $\bar{v}=0$ and $\sigma_v=1$.

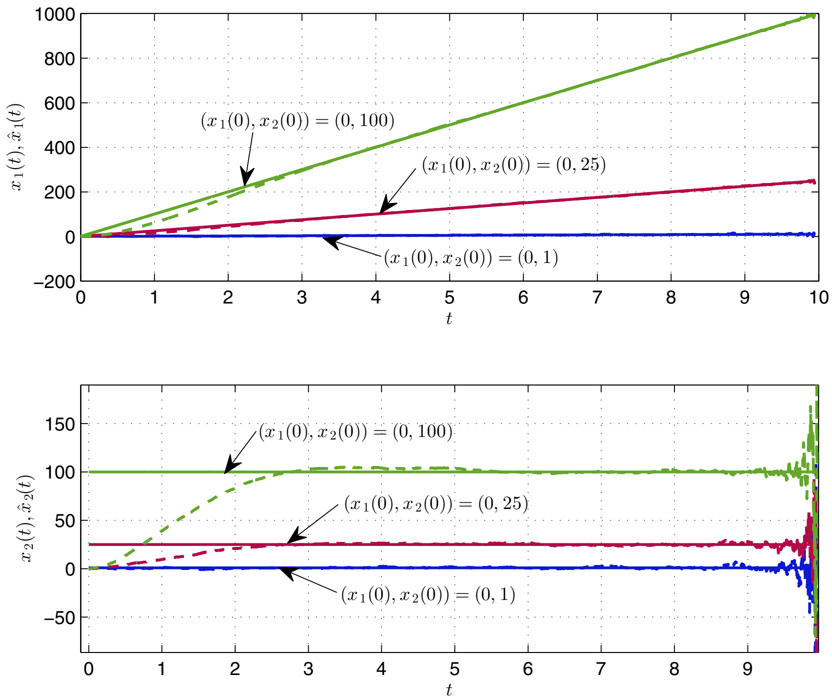

Figure 5.15: Time histories of states for Example 5.3 with $\bar{v} = 0$ and $\sigma_v = 25$.

Now, we repeat the same exercise, but use a much larger measurement disturbance standard deviation of twenty-five ($\sigma_v = 25$). The results are provided in Figure 5.15–Figure 5.17. With this example of a much larger σ_v, the impact on estimation error convergence is more evident. In Figure 5.16, for the largest initial condition ($x_2(0) = 100$), the estimation error still converges well relative to its initial condition, until near the end of the prescribed-convergence time window, where divergence from numerical instability is exacerbated by the disturbance. For the medium-sized initial condition ($x_2(0) = 25$), a sort of convergence is obtained for a while, but the measurement disturbance is much more of an issue because it is comparable to the initial condition. Then for the smallest initial condition ($x_2(0) = 1$), the disturbance prohibits any noticeable convergence relative to its initial condition (see the blue x_1 state in Figure 5.15).

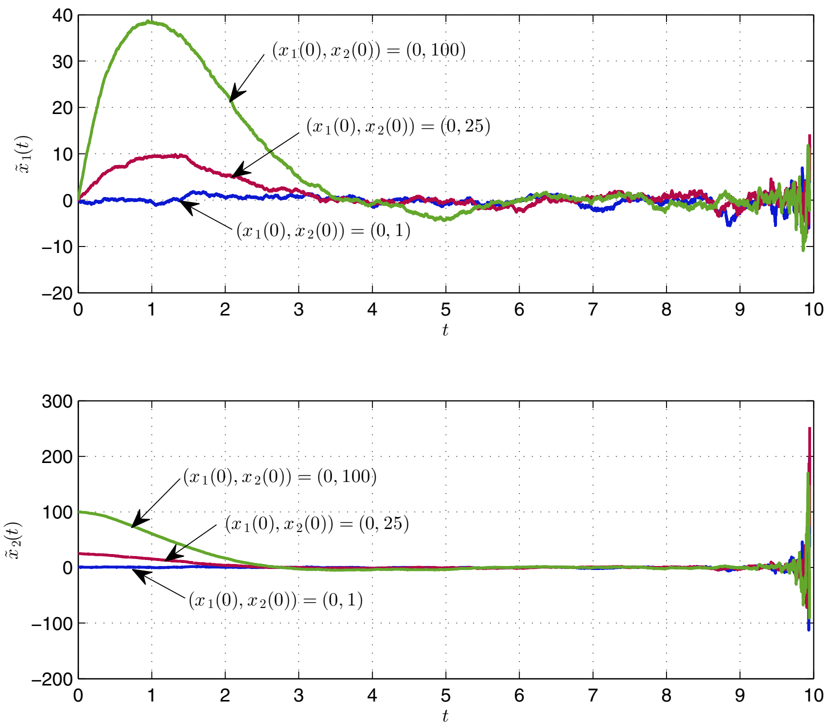

Figure 5.16: Time histories of state estimation errors for Example 5.3 with $\bar{v} = 0$ and $\sigma_v = 25$.

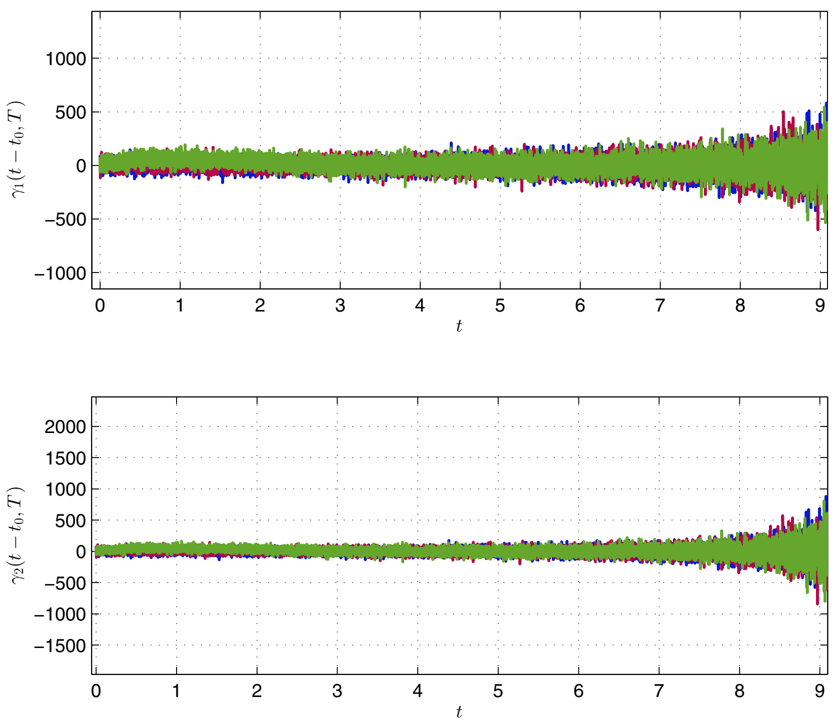

Figure 5.17: Time histories of output estimation error injections for Example 5.3 with $\bar{v} = 0$ and $\sigma_v = 25$.

Example 5.4. We repeat the simulation of the double integrator with zero control input, but now model the measurement disturbance as a sinusoid,

$$v(t) = 10\sin(10t).$$

Again, we selected the parameters as $t_0 = 0$, $T = 10$, $m = 1$, and $l_1 = l_2 = 1$, and we varied the initial conditions with the same values. Results are shown in Figure 5.18–Figure 5.20.

As before with the pseudo-random measurement disturbance, the effects of the measurement disturbance $v(t)$ are clearly seen in the dynamics of the output estimation error injections of Figure 5.20. Recall that in the nominal (disturbance-free) case, these injections go to zero as $t \to t_0 + T$. Here, however, after an initial transient due to the initial conditions, the injections tend to follow the dynamics of the measurement disturbance, before the disturbance exacerbates the numerical instability into divergence as time gets close to the prescribed convergence time. As in our previous example with the pseudo-random measurement disturbance, Figure 5.20 suggests that the amplitude of the disturbance, relative to the initial estimation error, has an enormous effect on the performance of the observer. This is just as we expect, since the system is linear.

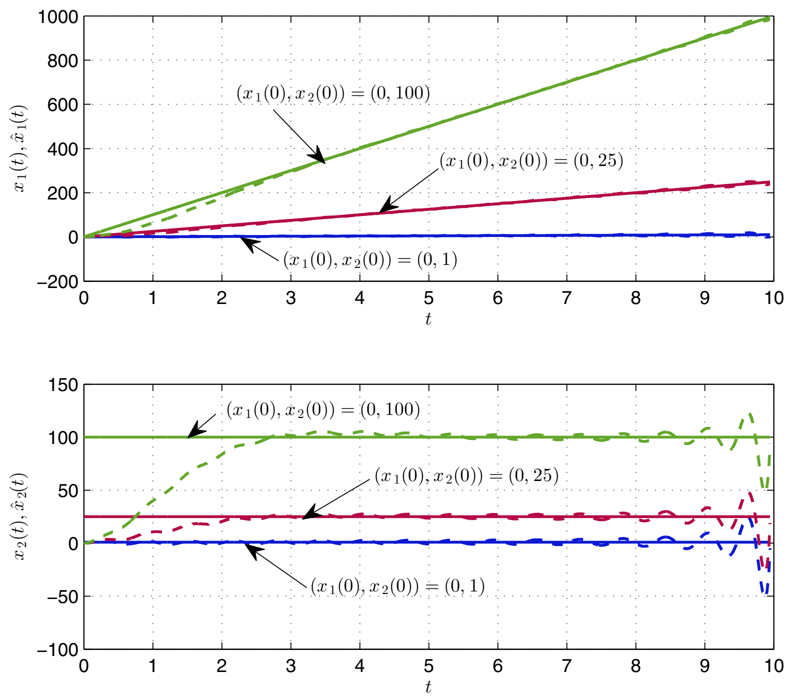

Figure 5.18: Time histories of states for Example 5.4 with $v(t) = 10\sin(10t)$.

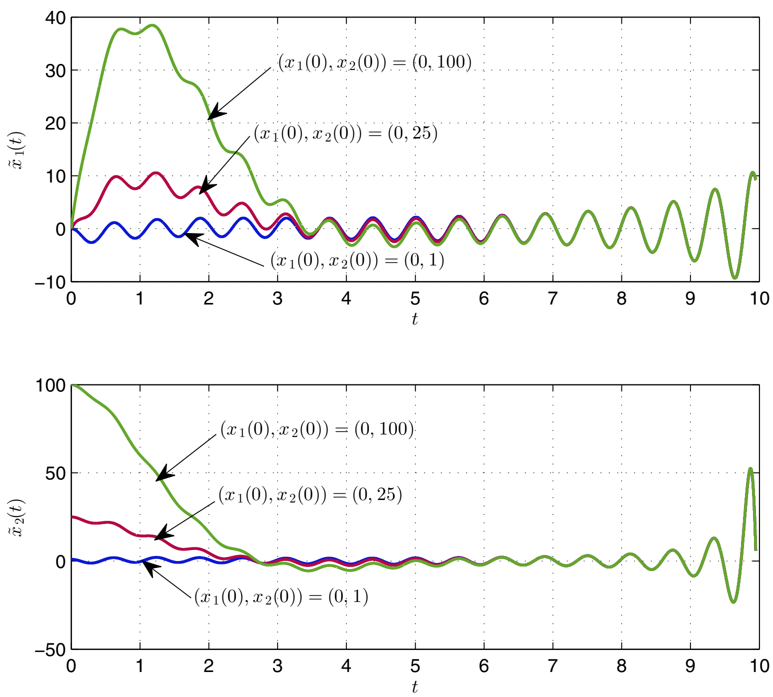

Figure 5.19: Time histories of state estimation errors for Example 5.4 with $v(t) = 10\sin(10t)$.

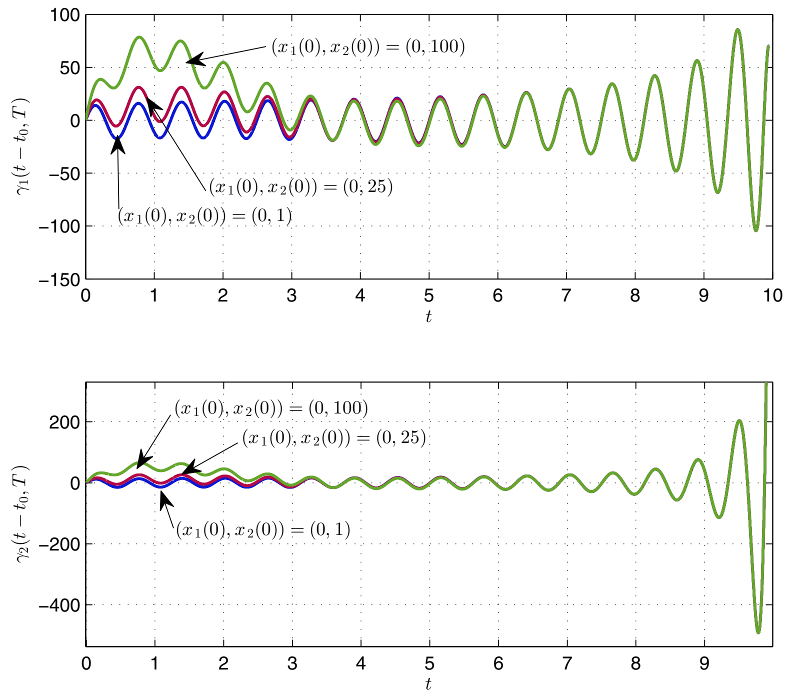

Figure 5.20: Time histories of output estimation error injections for Example 5.4 with $v(t) = 10\sin(10t)$.

Example 5.5. As a final example, consider the constant measurement disturbance,

$$v(t) = 10.$$

Using the same simulation parameters as in the previous examples, we provide the results in Figure 5.21–Figure 5.23.

Notice from Figure 5.23 that the output estimation error injections converge to zero as in the nominal case. And then from Figure 5.22, we see that the estimation errors are able to converge to constant values within the prescribed convergence time. The observer thinks it has converged to the origin, but it has no knowledge of the measurement disturbance. So although the estimation error for state x_2 has converged to zero, the estimate for the measured state x_1 has a steady state error equal to the magnitude of the constant measurement disturbance (see Figure 5.22). To summarize, in this example, the observer has not performed as desired, due to the existence of the persistent (constant) measurement disturbance.

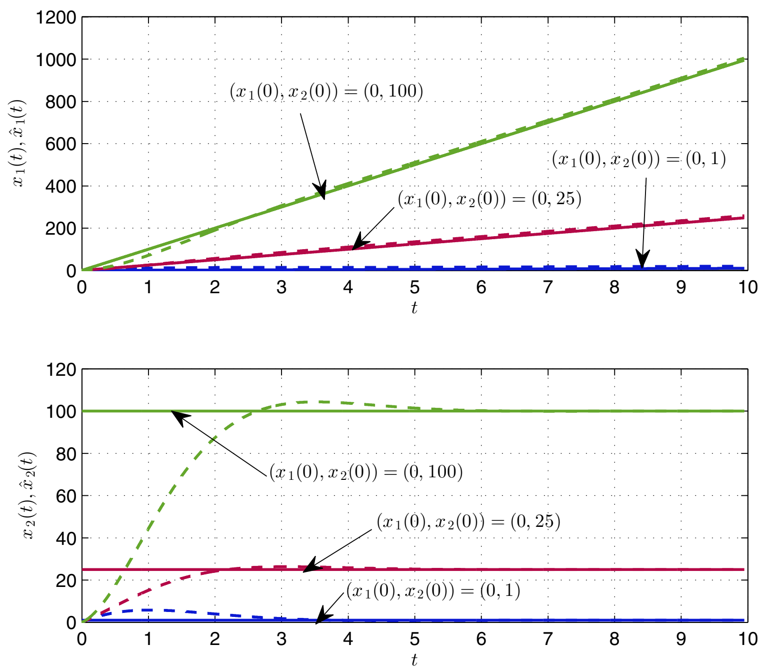

Figure 5.21: Time histories of states for Example 5.5 with $v(t) = 10\sin(10t)$.

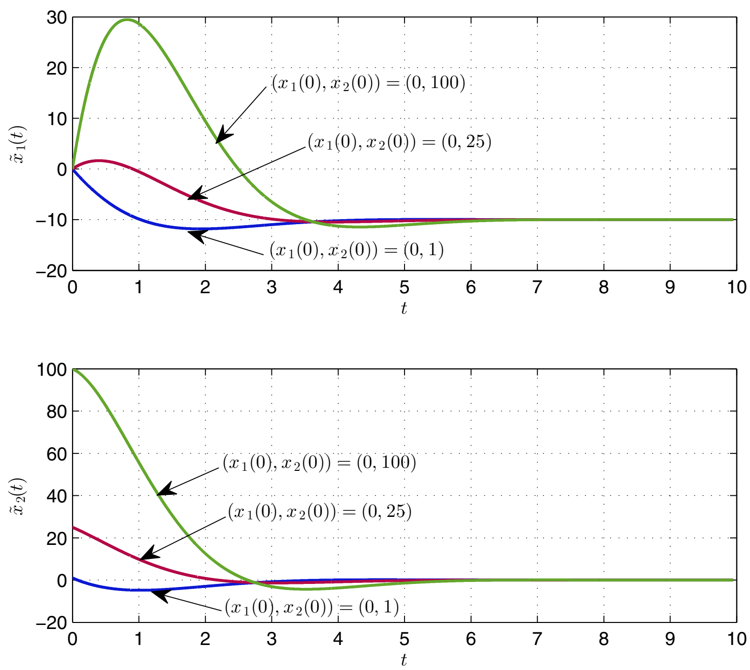

Figure 5.22: Time histories of state estimation errors for Example 5.5 with $v(t) = 10\sin(10t)$.

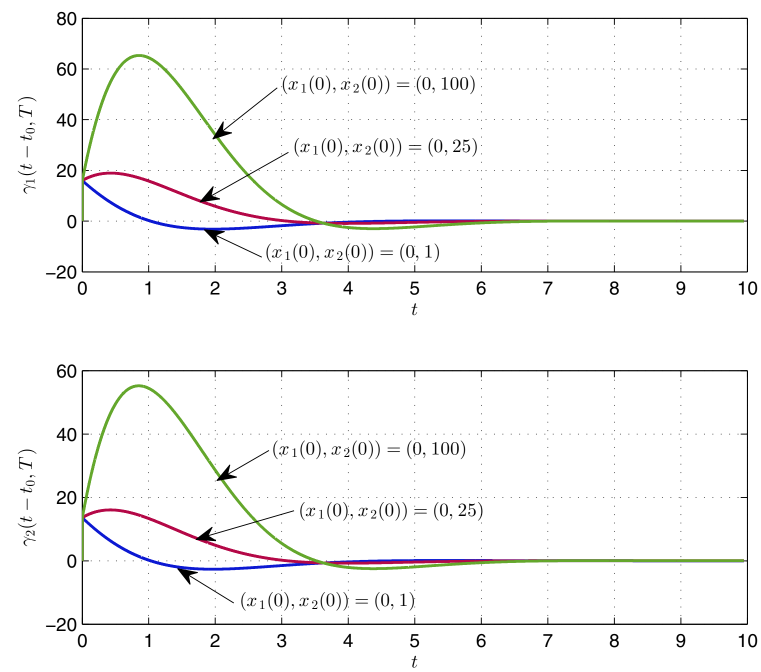

Figure 5.23: Time histories of output estimation error injections for Example 5.5 with $v(t) = 10\sin(10t)$.

5.5 Proofs of results

5.5.1 Proof of Lemma 5.1

Differentiating (5.10), we obtain

$$\dot{\tilde{z}}_i = \sum_{j=1}^{n} \dot{p}^*_{O_{i,j}}(\mu_1)\tilde{\zeta}_j + \sum_{j=1}^{n} p^*_{O_{i,j}}(\mu_1)\dot{\tilde{\zeta}}_j, \quad i = 1,2,...,n. \tag{5.34}$$

Note that differentiating (5.11) gives

$$\begin{aligned}\dot{p}^*_{O_{i,j}}(\mu_1) &= (i-j)\bar{p}_{O_{i,j}}\mu_1^{i-j-1}\left(\frac{1}{T}\mu_1^2\right)\\ &= \frac{i-j}{T}\bar{p}_{O_{i,j}}\mu_1^{i-j+1}.\end{aligned} \tag{5.35}$$

Next, substituting (5.35) and (5.11) into (5.34), and then using (5.13) gives for $i = 1,2,\ldots,n$

$$\begin{aligned}\dot{\tilde{z}}_i &= \sum_{j=1}^{i} \frac{i-j}{T}\bar{p}_{O_{i,j}}\mu_1^{i-j+1}\tilde{\zeta}_j + \sum_{j=1}^{i} \bar{p}_{O_{i,j}}\mu_1^{i-j}\dot{\tilde{\zeta}}_j\\ &= \frac{i-1}{T}\bar{p}_{O_{i,1}}\mu_1^{i}\tilde{\zeta}_1 + \sum_{j=2}^{i}\frac{i-j}{T}\bar{p}_{O_{i,j}}\mu_1^{i-j+1}\tilde{\zeta}_j + \sum_{j=1}^{i}\bar{p}_{O_{i,j}}\mu_1^{i-j}\dot{\tilde{\zeta}}_j.\end{aligned} \tag{5.36}$$

We rewrite the $\dot{\tilde{\zeta}}_j$ terms as follows. By differentiating (5.9) and substituting in (5.5) and (5.6), the transformed error dynamics are

$$\dot{\tilde{\zeta}}_i = -g_i\tilde{\zeta}_1 + \mu_2\tilde{\zeta}_i + \tilde{\zeta}_{i+1}, \quad i = 1,...,n-1, \tag{5.37}$$

$$\dot{\tilde{\zeta}}_n = -g_n\tilde{\zeta}_1 + \mu_2\tilde{\zeta}_n, \tag{5.38}$$

where we have defined $\mu_2 := \dot{\mu}_O/\mu_O = \mu_1(n+m_O)/T$ for notational convenience.

We next substitute in (5.37) and (5.38) for $\dot{\tilde{\zeta}}_j$ in (5.36), which will yield a different expression for $i = 1, \ldots, n-1$ than for $i = n$. For $i = 1, \ldots, n-1$, we obtain

$$\begin{aligned}
\dot{\tilde{z}}_i &= \frac{i-1}{T}\bar{p}_{O_{i,1}}\mu_1^i\tilde{\zeta}_1 + \sum_{j=2}^{i}\frac{i-j}{T}\bar{p}_{O_{i,j}}\mu_1^{i-j+1}\tilde{\zeta}_j + \sum_{j=1}^{i}\bar{p}_{O_{i,j}}\mu_1^{i-j}\left(-g_j\tilde{\zeta}_1 + \mu_2\tilde{\zeta}_j + \tilde{\zeta}_{j+1}\right) \\
&= \frac{i-1}{T}\bar{p}_{O_{i,1}}\mu_1^i\tilde{\zeta}_1 + \sum_{j=2}^{i}\frac{i-j}{T}\bar{p}_{O_{i,j}}\mu_1^{i-j+1}\tilde{\zeta}_j - \sum_{j=1}^{i}g_j\bar{p}_{O_{i,j}}\mu_1^{i-j}\tilde{\zeta}_1 + \frac{n+m_O}{T}\sum_{j=1}^{i}\bar{p}_{O_{i,j}}\mu_1^{i-j+1}\tilde{\zeta}_j \\
&\quad + \sum_{j=1}^{i}\bar{p}_{O_{i,j}}\mu_1^{i-j}\tilde{\zeta}_{j+1}. \qquad (5.39)
\end{aligned}$$

Note that for $i = 1$, from (5.10)–(5.13) we obtain $\tilde{z}_1 = \tilde{\zeta}_1$. Using this fact, writing out the $j = i$ term from the last summation, and using (5.12) gives

$$\begin{aligned}
\dot{\tilde{z}}_i &= \frac{i-1}{T}\bar{p}_{O_{i,1}}\mu_1^i\tilde{z}_1 + \sum_{j=2}^{i}\frac{i-j}{T}\bar{p}_{O_{i,j}}\mu_1^{i-j+1}\tilde{\zeta}_j - \sum_{j=1}^{i}g_j\bar{p}_{O_{i,j}}\mu_1^{i-j}\tilde{z}_1 + \frac{n+m_O}{T}\bar{p}_{O_{i,1}}\mu_1^i\tilde{z}_1 \\
&\quad + \frac{n+m_O}{T}\sum_{j=2}^{i}\bar{p}_{O_{i,j}}\mu_1^{i-j+1}\tilde{\zeta}_j + \sum_{j=1}^{i-1}\bar{p}_{O_{i,j}}\mu_1^{i-j}\tilde{\zeta}_{j+1} + \tilde{\zeta}_{i+1} \\
&= \frac{n+m_O+i-1}{T}\bar{p}_{O_{i,1}}\mu_1^i\tilde{z}_1 - \sum_{j=1}^{i}g_j\bar{p}_{O_{i,j}}\mu_1^{i-j}\tilde{z}_1 + \sum_{j=2}^{i}\frac{n+m_O+i-j}{T}\bar{p}_{O_{i,j}}\mu_1^{i-j+1}\tilde{\zeta}_j \\
&\quad + \sum_{j=1}^{i-1}\bar{p}_{O_{i,j}}\mu_1^{i-j}\tilde{\zeta}_{j+1} + \tilde{\zeta}_{i+1}, \quad i = 1, 2, \ldots, n-1. \qquad (5.40)
\end{aligned}$$

We rewrite the last two terms as follows. For the last summation, define $k := j+1$. Then $j = k-1$, and the summation can be rewritten over k as

$$\sum_{j=1}^{i-1}\bar{p}_{O_{i,j}}\mu_1^{i-j}\tilde{\zeta}_{j+1} = \sum_{k=2}^{i}\bar{p}_{O_{i,k-1}}\mu_1^{i-k+1}\tilde{\zeta}_k. \qquad (5.41)$$

Note, however, that k is a dummy index that will be replaced in order to combine this summation with the others in (5.40). To rewrite $\tilde{\zeta}_{i+1}$, we first obtain from (5.10)–(5.13)

$$\tilde{z}_i = \sum_{j=1}^{i-1}\bar{p}_{O_{i,j}}\mu_1^{i-j}\tilde{\zeta}_j + \tilde{\zeta}_i, \quad i = 1, \ldots, n,$$

or equivalently

$$\tilde{z}_{i+1} = \sum_{j=1}^{i}\bar{p}_{O_{i+1,j}}\mu_1^{i-j+1}\tilde{\zeta}_j + \tilde{\zeta}_{i+1}, \quad i = 0, 1, \ldots, n-1. \qquad (5.42)$$

Then for $i = 1, 2, ..., n-1$, we rewrite (5.40) using (5.41) and (5.42) as

$$\begin{aligned}
\dot{\tilde{z}}_i &= \frac{n+m_O+i-1}{T}\bar{p}_{O_{i,1}}\mu_1^i\tilde{z}_1 - \sum_{j=1}^{i} g_j\bar{p}_{O_{i,j}}\mu_1^{i-j}\tilde{z}_1 + \sum_{j=2}^{i}\frac{n+m_O+i-j}{T}\bar{p}_{O_{i,j}}\mu_1^{i-j+1}\tilde{\zeta}_j \\
&\quad + \sum_{j=2}^{i}\bar{p}_{O_{i,j-1}}\mu_1^{i-j+1}\tilde{\zeta}_j + \tilde{z}_{i+1} - \sum_{j=1}^{i}\bar{p}_{O_{i+1,j}}\mu_1^{i-j+1}\tilde{\zeta}_j \qquad (5.43) \\
&= \frac{n+m_O+i-1}{T}\bar{p}_{O_{i,1}}\mu_1^i\tilde{z}_1 - \sum_{j=1}^{i} g_j\bar{p}_{O_{i,j}}\mu_1^{i-j}\tilde{z}_1 - \bar{p}_{O_{i+1,1}}\mu_1^i\tilde{z}_1 + \tilde{z}_{i+1} \\
&\quad + \sum_{j=2}^{i}\frac{n+m_O+i-j}{T}\bar{p}_{O_{i,j}}\mu_1^{i-j+1}\tilde{\zeta}_j + \sum_{j=2}^{i}\bar{p}_{O_{i,j-1}}\mu_1^{i-j+1}\tilde{\zeta}_j - \sum_{j=2}^{i}\bar{p}_{O_{i+1,j}}\mu^{i-j+1}\tilde{\zeta}_j, \qquad (5.44)
\end{aligned}$$

after writing out the $j = 1$ term of the last summation and using $\tilde{\zeta}_1 = \tilde{z}_1$. Then we combine the summations from $j = 2, ..., i$ to obtain

$$\begin{aligned}
\dot{\tilde{z}}_i &= \frac{n+m_O+i-1}{T}\bar{p}_{O_{i,1}}\mu_1^i\tilde{z}_1 - \sum_{j=1}^{i} g_j\bar{p}_{O_{i,j}}\mu_1^{i-j}\tilde{z}_1 - \bar{p}_{O_{i+1,1}}\mu_1^i\tilde{z}_1 + \tilde{z}_{i+1} \\
&\quad + \sum_{j=2}^{i}\left(\frac{n+m_O+i-j}{T}\bar{p}_{O_{i,j}} + \bar{p}_{O_{i,j-1}} - \bar{p}_{O_{i+1,j}}\right)\mu_1^{i-j+1}\tilde{\zeta}_j. \qquad (5.45)
\end{aligned}$$

We then write out the $j = i$ term from the first summation, which yields for $i = 1, 2, ..., n-1$

$$\begin{aligned}
\dot{\tilde{z}}_i &= \frac{n+m_O+i-1}{T}\bar{p}_{O_{i,1}}\mu_1^i\tilde{z}_1 - \sum_{j=1}^{i-1} g_j\bar{p}_{O_{i,j}}\mu_1^{i-j}\tilde{z}_1 - g_i\tilde{z}_1 - \bar{p}_{O_{i+1,1}}\mu_1^i\tilde{z}_1 + \tilde{z}_{i+1} \\
&\quad + \sum_{j=2}^{i}\left(\frac{n+m_O+i-j}{T}\bar{p}_{O_{i,j}} + \bar{p}_{O_{i,j-1}} - \bar{p}_{O_{i+1,j}}\right)\mu_1^{i-j+1}\tilde{\zeta}_j \\
&= -\left(g_i + \sum_{j=1}^{i-1} g_j\bar{p}_{O_{i,j}}\mu_1^{i-j} + \bar{p}_{O_{i+1,1}}\mu_1^i - \frac{n+m_O+i-1}{T}\bar{p}_{O_{i,1}}\mu_1^i\right)\tilde{z}_1 + \tilde{z}_{i+1} \\
&\quad + \sum_{j=2}^{i}\left(\frac{n+m_O+i-j}{T}\bar{p}_{O_{i,j}} + \bar{p}_{O_{i,j-1}} - \bar{p}_{O_{i+1,j}}\right)\mu_1^{i-j+1}\tilde{\zeta}_j. \qquad (5.46)
\end{aligned}$$

Finally, by selecting the $\{\bar{p}_{O_{i,j}}\}$ for $j < i$ according to (5.14), and the gains $\{g_i(t-t_0,T)\}_{i=1}^{n-1}$ according to (5.16), we obtain (5.18).

Consider now the case for $i = n$. From (5.36) we have

$$\begin{aligned}
\dot{\tilde{z}}_n &= \frac{n-1}{T}\bar{p}_{O_{n,1}}\mu_1^n\tilde{\zeta}_1 + \sum_{j=2}^{n}\frac{n-j}{T}\bar{p}_{O_{n,j}}\mu_1^{n-j+1}\tilde{\zeta}_j + \sum_{j=1}^{n}\bar{p}_{O_{n,j}}\mu_1^{n-j}\dot{\tilde{\zeta}}_j \\
&= \frac{n-1}{T}\bar{p}_{O_{n,1}}\mu_1^n\tilde{\zeta}_1 + \sum_{j=2}^{n}\frac{n-j}{T}\bar{p}_{O_{n,j}}\mu_1^{n-j+1}\tilde{\zeta}_j + \sum_{j=1}^{n-1}\bar{p}_{O_{n,j}}\mu_1^{n-j}\dot{\tilde{\zeta}}_j + \dot{\tilde{\zeta}}_n. \qquad (5.47)
\end{aligned}$$

Now substituting in (5.37) and (5.38) for $\dot{\tilde{\zeta}}_j$ and $\dot{\tilde{\zeta}}_n$, we obtain

$$
\begin{aligned}
\dot{\tilde{z}}_n = & \frac{n-1}{T}\bar{p}_{O_{n,1}}\mu_1^n\tilde{\zeta}_1 + \sum_{j=2}^{n}\frac{n-j}{T}\bar{p}_{O_{n,j}}\mu_1^{n-j+1}\tilde{\zeta}_j + \sum_{j=1}^{n-1}\bar{p}_{O_{n,j}}\mu_1^{n-j}\left(-g_j\tilde{\zeta}_1 + \mu_2\tilde{\zeta}_j + \tilde{\zeta}_{j+1}\right) \\
& - g_n\tilde{\zeta}_1 + \mu_2\tilde{\zeta}_n \\
= & \frac{n-1}{T}\bar{p}_{O_{n,1}}\mu_1^n\tilde{\zeta}_1 + \sum_{j=2}^{n}\frac{n-j}{T}\bar{p}_{O_{n,j}}\mu_1^{n-j+1}\tilde{\zeta}_j - \sum_{j=1}^{n-1}g_j\bar{p}_{O_{n,j}}\mu_1^{n-j}\tilde{\zeta}_1 + \sum_{j=1}^{n-1}\mu_2\bar{p}_{O_{n,j}}\mu_1^{n-j}\tilde{\zeta}_j \\
& + \sum_{j=1}^{n-1}\bar{p}_{O_{n,j}}\mu_1^{n-j}\tilde{\zeta}_{j+1} - g_n\tilde{\zeta}_1 + \mu_2\tilde{\zeta}_n,
\end{aligned}
\tag{5.48}
$$

and after grouping the $\tilde{\zeta}_1$ terms and μ_2 terms, this reduces to

$$
\begin{aligned}
\dot{\tilde{z}}_n = & -\left(g_n + \sum_{j=1}^{n-1}g_j\bar{p}_{O_{n,j}}\mu_1^{n-j} - \frac{n-1}{T}\bar{p}_{O_{n,1}}\mu_1^n\right)\tilde{\zeta}_1 + \sum_{j=2}^{n}\frac{n-j}{T}\bar{p}_{O_{n,j}}\mu_1^{n-j+1}\tilde{\zeta}_j + \sum_{j=1}^{n}\mu_2\bar{p}_{O_{n,j}}\mu_1^{n-j}\tilde{\zeta}_j \\
& + \sum_{j=1}^{n-1}\bar{p}_{O_{n,j}}\mu_1^{n-j}\tilde{\zeta}_{j+1} \\
= & -\left(g_n + \sum_{j=1}^{n-1}g_j\bar{p}_{O_{n,j}}\mu_1^{n-j} - \frac{2n+m_O-1}{T}\bar{p}_{O_{n,1}}\mu_1^n\right)\tilde{\zeta}_1 + \sum_{j=2}^{n}\frac{n-j}{T}\bar{p}_{O_{n,j}}\mu_1^{n-j+1}\tilde{\zeta}_j \\
& + \sum_{j=2}^{n}\frac{n+m_O}{T}\bar{p}_{O_{n,j}}\mu_1^{n-j+1}\tilde{\zeta}_j + \sum_{j=1}^{n-1}\bar{p}_{O_{n,j}}\mu_1^{n-j}\tilde{\zeta}_{j+1},
\end{aligned}
\tag{5.49}
$$

after substituting in $\mu_2 = \mu_1(n+m_O)/T$ and writing out the $j=1$ term. Then after shifting the index of the last summation as before in (5.41), substituting in $\tilde{\zeta}_1 = \tilde{z}_1$, and combining the summations from $j = 2, \ldots, n$, we obtain

$$
\begin{aligned}
\dot{\tilde{z}}_n = & -\left(g_n + \sum_{j=1}^{n-1}g_j\bar{p}_{O_{n,j}}\mu_1^{n-j} - \frac{2n+m_O-1}{T}\bar{p}_{O_{n,1}}\mu_1^n\right)\tilde{z}_1 \\
& + \sum_{j=2}^{n}\left(\frac{2n+m_O-j}{T}\bar{p}_{O_{n,j}} + \bar{p}_{O_{n,j-1}}\right)\mu_1^{n-j+1}\tilde{\zeta}_j.
\end{aligned}
\tag{5.50}
$$

Finally, by selecting the $\{\bar{p}_{O_{n,j}}\}$ for $j < n$ according to (5.15), and the gain g_n according to (5.16) and (5.17), we obtain (5.19). ■

5.5.2 Proof of Lemma 5.2

The transformation (5.10) can be written as

$$\tilde{z} = P_O^*(\mu_1)\tilde{\zeta},$$

where $P_O^*(\mu_1)$ has elements given by (5.11)–(5.15), which show that $P_O^*(\mu_1)$ is unit lower triangular. Then substituting in (5.9) for $\tilde{\zeta}$ and using $\mu = \mu_1^{n+m_O}$ gives

$$\tilde{z} = P_O^*(\mu_1)\mu_1^{n+m_O}\tilde{x}. \tag{5.51}$$

Now factoring out $\mu_1^{m_O+1}$ to the left and defining the matrix $P_O(\mu_1) := P_O^*(\mu_1)\mu_1^{n-1}$ gives (5.20) and (5.21). ■

5.5.3 Proof of Lemma 5.3

From (5.11)–(5.15), it is clear that the matrix $P_O^*(\mu_1)$ is unit lower triangular. Then its inverse exists and is also unit lower triangular. Define $Q_O^* := (P_O^*)^{-1}(\mu_1)$. Since $P_O^*(\mu_1)$ is invertible, and since $\nu = \mu_1^{-1}$, we obtain from (5.51)

$$\tilde{x} = \nu^{n+m_O} Q_O^* \tilde{z}. \tag{5.52}$$

Since Q_O^* is the inverse of $P_O^*(\mu_1)$, the matrix Q_O^* obeys

$$P_O^*(\mu_1) Q_O^* = I_n, \tag{5.53}$$

where I_n is the $n \times n$ identity matrix. After obtaining the elements of $P_O^*(\mu_1)$ from (5.11)–(5.15), we can determine the elements of Q_O^* by solving (5.53) as follows. Denote the $j = 1, 2, \ldots, n$ columns of Q_O^* as $\{q^*_{O_{i,j}}\}_{j=1}^n$, where $i = 1, 2, \ldots, n$ denotes the ith (row) element of each column, such that $Q_O^* = [q^*_{O_{i,1}}, q^*_{O_{i,2}}, \ldots, q^*_{O_{i,n}}]$. Then (5.53) is equivalent to the system of equations

$$P_O^*(\mu_1) q^*_{O_{i,1}} = \mathrm{e}_1, \tag{5.54}$$

$$P_O^*(\mu_1) q^*_{O_{i,2}} = \mathrm{e}_2, \tag{5.55}$$

$$\vdots$$

$$P_O^*(\mu_1) q^*_{O_{i,n}} = \mathrm{e}_n. \tag{5.56}$$

where e_i denotes the ith unit vector. Therefore, after we obtain the elements of $P_O^*(\mu_1)$ from (5.11)–(5.15), we can then obtain the elements of Q_O^* by solving (5.54)–(5.56) with forward substitution.

To illustrate, beginning with (5.54), which corresponds to the $j = 1$ column of I_n, we find from the $i = j = 1$ row the redundant result that $q^*_{O_{1,1}} = 1$. But from the $i = j + 1 = 2$ row of (5.54), we obtain

$$\begin{aligned} q^*_{O_{2,1}} &= -p^*_{O_{2,1}} q^*_{O_{1,1}} \\ &= -p^*_{O_{2,1}}, \end{aligned} \tag{5.57}$$

and then using (5.11) in (5.57) gives

$$\begin{aligned} q^*_{O_{2,1}} &= -\bar{p}_{O_{2,1}} \mu_1^1 \\ &= -\bar{p}_{O_{2,1}} \left(\mu_1^{-1}\right)^{-1} \\ &= -\bar{p}_{O_{2,1}} \nu^{1-2}. \end{aligned}$$

Continuing with rows $i = j+2, j+3, \ldots, n$ gives us the remaining elements of $q^*_{O_{i,1}}$, with each result being of the form $q^*_{O_{i,1}} = f_{i,1}(\{\bar{p}_{O_{i,j}}\})\nu^{1-i}$, where each $f_{i,1}(\{\bar{p}_{O_{i,j}}\})$ is a function of the known constants $\{\bar{p}_{O_{i,j}}\}$. Next, having determined all of the elements of $q^*_{O_{i,1}}$, we proceed with (5.55) for the $j = 2$ column of I_n, and for rows $i = j+1, j+2, \ldots, n$ (in that order), solve for the elements of $q^*_{O_{i,2}}$. We continue this process with the remaining equations through (5.56), always beginning with row $i = j+1$ and working down the rows to finish with row $i = n$. The result of this process yields the matrix $Q^*_O(\nu)$ with elements $\{q^*_{O_{i,j}}(\nu)\}$ of the form

$$q^*_{O_{i,j}}(\nu) = \bar{q}_{O_{i,j}} \nu^{j-i},$$

where the $\{\bar{q}_{O_{i,j}}\}$ are known functions of the known constants $\{\bar{p}_{O_{i,j}}\}$. Having determined the $\{q^*_{O_{i,j}}(\nu)\}$ in this way, we return to (5.52), which now reads

$$\tilde{x} = \nu^{n+m_O} Q^*_O(\nu)\tilde{z}. \tag{5.58}$$

Now factoring out ν^{m_O+1} to the left and defining the matrix $Q_O(\nu) := \nu^{n-1}Q^*_O(\nu)$ gives (5.22) and (5.23).

The finiteness of $\bar{q}_O$ follows from the fact that $|Q_O(\nu)|$ is a continuous function of a bounded argument $\nu \in (0,1]$. ■

5.5.4 Proof of Lemma 5.4

We use induction to prove the claim. For $i = 1$, from (5.16) we have

$$\begin{aligned} g_1(t-t_0,T) &= h_1(\mu_1) \\ &= l_1 + \left(\frac{n+m_O}{T}\bar{p}_{O_{1,1}} - \bar{p}_{O_{2,1}}\right)\mu_1^1 \\ &= \bar{h}_{1,0} + \bar{h}_{1,1}\mu_1^1 \\ &= \sum_{k=0}^{1} \bar{h}_{1,k}\mu_1^k, \end{aligned}$$

where we have defined $\bar{h}_{1,0} := l_1$ and $\bar{h}_{1,1} := \left(\frac{n+m_O}{T}\bar{p}_{O_{1,1}} - \bar{p}_{O_{2,1}}\right)$. Now assume the induction hypothesis, say, for $i = l$,

$$\begin{aligned} g_l(t-t_0,T) &= h_l(\mu_1) \\ &= \sum_{k=0}^{l} \bar{h}_{l,k}\mu_1^k. \end{aligned} \tag{5.59}$$

Then for $i = l+1$, from (5.16) we have

$$\begin{aligned} g_{l+1}(t-t_0,T) &= h_{l+1}(\mu_1) \\ &= l_{l+1} + \left(\frac{n+m_O+l}{T}\bar{p}_{O_{l+1,1}} - \bar{p}_{O_{l+2,1}}\right)\mu_1^{l+1} - \sum_{j=1}^{l} g_j(t-t_0,T)\bar{p}_{O_{l+1,j}}\mu_1^{l+1-j}. \end{aligned} \tag{5.60}$$

For the products in the summation, combine $g_j(t-t_0,T)$ with μ_1^{l+1-j} to define a new polynomial by using (5.59),

$$\begin{aligned} \breve{h}_j(\mu_1) :&= g_j(t-t_0,T)\mu_1^{l+1-j} \\ &= h_j(\mu_1)\mu_1^{l+1-j} \\ &= \sum_{k=0}^{j} \bar{h}_{j,k}\mu_1^{l+1+k-j}. \end{aligned} \tag{5.61}$$

Then (5.60) becomes

$$g_{l+1}(t-t_0,T) = l_{l+1} + \left(\frac{n+m_O+l}{T}\bar{p}_{O_{l+1,1}} - \bar{p}_{O_{l+2,1}}\right)\mu_1^{l+1} - \sum_{j=1}^{l} \bar{p}_{O_{l+1,j}}\breve{h}_j(\mu_1). \tag{5.62}$$

From (5.61), it can be shown that for $j = 1, 2, ..., l$, every $\breve{h}_j(\mu_1)$ is an $(l+1)$th-order polynomial in μ_1. Then from (5.62), it is clear that

$$g_{l+1}(t - t_0, T) = \sum_{k=0}^{l+1} \bar{h}_{l+1,k}\mu_1^k, \tag{5.63}$$

for some constants $\{\bar{h}_{l+1,k}\}$, thus finishing the induction and proving (5.24) for $i = 1, 2, ..., n-1$.

For $i = n$, from (5.17) we have

$$\begin{aligned} g_n(t - t_0, T) &= h_n(\mu_1) \\ &= l_n + \frac{2n + m_O - 1}{T}\bar{p}_{O_{n,1}}\mu_1^n - \sum_{j=1}^{n-1} g_j(t - t_0, T)\bar{p}_{O_{n,j}}\mu_1^{n-j}. \end{aligned} \tag{5.64}$$

In the summation, combine $g_j(t - t_0, T)$ with μ_1^{n-j} to define a new polynomial, by using (5.24) for $i = 1, 2, ..., n-1$ (which we just proved),

$$\begin{aligned} \breve{h}_j^*(\mu_1) :&= g_j(t - t_0, T)\mu_1^{n-j} \\ &= h_j(\mu_1)\mu_1^{n-j} \\ &= \sum_{k=0}^{j} \bar{h}_{j,k}\mu_1^{n+k-j}. \end{aligned} \tag{5.65}$$

Then (5.64) becomes

$$g_n(t - t_0, T) = l_n + \frac{2n + m_O - 1}{T}\bar{p}_{O_{n,1}}\mu_1^n - \sum_{j=1}^{n-1} \bar{p}_{O_{n,j}}\breve{h}_j^*(\mu_1). \tag{5.66}$$

From (5.65), it can be shown that for $j = 1, 2, ..., n-1$, every $\breve{h}_j^*(\mu_1)$ is an nth-order polynomial in μ_1. Then from (5.66), it is clear that (5.24) is true for $i = n$ with some constants $\{\bar{h}_{n,k}\}$ for $k = 0, 1, ..., n$. ■

5.5.5 Proof of Theorem 5.1

The proof of Theorem 5.1 leverages Lemma 5.1, Lemma 5.2, Lemma 5.3, and Lemma 5.4. In the proof of Lemma 5.1, we showed that substituting (5.16) and (5.17) into (5.5) and (5.6) yield (5.18) and (5.19), which can be written as

$$\dot{\tilde{z}}(t) = \Lambda_O \tilde{z}(t),$$

where Λ_O was defined in (5.25). By selecting the constants $\{l_i\}_{i=1}^n$ to make the polynomial $s^n + l_1 s^{n-1} + \ldots + l_n$ and companion matrix Λ_O Hurwitz, there exist positive constants M_z, $\delta_z > 0$ such that for all $t \in [t_0, t_0 + T)$,

$$|\tilde{z}(t)| \leq M_z \mathrm{e}^{-\delta_z(t-t_0)} |\tilde{z}(t_0)|. \tag{5.67}$$

From (5.22) and the last statement in Lemma 5.3, we obtain the estimate

$$\begin{aligned} |\tilde{x}(t)| &\leq |\nu^{m_O+1}||Q_O(\nu)||\tilde{z}(t)| \\ &\leq \nu^{m+1} \bar{q}_O |\tilde{z}(t)|, \end{aligned} \tag{5.68}$$

and from (5.20), we obtain the estimate

$$\begin{aligned} |\tilde{z}(t_0)| &\leq |\mu_1(0,T)^{m_O+1}||P_O(\mu_1(0,T))||\tilde{x}(t_0)| \\ &= |P_O(1)||\tilde{x}(t_0)|. \end{aligned} \tag{5.69}$$

Substituting (5.69) into (5.67), and then the result into (5.68) then give

$$|\tilde{x}(t)| \leq \nu^{m_O+1} \bar{q}_O |P_O(1)| M_z \mathrm{e}^{-\delta_z(t-t_0)} |\tilde{x}(t_0)|. \tag{5.70}$$

Thus we have obtained (5.26) with $\tilde{M} := \bar{q}_O |P_O(1)| M_z$ and $\tilde{\delta} := \delta_z$.

We now consider our claim regarding the output estimation error injection terms, $\{\gamma_i(t - t_0, T)\}_{i=1}^n$. For $i = 1, 2, \ldots, n-1$, multiplying $g_i(t - t_0, T)$ by $\tilde{x}_1(t)$ and then using (5.9) and (2.43) to replace $\tilde{x}_1(t)$ gives

$$\begin{aligned}\gamma_i(t-t_0,T) &= g_i(t-t_0,T)\tilde{x}_1(t),\\ &= g_i(t-t_0,T)\frac{1}{\mu_1^{n+m_O}}\tilde{\zeta}_1(t)\\ &= \nu^{m_O} g_i(t-t_0,T)\nu^n\tilde{z}_1(t),\end{aligned} \tag{5.71}$$

since $\nu = \mu_1^{-1}$ and $\tilde{z}_1(t) = \tilde{\zeta}_1(t)$ by (5.10)–(5.13). Now combine $g_i(t-t_0,T)$ with ν^n to define a new polynomial using (5.24) from Lemma 5.4, such that for $i = 1,2,\ldots,n-1$

$$\begin{aligned}\eta_i(\nu) :&= g_i(t-t_0,T)\nu^n\\ &= h_i(\mu_1)\nu^n\\ &= \sum_{k=0}^{i}\bar{h}_{i,k}\mu_1^k\nu^n\\ &= \sum_{k=0}^{i}\bar{h}_{i,k}\nu^{n-k}.\end{aligned} \tag{5.72}$$

Then (5.71) becomes

$$\gamma_i(t-t_0,T) = \nu^{m_O}\eta_i(\nu)\tilde{z}_1(t), \quad i = 1,2,\ldots,n-1. \tag{5.73}$$

The transformed error $\tilde{z}_1(t)$ is asymptotically stabilized by our choice of the constants $\{l_i\}_{i=1}^n$. Then from (5.72), it is clear that for $i = 1,2,\ldots,n-1$, every $\eta_i(\nu)$ is a polynomial in the argument $\nu \in (0,1]$ for $t \in [t_0,t_0+T)$, thus is bounded and goes to zero as $t \to t_0+T$. Therefore, with $m_O \geq 1$, $\gamma_i(t-t_0,T)$ is uniformly bounded and goes to zero as $t \to t_0+T$ for $i = 1,2,\ldots,n-1$. The claim for $i = n$ is proven the same way. ■

5.5.6 Proof of Lemma 5.5

Consider first the autonomous case with $u(j) = 0$ for all j. The first step back from the initial condition is found from (5.27) with $j = i$,

$$x(i-1) = a(i)x(i). \tag{5.74}$$

Then the second step back is found from (5.27) with $j = i-1$,

$$\begin{aligned} x(i-2) &= a(i-1)x(i-1) \\ &= a(i-1)a(i)x(i), \end{aligned} \tag{5.75}$$

by using (5.74). By now it is clear that the solution to the autonomous case for k steps back from the initial condition is

$$x(i-k) = \Gamma(i-k,i)x(i), \tag{5.76}$$

where we have used (5.28) with $l = 0$. Consider now when $u(j) \neq 0$. Using the same method of substitution above, we find that the expression for k steps back is

$$\begin{aligned} x(i-k) = a(i-(k-1))a(i-(k-2))...a(i-1)a(i)x(i) \\ +a(i-(k-1))a(i-(k-2))...a(i-1)u(i) \\ +a(i-(k-1))a(i-(k-2))...a(i-2)u(i-1) \\ +a(i-(k-1))a(i-(k-2))...a(i-3)u(i-2)+... \\ +a(i-(k-1))u(i-(k-2))+u(i-(k-1)). \end{aligned} \tag{5.77}$$

Then rewriting (5.77) with (5.28) gives

$$\begin{aligned} x(i-k) &= \Gamma(i-k,i)x(i) + \Gamma(i-k,i-1)u(i) \\ &\quad + \Gamma(i-k,i-2)u(i-1) + \ldots \\ &\quad + \Gamma(i-k,i-(k-1))u(i-(k-2)) + u(i-(k-1)) \\ &= \Gamma(i-k,i)x(i) + \sum_{l=0}^{k-1} \Gamma(i-k,i-(l+1))u(i-l). \end{aligned} \tag{5.78}$$

■

5.5.7 Proof of Proposition 5.1

Observe that both (5.14), (5.15) are linear difference equations that can be viewed as discrete-time dynamic systems stepping backward in time, with j playing the role of time, so their solutions are provided by Lemma 5.5. For $i = n$, (5.15) is autonomous, whereas for each $i = n-1, n-2, \ldots, 2$, each equation defined by (5.14) is forced by $\{\bar{p}_{O_{i+1,j}}\}$, for $j = i, i-1, \ldots, 2$. Constrained by the latter, we must solve (5.15) first. Define

$$\begin{aligned} x_n(j) &:= \bar{p}_{O_{n,j}} \\ a_n(j) &:= -\frac{2n + m_O - j}{T}. \end{aligned}$$

Then (5.15) with initial condition (5.12) is written as

$$x_n(j-1) = a_n(j)x_n(j), \quad x_n(n) = 1. \tag{5.79}$$

From Lemma 5.5 and its proof, the solution to (5.79) is given by (5.76) and (5.28) (with $l = 0$),

$$x_n(n-k) = \Gamma(n-k,n)x_n(n). \tag{5.80}$$

But consider now (5.28) (with $l = 0$) for step k, where $0 < k \leq n-1$,

$$\begin{aligned}
\Gamma(n-k,n) &= \prod_{s=0}^{k-1} a_n(n-s) \\
&= \prod_{s=0}^{k-1} \left(-\frac{n+m_O+s}{T} \right) && (5.81) \\
&= \left(\frac{-1}{T} \right)^k (n+m_O+k-1)(n+m_O+k-2)...(n+m_O+1)(n+m_O). && (5.82)
\end{aligned}$$

Now multiplying the numerator and denominator of (5.82) by $(n+m_O-1)!$ results in

$$\Gamma(n-k,n) = \frac{(-1)^k (n+m_O+k-1)!}{T^k (n+m_O-1)!}, \quad 0 < k \leq n-1. \tag{5.83}$$

Then the solution to (5.79) is provided by (5.80), (5.83), and the initial condition $x_n(n) = 1$, which gives

$$x_n(n-k) = \frac{(-1)^k (n+m_O+k-1)!}{T^k (n+m_O-1)!}, \quad 0 < k \leq n-1. \tag{5.84}$$

Define $j := n-k$, so that $k = n-j$. Then since $x_n(j) = \bar{p}_{O_{n,j}}$, (5.84) is rewritten as

$$\begin{aligned}
x_n(j) &= \bar{p}_{O_{n,j}} \\
&= \frac{(-1)^{n-j} (2n+m_O-j-1)!}{T^{n-j} (n+m_O-1)!}, \quad 1 \leq j \leq n-1.
\end{aligned}$$

Now for the systems defined by (5.14) for $i = n-1, n-2, ..., 2$, define

$$\begin{aligned}
x_i(j) &:= \bar{p}_{O_{i,j}} \\
a_i(j) &:= -\frac{n+m_O+i-j}{T} \\
u_i(j) &:= \bar{p}_{O_{i+1,j}}.
\end{aligned}$$

Then (5.14) can be expressed as

$$x_i(j-1) = a_i(j) x_i(j) + u_i(j), \quad x_i(i) = 1. \tag{5.85}$$

From (5.29) under Lemma 5.5, the solution to (5.85) is

$$x_i(i-k) = \Gamma(i-k,i)x_i(i) + \sum_{l=0}^{k-1} \Gamma(i-k,i-(l+1))u_i(i-l). \tag{5.86}$$

As for $i = n$, the transition from the initial condition is

$$\begin{aligned}\Gamma(i-k,i) &= \prod_{s=0}^{k-1} a_i(i-s) \\ &= \frac{(-1)^k(n+m_O+k-1)!}{T^k(n+m_O-1)!},\end{aligned} \tag{5.87}$$

by using (5.81)–(5.83). Then for the inputs,

$$\begin{aligned}\Gamma(i-k,i-(l+1)) &= \prod_{s=l+1}^{k-1} a_i(i-s) \\ &= \prod_{s=l+1}^{k-1}\left(-\frac{n+m_O+s}{T}\right) \\ &= \left(-\frac{1}{T}\right)^{k-(l+1)}(n+m_O+k-1)(n+m_O+k-2)\ldots(n+m_O+l+2)(n+m_O+l+1) \\ &= \frac{(-1)^{k-(l+1)}(n+m_O+k-1)!}{T^{k-(l+1)}(n+m_O+l)!}.\end{aligned} \tag{5.88}$$

Then rewriting (5.86) with (5.87) and (5.88) gives

$$x_i(i-k) = \frac{(-1)^k(n+m_O+k-1)!}{T^k(n+m_O-1)!}x_i(i) + \sum_{l=0}^{k-1}\frac{(-1)^{k-(l+1)}(n+m_O+k-1)!}{T^{k-(l+1)}(n+m_O+l)!}u_i(i-l). \tag{5.89}$$

Define $j := i-k$, so that $k = i-j$. Then (5.89) is rewritten as

$$x_i(j) = \frac{(-1)^{i-j}(n+m_O+i-j-1)!}{T^{i-j}(n+m_O-1)!} + \sum_{l=0}^{i-j-1}\frac{(-1)^{i-j-(l+1)}(n+m_O+i-j-1)!}{T^{i-j-(l+1)}(n+m_O+l)!}u_i(i-l) \tag{5.90}$$

after using $x_i(i) = 1$. Then since $x_i(j) = \bar{p}_{O_{i,j}}$ and $u_i(i-l) = \bar{p}_{O_{i+1,i-l}}$, (5.90) becomes

$$\bar{p}_{O_{i,j}} = \frac{(-1)^{i-j}(n+m_O+i-j-1)!}{T^{i-j}(n+m_O-1)!} + \sum_{l=0}^{i-j-1}\frac{(-1)^{i-j-(l+1)}(n+m_O+i-j-1)!}{T^{i-j-(l+1)}(n+m_O+l)!}\bar{p}_{O_{i+1,i-l}}. \tag{5.91}$$

■

5.6 Acknowledgement

Most of the material in Chapter 5 may appear in a paper by Prof. Krstic and myself entitled "Prescribed-time observers for linear systems in observer canonical form," which is under review for possible publication in *IEEE Transactions on Automatic Control*.

Chapter 6

Prescribed-Time Output Feedback

For linear systems in the controllable canonical form, we introduce a prescribed-time output feedback controller which allows for both easy prescription of the estimation and stabilization convergence times and minimal tuning of the observer and controller parameters. We show that the closed-loop output feedback system exhibits the FT-ISS+C property with respect to the disturbance caused by the estimation error, and in a time that is freely prescribed by the user and independent of initial conditions. In addition, we show that a separation principle holds between the prescribed-time controller and the prescribed-time observer provided the scaling power of the time-varying observer gains exceeds the scaling power of the controller gains by twice the order of the system, i.e., provided the observer is fast enough relative to the controller, irrespective of the constant gains of both.

6.1 Introduction

In this chapter, we leverage the nominal prescribed-time controller of Chapter 4 and the prescribed-time observer of Chapter 5 to develop a prescribed-time output feedback controller for linear systems in the controllable canonical form. In addition, we provide stability results of the output-feedback controller, and demonstrate that a separation principle holds between the observer and the state feedback controller provided the scaling power of the time-varying observer gains exceeds the scaling power of the controller gains by twice the order of the system, i.e., provided the observer is fast enough relative to the controller, irrespective of the constant gains of both.

6.1.1 Existing approaches to finite-time output feedback

Existing approaches to estimation and control in finite time are dominated by sliding modes ([47–50,58,59]) and approaches based on concepts of homogeneity ([37,48,49,71,101]). However, for higher-order systems, these approaches lack constructive methods for selecting observer and controller parameters that allow for prescription of the convergence times a priori. The Implicit Lyapunov Function (ILF) approach used by [19] and [21] does offer controllers and observers for higher-order systems that make *fixed-time* convergence possible (i.e., where the convergence time is independent of initial conditions). However, the parameter tuning process is complicated, since it requires numerical schemes to solve systems of linear matrix inequalities (LMIs). There also exist other state observers that provide for prescription of convergence time, but their implementations are relatively complicated also, since they require the use of time delays ([22]) or a hybrid-systems framework ([54,73]). Some results on finite-time output feedback were provided by [12,16,20,37, 48,52,71], however none of these works offer simple or constructive ways to select controller and observer parameters that allow the user to prescribe the convergence times.

6.1.2 Problem statement

In this chapter, we study output feedback for systems whose solutions are only required to exist on a finite-time interval, $t \in [t_0, t_0 + t_f)$, where $t_0 \geq 0$ is the initial time, and $t_f > t_0$ is the final or terminal time by which we are required to meet the estimation and control objectives. We restrict our analysis to linear single-input single-output (SISO) systems in the controllable canonical form,

$$\dot{x}(t) = Ax(t) + Bu(t) \tag{6.1}$$

$$y(t) = Cx(t), \tag{6.2}$$

where

$$A := \begin{bmatrix} 0 & I_{n-1} & & \\ \vdots & & & \\ -a_0 & -a_1 & \dots & -a_{n-1} \end{bmatrix}, \quad B := \begin{bmatrix} 0 \\ \vdots \\ 1 \end{bmatrix} \tag{6.3}$$

$$C := \begin{bmatrix} b_0 & b_1 & \dots & b_{n-1} \end{bmatrix}. \tag{6.4}$$

Here, $x(t) \in \mathbb{R}^n$ is the state, $u(t) \in \mathbb{R}$ is a known and bounded control input, and $y(t) \in \mathbb{R}$ is the measured output. Our objective is to achieve perfect estimation of the state and stabilize it to the origin within a finite time $T : 0 < T \leq t_f$, in a manner in which T is fixed (independent of initial conditions) and freely prescribed by the user a priori.

6.1.3 Design approach

Our output feedback controller employs the nominal prescribed-time controller of Chapter 4 and the prescribed-time observer of Chapter 5. The controller was developed for nonlinear systems in the normal form, which reduces to the controllable canonical form in the case where the nonlinearities vanish. The observer, however, was developed for linear systems in the observer canonical form. Therefore, to use this controller and observer together, we require a state transformation to relate the different canonical realizations. Toward this end, note that there exists a linear time-invariant coordinate transformation $\mathscr{T}$, such that by defining a new state $\xi(t)$ as

$$\xi(t) := \mathscr{T} x(t), \tag{6.5}$$

the system in controllable canonical form (6.1), (6.2) is transformed into the observer canonical form,

$$\dot{\xi}(t) = \mathscr{A}\xi(t) + \mathscr{B}u(t) - \mathscr{D}y(t) \tag{6.6}$$

$$y(t) = \mathrm{e}_1^T \xi(t), \tag{6.7}$$

where

$$\mathscr{A} := \begin{bmatrix} 0 & I_{n-1} & \\ \vdots & & \\ 0 & \dots & 0 \end{bmatrix}, \quad \mathscr{B} := \begin{bmatrix} b_{n-1} \\ \vdots \\ b_0 \end{bmatrix}, \quad \mathscr{D} := \begin{bmatrix} a_{n-1} \\ \vdots \\ a_0 \end{bmatrix},$$

the a_is and b_is are the same as those in (6.1)–(6.4), and $\mathrm{e}_1 = [1, 0, \dots, 0]^T \in \mathbb{R}^n$ is the first of the n-dimensional unit vectors. Now, we construct a prescribed-time observer for the system (6.6), (6.7) according to Chapter 5 as

$$\dot{\hat{\xi}}(t) = \mathscr{A}\hat{\xi}(t) + \mathscr{B}u(t) - \mathscr{D}y(t) + \begin{bmatrix} g_1(t - t_0, T) \\ \vdots \\ g_n(t - t_0, T) \end{bmatrix} \Big(y(t) - \hat{\xi}_1(t) \Big) \tag{6.8}$$

where the time-varying observer gains $\{g_i(t - t_0, T)\}_{i=1}^n$ are functions of the prescribed convergence time T, with $0 < T \leq t_f$, and must be designed. Then since the relationship (6.5) is known, we calculate the state estimate $\hat{x}(t)$ with

$$\hat{x}(t) = \mathscr{T}^{-1}\hat{\xi}(t). \tag{6.9}$$

The estimate (6.9) is based on the idea that, if the estimate $\hat{\xi}(t)$ tracks $\xi(t)$ well, then $\hat{x}(t)$ might track $x(t)$ with comparable performance by virture of (6.5). Finally, using the state estimate (6.9), we construct a prescribed-time output feedback controller of the form

$$u(t) = -\hat{L}_0(t) - \hat{L}_1(t) - \hat{L}_2(t) - \hat{L}_3(t), \tag{6.10}$$

where $\hat{L}_0(t)$, $\hat{L}_1(t)$, $\hat{L}_2(t)$, and $\hat{L}_3(t)$ are linear time-varying functions of the state estimates. In the following sections, we develop explicit expressions for each of the terms in (6.10).

6.2 Results

6.2.1 Prescribed-time observer

Define the observer error states as

$$\tilde{\xi}_i(t) := \xi_i(t) - \hat{\xi}_i(t), \quad i = 1, \ldots, n. \tag{6.11}$$

Then with (6.6), (6.7), and (6.8), we obtain the error dynamics

$$\dot{\tilde{\xi}}_i(t) = \tilde{\xi}_{i+1}(t) - g_i(t - t_0, T)\tilde{\xi}_1(t), \quad i = 1, \ldots, n-1 \tag{6.12}$$

$$\dot{\tilde{\xi}}_n(t) = -g_n(t - t_0, T)\tilde{\xi}_1(t). \tag{6.13}$$

To facilitate the selection of the observer gains $\{g_i(t - t_0, T)\}_{i=1}^{n}$, we transform the error system (6.12), (6.13) using Lemma 5.1, which we repeat here for the observer (6.8) (written for $\hat{\xi}(t)$).

Lemma 6.1. *Consider the transformation $\tilde{\xi}_i(t) \mapsto \tilde{\zeta}_i(t)$ defined by*

$$\tilde{\zeta}_i(t) := \mu_O(t-t_0,T)\tilde{\xi}_i(t), \quad i=1,...,n, \tag{6.14}$$

and the transformation $\tilde{\zeta}_i(t) \mapsto \tilde{z}_i(t)$ defined by

$$\tilde{z}_i(t) := \sum_{j=1}^{n} p^*_{O_{i,j}}(\mu_1)\tilde{\zeta}_j(t), \quad i=1,...,n, \tag{6.15}$$

where the functions $\{p^*_{O_{i,j}}(\mu_1)\}$ are defined by

$$p^*_{O_{i,j}}(\mu_1) := \bar{p}_{O_{i,j}}\mu_1^{i-j}, \quad 1 \le j \le i \le n, \tag{6.16}$$

and the coefficients $\{\bar{p}_{O_{i,j}}\}$ are constants to be determined. By selecting the $\{\bar{p}_{O_{i,j}}\}$ according to

$$\bar{p}_{O_{i,i}} = 1, \tag{6.17}$$

$$\bar{p}_{O_{i,j}} = 0, \quad j > i, \tag{6.18}$$

for $\{\bar{p}_{O_{i,j}}\}$ with $j \ge i$, the recursion relations

$$\bar{p}_{O_{i,j-1}} = -\frac{n+m_O+i-j}{T}\bar{p}_{O_{i,j}} + \bar{p}_{O_{i+1,j}}, \quad n-1 \ge i \ge j \ge 2, \tag{6.19}$$

$$\bar{p}_{O_{n,j-1}} = -\frac{2n+m_O-j}{T}\bar{p}_{O_{n,j}}, \qquad j=n,n-1,...,2, \tag{6.20}$$

for $\{\bar{p}_{O_{i,j}}\}$ with $j < i$, and the observer gains $\{g_i(t-t_0,T)\}_{i=1}^{n-1}$ according to

$$g_i(t-t_0,T) = l_i + \left(\frac{n+m_O+i-1}{T}\bar{p}_{O_{i,1}} - \bar{p}_{O_{i+1,1}}\right)\mu_1^i - \sum_{j=1}^{i-1} g_j(t-t_0,T)\bar{p}_{O_{i,j}}\mu_1^{i-j}, \tag{6.21}$$

and $g_n(t-t_0,T)$ according to

$$g_n(t-t_0,T) = l_n + \frac{2n+m_O-1}{T}\bar{p}_{O_{n,1}}\mu_1^n - \sum_{j=1}^{n-1} g_j(t-t_0,T)\bar{p}_{O_{n,j}}\mu_1^{n-j}, \tag{6.22}$$

where the $\{l_i\}_{i=1}^n$ are constants to be selected, the observer error system (6.12), (6.13) is transformed into

$$\dot{\tilde{z}}_i(t) = \tilde{z}_{i+1}(t) - l_i\tilde{z}_1(t), \quad i=1,...,n-1, \tag{6.23}$$

$$\dot{\tilde{z}}_n(t) = -l_n\tilde{z}_1(t). \tag{6.24}$$

The system (6.23), (6.24) is stabilized by selecting the constants $\{l_i\}_{i=1}^n$ to make the polynomial $s^n + l_1 s^{n-1} + \ldots + l_n$ and the companion matrix Λ_O Hurwitz, where Λ_O is defined from (6.23), (6.24) as

$$\Lambda_O := \begin{bmatrix} -l_1 & I_{n-1} \\ \vdots & \\ -l_n & 0 \end{bmatrix}. \tag{6.25}$$

Prescribed-time convergence of the observer (6.8) is provided by Theorem 5.1, restated here as a lemma (written for $\hat{\xi}(t)$).

Lemma 6.2. *For the dynamic system (6.1), (6.2) defined on the finite time interval $t \in [t_0, t_0 + T)$, consider the observer (6.8) having error dynamics (6.12), (6.13) and observer gains $\{g_i(t - t_0, T)\}_{i=1}^n$ given by (6.21), (6.22) where the $\{l_i\}_{i=1}^n$ are constants to be selected. If the constants $\{l_i\}_{i=1}^n$ are selected such that the polynomial $s^n + l_1 s^{n-1} + \ldots + l_n$ and the companion matrix (6.25) are both Hurwitz, then the system (6.12), (6.13) has a FT-GUAS equilibrium at the origin, with a prescribed convergence time T, and there exist positive constants $\tilde{M}$, $\tilde{\delta} > 0$ such that*

$$|\tilde{\xi}(t)| \leq \nu(t - t_0, T)^{m_O+1} \tilde{M} \mathrm{e}^{-\tilde{\delta}(t-t_0)} |\tilde{\xi}(t_0)|, \tag{6.26}$$

for all $t \in [t_0, t_0 + T)$, where $\nu(t - t_0, T)$ is defined in (2.42), and $m_O \geq 1$ is an integer and a design parameter. Furthermore, the output estimation error injection terms $\gamma_i(t - t_0, T) := g_i(t - t_0, T)\tilde{\xi}_1(t)$ for $i = 1, \ldots, n$ remain uniformly bounded over $[t_0, t_0 + T)$, and also converge to zero as $t \to t_0 + T$.

In summary, the convergence time $T : 0 < T \leq t_f$ is a free parameter selected by the user, the parameters $\{l_i\}_{i=1}^n$ are selected by pole placement, and m_O is an integer tuning parameter. The constant coefficients $\{\bar{p}_{O_{i,j}}\}$ for $j < i$ are explicitly provided by the recursion relations (6.19), (6.20), and are calculated using the algorithm of Section 5.2.4. Finally, the observer gains $\{g_i(t - t_0, T)\}_{i=1}^n$ provided by (6.21), (6.22) are then easily calculated recursively.

6.2.2 Prescribed-time controller

Prescribed-time stabilization of the state to the origin will be achieved using the nominal controller provided by Theorem 4.2. The controller employs a change-of-coordinates transformation of the state,

$$w_1(t) = \mu_C(t-t_0,T)x_1(t), \tag{6.27}$$

$$w_q(t) = dw_{q-1}(t)/dt, \quad q = 2,...,n+1, \tag{6.28}$$

and we denote $w_{n+1}(t) = \dot{w}_n(t)$ and $x_{n+1}(t) = \dot{x}_n(t)$. We also define

$$r_1(t) := [w_1(t),...,w_{n-1}(t)]^T = J_1 w(t) \in \mathbb{R}^{n-1} \tag{6.29}$$

$$r_2(t) := \dot{r}_1(t) = [w_2(t),...,w_n(t)]^T = J_2 w(t) \in \mathbb{R}^{n-1}$$

where

$$J_1 := [I_{n-1}, 0_{(n-1)\times 1}], \quad J_2 := [0_{(n-1)\times 1}, I_{n-1}],$$

and $K_{n-1} := [k_1,...,k_{n-1}]^T \in \mathbb{R}^{n-1}$, where K_{n-1} is an appropriately chosen coefficient vector so that the polynomial $s^{n-1} + k_{n-1}s^{n-2} + ... + k_1$ and the matrix

$$\Lambda_C := \begin{bmatrix} 0 & & I_{n-2} & \\ & & & \\ -k_1 & -k_2 & \dots & -k_{n-1} \end{bmatrix} \tag{6.30}$$

are both Hurwitz. The state $w_n(t)$ is replaced by a new variable $\sigma(t)$ defined as

$$\sigma(t) := w_n(t) + K_{n-1}^T r_1(t), \tag{6.31}$$

which results in the transformed system

$$\dot{r}_1(t) = \Lambda_C r_1(t) + \mathrm{e}_{n-1}\sigma(t) \tag{6.32}$$

$$\dot{\sigma}(t) = \dot{w}_n(t) + K_{n-1}^T J_2 w(t). \tag{6.33}$$

The latter equation (6.33) is rewritten by substitution of $\dot{w}_n(t) = w_{n+1}(t)$ first, then using (4.48) and writing out the $k = 0$ term from the sum, and lastly, using $\dot{x}_n(t) = x_{n+1}(t)$. This yields

$$\begin{aligned}\dot{\sigma}(t) &= \mu_C \dot{x}_n(t) + \sum_{k=1}^{n} \begin{pmatrix} n \\ k \end{pmatrix} \mu_C^{(k)} x_{n+1-k}(t) + K_{n-1}^T J_2 w(t) \\ &= \mu_C \left(\dot{x}_n(t) + \sum_{k=1}^{n} \begin{pmatrix} n \\ k \end{pmatrix} \frac{\mu_C^{(k)}}{\mu_C} x_{n+1-k}(t) + \nu^{n+m_C} K_{n-1}^T J_2 w(t) \right). \end{aligned} \tag{6.34}$$

We now substitute in the last row of (6.1) to obtain

$$\dot{\sigma}(t) = \mu_C \left(u(t) - a^T x(t) + \sum_{k=1}^{n} \begin{pmatrix} n \\ k \end{pmatrix} \frac{\mu_C^{(k)}}{\mu_C} x_{n+1-k}(t) + \nu^{n+m_C} K_{n-1}^T J_2 w(t) \right) \tag{6.35}$$

where the vector $a \in \mathbb{R}^n$ is defined from (6.1) as $a := [a_0, a_1, ..., a_{n-1}]^T$. Finally, (6.35) is rewritten as

$$\dot{\sigma}(t) = \mu_C \left(u(t) + L_0(t) + L_1(t) + L_2(t) \right) \tag{6.36}$$

where

$$L_0(t) := \sum_{k=1}^{n} \begin{pmatrix} n \\ k \end{pmatrix} \frac{\mu_C^{(k)}}{\mu_C} x_{n+1-k}(t), \tag{6.37}$$

$$L_1(t) := \nu^{n+m_C} K_{n-1}^T J_2 w(t) \tag{6.38}$$

$$L_2(t) := -a^T x(t). \tag{6.39}$$

Using these definitions, we paraphrase Theorem 4.2 as another lemma. Note that in this case, the known $f(x,t)$ in Theorem 4.2 equals $L_2(t)$ as defined in (6.39).

Lemma 6.3. *Select $k_n > 0$. Then the system (6.1), (6.3) with the controller*

$$u(t) = -\left(L_0(t) + L_1(t) + L_2(t) + k_n\sigma(t)\right) \tag{6.40}$$

with $L_0(t)$, $L_1(t)$, and $L_2(t)$ as defined in (6.37)–(6.39) and $\sigma(t)$ as defined in (6.31) has a FT-GUAS equilibrium at the origin, with a prescribed convergence time T, and there exist $\tilde{M}$, $\tilde{\delta} > 0$ such that

$$|x(t)| \leq \nu(t - t_0, T)^{m_C+1}\tilde{M}\mathrm{e}^{-\tilde{\delta}(t-t_0)}|x(t_0)| \tag{6.41}$$

for all $t \in [t_0, t_0 + T)$. Furthermore, the control $u(t)$ remains uniformly bounded over $[t_0, t_0 + T)$, and also converges to zero as $t \to t_0 + T$.

Because of Lemma 6.3, we define the linear feedback with $k_n > 0$ as

$$\begin{aligned} L_3(t) &:= k_n\sigma(t) \qquad (6.42)\\ &= k_n\left(w_n(t) + K_{n-1}^T r_1(t)\right)\\ &= k_n\left(\mathrm{e}_n^T + K_{n-1}^T J_1\right)w(t) \qquad (6.43) \end{aligned}$$

after using (6.31) and (6.29). Then using (6.42), the controller (6.40) becomes

$$u(t) = -\left(L_0(t) + L_1(t) + L_2(t) + L_3(t)\right). \tag{6.44}$$

The quantities $L_0(t)$, $L_1(t)$, $L_2(t)$, and $L_3(t)$ are linear feedbacks of the state, and can be written in terms of either the original state variables or the transformed ones. The former are more useful for implementation, while the latter facilitate stability analyses. In terms of the transformed variables, we have

$$L_0(t) = \nu^{m_C} l_0(\nu)w(t) \tag{6.45}$$

$$L_1(t) = \nu^{n+m_C} K_{n-1}^T J_2 w(t) \tag{6.46}$$

$$L_2(t) = -\nu^{m_C+1} a^T Q_C(\nu)w(t) \tag{6.47}$$

$$L_3(t) = k_n\left(\mathrm{e}_n^T + K_{n-1}^T J_1\right)w(t) \tag{6.48}$$

where (6.45) comes from (4.33) in Lemma 4.4, and (6.47) results from using (4.19) of Lemma 4.3 in (6.39). Then to summarize $L_0(t)$, $L_1(t)$, $L_2(t)$, and $L_3(t)$ in terms of the original state variables, we use (4.16) of Lemma 4.2 to replace $w(t)$ in (6.45)–(6.48), which gives

$$L_0(t) = \mu_1 l_0(\nu) P_C(\mu_1) x(t) \tag{6.49}$$

$$L_1(t) = \mu_1^{1-n} K_{n-1}^T J_2 P_C(\mu_1) x(t) \tag{6.50}$$

$$L_2(t) = -a^T x(t) \tag{6.51}$$

$$L_3(t) = \mu_1^{m_C+1} k_n \left(\mathrm{e}_n^T + K_{n-1}^T J_1\right) P_C(\mu_1) x(t). \tag{6.52}$$

Lastly, note that as with the observer, $T : 0 < T \leq t_f$ is a free parameter selected by the user, the parameters $\{k_i\}_{i=1}^{n-1}$ are selected by pole placement, and m_C is an integer tuning parameter. The user can select any $k_n > 0$, and then the remaining coefficients needed to build the controller are provided by the explicit formulas of Lemma 4.2 and Lemma 4.4.

6.2.3 Synthesis

Having only the measured output and state estimate available for feedback, define the quantities

$$\hat{L}_0(t) := \mu_1 l_0(\nu) P_C(\mu_1) \hat{x}(t) \tag{6.53}$$

$$\hat{L}_1(t) := \mu_1^{1-n} K_{n-1}^T J_2 P_C(\mu_1) \hat{x}(t) \tag{6.54}$$

$$\hat{L}_2(t) = -a^T \hat{x}(t) \tag{6.55}$$

$$\hat{L}_3(t) := \mu_1^{m_C+1} k_n \left(\mathrm{e}_n^T + K_{n-1}^T J_1\right) P_C(\mu_1) \hat{x}(t) \tag{6.56}$$

where $\hat{L}_0(t)$, $\hat{L}_1(t)$, $\hat{L}_2(t)$, and $\hat{L}_3(t)$ are simply (6.49)–(6.52) with $x(t)$ replaced by $\hat{x}(t)$. We then replace the controller (6.44) with the output feedback

$$u(t) = -(\hat{L}_0(t)+\hat{L}_1(t)+\hat{L}_2(t)+\hat{L}_3(t)) \tag{6.57}$$

$$= -\Big(\mu_1 l_0(\nu)P_C(\mu_1)+\mu_1^{1-n}K_{n-1}^T J_2 P_C(\mu_1) - a^T + \mu_1^{m_C+1}k_n\left(\mathrm{e}_n^T + K_{n-1}^T J_1\right)P_C(\mu_1)\Big)\hat{x}(t). \tag{6.58}$$

Using (6.9), (6.11), and (6.5), we obtain

$$\hat{x}(t) = x(t) - \mathscr{T}^{-1}\tilde{\xi}(t). \tag{6.59}$$

Then substituting (6.59) into (6.58) gives

$$u(t) = -\Big(\mu_1 l_0(\nu)P_C(\mu_1)+\mu_1^{1-n}K_{n-1}^T J_2 P_C(\mu_1) - a^T \tag{6.60}$$

$$+\mu_1^{m_C+1}k_n\left(\mathrm{e}_n^T + K_{n-1}^T J_1\right)P_C(\mu_1)\Big)\left(x(t)-\mathscr{T}^{-1}\tilde{\xi}(t)\right)$$

$$= -(L_0(t)+L_1(t)+L_2(t)+L_3(t)) + (\tilde{L}_0(t)+\tilde{L}_1(t)+\tilde{L}_2(t)+\tilde{L}_3(t)) \tag{6.61}$$

where we have defined

$$\tilde{L}_0(t) := \mu_1 l_0(\nu)P_C(\mu_1)\mathscr{T}^{-1}\tilde{\xi}(t) \tag{6.62}$$

$$\tilde{L}_1(t) := \mu_1^{1-n}K_{n-1}^T J_2 P_C(\mu_1)\mathscr{T}^{-1}\tilde{\xi}(t) \tag{6.63}$$

$$\tilde{L}_2(t) := -a^T\mathscr{T}^{-1}\tilde{\xi}(t) \tag{6.64}$$

$$\tilde{L}_3(t) := \mu_1^{m_C+1}k_n\left(\mathrm{e}_n^T + K_{n-1}^T J_1\right)P_C(\mu_1)\mathscr{T}^{-1}\tilde{\xi}(t). \tag{6.65}$$

The second group of terms in parentheses on the right-hand side of (6.61) can be viewed as an "input error" that acts as a disturbance against the controller, which we define as the quantity

$$\tilde{u}(t) := \tilde{L}_0(t)+\tilde{L}_1(t)+\tilde{L}_2(t)+\tilde{L}_3(t). \tag{6.66}$$

Then with (6.66), (6.61) becomes

$$u(t) = -(L_0(t) + L_1(t) + L_2(t) + L_3(t)) + \tilde{u}(t). \tag{6.67}$$

In summary, (6.57) is equivalent to (6.67).

6.2.4 Stability analysis

Observe from (6.67) that the stability of the output feedback system obtained by using the controller (6.57) depends on the behavior of the input error, $\tilde{u}(t)$. The following lemmas show how desirable $\tilde{u}(t)$ dynamics can be obtained. The proofs are provided later in Section 6.5.

Lemma 6.4. *By selecting the constants $\{l_i\}_{i=1}^{n}$ to make the polynomial $s^n + l_1 s^{n-1} + \ldots + l_n$ and the companion matrix Λ_O Hurwitz, and selecting the integers $m_O \geq 1$ and $m_C \geq 1$ according to*

$$m_O \geq m_C + 2n - 1, \tag{6.68}$$

the input error $\tilde{u}(t)$ defined by (6.66) remains bounded for all $t \in [t_0, t_0 + T)$, and also goes to zero as $t \to t_0 + T$.

When the dynamic system (6.1), (6.2) is reduced to a chain of integrators, the method of proving Lemma 6.4 results in a less-restrictive constraint on m_O, as captured in the next lemma.

Lemma 6.5. *Suppose (6.1), (6.2) is replaced by an nth-order chain of integrators. Then by selecting the constants $\{l_i\}_{i=1}^{n}$ to make the polynomial $s^n + l_1 s^{n-1} + \ldots + l_n$ and the companion matrix Λ_O Hurwitz, and the integers $m_O \geq 1$ and $m_C \geq 1$ such that*

$$m_O \geq m_C + n, \tag{6.69}$$

the input error $\tilde{u}(t)$ defined by (6.66) remains uniformly bounded over $t \in [t_0, t_0 + T)$, and also goes to zero as $t \to t_0 + T$.

As shown in the proofs later, the first part of Lemma 6.4 can be proven using a slightly different approach which yields an additional result as captured in the next lemma.

Lemma 6.6. *By selecting the constants $\{l_i\}_{i=1}^n$ to make the polynomial $s^n + l_1 s^{n-1} + \ldots + l_n$ and the companion matrix Λ_O Hurwitz, and the integers $m_O \geq 1$ and $m_C \geq 1$ according to (6.68), the function $|\tilde{u}(t)|$ remains uniformly bounded over $t \in [t_0, t_0 + T)$, and also goes to zero as $t \to t_0 + T$. Furthermore, there exists a positive integer α and positive constants M_α, δ_α such that*

$$|\tilde{u}(t)| \leq \nu(t - t_0, T)^{\alpha} M_\alpha \mathrm{e}^{-\delta_\alpha (t - t_0)} |\tilde{\xi}(t_0)|. \tag{6.70}$$

As shown in the proof later, Lemma 6.6 is required to prove the following stability result for the closed-loop system.

Lemma 6.7. *Consider the system (6.1)–(6.4) with observer (6.8) and the controller given by (6.67). If the constants $\{k_i\}_{i=1}^{n-1}$ and $\{l_i\}_{i=1}^n$ are selected such that the matrices Λ_C and Λ_O are Hurwitz, k_n is selected positive, and if the integers $m_O \geq 1$ and $m_C \geq 1$ are selected according to (6.68), then the closed-loop output feedback system is FT-ISS+C, and there exist $\check{M}$, $\check{\delta}, \check{\gamma} > 0$ such that for all $t \in [t_0, t_0 + T)$,*

$$|x(t)| \leq \nu(t - t_0, T)^{m_C + 1} \left(\check{M} \mathrm{e}^{-\check{\delta}(t - t_0)} |x(t_0)| + \check{\gamma} ||\tilde{u}||_{[t_0, t]} \right). \tag{6.71}$$

Furthermore, the control $u(t)$ remains uniformly bounded over $[t_0, t_0 + T)$.

By leveraging the previous results, we are able to prove our main result for our prescribed-time output feedback controller, which is the separation principle between the prescribed-time observer (6.8) and the prescribed-time controller (6.57).

Theorem 6.1. *Consider the system (6.1)–(6.4) with observer (6.8) and the controller given by (6.57). If the constants $\{k_i\}_{i=1}^{n-1}$ and $\{l_i\}_{i=1}^{n}$ are selected such that the matrices Λ_C and Λ_O are Hurwitz, k_n is selected positive, and the integers $m_O \geq 1$ and $m_C \geq 1$ are selected according to (6.68), then the quantity $|x(t)| + |\hat{\bar{\xi}}(t)|$ is FT-GUAS, and there exists a positive constant $\bar{M}$ such that for all $t \in [t_0, t_0 + T)$,*

$$|x(t)| + |\hat{\bar{\xi}}(t)| \leq \nu(t - t_0, T)^{m_C + 1} \bar{M} \left(|x(t_0)| + |\hat{\bar{\xi}}(t_0)| \right). \tag{6.72}$$

6.3 Discussion

6.3.1 Implementation

The main benefit of this approach to finite-time stabilization is the ability to very simply select observer and controller parameters that prescribe the convergence times. The parameters $\{l_i\}_{i=1}^{n}$ and $\{k_i\}_{i=1}^{n}$, which stabilize the transformed systems, are selected by pole placement, and the integer tuning parameters $m_O \geq 1$, $m_C \geq 1$ are arbitrary. But most importantly, the parameter $T : 0 < T \leq t_f$ is arbitrary, in contrast to most existing methods for finite-time stabilization, wherein the convergence time depends upon initial conditions.

On the other hand, the main drawback of our approach is clear; our output feedback controller was developed for linear systems having no plant or measurement uncertainties, which is limiting in practice. The robust controller of Theorem 4.3 is able to accommodate plant nonlinearities and uncertainties, however the observer of Chapter 5 was designed assuming no such disturbances and perfect measurements. Simulation analyses suggest the observer has some robustness to pseudo-random measurement noise (see Example 5.3), but rigorous treatments of measurement disturbances have not yet been initiated and are open problems for future work.

Lastly, as discussed in Chapter 4 and Chapter 5, the use of the observer (6.8) and controller

(6.57) in practice will exhibit numerical instability in the final instants as $t \to t_0 + T$. This feature of the approach considered here is simply the unavoidable result of implementation on digital computers, wherein the precision of arithmetic with very large and very small numbers is limited to finite values. For a given problem, the exact time at which instability will occur is difficult to determine a priori, because it depends upon the maximum real number representation of the computer performing the calculations, as well as the numerical method and time step size employed. However, as also discussed in these works, there exist simple solutions to circumvent the numerical instability, and yield effective observers and controllers in practice. Section 4.3.1 discussed two options: *1)* the use of a deadzone, in which the feedback is turned off once the state is within an acceptable neighborhood of the origin, and *2)* setting T to some value slightly larger than t_f. Section 5.3.1 proposed yet another option, in which the gains are monitored until they approach some large value set by the user, in order to turn off the observer (or controller) feedbacks once the gains approach this large value. All of these solutions decrease the accuracy of the approach, but in manageable ways that can be tuned if desired. Adding this tuning to the minimal parameter tuning mentioned above still results in constructive, straightforward ways to select parameters for the observer and controller to achieve the desired convergence times.

6.4 Example

We illustrate the performance of the output feedback controller (6.57) through a pedagogical example.

Example 6.1. Consider the double integrator with only the first state measured as output,

$$\dot{x}_1(t) = x_2(t),$$

$$\dot{x}_2(t) = u(t),$$

$$y(t) = x_1(t).$$

Using (6.49)–(6.52) and Lemma 4.2 and Lemma 4.4, we find the state feedback controller (6.44) to be

$$u(t) = -\kappa(t-t_0,T)x(t) \tag{6.73}$$

where $\kappa(t-t_0,T) := [\kappa_1(t-t_0,T), \kappa_2(t-t_0,T)]$, and

$$\kappa_1(t-t_0,T) = k_1\frac{m_C+2}{T}\mu_1 + \frac{(m_C+3)(m_C+2)}{T^2}\mu_1^2 + k_1k_2\mu_1^{m_C+2} + k_2\frac{m_C+2}{T}\mu_1^{m_C+3}$$
$$\kappa_2(t-t_0,T) = k_1 + 2\frac{m_C+2}{T}\mu_1 + k_2\mu_1^{m_C+2}.$$

However, having only the measured output and state estimate available for feedback, we replace $x(t)$ in (6.73) with $\hat{x}(t)$ and use (6.9) to implement the control

$$u(t) = -\kappa(t-t_0,T)\hat{\xi}(t),$$

since $\mathscr{T}^{-1}$ equals identity for the chain of integrators. The state estimate $\hat{\xi}(t)$ is obtained from the observer (6.8), which for this example becomes

$$\dot{\hat{\xi}}_1(t) = \hat{\xi}_2(t) + g_1(t-t_0,T)\left(y(t) - \hat{\xi}_1(t)\right),$$
$$\dot{\hat{\xi}}_2(t) = u(t) + g_2(t-t_0,T)\left(y(t) - \hat{\xi}_1(t)\right).$$

Using (6.17)–(6.20) and the algorithm provided in Section 5.2.4, we obtain the constants $\bar{p}_{O_{1,1}} = \bar{p}_{O_{2,2}} = 1$, $\bar{p}_{O_{1,2}} = 0$, and $\bar{p}_{O_{2,1}} = -\frac{m_O+2}{T}$. Then from (6.21) and (6.22), $g_1(t-t_0,T)$ and $g_2(t-t_0,T)$

are found to be

$$g_1(t-t_0,T) = l_1 + 2\frac{m_O+2}{T}\mu_1,$$
$$g_2(t-t_0,T) = l_2 + l_1\frac{m_O+2}{T}\mu_1 + \frac{(m_O+1)(m_O+2)}{T^2}\mu_1^2.$$

Figures 6.1–6.5 show simulation results of this example with $t_0 = 0$, $t_f = 10$, $m_C = 1$ and $m_O = 3$ (see Lemma 6.5), and $l_1 = l_2 = k_1 = k_2 = 1$, for three sets of initial conditions: $(x_1(0), x_2(0)) = (20, -8)$, $(x_1(0), x_2(0)) = (-12, 10)$, and $(x_1(0), x_2(0)) = (-30, 25)$. In all cases, the state observer was initialized to $(\hat{\xi}_1(0), \hat{\xi}_2(0)) = (0,0)$. To ensure stabilization at $t = t_f$ without numerical instability, as discussed in Section 6.3.1, we set $T = 10.8$. Figure 6.1 shows the dynamics of the state and state estimate, and Figure 6.2 shows the dynamics of the estimation error. As proven in Theorem 6.1, stabilization of both the state and state estimate is obtained in the prescribed time. The control input is shown in Figure 6.4, and the observer gains and controller gains are shown in Figure 6.5. Despite the latter going to infinity as $t \to t_0 + T$, the control input remains bounded, as proven in Lemma 6.7, and in this case goes to zero as $t \to t_0 + T$.

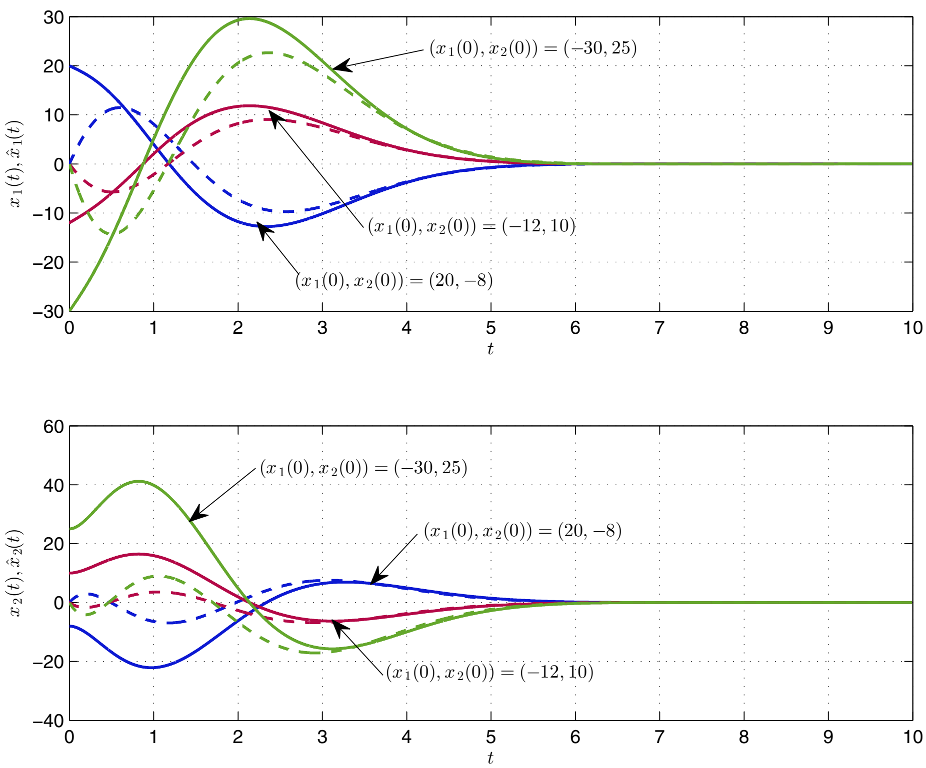

Figure 6.1: Time histories of states and state estimates for Example 6.1. Solid lines denote the states, and dashed lines denote the state estimates.

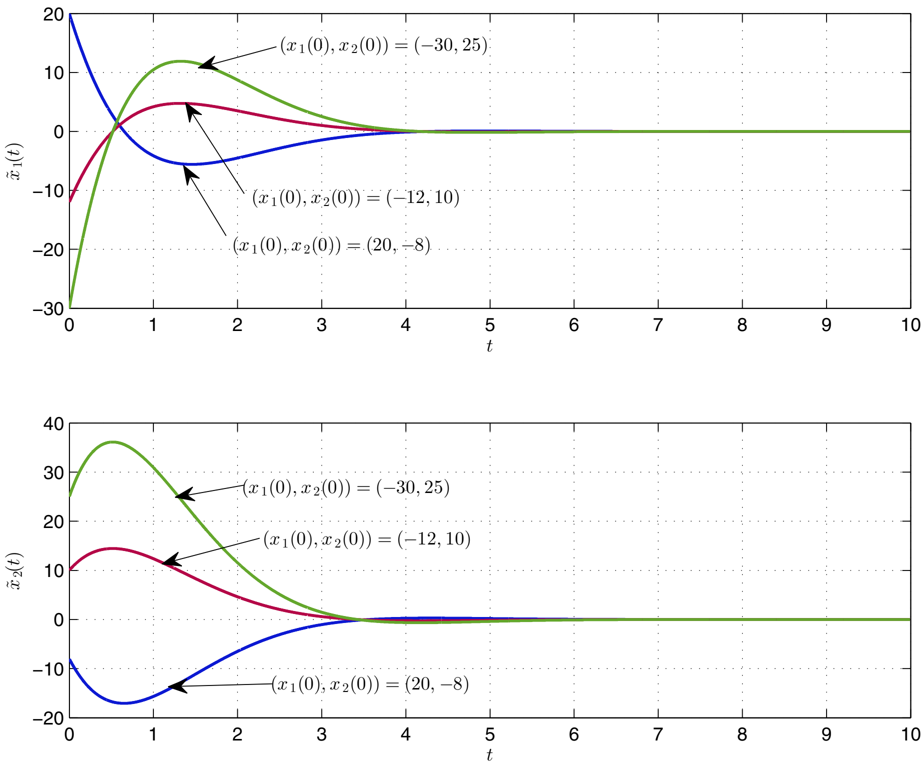

Figure 6.2: Time histories of state estimation errors for Example 6.1.

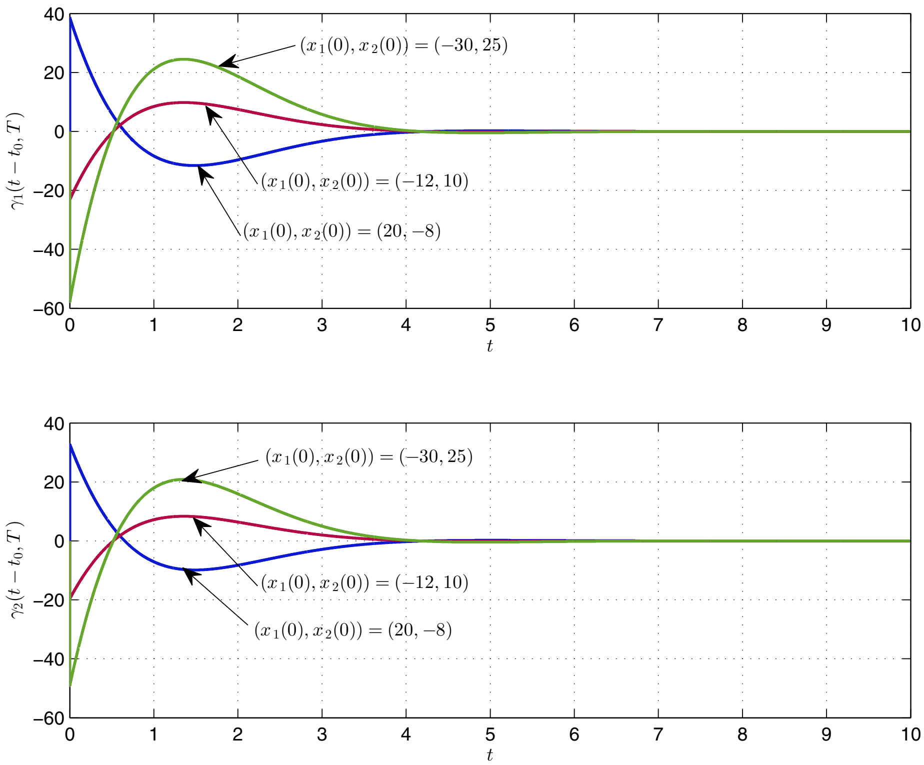

Figure 6.3: Time histories of output estimation error injections for Example 6.1.

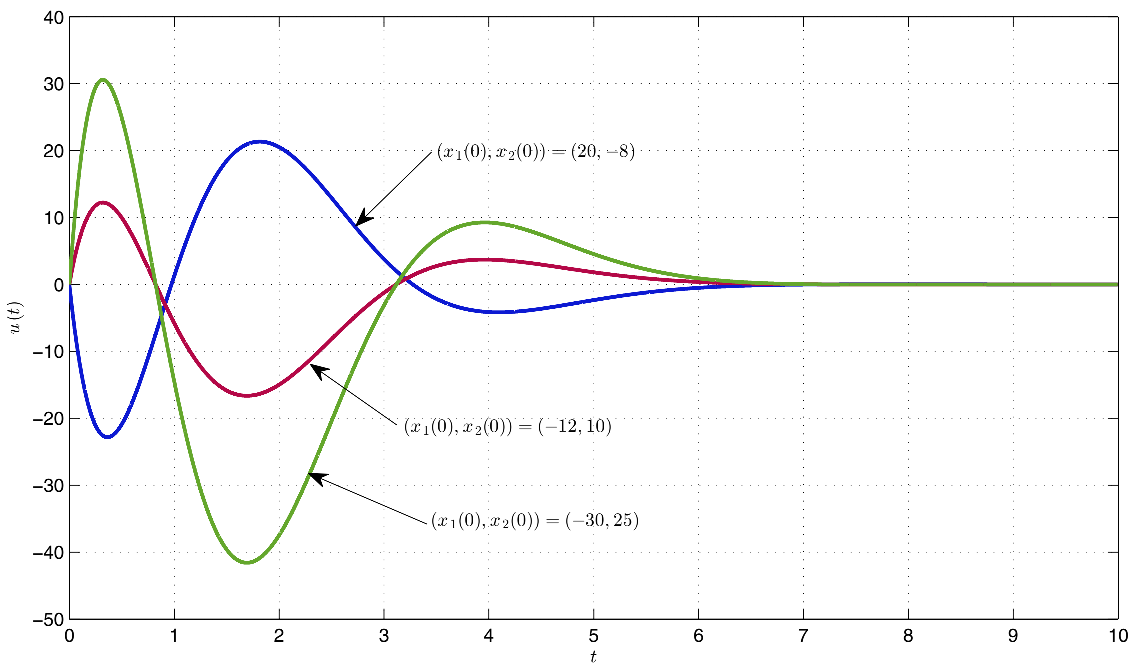

Figure 6.4: Time histories of control input for Example 6.1.

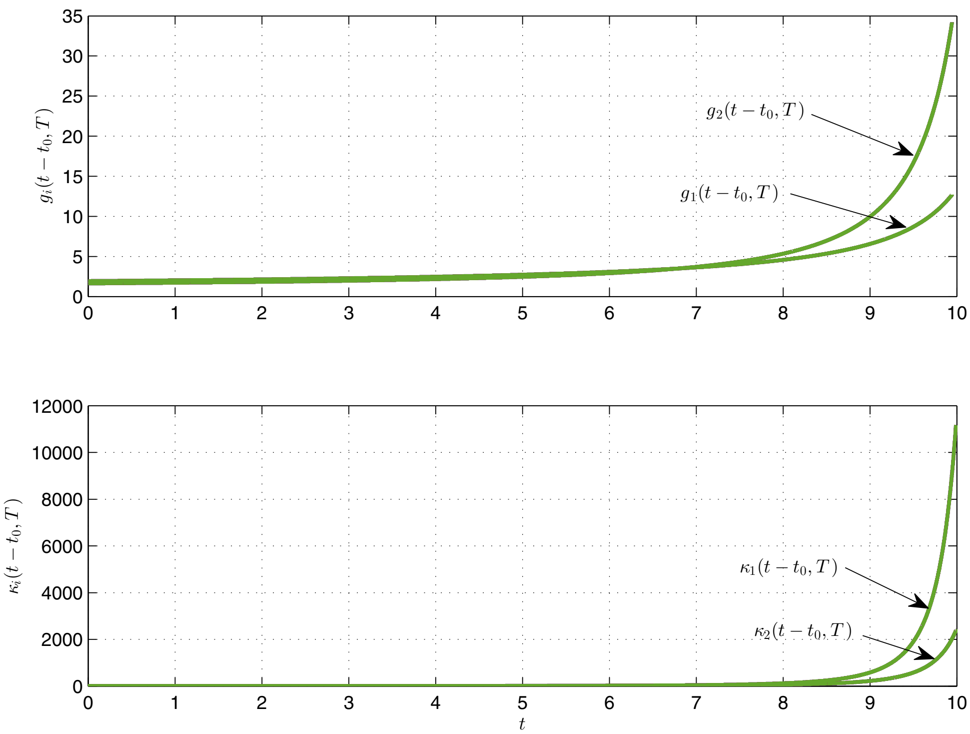

Figure 6.5: Time histories of observer and controller gains for Example 6.1.

6.5 Proofs of results

6.5.1 Proof of Lemma 6.4

Since $\tilde{u}(t)$ is the sum of $\tilde{L}_0$, $\tilde{L}_1$, $\tilde{L}_2$, and $\tilde{L}_3$, we will prove the claims if we can show that each of those terms remain bounded for all $t \in [t_0, t_0+T)$ and also go to zero as $t \to t_0 + T$. We begin by rewriting $\tilde{u}(t)$ using the transformed variables as follows.

Inserting (6.62)–(6.65) into (6.66), $\tilde{u}(t)$ becomes

$$\begin{aligned}\tilde{u}(t) = \mu_1 l_0(\nu) P_C(\mu_1)\mathscr{T}^{-1}\tilde{\xi}(t) + \mu_1^{1-n} K_{n-1}^T J_2 P_C(\mu_1)\mathscr{T}^{-1}\tilde{\xi}(t) \\ - a^T \mathscr{T}^{-1}\tilde{\xi}(t) + \mu_1^{m_C+1} k_n \left(\mathrm{e}_n^T + K_{n-1}^T J_1\right) P_C(\mu_1)\mathscr{T}^{-1}\tilde{\xi}(t).\end{aligned} \tag{6.74}$$

Now use Lemma 5.3 to replace $\tilde{\xi}(t)$, which gives

$$\begin{aligned}\tilde{u}(t) = \mu_1 l_0(\nu) P_C(\mu_1)\mathscr{T}^{-1}\nu^{m_O+1} Q_O(\nu)\tilde{z}(t) + \mu_1^{1-n} K_{n-1}^T J_2 P_C(\mu_1)\mathscr{T}^{-1}\nu^{m_O+1} Q_O(\nu)\tilde{z}(t) \\ - \nu^{m_O+1} a^T \mathscr{T}^{-1} Q_O(\nu)\tilde{z}(t) + \mu_1^{m_C+1} k_n \left(\mathrm{e}_n^T + K_{n-1}^T J_1\right) P_C(\mu_1)\mathscr{T}^{-1}\nu^{m_O+1} Q_O(\nu)\tilde{z}(t).\end{aligned} \tag{6.75}$$

Define the matrix

$$R^*(\mu_1, \nu) := P_C(\mu_1)\mathscr{T}^{-1} Q_O(\nu), \tag{6.76}$$

which reduces (6.75) to

$$\begin{aligned}\tilde{u}(t) = \nu^{m_O} l_0(\nu) R^*(\mu_1,\nu)\tilde{z}(t) + \nu^{m_O+n} K_{n-1}^T J_2 R^*(\mu_1,\nu)\tilde{z}(t) \\ - \nu^{m_O+1} a^T \mathscr{T}^{-1} Q_O(\nu)\tilde{z}(t) + \nu^{m_O-m_C} k_n \left(\mathrm{e}_n^T + K_{n-1}^T J_1\right) R^*(\mu_1,\nu)\tilde{z}(t).\end{aligned} \tag{6.77}$$

The elements of $R^*(\mu_1,\nu)$ in (6.76) are written as

$$r_{i,j}^* = \sum_{l=1}^{n} p_{C_{i,l}}(\mu_1)\left(\sum_{k=1}^{n} \bar{\tau}_{l,k}^{-1} q_{O_{k,j}}(\nu)\right), \tag{6.78}$$

where $\bar{\tau}_{l,k}^{-1}$ denotes the l,k element of $\mathscr{T}^{-1}$. Next, using the definition of $P_C(\mu_1)$ from Lemma 4.2, and the definition of $Q_O(\nu)$ from Lemma 5.3, (6.78) becomes

$$\begin{aligned}
r_{i,j}^* &= \sum_{l=1}^{n} \bar{p}_{C_{i,l}} \mu_1^{n+i-l-1} \left(\sum_{k=1}^{n} \bar{\tau}_{l,k}^{-1} \bar{q}_{O_{k,j}} \nu^{n+j-k-1} \right) \\
&= \sum_{l=1}^{n} \bar{p}_{C_{i,l}} \left(\nu^{-1}\right)^{n+i-l-1} \left(\sum_{k=1}^{n} \bar{\tau}_{l,k}^{-1} \bar{q}_{O_{k,j}} \nu^{n+j-k-1} \right) \\
&= \sum_{l=1}^{n} \bar{p}_{C_{i,l}} \nu^{-n-i+l+1} \left(\sum_{k=1}^{n} \bar{\tau}_{l,k}^{-1} \bar{q}_{O_{k,j}} \nu^{n+j-k-1} \right) \\
&= \sum_{l=1}^{n} \sum_{k=1}^{n} \bar{p}_{C_{i,l}} \bar{\tau}_{l,k}^{-1} \bar{q}_{O_{k,j}} \nu^{j+l-i-k} \qquad (6.79)
\end{aligned}$$

for $1 \le i \le j \le n$. It would be convenient if every element of $R^*(\mu_1, \nu)$ remained bounded as $t \to t_0 + T$; however, that would require a nonnegative exponent on ν in (6.79). The indices i and k can each be as large as n, but both j and l are at least equal to one. So, the most negative the exponent on ν can be in (6.79) is $2 - 2n = 2(1-n)$. Therefore, to ensure a nonnegative exponent, we multiply and divide (6.79) by ν^{2n-2} to obtain

$$r_{i,j}^* = \frac{1}{\nu^{2n-2}} \sum_{l=1}^{n} \sum_{k=1}^{n} \bar{p}_{C_{i,l}} \bar{\tau}_{l,k}^{-1} \bar{q}_{O_{k,j}} \nu^{2n-2+j+l-i-k}. \qquad (6.80)$$

Now, using (6.80), we define a new matrix,

$$R = R(\nu) := \nu^{2n-2} R^*(\mu_1, \nu) \qquad (6.81)$$

having elements

$$r_{i,j}(\nu) = \sum_{l=1}^{n} \sum_{k=1}^{n} \bar{p}_{C_{i,l}} \bar{\tau}_{l,k}^{-1} \bar{q}_{O_{k,j}} \nu^{2n-2+j+l-i-k}, \quad 1 \le i \le j \le n, \qquad (6.82)$$

where it is clear that $r_{i,j}(\nu)$ remains bounded for every i, j as $t \to t_0 + T$. Then (6.80) is rewritten as

$$\begin{aligned}
R^*(\mu_1, \nu) &= P(\mu_1) \mathscr{T}^{-1} Q(\nu) \\
&= \frac{1}{\nu^{2n-2}} R(\nu). \qquad (6.83)
\end{aligned}$$

Next, substituting (6.83) into (6.77) leads to

$$\tilde{u}(t) = \nu^{m_O-2n+2} l_0(\nu)R(\nu)\tilde{z}(t) + \nu^{m_O-n+2} K_{n-1}^T J_2 R(\nu)\tilde{z}(t)$$
$$- \nu^{m_O+1} a^T \mathscr{T}^{-1} Q_O(\nu)\tilde{z}(t) + \nu^{m_O-m_C-2n+2} k \left(\mathrm{e}_n^T + K_{n-1}^T J_1\right) R(\nu)\tilde{z}(t). \tag{6.84}$$

From (6.84), it is clear that all of the rewritten terms $\tilde{L}_0$, $\tilde{L}_1$, $\tilde{L}_2$, and $\tilde{L}_3$ are comprised of three kinds of quantities: 1) $\tilde{z}$, which is asymptotically stabilized (and therefore bounded) for all $t \in [t_0, t_0+T)$ by our special selection of the constants $\{l_i\}_{i=1}^n$, 2) linear functions in the argument $\nu \in [0,1)$ which are bounded for all $t \in [t_0, t_0+T)$, and 3) some factor of ν whose exponent depends on n and the design parameters m_C and m_O. Therefore, if we select the design parameters m_C and m_O to make the exponent on ν positive on each of the terms in (6.84), then we ensure that all of the terms in (6.84) not only remain bounded for all $t \in [t_0, t_0+T)$, but also go to zero as $t \to t_0+T$. Since $m_O \geq 1$ by definition, then the exponent on ν is always positive on the third term in (6.84). Then for the other terms, we see that we ensure positive exponents on ν by selecting

$$m_O \geq 2n-1, \quad m_O \geq n-1, \quad m_O \geq m_C + 2n - 1. \tag{6.85}$$

All three conditions are satisfied simultaneously by selecting $m_O \geq 1$ and $m_C \geq 1$ according to $m_O \geq m_C + 2n - 1$. Doing so ensures that the quantities $\tilde{L}_0$, $\tilde{L}_1$, $\tilde{L}_2$, and $\tilde{L}_3$ remain bounded for all $t \in [t_0, t_0+T)$, and also go to zero as $t \to t_0+T$. Therefore, the sum of all the terms in (6.84) also remains bounded for all $t \in [t_0, t_0+T)$ and go to zero as $t \to t_0+T$, which proves the claim. ■

6.5.2 Proof of Lemma 6.5

The proof follows the exact same approach as the proof of Lemma 6.4. The main difference is that for the chain of integrators, the transformation $\mathscr{T}^{-1}$ equals the identity matrix. With $\mathscr{T}^{-1} = I$, inserting (6.62)–(6.65) into (6.66) gives

$$\begin{aligned}\tilde{u}(t) = {} & \mu_1 l_0(\nu) P_C(\mu_1)\tilde{\xi}(t) + \mu_1^{1-n} K_{n-1}^T J_2 P_C(\mu_1)\tilde{\xi}(t) \\ & - a^T \tilde{\xi}(t) + \mu_1^{m_C+1} k_n \left(\mathrm{e}_n^T + K_{n-1}^T J_1\right) P_C(\mu_1)\tilde{\xi}(t).\end{aligned} \tag{6.86}$$

Now use Lemma 5.3 to replace $\tilde{\xi}(t)$, which gives

$$\begin{aligned}\tilde{u}(t) = {} & \mu_1 l_0(\nu) P_C(\mu_1)\nu^{m_O+1} Q_O(\nu)\tilde{z}(t) + \mu_1^{1-n} K_{n-1}^T J_2 P_C(\mu_1)\nu^{m_O+1} Q_O(\nu)\tilde{z}(t) \\ & - \nu^{m_O+1} a^T Q_O(\nu)\tilde{z}(t) + \mu_1^{m_C+1} k_n \left(\mathrm{e}_n^T + K_{n-1}^T J_1\right) P_C(\mu_1)\nu^{m_O+1} Q_O(\nu)\tilde{z}(t).\end{aligned} \tag{6.87}$$

Define the matrix

$$R^*(\mu_1, \nu) := P_C(\mu_1) Q_O(\nu), \tag{6.88}$$

which reduces (6.87) to

$$\begin{aligned}\tilde{u}(t) = {} & \nu^{m_O} l_0(\nu) R^*(\mu_1,\nu)\tilde{z}(t) + \nu^{m_O+n} K_{n-1}^T J_2 R^*(\mu_1,\nu)\tilde{z}(t) \\ & - \nu^{m_O+1} a^T Q_O(\nu)\tilde{z}(t) + \nu^{m_O-m_C} k_n \left(\mathrm{e}_n^T + K_{n-1}^T J_1\right) R^*(\mu_1,\nu)\tilde{z}(t).\end{aligned} \tag{6.89}$$

The elements of $R^*(\mu_1, \nu)$ in (6.88) are written as

$$r_{i,j}^* = \sum_{k=1}^{n} p_{C_{i,k}}(\mu_1) q_{O_{k,j}}(\nu). \tag{6.90}$$

Next, using the definition of $P_C(\mu_1)$ from Lemma 4.2, and the definition of $Q_O(\nu)$ from Lemma 5.3, (6.90) becomes

$$\begin{aligned}
r^*_{i,j} &= \sum_{k=1}^{n} \bar{p}_{C_{i,k}} \mu_1^{n+i-k-1} \bar{q}_{O_{k,j}} \nu^{n+j-k-1} \\
&= \sum_{k=1}^{n} \bar{p}_{C_{i,k}} \left(\nu^{-1}\right)^{n+i-k-1} \bar{q}_{O_{k,j}} \nu^{n+j-k-1} \\
&= \sum_{k=1}^{n} \bar{p}_{C_{i,k}} \nu^{-n-i+k+1} \bar{q}_{O_{k,j}} \nu^{n+j-k-1} \\
&= \sum_{k=1}^{n} \bar{p}_{C_{i,k}} \bar{q}_{O_{k,j}} \nu^{j-i} \\
&= \bar{r}_{i,j} \nu^{j-i}
\end{aligned} \tag{6.91}$$

for $1 \le i \le j \le n$, where we have defined the constants

$$\bar{r}_{i,j} = \sum_{k=1}^{n} \bar{p}_{C_{i,k}} \bar{q}_{O_{k,j}}. \tag{6.92}$$

It would be convenient if every element of $R^*(\mu_1, \nu)$ remained bounded as $t \to t_0 + T$; however, that would require a nonnegative exponent on ν in (6.91). The indices i and j can each be as large as n, but are no less than one. So, the most negative the exponent on ν can be in (6.91) is $1-n$. Therefore, to ensure a nonnegative exponent, we multiply and divide (6.91) by ν^{n-1} to obtain

$$r^*_{i,j} = \bar{r}_{i,j} \frac{1}{\nu^{n-1}} \nu^{n-1+j-i}. \tag{6.93}$$

Now, using (6.93), we define a new matrix,

$$R = R(\nu) := \nu^{n-1} R^*(\mu_1, \nu) \tag{6.94}$$

having elements

$$r_{i,j}(\nu) = \bar{r}_{i,j} \nu^{n-1+j-i}, \quad 1 \le i \le j \le n, \tag{6.95}$$

where it is clear that $r_{i,j}(\nu)$ remains bounded for every i, j as $t \to t_0 + T$. Then (6.93) is rewritten as

$$R^*(\mu_1, \nu) = P(\mu_1)Q(\nu)$$
$$= \frac{1}{\nu^{n-1}} R(\nu). \tag{6.96}$$

Next, substituting (6.96) into (6.89) leads to

$$\tilde{u}(t) = \nu^{m_O - n + 1} l_0(\nu) R(\nu) \tilde{z}(t) + \nu^{m_O + 1} K_{n-1}^T J_2 R(\nu) \tilde{z}(t)$$
$$- \nu^{m_O + 1} a^T Q_O(\nu) \tilde{z}(t) + \nu^{m_O - m_C - n + 1} k \left(\mathrm{e}_n^T + K_{n-1}^T J_1 \right) R(\nu) \tilde{z}(t). \tag{6.97}$$

From (6.97), it is clear that all of the rewritten terms $\tilde{L}_0$, $\tilde{L}_1$, $\tilde{L}_2$, and $\tilde{L}_3$ are comprised of three kinds of quantities: 1) $\tilde{z}$, which is asymptotically stabilized (and therefore bounded) for all $t \in [t_0, t_0 + T)$ by our special selection of the constants $\{l_i\}_{i=1}^n$, 2) linear functions in the argument $\nu \in [0, 1)$ which are bounded for all $t \in [t_0, t_0 + T)$, and 3) some factor of ν whose exponent depends on n and the design parameters m_C and m_O. Therefore, if we select the design parameters m_C and m_O to make the exponent on ν positive on each of the terms in (6.97), then we ensure that all of the terms in (6.97) not only remain bounded for all $t \in [t_0, t_0 + T)$, but also go to zero as $t \to t_0 + T$. Since $m_O \geq 1$ by definition, then the exponent on ν is always positive on the second and third terms in (6.97). Then for the other terms, we see that we ensure positive exponents on ν by selecting

$$m_O \geq n, \quad m_O \geq m_C + n. \tag{6.98}$$

Both conditions are satisfied simultaneously by selecting $m_O \geq 1$ and $m_C \geq 1$ according to $m_O \geq m_C + n$. Doing so ensures that the quantities $\tilde{L}_0$, $\tilde{L}_1$, $\tilde{L}_2$, and $\tilde{L}_3$ remain bounded for all $t \in [t_0, t_0 + T)$, and also go to zero as $t \to t_0 + T$. Therefore, the sum of all the terms in (6.97) also remains bounded for all $t \in [t_0, t_0 + T)$ and go to zero as $t \to t_0 + T$, which proves the claim. ■

6.5.3 Proof of Lemma 6.6

From (6.66), the triangle inequality, and (6.62)–(6.65), and since $\mu_1 > 0$, we obtain

$$\begin{aligned}
|\tilde{u}(t)| &\leq |\tilde{L}_0(t)| + |\tilde{L}_1(t)| + |\tilde{L}_2(t)| + |\tilde{L}_3(t)| \\
&\leq |\mu_1 l_0(\nu) P_C(\mu_1) \mathscr{T}^{-1} \tilde{\xi}(t)| + |\mu_1^{1-n} K_{n-1}^T J_2 P_C(\mu_1) \mathscr{T}^{-1} \tilde{\xi}(t)| \\
&\quad + |a^T \mathscr{T}^{-1} \tilde{\xi}(t)| + |\mu_1^{m_C+1} k_n (\mathrm{e}_n^T + K_{n-1}^T J_1) P_C(\mu_1) \mathscr{T}^{-1} \tilde{\xi}(t)| \\
&\leq |\mu_1||l_0(\nu)||P_C(\mu_1)||\mathscr{T}^{-1}||\tilde{\xi}(t)| + |\mu_1^{1-n}||K_{n-1}^T||J_2||P_C(\mu_1)||\mathscr{T}^{-1}||\tilde{\xi}(t)| \\
&\quad + |a||\mathscr{T}^{-1}||\tilde{\xi}(t)| + |\mu_1^{m_C+1}||k_n(\mathrm{e}_n^T + K_{n-1}^T J_1)||P_C(\mu_1)||\mathscr{T}^{-1}||\tilde{\xi}(t)| \\
&= \mu_1 |l_0(\nu)||P_C(\mu_1)||\mathscr{T}^{-1}||\tilde{\xi}(t)| + \mu_1^{1-n}|K_{n-1}^T||J_2||P_C(\mu_1)||\mathscr{T}^{-1}||\tilde{\xi}(t)| \\
&\quad + |a||\mathscr{T}^{-1}||\tilde{\xi}(t)| + \mu_1^{m_C+1}|k_n(\mathrm{e}_n^T + K_{n-1}^T J_1)||P_C(\mu_1)||\mathscr{T}^{-1}||\tilde{\xi}(t)| \\
&= \Big(\mu_1 |l_0(\nu)| + \mu_1^{1-n}|K_{n-1}^T||J_2| + \mu_1^{m_C+1}|k_n(\mathrm{e}_n^T + K_{n-1}^T J_1)|\Big)|P_C(\mu_1)||\mathscr{T}^{-1}||\tilde{\xi}(t)| \\
&\quad + |a||\mathscr{T}^{-1}||\tilde{\xi}(t)|. \qquad (6.99)
\end{aligned}$$

Now, since $\mu_1 = \nu^{-1}$, from (4.17) we have

$$\begin{aligned}
p_{C_{i,j}}(\mu_1) &= \bar{p}_{C_{i,j}} \mu_1^{n+i-j-1} \\
&= \bar{p}_{C_{i,j}} \nu^{-n-i+j+1}, \qquad (6.100)
\end{aligned}$$

and multiplying and dividing by ν^{2n-2} gives

$$p_{C_{i,j}}(\mu_1) = \frac{1}{\nu^{2n-2}} \bar{p}_{C_{i,j}} \nu^{n+j-i-1}. \qquad (6.101)$$

Now define the matrix $P_C^*(\nu)$ having elements

$$p^*_{C_{i,j}}(\nu) = \bar{p}_{C_{i,j}} \nu^{n+j-i-1}. \qquad (6.102)$$

Since i can be at most equal to n, and j is at least equal to one, for all i, j, the exponent on ν in (6.102) is nonnegative. This means that $|P_C^*(\nu)|$ is a continuous function of the bounded argument

$\nu \in (0,1]$, so it remains bounded for all $t \in [t_0, t_0+T)$. Now, from (6.101) and (6.102) we obtain

$$p_{C_{i,j}}(\mu_1) = \frac{1}{\nu^{2n-2}} p^*_{C_{i,j}}(\nu), \tag{6.103}$$

and therefore

$$\begin{aligned} P_C(\mu_1) &= \frac{1}{\nu^{2n-2}} P^*_C(\nu) \\ &= \mu_1^{2n-2} P^*_C(\nu). \end{aligned} \tag{6.104}$$

Then from (6.104) we have

$$\begin{aligned} |P_C(\mu_1)| &\leq |\mu_1^{2n-2}||P^*_C(\nu)| \\ &= \mu_1^{2n-2}|P^*_C(\nu)| \end{aligned} \tag{6.105}$$

since $\mu_1 > 0$ for all $t \in [t_0, t_0+T)$.

Substituting (6.105) into (6.99) obtains

$$\begin{aligned} |\tilde{u}(t)| \leq &\left(\mu_1^{2n-1}|l_0(\nu)| + \mu_1^{n-1}|K^T_{n-1}||J_2| + \mu_1^{2n+m_C-1}|k_n(\mathrm{e}^T_n + K^T_{n-1}J_1)|\right)|P^*_C(\nu)||\mathscr{T}^{-1}||\tilde{\xi}(t)| \\ &+ |a||\mathscr{T}^{-1}||\tilde{\xi}(t)| \\ = &\left(\nu^{-2n+1}|l_0(\nu)| + \nu^{-n+1}|K^T_{n-1}||J_2| + \nu^{-2n-m_C+1}|k_n(\mathrm{e}^T_n + K^T_{n-1}J_1)|\right)|P^*_C(\nu)||\mathscr{T}^{-1}||\tilde{\xi}(t)| \\ &+ |a||\mathscr{T}^{-1}||\tilde{\xi}(t)| \end{aligned} \tag{6.106}$$

and then substituting (6.26) into (6.106) gives

$$\begin{aligned} |\tilde{u}(t)| \leq &\left(\nu^{m_O-2n+2}|l_0(\nu)| + \nu^{m_O-n+2}|K^T_{n-1}||J_2| + \nu^{m_O-m_C-2n+2}|k_n(\mathrm{e}^T_n + K^T_{n-1}J_1)|\right) \\ &\times |P^*_C(\nu)||\mathscr{T}^{-1}|\tilde{M}\mathrm{e}^{-\tilde{\delta}(t-t_0)}|\tilde{\xi}(t_0)| + \nu^{m_O+1}|a||\mathscr{T}^{-1}|\tilde{M}\mathrm{e}^{-\tilde{\delta}(t-t_0)}|\tilde{\xi}(t_0)| \\ = &\left\{\left(\nu^{m_O-2n+2}|l_0(\nu)| + \nu^{m_O-n+2}|K^T_{n-1}||J_2| + \nu^{m_O-m_C-2n+2}|k_n(\mathrm{e}^T_n + K^T_{n-1}J_1)|\right)|P^*_C(\nu)| \right. \\ &\left. + \nu^{m_O+1}|a|\right\}|\mathscr{T}^{-1}|\tilde{M}\mathrm{e}^{-\tilde{\delta}(t-t_0)}|\tilde{\xi}(t_0)|. \end{aligned} \tag{6.107}$$

Since $\nu \in (0,1]$, for positive integers i, j with $i < j$, it is true that $\nu^j \leq \nu^i$. Similarly, $\nu^{m_O-n+2} \leq \nu^{m_O-2n+2} \leq \nu^{m_O-m_C-2n+2}$, and $\nu^{m_O+1} \leq \nu^{m_O-m_C-2n+2}$. Then from (6.107) we obtain

$$|\tilde{u}(t)| \leq \nu^{m_O-m_C-2n+2}\left\{\Big(|l_0(\nu)|+|K_{n-1}^T||J_2|+|k_n(\mathrm{e}_n^T+K_{n-1}^T J_1)|\Big)|P_C^*(\nu)|+|a|\right\}$$

$$\times|\mathscr{T}^{-1}|\tilde{M}\mathrm{e}^{-\tilde{\delta}(t-t_0)}|\tilde{\xi}(t_0)|. \tag{6.108}$$

Define the function

$$\phi(\nu) := \Big(|l_0(\nu)|+|K_{n-1}^T||J_2|+|k_n(\mathrm{e}_n^T+K_{n-1}^T J_1)|\Big)|P_C^*(\nu)|+|a| \tag{6.109}$$

and the quantity

$$\bar{\phi} := \sup_{0<\nu\leq 1} |\phi(\nu)|. \tag{6.110}$$

By (6.102) and the statements that immediately followed, it is clear that $|P_C^*(\nu)|$ remains bounded for all $t \in [t_0, t_0+T)$. Furthermore, $|l_0(\nu)|$ remains bounded for all $t \in [t_0, t_0+T)$ by the last statement of Lemma 4.4. Therefore, from (6.109) and (6.110), it is clear that $\bar{\phi}$ is bounded for all $t \in [t_0, t_0+T)$.

And so, with (6.108), (6.109), and (6.110), we obtain

$$|\tilde{u}(t)| \leq \nu^{m_O-m_C-2n+2}\bar{\phi}|\mathscr{T}^{-1}|\tilde{M}\mathrm{e}^{-\tilde{\delta}(t-t_0)}|\tilde{\xi}(t_0)|, \tag{6.111}$$

where $\bar{\phi}$ is a positive constant. Then by selecting $m_O \geq m_C+2n-1$, the exponent on ν in (6.111) is positive, and we have proven the claim with $\alpha = m_O - m_C - 2n + 2$, $M_\alpha = \bar{\phi}|\mathscr{T}^{-1}|\tilde{M}$, and $\delta_\alpha = \tilde{\delta}$.

■

6.5.4 Proof of Lemma 6.7

Substituting the controller (6.67) into the transformed system (6.32), (6.36) yields

$$\dot{r}_1(t) = \Lambda_C r_1(t) + \mathrm{e}_{n-1}\sigma(t) \tag{6.112}$$

$$\begin{aligned}\dot{\sigma}(t) &= \mu_C\left(u(t) + L_0(t) + L_1(t) + L_2(t)\right)\\ &= \mu_C\left(-k_n\sigma(t) + \tilde{u}(t)\right)\\ &= -k_n\mu_C\sigma(t) + \mu_C\tilde{u}(t).\end{aligned} \tag{6.113}$$

Define the Lyapunov function candidate

$$V(t) := \frac{1}{2}\sigma(t)^2. \tag{6.114}$$

Then with (6.113) we obtain

$$\begin{aligned}\dot{V}(t) &= \sigma(t)\left(-k_n\mu_C\sigma(t) + \mu_C\tilde{u}(t)\right)\\ &= -k_n\mu_C\sigma(t)^2 + \mu_C\sigma(t)\tilde{u}(t).\end{aligned} \tag{6.115}$$

With $\lambda = k_n/2 > 0$, Young's inequality gives

$$\mu_C\sigma(t)\tilde{u}(t) \leq \frac{k_n\mu_C}{2}\sigma(t)^2 + \frac{\mu_C}{2k_n}\tilde{u}(t)^2. \tag{6.116}$$

Inserting (6.116) into (6.115) gives

$$\begin{aligned}\dot{V}(t) &\leq -\frac{k_n\mu_C}{2}\sigma(t)^2 + \frac{\mu_C}{2k_n}\tilde{u}(t)^2\\ &= -k_n\mu_C V(t) + \frac{\mu_C}{2k_n}\tilde{u}(t)^2.\end{aligned} \tag{6.117}$$

Then by Lemma 4.1, for all $t \in [t_0, t_0 + T)$, it is true that

$$V(t) \leq \zeta_C(t - t_0, T)^{k_n} V(t_0) + \frac{||\tilde{u}||^2_{[t_0,t]}}{2k_n^2}. \tag{6.118}$$

Then using (6.114) in (6.118) results in

$$\sigma(t)^2 \leq \zeta_C(t-t_0,T)^{k_n}\sigma(t_0)^2 + \frac{||\tilde{u}||^2_{[t_0,t]}}{k_n^2}, \tag{6.119}$$

from which we obtain for all $t \in [t_0, t_0+T)$,

$$|\sigma(t)| \leq \zeta_C(t-t_0,T)^{\frac{k_n}{2}}|\sigma(t_0)| + \gamma_\sigma||\tilde{u}||_{[t_0,t]}, \tag{6.120}$$

where $\gamma_\sigma := 1/k_n$. Now, by Lemma 6.4, by selecting $m_O \geq m_C + 2n - 1$, we guarantee that $\tilde{u}(t)$ not only remains bounded, but also goes to zero as $t \to t_0 + T$. The former fact combined with (6.120) shows that the $\sigma(t)$ system is FT-ISS with respect to $\tilde{u}(t)$.

The $r_1(t)$ and $\sigma(t)$ systems (6.112) and (6.113) combine to form a cascade system whose stability depends upon the stability of each subsystem. Define

$$\bar{w}(t) := \begin{bmatrix} r_1(t) \\ \sigma(t) \end{bmatrix}. \tag{6.121}$$

Then it is true that

$$|\bar{w}(t)| \leq |r_1(t)| + |\sigma(t)| \tag{6.122}$$

$$|r_1(t_0)| \leq |\bar{w}(t_0)| \tag{6.123}$$

$$|\sigma(t_0)| \leq |\bar{w}(t_0)|. \tag{6.124}$$

Recall that the $r_1(t)$ system is a linear system that is ISS w.r.t. $\sigma(t)$. This means there exist positive constants M_1, δ_1, γ_1 such that for all $t \in [t_0, t_0+T)$,

$$|r_1(t)| \leq M_1 \mathrm{e}^{-\delta_1(t-t_0)}|r_1(t_0)| + \gamma_1||\sigma||_{[t_0,t]}. \tag{6.125}$$

We obtain a "fading memory" stability estimate for $|r_1(t)|$ as follows. For any time $t \in [t_0, t_0+T)$, (6.125) provides

$$|r_1(t)| \leq M_1 \mathrm{e}^{-\delta_1\left(t-\frac{t+t_0}{2}\right)}\left|r_1\left(\frac{t+t_0}{2}\right)\right| + \gamma_1 \sup_{\frac{t+t_0}{2}\leq\tau\leq t}|\sigma(\tau)|. \tag{6.126}$$

Now, from (6.120) we obtain

$$\begin{aligned}
\sup_{\frac{t+t_0}{2}\le\tau\le t}|\sigma(\tau)| &\le \sup_{\frac{t+t_0}{2}\le\tau\le t}\left(\zeta_C(\tau-t_0,T)^{\frac{k_n}{2}}|\sigma(t_0)|+\gamma_\sigma||\tilde{u}||_{[t_0,\tau]}\right)\\
&= \sup_{\frac{t+t_0}{2}\le\tau\le t}\left(\zeta_C(\tau-t_0,T)^{\frac{k_n}{2}}|\sigma(t_0)|+\gamma_\sigma\sup_{t_0\le s\le\tau}|\tilde{u}(s)|\right)\\
&= \sup_{\frac{t+t_0}{2}\le\tau\le t}\left(\zeta_C(\tau-t_0,T)^{\frac{k_n}{2}}|\sigma(t_0)|\right)+\sup_{\frac{t+t_0}{2}\le\tau\le t}\left(\gamma_\sigma\sup_{t_0\le s\le\tau}|\tilde{u}(s)|\right)\\
&\le \zeta_C\left(\frac{t+t_0}{2}-t_0,T\right)^{\frac{k_n}{2}}|\sigma(t_0)|+\gamma_\sigma\sup_{t_0\le\tau\le t}|\tilde{u}(\tau)|\\
&= \zeta_C\left(\frac{t+t_0}{2}-t_0,T\right)^{\frac{k_n}{2}}|\sigma(t_0)|+\gamma_\sigma||\tilde{u}||_{[t_0,t]}.
\end{aligned}\tag{6.127}$$

Then also from (6.125), we obtain

$$\begin{aligned}
\left|r_1\left(\frac{t+t_0}{2}\right)\right| &\le M_1\mathrm{e}^{-\delta_1\left(\frac{t+t_0}{2}-t_0\right)}|r_1(t_0)|+\gamma_1\sup_{t_0\le\tau\le\frac{t+t_0}{2}}|\sigma(\tau)|\\
&\le M_1\mathrm{e}^{-\delta_1\left(\frac{t+t_0}{2}-t_0\right)}|r_1(t_0)|+\gamma_1\sup_{t_0\le\tau\le\frac{t+t_0}{2}}\left(\zeta_C(\tau-t_0,T)^{\frac{k_n}{2}}|\sigma(t_0)|+\gamma_\sigma||\tilde{u}||_{[t_0,\tau]}\right)\\
&= M_1\mathrm{e}^{-\delta_1\left(\frac{t+t_0}{2}-t_0\right)}|r_1(t_0)|+\gamma_1\sup_{t_0\le\tau\le\frac{t+t_0}{2}}\zeta_C(\tau-t_0,T)^{\frac{k_n}{2}}|\sigma(t_0)|+\gamma_1\sup_{t_0\le\tau\le\frac{t+t_0}{2}}\gamma_\sigma||\tilde{u}||_{[t_0,\tau]}\\
&\le M_1\mathrm{e}^{-\delta_1\left(\frac{t+t_0}{2}-t_0\right)}|r_1(t_0)|+\gamma_1\zeta_C(t_0-t_0,T)^{\frac{k_n}{2}}|\sigma(t_0)|+\gamma_1\gamma_\sigma||\tilde{u}||_{[t_0,\frac{t+t_0}{2}]}\\
&= M_1\mathrm{e}^{-\delta_1\left(\frac{t+t_0}{2}-t_0\right)}|r_1(t_0)|+\gamma_1|\sigma(t_0)|+\gamma_1\gamma_\sigma||\tilde{u}||_{[t_0,\frac{t+t_0}{2}]}
\end{aligned}\tag{6.128}$$

since $\zeta_C(0,T)=1$. Now, inserting (6.128) and (6.127) into (6.126) gives

$$\begin{aligned}
|r_1(t)| &\le M_1 \mathrm{e}^{-\delta_1\left(t-\frac{t+t_0}{2}\right)}\left(M_1 \mathrm{e}^{-\delta_1\left(\frac{t+t_0}{2}-t_0\right)}|r_1(t_0)|+\gamma_1|\sigma(t_0)|+\gamma_1\gamma_\sigma||\tilde{u}||_{[t_0,\frac{t+t_0}{2}]}\right)\\
&\quad+\gamma_1\left(\zeta_C\left(\frac{t+t_0}{2}-t_0,T\right)^{\frac{k_n}{2}}|\sigma(t_0)|+\gamma_\sigma||\tilde{u}||_{[t_0,t]}\right)\\
&\le M_1^2\mathrm{e}^{-\delta_1(t-t_0)}|r_1(t_0)|+M_1\gamma_1\mathrm{e}^{-\delta_1\left(t-\frac{t+t_0}{2}\right)}|\sigma(t_0)|+\gamma_1\gamma_\sigma M_1\mathrm{e}^{-\delta_1\left(t-\frac{t+t_0}{2}\right)}||\tilde{u}||_{[t_0,t]}\\
&\quad+\gamma_1\zeta_C\left(\frac{t+t_0}{2}-t_0,T\right)^{\frac{k_n}{2}}|\sigma(t_0)|+\gamma_1\gamma_\sigma||\tilde{u}||_{[t_0,t]}\\
&= M_1^2\mathrm{e}^{-\delta_1(t-t_0)}|r_1(t_0)|+\gamma_1\left(M_1\mathrm{e}^{-\delta_1\left(t-\frac{t+t_0}{2}\right)}+\zeta_C\left(\frac{t+t_0}{2}-t_0,T\right)^{\frac{k_n}{2}}\right)|\sigma(t_0)|\\
&\quad+\gamma_1\gamma_\sigma\left(M_1\mathrm{e}^{-\delta_1\left(t-\frac{t+t_0}{2}\right)}+1\right)||\tilde{u}||_{[t_0,t]}\\
&\le M_1^2\mathrm{e}^{-\delta_1(t-t_0)}|r_1(t_0)|+\gamma_1\left(M_1\mathrm{e}^{-\delta_1\left(t-\frac{t+t_0}{2}\right)}+\zeta_C\left(\frac{t+t_0}{2}-t_0,T\right)^{\frac{k_n}{2}}\right)|\sigma(t_0)|\\
&\quad+\gamma_1\gamma_\sigma(M_1+1)||\tilde{u}||_{[t_0,t]}.
\end{aligned}\tag{6.129}$$

Next, using (6.129) and (6.120) in (6.122), we obtain for all $t\in[t_0,t_0+T)$

$$\begin{aligned}
|\bar{w}(t)| &\le M_1^2\mathrm{e}^{-\delta_1(t-t_0)}|r_1(t_0)|+\left(\gamma_1 M_1\mathrm{e}^{-\delta_1\left(t-\frac{t+t_0}{2}\right)}+\gamma_1\zeta_C\left(\frac{t+t_0}{2}-t_0,T\right)^{\frac{k_n}{2}}+\zeta_C(t-t_0,T)^{\frac{k_n}{2}}\right)|\sigma(t_0)|\\
&\quad+(\gamma_1\gamma_\sigma(M_1+1)+\gamma_\sigma)||\tilde{u}||_{[t_0,t]}.
\end{aligned}\tag{6.130}$$

Then using (6.123) and (6.124), (6.130) gives

$$\begin{aligned}
|\bar{w}(t)| &\le \left(M_1^2\mathrm{e}^{-\delta_1(t-t_0)}+\gamma_1 M_1\mathrm{e}^{-\delta_1\left(t-\frac{t+t_0}{2}\right)}+\gamma_1\zeta_C\left(\frac{t+t_0}{2}-t_0,T\right)^{\frac{k_n}{2}}+\zeta_C(t-t_0,T)^{\frac{k_n}{2}}\right)|\bar{w}(t_0)|\\
&\quad+(\gamma_1\gamma_\sigma(M_1+1)+\gamma_\sigma)||\tilde{u}||_{[t_0,t]}.
\end{aligned}\tag{6.131}$$

For all $t\in[t_0,t_0+T)$, every term in the parentheses has decayed from its initial value at t_0. So, there exist some positive constants $M_{\bar{w}}$, $\delta_{\bar{w}}$, and $\gamma_{\bar{w}}$ such that

$$|\bar{w}(t)|\le M_{\bar{w}}\mathrm{e}^{-\delta_{\bar{w}}(t-t_0)}|\bar{w}(t_0)|+\gamma_{\bar{w}}||\tilde{u}||_{[t_0,t]}\tag{6.132}$$

where $\gamma_{\bar{w}} := (\gamma_1\gamma_\sigma(M_1+1)+\gamma_\sigma)$. Therefore, the $\bar{w}(t)$ cascade system is ISS w.r.t. the disturbance $\tilde{u}(t)$.

It remains to invert the dynamics of the scaled state to obtain those of the original state. Define the matrix $\mathscr{R}$ and its inverse from the equation

$$\begin{aligned}\bar{w}(t) &= \left(J_1^T + \mathrm{e}_n K_{n-1}^T\right) r_1(t) + \mathrm{e}_n w_n(t)\\ &= \mathscr{R} w(t),\end{aligned} \tag{6.133}$$

such that

$$\mathscr{R} := I + \mathrm{e}_n K_{n-1}^T J_1, \quad \mathscr{R}^{-1} = I - \mathrm{e}_n K_{n-1}^T J_1. \tag{6.134}$$

From Lemma 4.3 and (6.133) we obtain

$$x(t) = \nu^{m_C+1} Q_C(\nu)\mathscr{R}^{-1}\bar{w}(t), \tag{6.135}$$

and then from (6.133) and Lemma 4.2, we have

$$\begin{aligned}\bar{w}(t_0) &= \mathscr{R} w(t_0)\\ &= \mathscr{R}\mu_1(0,T)^{m_C+1} P_C(\mu_1(0,T))x(t_0)\\ &= \mathscr{R} P_C(1)x(t_0)\end{aligned} \tag{6.136}$$

since $\mu_1(0,T)=1$. Then (6.135) gives

$$\begin{aligned}|x(t)| &\le |\nu^{m_C+1}||Q_C(\nu)||\mathscr{R}^{-1}||\bar{w}(t)|\\ &\le \nu^{m_C+1}\bar{q}_C|\mathscr{R}^{-1}|\left(M_{\bar{w}}\mathrm{e}^{-\delta_{\bar{w}}(t-t_0)}|\bar{w}(t_0)| + \gamma_{\bar{w}}||\tilde{u}||_{[t_0,t]}\right)\end{aligned} \tag{6.137}$$

after invoking the last statement of Lemma 4.3 and substituting in (6.132). Then from (6.136), we obtain

$$|\bar{w}(t_0)| \le |\mathscr{R} P_C(1)||x(t_0)|, \tag{6.138}$$

which after substituting into (6.137) obtains

$$
\begin{aligned}
|x(t)| &\leq \nu^{m_C+1}\bar{q}_C|\mathscr{R}^{-1}|\left(M_{\bar{w}}|\mathscr{R}P_C(1)|\mathrm{e}^{-\delta_{\bar{w}}(t-t_0)}|x(t_0)| + \gamma_{\bar{w}}||\tilde{u}||_{[t_0,t]}\right) \\
&= \nu^{m_C+1}\left(\check{M}\mathrm{e}^{-\check{\delta}(t-t_0)}|x(t_0)| + \check{\gamma}||\tilde{u}||_{[t_0,t]}\right) \qquad (6.139)
\end{aligned}
$$

with $\check{M} := \bar{q}_C|\mathscr{R}^{-1}||\mathscr{R}P_C(1)|M_{\bar{w}}$, $\check{\delta} := \delta_{\bar{w}}$, and $\check{\gamma} := \bar{q}_C|\mathscr{R}^{-1}|\gamma_{\bar{w}}$. Therefore, the output feedback system is FT-ISS+C.

As for the claim regarding $u(t)$, from (6.67), (6.45)–(6.47), and (6.42), we obtain

$$
\begin{aligned}
u(t) &= -\nu^{m_C}l_0(\nu)w(t) - \nu^{m_C+n}K_{n-1}^T J_2 w(t) + \nu^{m_C+1}a^T Q_C(\nu)w(t) - k_n\sigma(t) + \tilde{u}(t) \\
&= -\nu^{m_C}\left(l_0(\nu) + \nu^n K_{n-1}^T J_2 - \nu a^T Q_C(\nu)\right)w(t) - k_n\sigma(t) + \tilde{u}(t). \qquad (6.140)
\end{aligned}
$$

The terms involving $w(t)$ are uniformly bounded for $t \in [t_0, t_0+T)$ and go to zero as $t \to t_0+T$. By Lemma 6.4 and our choice of the observer and controller parameters, the same is true for $\tilde{u}(t)$. Finally, by Lemma 6.6 and (6.120), $\sigma(t)$ remains uniformly bounded for $t \in [t_0, t_0+T)$. The claim on $u(t)$ is proven. ■

6.5.5 Proof of Theorem 6.1

From (6.11), the triangle inequality, and (6.9) we obtain

$$
\begin{aligned}
|\tilde{\xi}(t_0)| &\leq |\mathscr{T}||x(t_0)| + |\hat{\xi}(t_0)| \\
&\leq |\mathscr{T}|\left(|x(t_0)| + |\hat{\xi}(t_0)|\right). \qquad (6.141)
\end{aligned}
$$

Inserting (6.141) into (6.26) then gives

$$
|\tilde{\xi}(t)| \leq \nu^{m_O+1}\tilde{M}|\mathscr{T}|\mathrm{e}^{-\tilde{\delta}(t-t_0)}\left(|x(t_0)| + |\hat{\xi}(t_0)|\right). \qquad (6.142)
$$

With (6.71) and (6.142), we obtain

$$
\begin{aligned}
|x(t)| + |\hat{\xi}(t)| &\leq \nu^{m_C+1}\left(\check{M}\mathrm{e}^{-\check{\delta}(t-t_0)}|x(t_0)| + \check{\gamma}||\tilde{u}||_{[t_0,t]}\right) + \nu^{m_O+1}\tilde{M}|\mathscr{T}|\mathrm{e}^{-\tilde{\delta}(t-t_0)}\left(|x(t_0)| + |\hat{\xi}(t_0)|\right) \\
&\leq \nu^{m_C+1}\left(\check{M}\mathrm{e}^{-\check{\delta}(t-t_0)}|x(t_0)| + \check{\gamma}||\tilde{u}||_{[t_0,t]}\right) + \nu^{m_C+1}\tilde{M}|\mathscr{T}|\mathrm{e}^{-\tilde{\delta}(t-t_0)}\left(|x(t_0)| + |\hat{\xi}(t_0)|\right) \\
&\leq \nu^{m_C+1}\check{M}\mathrm{e}^{-\check{\delta}(t-t_0)}|x(t_0)| + \nu^{m_C+1}\tilde{M}|\mathscr{T}|\mathrm{e}^{-\tilde{\delta}(t-t_0)}\left(|x(t_0)| + |\hat{\xi}(t_0)|\right) + \nu^{m_C+1}\check{\gamma}||\tilde{u}||_{[t_0,t]} \\
&\leq \nu^{m_C+1}\left(\check{M}\mathrm{e}^{-\check{\delta}(t-t_0)} + \tilde{M}|\mathscr{T}|\mathrm{e}^{-\tilde{\delta}(t-t_0)}\right)\left(|x(t_0)| + |\hat{\xi}(t_0)|\right) + \nu^{m_C+1}\check{\gamma}||\tilde{u}||_{[t_0,t]}.
\end{aligned}
$$

$$(6.143)$$

From (6.111) we have

$$
\begin{aligned}
\sup_{t_0 \leq \tau \leq t}|\tilde{u}(\tau)| &= \bar{\phi}|\mathscr{T}^{-1}|\tilde{M}|\tilde{\xi}(t_0)| \\
&\leq \bar{\phi}|\mathscr{T}^{-1}|\tilde{M}|\mathscr{T}|\left(|x(t_0)| + |\hat{\xi}(t_0)|\right)
\end{aligned}
$$

after using (6.141). Using this result in (6.143) obtains

$$
\begin{aligned}
|x(t)| + |\hat{\xi}(t)| &\leq \nu^{m_C+1}\left(\check{M}\mathrm{e}^{-\check{\delta}(t-t_0)} + \tilde{M}|\mathscr{T}|\mathrm{e}^{-\tilde{\delta}(t-t_0)} + \check{\gamma}\bar{\phi}|\mathscr{T}^{-1}|\tilde{M}|\mathscr{T}|\right)\left(|x(t_0)| + |\hat{\xi}(t_0)|\right) \\
&\leq \nu^{m_C+1}\bar{M}\left(|x(t_0)| + |\hat{\xi}(t_0)|\right) \qquad (6.144)
\end{aligned}
$$

for some positive constant $\bar{M}$. Define $r := |x(t_0)| + |\hat{\xi}(t_0)|$, and $s := \mu_1 - 1$. Then ν can be expressed as $\nu = 1/(s+1)$, and it is clear that the right-hand side of (6.144) is a class $\mathscr{K}\mathscr{L}$ function of the form $\beta(r,s) = \bar{M}r/(s+1)^{m_c+1}$. Thus we have proven the claim. ■

6.6 Acknowledgement

Most of the material in Chapter 6 may appear in a paper by Prof. Krstic and myself entitled "Prescribed-time output feedback for linear systems in controllable canonical form," which has been provisionally accepted to appear in *Automatica*.

Part III

Prescribed-Time Missile Guidance

Chapter 7

State Feedback Guidance Laws

We propose a solution to the general tactical missile guidance problem in which the objective is to stabilize the missile-to-target line-of-sight (LOS) rate to zero within a finite time. Unlike existing approaches to this problem which use sliding mode control (SMC), which does not offer a means to prescribe the stabilization time in a straightforward manner, we propose an alternative approach which employs time-varying feedback of transformed state variables that can achieve full-state stabilization in a *prescribed* finite time. After reviewing the mathematical results required for the new approach, we apply it to a homing missile guidance near-collision course (NCC) engagement for both the ideal case which has a non-maneuvering target and ideal missile autopilot dynamics, and the more general case which has a maneuvering target and uncertain missile autopilot dynamics. We show that with proper selection of the control gains, for which we have closed formulas, the new prescribed-time guidance laws are able to achieve full-state stabilization in a time that is freely prescribed by the user and independent of initial conditions.

7.1 Introduction

In this chapter, we apply the prescribed-time controllers of Chapter 4 to the problem of homing missile guidance in the near-collision course (NCC) (see Section 3.5). We explore the effectiveness of the nominal controller for an ideal scenario with ideal missile autopilot and a non-maneuvering target, and then the robust controller for the more general case of uncertain autopilot dynamics and a maneuvering target.

7.1.1 An alternative approach to finite-time missile guidance

Most existing finite-time tactical missile guidance laws use some form of sliding mode control (SMC) [39, 61, 81, 89, 109]. Although they can be made robust to matched uncertainties such as target maneuvers, these guidance laws do not offer a straightforward way to stabilize the LOS rate in *prescribed* time. In particular, for some SMC guidance laws, it has been shown that the finite time in which stabilization to the origin is achieved is proportional to a Lyapunov function of the initial conditions [89]. These methods make it difficult to prescribe the convergence time because they require accurate knowledge of the initial conditions, which in general is not available in practice.

In Chapter 4, we presented new prescribed-time controllers for normal form nonlinear systems that offer another solution to this problem. The Chapter 4 controllers employ state variable transformations based on time-varying scaling functions that go to infinity at a prescribed time, T, which with carefully-designed time-varying gains results in the state going to zero at the prescribed time. These controllers also offer robustness to matched uncertainties such as target maneuvering, just as SMCs do.

7.1.2 Engagement model

In this section and the next, we lay the foundation for the development of prescribed-time state feedback guidance laws for homing missiles in the NCC (see Section 3.5). Figure 3.5 illustrates the geometry of the engagement. Recall that the purpose of the missile guidance law and missile flight control system (autopilot) are to effect maneuvers through $a_M(t)$ that result in target intercept, i.e., make $y(t) \to 0$ at $t = t_0 + t_f$, since at that time, $r(t) = 0$. The target maneuver $a_T(t)$ acts as a disturbance against this guidance and control objective. When $t = t_0 + t_f$, any remaining displacement, i.e., $M := y(t_0 + t_f)$, is called the *miss distance*.

As in Section 3.5, we define the state as $x(t) = \begin{bmatrix} y(t) & \dot{y}(t) \end{bmatrix}^T$, and express the engagement kinematics as (3.10). In this chapter, we will explore both an ideal engagement in which the target is not maneuvering and the missile exhibits perfect autopilot dynamics ($a_M(t) = a_{M_c}(t)$), and a non-ideal engagement in which the target is maneuvering and the missile autopilot exhibits first-order dynamics according to (3.4).

7.1.3 Prescribed-time controller

To better understand the mechanics of the controllers we will use, we review some of the relevant material from Chapter 4.

In regards to tactical missile guidance applications, Assumption 4.1 says the only knowledge we require about the performance of the missile actuator system is some lower bound on its output once it is commanded an input. Specifically, we do not need to know its detailed dynamical behavior according to some model. Assumption 4.2 imposes a requirement on the kind of uncertain nonlinearity that can be dominated by the controller. For our prescribed-time missile guidance laws, we assume $\psi(x) = 1$, and treat deterministic target maneuver disturbances of the form $f(x,t) = a_T(t)$. Note that Assumption 4.2 does not require that we know an upper bound of the target maneuver.

Next, recall that our controllers employ the prescribed-time scaling functions of Section 2.3.3 and the prescribed-time stability definitions of Section 2.3.4. Last, note that our new prescribed-time guidance laws are based on Theorem 4.2 and Theorem 4.3 of Chapter 4. In the next sections, we show how the results of Chapter 4 could be used to aid in the design of full-state feedback missile guidance laws.

7.2 State feedback guidance law design

7.2.1 Non-maneuvering target and ideal autopilot dynamics

By tailoring the control law of Theorem 4.2 to our NCC engagement model (3.10), for ideal missile autopilot dynamics and a target maneuver $a_T(t)$ that is either non-zero but known (unlikely) or zero (more likely), we obtain the following corollary.

Corollary 7.1. *Select (prescribe) some fixed time $T > 0$ as the time at which stabilization of the LOS rate, $\dot{\lambda}(t)$, is desired. Then for a known target maneuver, $a_T(t)$, and ideal missile autopilot dynamics ($a_M(t) = a_{M_c}(t)$), the guidance law*

$$a_{M_c}(t) = a_T(t) + \kappa_1(t)y(t) + \kappa_2(t)\dot{y}(t), \tag{7.1}$$

with time-varying gains

$$\kappa_1(t) = \frac{\mu_C^{(2)}(t-t_0,T)}{\mu_C(t-t_0,T)} + \mu_C^{(1)}(t-t_0,T)\left(\frac{k_1}{\mu_C(t-t_0,T)} + k_2\right) + k_1k_2\mu_C(t-t_0,T),$$
$$\kappa_2(t) = 2\frac{\mu_C^{(1)}(t-t_0,T)}{\mu_C(t-t_0,T)} + k_2\mu_C(t-t_0,T) + k_1,$$

where $k_1, k_2 > 0$ are design parameters, and

$$\mu_C(t-t_0,T) = \frac{T^{m_C+2}}{(T+t_0-t,T)^{m_C+2}},$$
$$\mu_C^{(1)}(t-t_0,T) = (m_C+2)\frac{T^{m_C+2}}{(T+t_0-t)^{m_C+3}},$$
$$\mu_C^{(2)}(t-t_0,T) = (m_C+3)(m_C+2)\frac{T^{m_C+2}}{(T+t_0-t)^{m_C+4}},$$

with integer $m_C \geq 1$ a third design parameter, achieves stabilization of $y(t)$ and $\dot{y}(t)$ within the prescribed time T. Furthermore, this guarantees that the LOS rate, $\dot{\lambda}(t)$, is stabilized to zero in time T.

Example 7.1. First, we consider the prescribed-time guidance law (7.1) of Corollary 1, denoted here as FTG1, for an engagement having a known target maneuver ($a_T(t) = 0$) and ideal autopilot dynamics ($a_M(t) = a_{M,c}(t)$). Figure 7.1 shows an example of using FTG1 in an engagement with initial conditions $t_0 = 0$, $(y(t_0), \dot{y}(t_0)) = (5,2)$, total time-of-flight $t_f = 5$, prescribed stabilization time $T = 6.5$, and three different values of m_C ($m_C = 1,2,3$). We see that with all three values of m_C, fixed-time stabilization of y and $\dot{y}$ is achieved within the prescribed time $T = 6.5$. Also, as m_C is increased, stabilization is achieved in a shorter amount of time. Figure 7.2 shows the corresponding time histories of the control gains and missile acceleration, which in this case of ideal autopilot dynamics is equal to the commanded missile acceleration from guidance. For all three values of m_C, the missile acceleration is not only continuous, but is also smooth, and decreases to zero as stabilization is achieved. Finally, note that as m_C increases, the initial acceleration output increases as well. We therefore see a design trade for FTG1 from (7.1), i.e., that as $m_C \geq 1$ is increased, stabilization of the state can be obtained more quickly, but it comes at the cost of increased acceleration requirements by the guidance and control system.

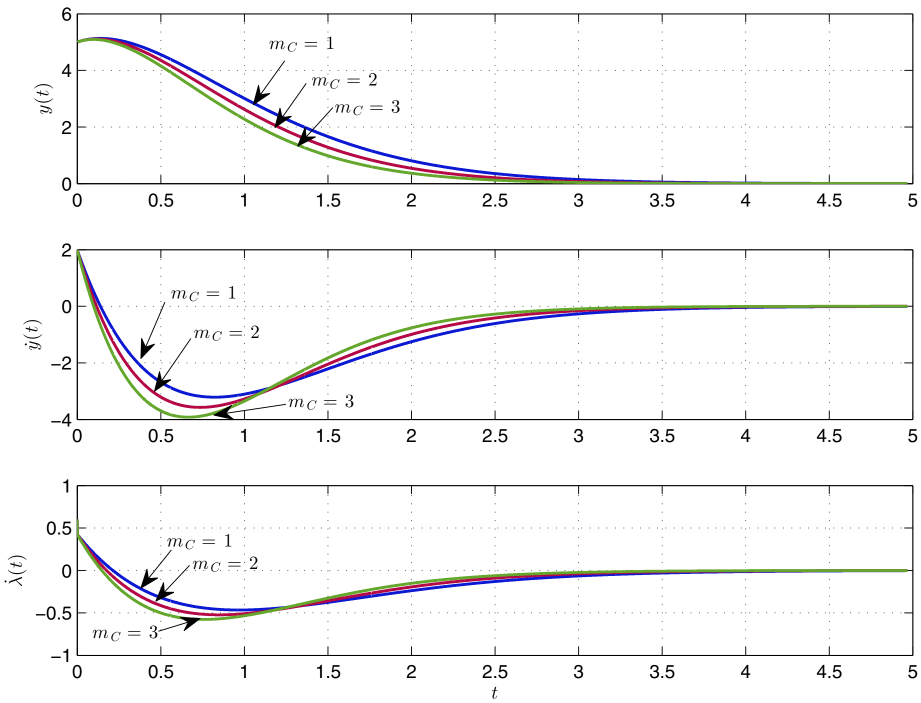

Figure 7.1: Time histories of states for Example 7.1. The parameter m_C is varied.

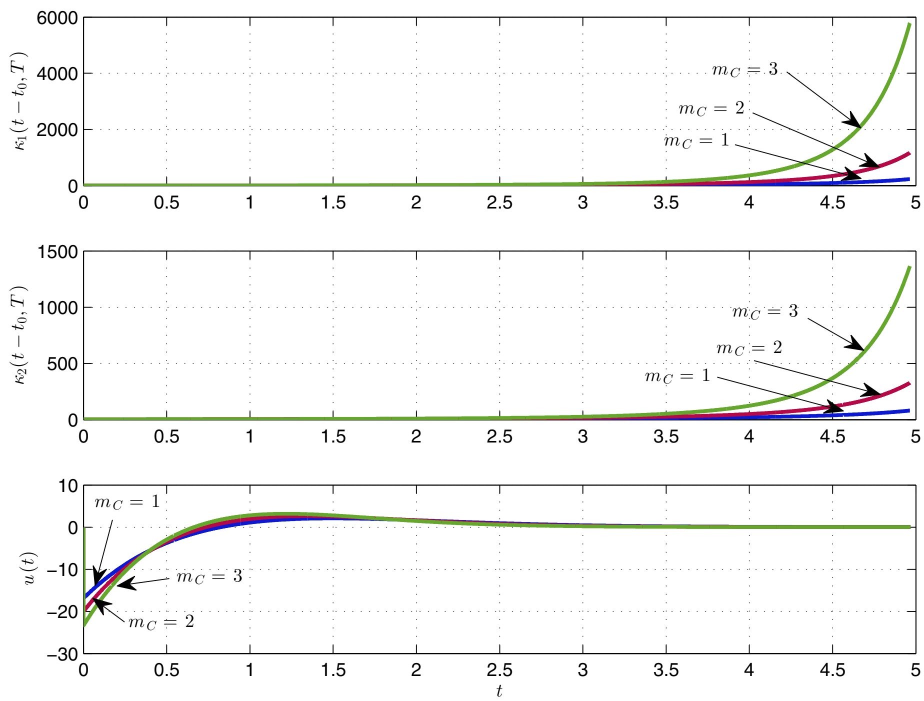

Figure 7.2: Time histories of control gains and missile acceleration for Example 7.1. The parameter m_C is varied.

Example 7.2. In Figure 7.3 and Figure 7.4, we compare the performance of FTG1 to the classical tactical missile guidance law, Proportional Navigation (PN) (see Section 3.6), with ideal missile autopilot dynamics ($a_M(t) = a_{M_c}(t)$). In the NCC, by substituting (3.7) into (3.15), PN can be expressed as

$$a_{M_c}(t) = \frac{N'}{t_{go}(t)^2} y(t) + \frac{N'}{t_{go}(t)} \dot{y}(t), \tag{7.2}$$

where N' is the *effective navigation ratio* (see Section 3.6.2). For our comparison, we set $N' = 4$ and consider an engagement with initial conditions $t_0 = 0$, $(y(t_0), \dot{y}(t_0)) = (0, -10)$, and $t_f = 4$. For FTG1, we selected $T = 6$ and $m_C = 1$. Figure 7.3 shows that FTG1 achieves stabilization of both $y(t)$ and $\dot{y}(t)$ prior to $t_f = 4$, whereas PN only achieves stabilization of $y(t)$. Figure 7.3 also shows that both FTG1 and PN eventually null the LOS rate $\dot{\lambda}(t)$, but FTG1 is able to do so more quickly. For both simulations, $\dot{\lambda}(t)$ eventuallly diverges due to numerical instability in the calculation of $\dot{\lambda}(t)$. Figure 7.4 shows that the FTG1 demands greater missile acceleration initially, and other simulations not shown here have suggested that this behavior is strongly dependent on the choice of the parameter T. Therefore, the guidance law (7.1) exhibits a second design trade to consider.

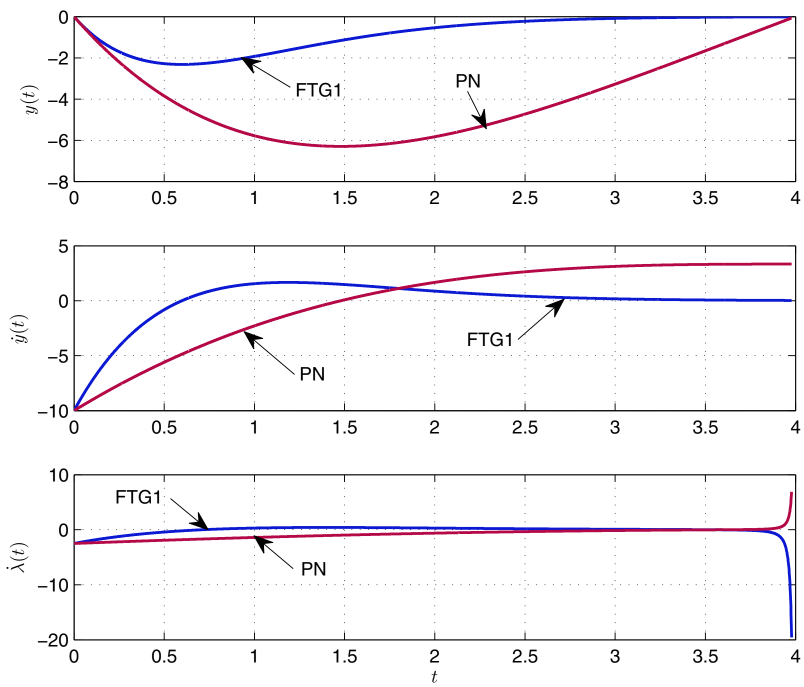

Figure 7.3: Time histories of states for Example 7.2, in which FTG1 is compared to PN.

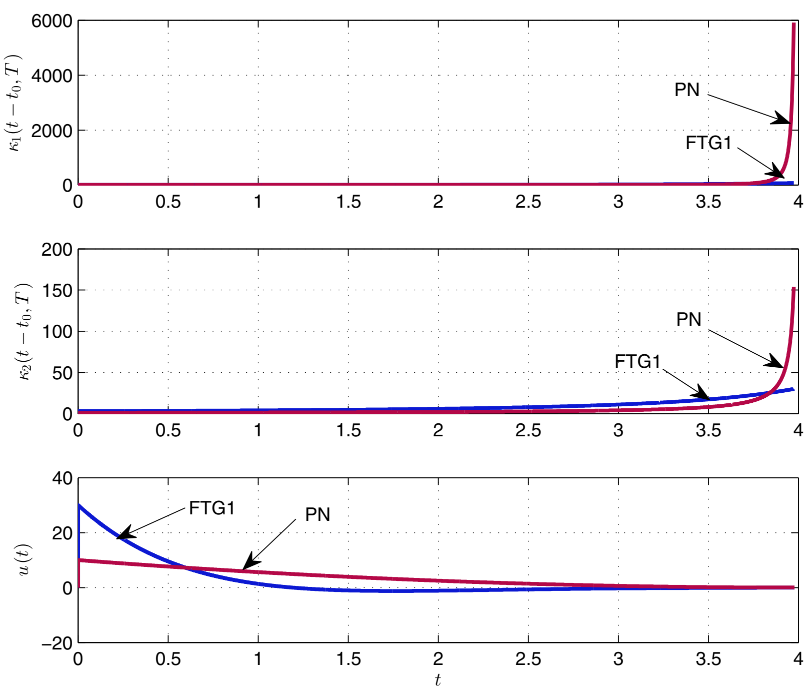

Figure 7.4: Time histories of control gains and missile acceleration for Example 7.2, in which FTG1 is compared to PN.

7.2.2 Maneuvering target and uncertain autopilot dynamics

For the more general case in which the target maneuvers in an unknown fashion, and there exist non-ideal missile autopilot dynamics that the guidance law does not explicitly account for, we leverage Theorem 4.3. By tailoring the result and proof of Theorem 4.3 to this particular homing missile guidance problem, we obtain the following corollary.

Corollary 7.2. *Select (prescribe) some fixed time $T > 0$ as the time at which stabilization of the LOS rate, $\dot{\lambda}(t)$, is desired, and calculate the static gain $\overline{\kappa} > 0$ according to*

$$\overline{\kappa} = \frac{1}{\underline{b}}(\lambda + \theta + k),$$

where $\underline{b} > 0$ is the minimum autopilot acceleration expected upon command, $\lambda > 0$, $\theta \geq \theta_*$, where for $k_1, \rho > 0$ and integer $m_C \geq 1$,

$$\theta_* = k_1 + \frac{2(m_C+2)}{T} + \rho \max_{\nu \in [0,1]} |\Gamma(\nu)|^2,$$
$$\Gamma(\nu) = -\left[\frac{1}{T^2}(m_C+2)(m_C+1) + \frac{2k_1(m_C+2)}{T}\nu + k_1^2\nu^2\right],$$

and $k > 0$ is selected such that

$$k > \frac{1}{4k_1\rho}.$$

Then, the guidance law

$$a_{M_c}(t) = \kappa_1(t-t_0,T)y(t) + \kappa_2(t-t_0,T)\dot{y}(t), \tag{7.3}$$

with time-varying gains $\kappa_1(t-t_0,T)$ and $\kappa_2(t-t_0,T)$ given by

$$\kappa_1(t-t_0,T) = \overline{\kappa}\left(\mu_C^{(1)}(t-t_0,T) + k_1\mu_C(t-t_0,T)\right),$$
$$\kappa_2(t-t_0,T) = \overline{\kappa}\mu_C(t-t_0,T),$$

achieves FT-ISS+C stabilization of $y(t)$, $\dot{y}(t)$ in the prescribed time T.

Example 7.3. We now consider the prescribed-time guidance law (7.3) of Corollary 2, denoted FTG2, for an engagement having an unknown target maneuver and first-order missile autopilot dynamics according to (3.4). Figure 7.5–Figure 7.7 show simulation results of using FTG2 for an engagement in which the initial conditions are $t_0 = 0$, $(y(t_0), \dot{y}(t_0)) = (10, -20)$, the total time-of-flight is $t_f = 5$, the target maneuvers according to $a_T(t) = 5\sin(2t)$, and the missile autopilot has a time constant of $T_A = 0.2$ but the missile guidance law does not directly account for this. To achieve the intercept objective, we selected $T = 6.5$ as the prescribed stabilization time, and $m_C = 1$, $\rho = 1$, $\underline{b} = 3.0$, $k_1 = 0.1$, $\lambda = 0.1$, $\theta = 1.08$, and $k = 2.51$ for the controller parameters. Figure 7.5 shows time histories of the states and LOS rate, Figure 7.6 shows time histories of the control gains and commanded missile acceleration, and Figure 7.7 shows time histories of the target acceleration, commanded missile acceleration, and actual missile acceleration. Figure 7.5 shows that, despite the target maneuvering and autopilot dynamics, FTG2 is able to stabilize both y and $\dot{y}$ to zero within the prescribed time $T = 6.5$. Figure 7.6 shows that despite the gains going to infinity, the overall control input remains bounded.

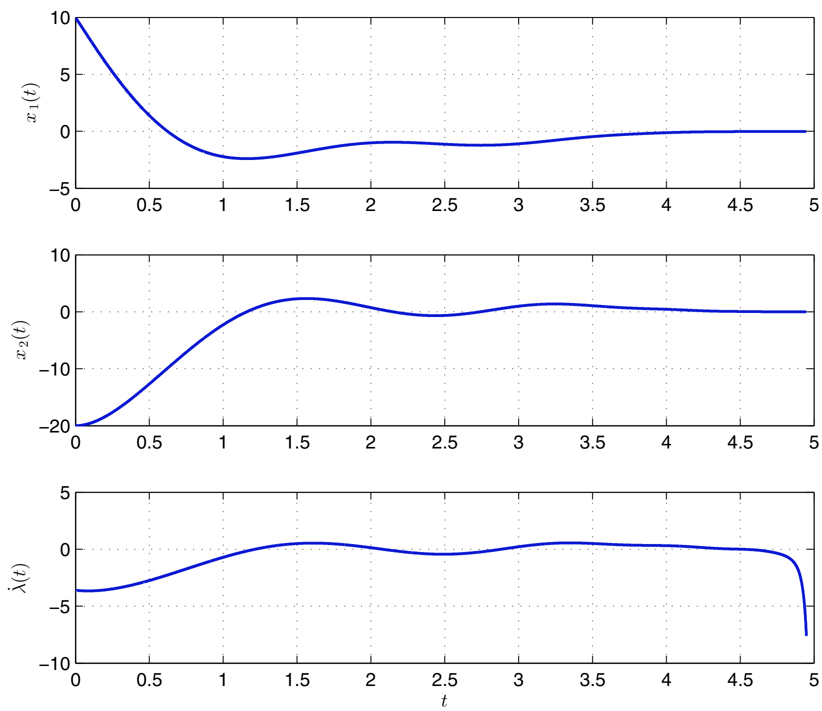

Figure 7.5: Time histories of states for Example 7.3.

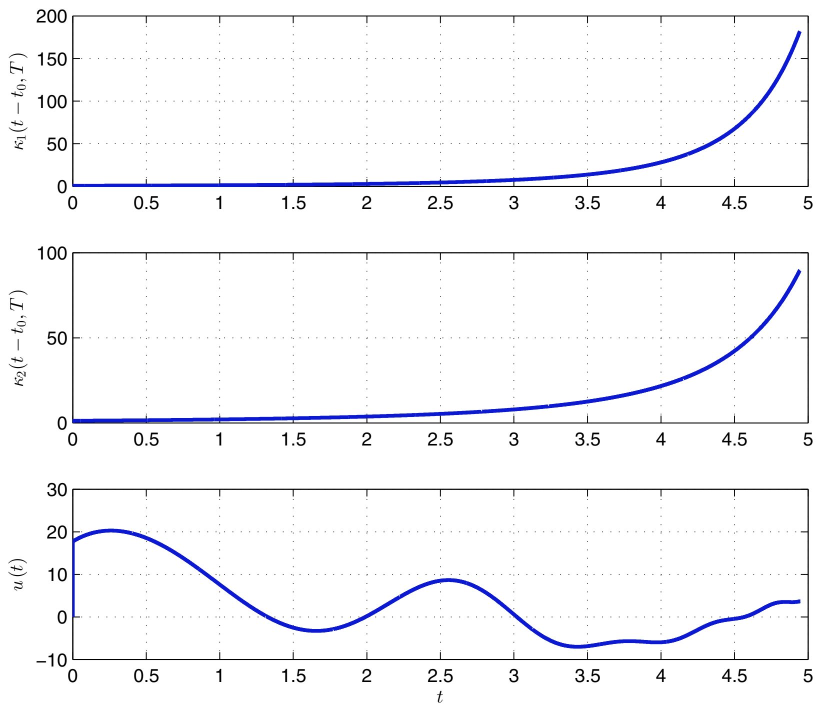

Figure 7.6: Time histories of gains and commanded missile acceleration for Example 7.3.

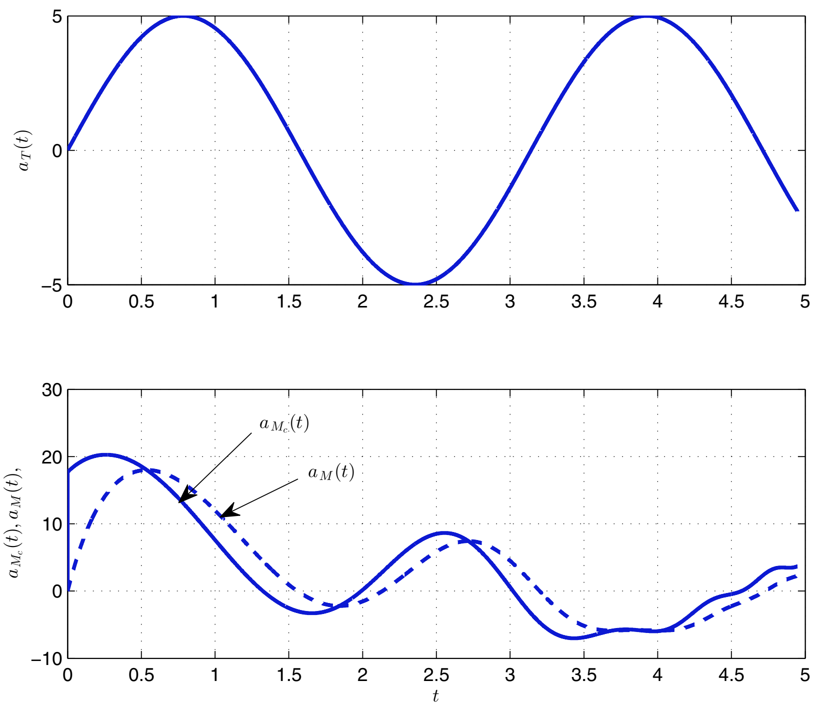

Figure 7.7: Time histories of target and missile acceleration for Example 7.3.

7.3 Discussion

Our proposed prescribed-time guidance laws offer a new approach for homing missile guidance systems to null the LOS rate in a prescribed finite time. The first guidance law we explored for a non-maneuvering target and ideal missile autopilot dynamics offers design trades with the parameters T and m_C. Increasing m_C can decrease the time in which stabilization is achieved, but it comes at the cost of demanding greater acceleration output from the missile autopilot. This suggests that actuator saturation could become a limiting factor in using this guidance law in practice. The second guidance law, which was designed as a robust guidance law to dominate target maneuvering and autopilot uncertainties, offers similar trades but with a larger number of controller parameters that must be tuned. With better understanding of the design trades, and satisfactory tuning of the controller parameters for the particular application considered, these guidance laws could potentially be useful starting points in the design of guidance laws for real homing missile systems for which the engagement kinematics can be sufficiently modeled as uncertain systems in normal form. However, a key layer of realism must still be added to yield a viable guidance law in practice, and that is the on-line estimation of the states required to implement the guidance law. This is the subject of the next chapter.

7.4 Proofs of results

7.4.1 Proof of Corollary 7.1

First, note that by comparing (3.8) to (4.1), we see that $n = 2$, $b(x,t) = -1$, and $f(x,t) = a_T(t)$. Next, for ideal autopilot dynamics, we also have $a_M(t) = a_{M,c}(t)$. Then to construct the guidance law, we simply require expressions for $L_0(t)$, $L_1(t)$, and $z(t)$. For our engagement model, $n = 2$, and the transformed variables w_1 and w_2 are found using the scaling function $\mu_C(t-t_0,T)$ and differentiating,

$$\begin{aligned} w_1 &= \mu_C x_1, \\ w_2 &= \dot{w}_1 \\ &= \mu_C^{(1)} x_1 + \mu_C \dot{x}_1 \\ &= \mu_C^{(1)} x_1 + \mu_C x_2. \end{aligned} \tag{7.4}$$

The r variables are given by

$$r_1 = w_1 = J_1 w = \begin{bmatrix} 1 & 0 \end{bmatrix} \begin{bmatrix} w_1 \\ w_2 \end{bmatrix}, \tag{7.5}$$

$$r_2 = w_2 = J_2 w = \begin{bmatrix} 0 & 1 \end{bmatrix} \begin{bmatrix} w_1 \\ w_2 \end{bmatrix}, \tag{7.6}$$

and then from (4.27), we have

$$\dot{r}_1 = -k_1 r_1 + z. \tag{7.7}$$

Recall that (7.7) is ISS with respect to the disturbance z. Then from (4.26) and (4.29), and with $x_1 = y$ and $x_2 = \dot{y}$,

$$
\begin{aligned}
z &= w_2 + k_1 r_1 \\
&= w_2 + k_1 w_1 \\
&= \mu_C^{(1)} x_1 + \mu_C x_2 + k_1 \mu_C x_1 \\
&= \left(\mu_C^{(1)} + k_1 \mu_C\right) x_1 + \mu_C x_2 \\
&= \left(\mu_C^{(1)} + k_1 \mu_C\right) y + \mu_C \dot{y}.
\end{aligned} \tag{7.8}
$$

Explicit expressions for the feedbacks L_0 and L_1 are obtained easily since they are provided by the closed-form expressions (4.31) and (4.32). That is,

$$
\begin{aligned}
L_0 &= \sum_{k=1}^{2} \begin{pmatrix} 2 \\ k \end{pmatrix} \frac{\mu_C^{(k)}}{\mu_C} x_{3-k} \\
&= 2\frac{\mu_C^{(1)}}{\mu_C} x_2 + \frac{\mu_C^{(2)}}{\mu_C} x_1 \\
&= 2\frac{\mu_C^{(1)}}{\mu_C} \dot{y} + \frac{\mu_C^{(2)}}{\mu_C} y
\end{aligned} \tag{7.9}
$$

and

$$
\begin{aligned}
L_1 &= \frac{1}{\mu_C} k_1 w_2 \\
&= \frac{1}{\mu_C} k_1 \left(\mu_C^{(1)} x_1 + \mu_C x_2\right) \\
&= k_1 \frac{\mu^{(1)}}{\mu_C} y + k_1 \dot{y}.
\end{aligned} \tag{7.10}
$$

Combining these expressions gives the feedback

$$
\begin{aligned}
a_{M,c} &= a_M \\
&= a_T + L_0 + L_1 + k_2 z \\
&= a_T + 2\frac{\mu_C^{(1)}}{\mu_C}\dot{y} + \frac{\mu_C^{(2)}}{\mu_C}y + k_1\frac{\mu_C^{(1)}}{\mu_C}y + k_1\dot{y} + k_2\left(\mu_C^{(1)} + k_1\mu_C\right)y + k_2\mu_C\dot{y} \\
&= a_T + \left(\frac{\mu_C^{(2)}}{\mu_C} + k_1\frac{\mu_C^{(1)}}{\mu_C} + k_2\mu_C^{(1)} + k_1k_2\mu_C\right)y + \left(2\frac{\mu_C^{(1)}}{\mu_C} + k_2\mu_C + k_1\right)\dot{y} \\
&= a_T + \left(\frac{\mu_C^{(2)}}{\mu_C} + \mu_C^{(1)}\left(\frac{k_1}{\mu_C} + k_2\right) + k_1k_2\mu_C\right)y + \left(2\frac{\mu_C^{(1)}}{\mu_C} + k_2\mu_C + k_1\right)\dot{y},
\end{aligned}
\tag{7.11}
$$

which obtains (7.1). ∎

7.4.2 Proof of Corollary 7.2

To implement this controller, we must determine appropriate values for $\underline{b}, k, \theta$, and λ that appear in (4.38) of Theorem 4.3 (recall that we assume that $\psi(x) = 1$ for our engagements). First, an appropriate value for $\underline{b}$ can be selected based on judgement and experience with the particular actuator system employed. It is simply a lower bound on the output of the actuators given an acceleration command. Next, we must tailor the θ_* expression (4.42) to our problem. For $n = 2$,

$$\begin{aligned} l_0(\nu) &= \begin{bmatrix} l_{0,1} & l_{0,2} \end{bmatrix} \\ &= \begin{bmatrix} \bar{l}_{0,1} & \bar{l}_{0,2}\nu \end{bmatrix}, \end{aligned} \tag{7.12}$$

and computation of $\bar{l}_{0,1}$ and $\bar{l}_{0,2}$ result in

$$\begin{aligned} \bar{l}_{0,1} &= -\frac{1}{T^2}(m_C+2)(m_C+1), \\ \bar{l}_{0,2} &= \frac{2(m_C+2)}{T}, \end{aligned} \tag{7.13}$$

so that

$$l_0(\nu) = \begin{bmatrix} -\frac{1}{T^2}(m_C+2)(m_C+1) & \frac{2(m_C+2)}{T}\nu \end{bmatrix}. \tag{7.14}$$

Define

$$\Gamma(\nu) := \left(\nu^n K_{n-1}^T J_2 + l_0(\nu)\right)\left(J_1^T - \mathrm{e}_n K_{n-1}^T\right). \tag{7.15}$$

Then since for $n = 2$, $J_1 = \begin{bmatrix} 1 & 0 \end{bmatrix}$ and $J_2 = \begin{bmatrix} 0 & 1 \end{bmatrix}$, and $K_{n-1}^T = k_1$, it is easy to verify that

$$\begin{aligned} \Gamma(\nu) &= \bar{l}_{0,1} - k_1\bar{l}_{0,2}\nu - k_1^2\nu^2 \\ &= -\frac{1}{T^2}(m_C+2)(m_C+1) - \frac{2k_1(m_C+2)}{T}\nu - k_1^2\nu^2 \\ &= -\left[\frac{1}{T^2}(m_C+2)(m_C+1) + \frac{2k_1(m_C+2)}{T}\nu + k_1^2\nu^2\right]. \end{aligned} \tag{7.16}$$

Clearly, the maximum of $|\Gamma(\nu)|^2$ over $\nu \in [0,1]$ depends on the choices for T, m_C, and k_1.

To determine γ_1, we must complete the ISS proof for the r_1 system. We seek to find M_1, δ_1, and γ_1 such that

$$|r_1(t)| \leq M_1 \mathrm{e}^{-\delta_1(t-t_0)}|r_1(t_0)| + \gamma_1 \|z\|_{\tau\in[t_0,t]}, \quad \forall t \in [t_0, t_0+T). \tag{7.17}$$

Since the matrix Λ is Hurwitz, given $Q = Q^T > 0$, there exists a $P = P^T > 0$ such that P is the solution to the Lyapunov equation

$$P\Lambda + \Lambda^T P = -Q. \tag{7.18}$$

For $n = 2$, this reduces to a scalar equation, such that $\Lambda = -k_1$, $P = p$, and choosing $Q = 1$, we obtain

$$-pk_1 - k_1 p = -1, \quad \Rightarrow p = \frac{1}{2k_1}. \tag{7.19}$$

To prove ISS for the r_1 system, we choose the Lyapunov function candidate

$$V[r_1(t)] := r_1(t)^T P r_1(t), \tag{7.20}$$

such that

$$\underline{\lambda}(P)|r_1|^2 \leq V[r_1] \leq \overline{\lambda}(P)|r_1|^2, \tag{7.21}$$

where $\underline{\lambda}(\cdot)$ and $\overline{\lambda}(\cdot)$ denote the minimum and maximum eigenvalues of a matrix, respectively. For $n = 2$, since $\lambda = 1/2k_1$ is the only eigenvalue of P, this reduces to

$$V = \frac{1}{2k_1} r_1^2, \tag{7.22}$$

$$\frac{1}{2k_1} r_1^2 \leq V \leq \frac{1}{2k_1} r_1^2. \tag{7.23}$$

Taking the derivative of the Lyapunov function, we have

$$\begin{aligned}\dot{V} &= \frac{1}{k_1} r_1 \dot{r}_1 \\ &= \frac{1}{k_1} r_1 \left(-k_1 r_1 + z\right) \\ &= -r_1^2 + \frac{1}{k_1} r_1 z. \end{aligned} \tag{7.24}$$

Then using Young's inequality in the form $ab \leq \frac{1}{2}\gamma a^2 + \frac{1}{2\gamma} b^2$ with $\gamma = k_1$ gives

$$\begin{aligned}\dot{V} &\leq -r_1^2 + \frac{1}{2} r_1^2 + \frac{1}{2k_1^2} z^2 \\ &= -\frac{1}{2} r_1^2 + \frac{1}{2k_1^2} z^2 \\ &\leq -k_1 V + \frac{1}{2k_1^2} z^2. \end{aligned} \tag{7.25}$$

We next employ Lemma C.5 of [41] (with $c = k_1$ and $b = \frac{1}{2k_1^2}$), and obtain

$$V(t) \leq V(t_0) \mathrm{e}^{-k_1 (t-t_0)} + \frac{1}{2k_1^3} \|z\|_\infty^2, \tag{7.26}$$

where $\|z\|_\infty := \sup_{\tau \in [t_0, t)} z(\tau)$. From (7.23) we have

$$\begin{aligned} r_1^2 &\leq 2k_1 V \\ &\leq 2k_1 V(t_0) \mathrm{e}^{-k_1 (t-t_0)} + \frac{1}{k_1^2} \|z\|_\infty^2 \qquad (7.27) \\ &\leq r_1(t_0)^2 \mathrm{e}^{-k_1 (t-t_0)} + \frac{1}{k_1^2} \|z\|_\infty^2, \qquad (7.28) \end{aligned}$$

which means that

$$r_1(t) \leq \mathrm{e}^{-\frac{k_1}{2}(t-t_0)} r_1(t_0) + \frac{1}{k_1} \|z\|_\infty, \tag{7.29}$$

thus proving the r_1 system is ISS for $n = 2$. Comparing (7.29) to (4.28) for the definition of ISS, we see that for $n = 2$,

$$M_1 = 1, \quad \delta_1 = \frac{k_1}{2}, \quad \gamma_1 = \frac{1}{k_1}. \tag{7.30}$$

To obtain the remaining control gains, we must choose $\theta \geq \theta_*$ with

$$\theta_* = k_1 + \frac{2(m_C + 2)}{T} + \rho \max_{\nu \in [0,1]} |\Gamma(\nu)|^2, \quad \rho > 0 \tag{7.31}$$

where ρ and k are chosen such that

$$\rho k > \frac{\gamma_1}{4} = \frac{1}{4k_1} \tag{7.32}$$

■

7.5 Acknowledgement

Most of the material in Chapter 7 was accepted for inclusion in the AIAA SciTech 2017 conference in a paper by Prof. Krstic and myself entitled "Finite-time terminal guidance laws based on robust time-varying feedback for uncertain normal form systems." We later withdrew the paper because I was unable to attend the conference to present it. However, we may submit this material elsewhere for possible publication in the future.

Chapter 8

Output Feedback Guidance Laws

In realistic tactical missile guidance applications, the missile-to-target line-of-sight (LOS) rate must be estimated accurately before it can be stabilized to zero through guidance and control to enforce collision-course (CC) kinematic conditions. Here, we introduce two prescribed-time output feedback guidance laws that are capable of both estimating the LOS rate accurately and stabilizing it to within a small neighborhood of the origin in a fixed time that is freely prescribed by the user and independent of initial conditions. The first prescribed-time output feedback guidance law may be useful for applications in which the target is either not maneuvering or the maneuver is known, and the missile autopilot dynamics are fast relative to the engagement time. The second prescribed-time output feedback guidance law is designed for the more common situation in which the target is maneuvering in an unknown fashion, and there exist unmodeled or uncertain missile autopilot dynamics.

8.1 Introduction

In this chapter, we leverage the results of the previous chapters to develop two prescribed-time output feedback guidance laws. Having knowledge of the separation principle introduced in Chapter 6, the basic idea we employ here is to combine the prescribed-time observer of Chapter 5 with the prescribed-time state feedback guidance laws of Chapter 7. This short chapter introduces two prescribed-time output feedback guidance laws through three examples.

8.2 Output feedback guidance law design

8.2.1 Non-maneuvering target and ideal autopilot dynamics

Our first prescribed-time output feedback guidance law consists of using the prescribed-time observer of Chapter 5 with the prescribed-time guidance law of Corollary 7.1. This guidance law is intended for use in applications in which the missile autopilot dynamics are fast relative to the engagement time, and the target is either not maneuvering or maneuvering in a known fashion. Note that when no missile autopilot dynamics or target maneuvering are present, this guidance law is the same as the output feedback controller of Example 6.1.

Example 8.1. We simulate the prescribed-time guidance law (7.1) but with the state estimated by the observer of Example 6.1, denoted here as FTOFG1, for an engagement with a non-maneuvering target and ideal autopilot dynamics. Figure 8.1–Figure 8.4 show the results of using FTOFG1 in an engagement having initial conditions $t_0 = 0$, $(y(t_0), \dot{y}(t_0)) = (21, 4)$, total time-of-flight of $t_f = 7$, prescribed stabilization time of $T = 9$, $l_1 = l_2 = k_1 = k_2 = 1$, and $m_C = 1$ and $m_O = 3$. Fixed-time stabilization of y and $\dot{y}$ is achieved within the prescribed time $T = 9$. Figure 8.2 shows time histories of the state estimation errors, and Figure 8.3 shows time histories of the output estimation error injections. Both of these remain bounded and go to zero as time approaches the prescribed time, despite the observer gains going to infinity. Figure 8.4 shows the corresponding time histories of the control gains and commanded missile acceleration, which in this case of ideal autopilot dynamics is equal to the actual resulting missile acceleration. The commanded missile acceleration remains bounded despite the control gains going to infinity.

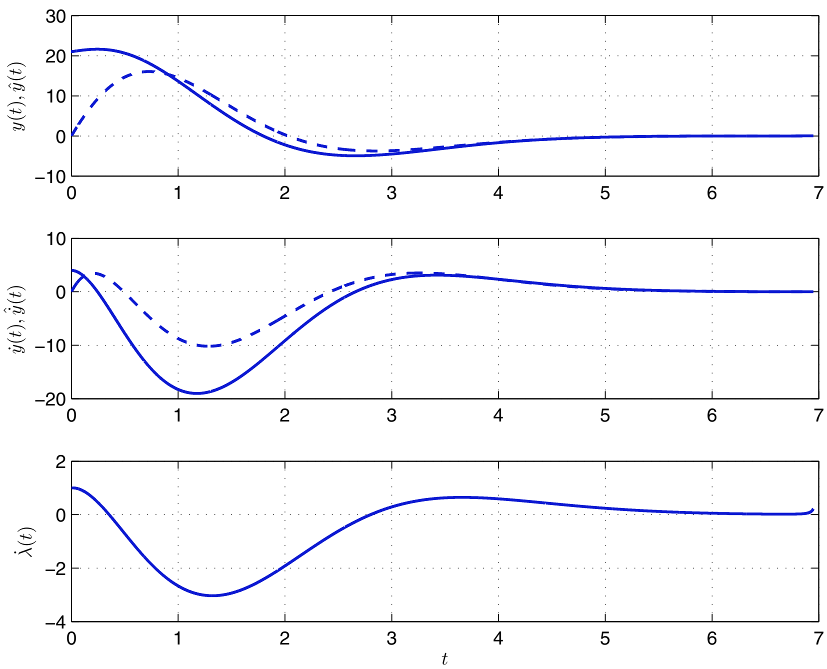

Figure 8.1: Time histories of states and state estimates for Example 8.1. Solid lines denote the states, and dashed lines denote the state estimates.

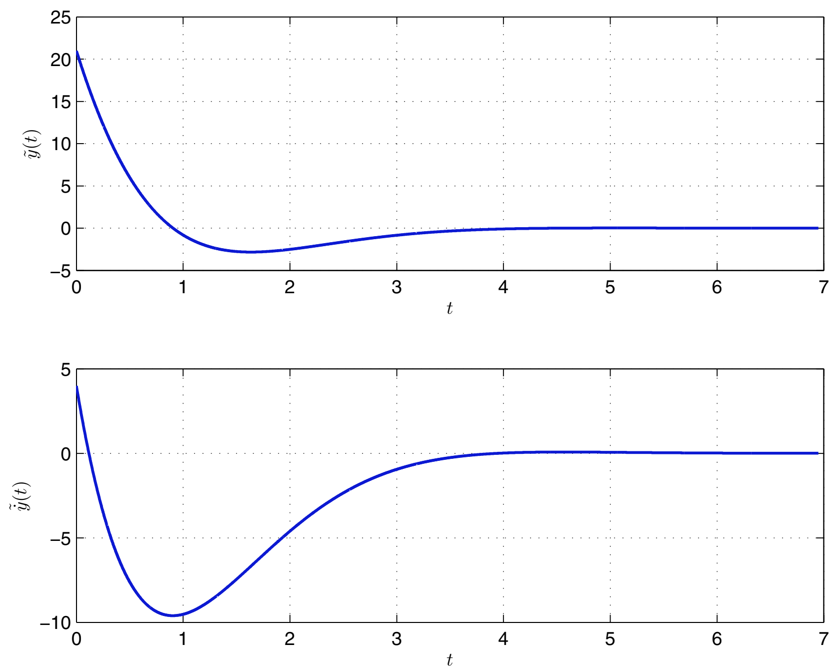

Figure 8.2: Time histories of state estimation errors for Example 8.1.

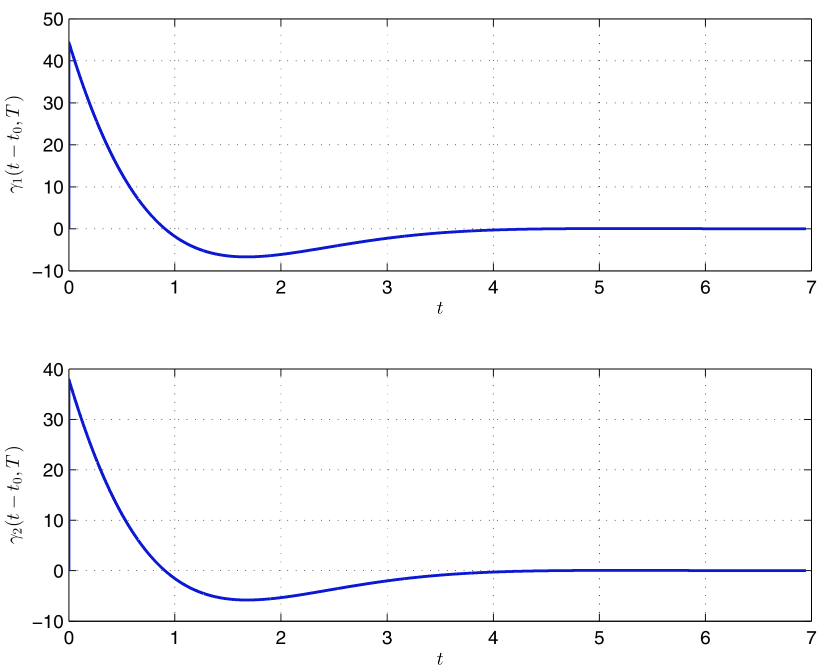

Figure 8.3: Time histories of output estimation error injections for Example 8.1.

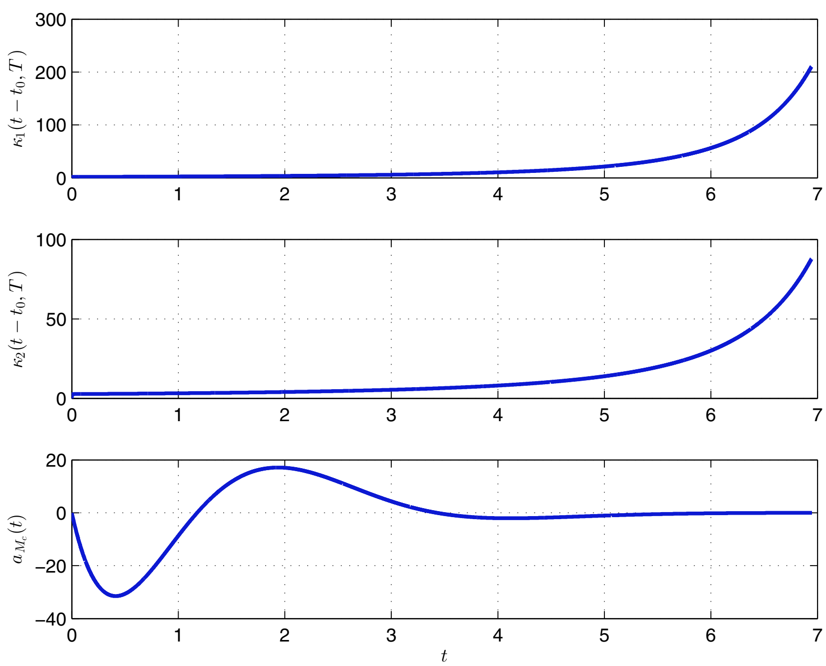

Figure 8.4: Time histories of gains and missile acceleration for Example 8.1.

8.2.2 Maneuvering target and uncertain autopilot dynamics

Our second prescribed-time output feedback guidance law consists of using the prescribed-time observer of Chapter 5 with the prescribed-time guidance law of Corollary 7.2. With proper tuning of the controller and observer parameters, this guidance law may be appropriate when the missile has unmodeled autopilot dynamics that must be accounted for and the target is maneuvering. Note, however, that the observer of Chapter 5 was designed assuming no plant disturbances such as target maneuvering and unmodeled autopilot dynamics. Therefore, we do not necessarily expect the observer to perform as well here as it does for cases having no disturbances, such as Example 8.1. Also, if the observer does not perform optimally, then intuitively we should not expect the controller to perform as well as in the state feedback case of Example 7.3. Last, note that we have not yet sought to rigorously prove whether the separation principle holds when plant disturbances are present, so we may encounter additional challenges resulting from combining the observer and the guidance law of Corollary 7.2.

Example 8.2. In this example, we simulate the prescribed-time guidance law (7.3) but with state estimated by the observer of Example 6.1, denoted here as FTOFG2, for an engagement having a maneuvering target and first-order missile autopilot dynamics according to (3.4). Figure 8.5–Figure 8.9 show the results of applying FTOFG2 in an engagement identical to that of Example 7.3, having initial conditions $t_0 = 0$, $(y(t_0), \dot{y}(t_0)) = (10, -20)$, total time-of-flight of $t_f = 5$, the target maneuvers according to $a_T(t) = 5\sin(2t)$, and the missile autopilot time constant is $T_A = 0.2$. To achieve the intercept objective, we selected $T = 6.5$ for the prescribed stabilization time, $l_1 = l_2 = 1$ and $m_O = 6$ for the observer parameters, and $m_C = 1$, $\rho = 1$, $\underline{b} = 3.0$, $k_1 = 0.1$, $\lambda = 0.1$, $\theta = 1.08$, and $k = 2.51$ for the controller parameters. Figure 8.5 shows that fixed-time stabilization of y and $\dot{y}$ is achieved to within a small neighborhood of the origin within the prescribed time $T = 6.5$. Figure

8.6 shows time histories of the state estimation errors, and Figure 8.7 shows time histories of the output estimation error injections. Notice that in this example, these do not completely go to zero as usual, due to the presence of the unmodeled autopilot dynamics and target maneuver which the observer was not designed to accommodate. However, they still remain bounded and converge to within a neighborhood of the origin that is small relative to initial conditions. Figure 8.8 shows the corresponding time histories of the control gains and commanded missile acceleration. The latter remains bounded despite the former going to infinity. Last, Figure 8.9 shows time histories of the target acceleration, commanded missile acceleration, and actual missile acceleration for comparison.

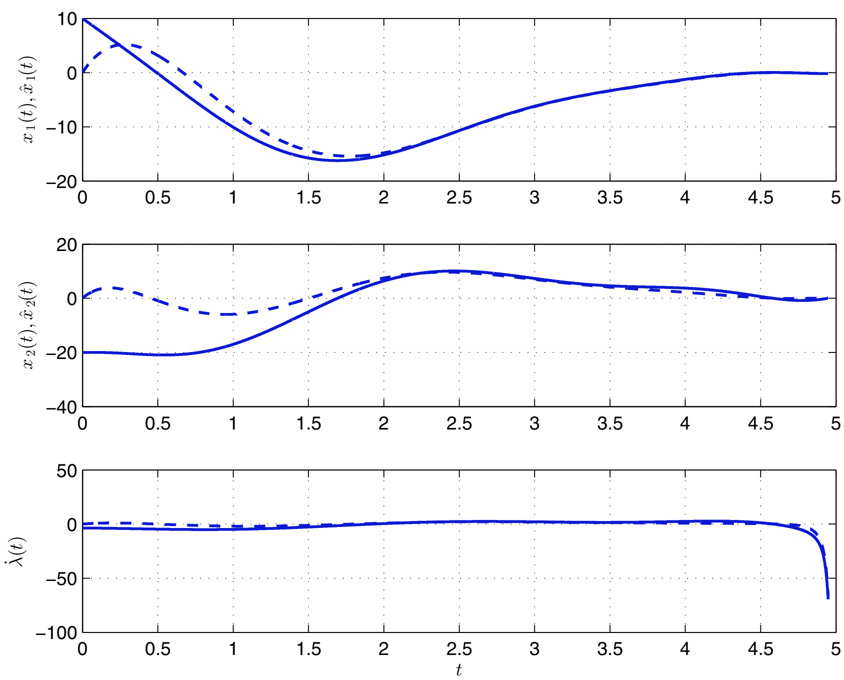

Figure 8.5: Time histories of states and state estimates for Example 8.2. Solid lines denote the states, and dashed lines denote the state estimates.

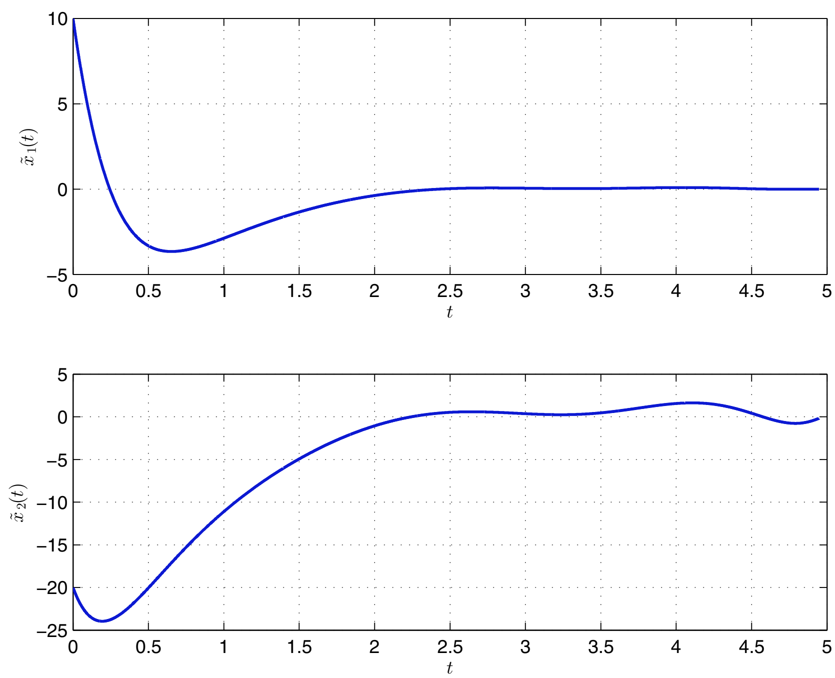

Figure 8.6: Time histories of state estimation errors for Example 8.2.

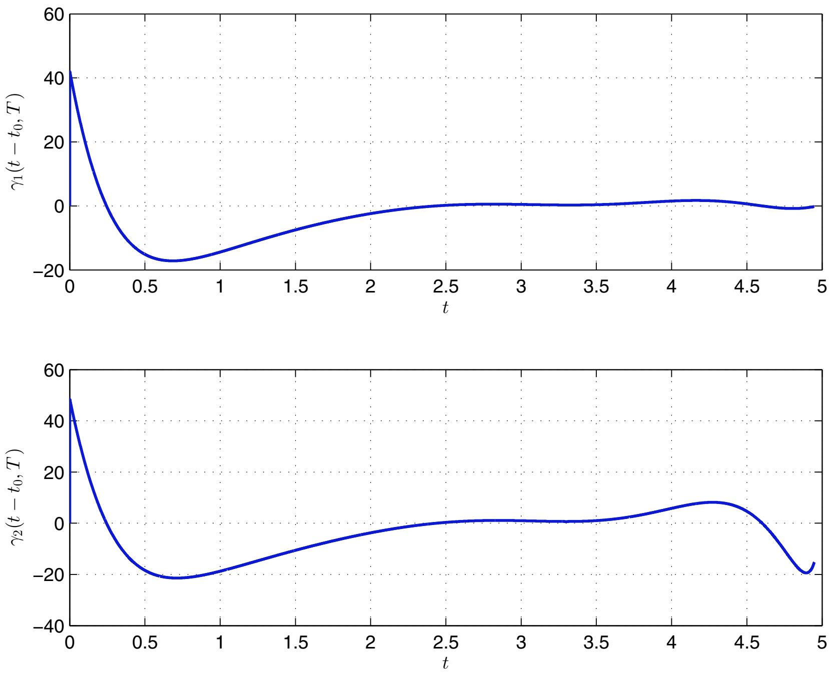

Figure 8.7: Time histories of output estimation error injections for Example 8.2.

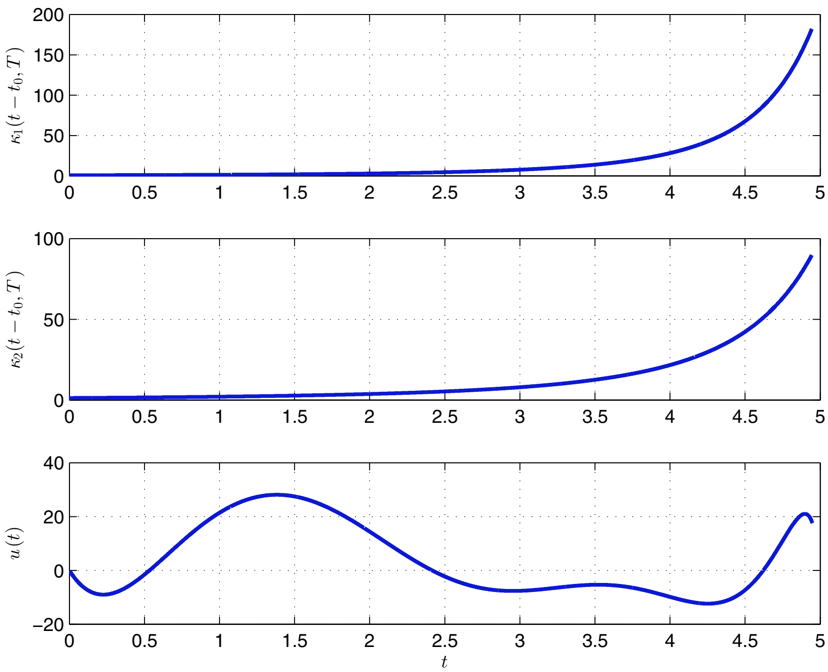

Figure 8.8: Time histories of control gains and missile acceleration command for Example 8.2.

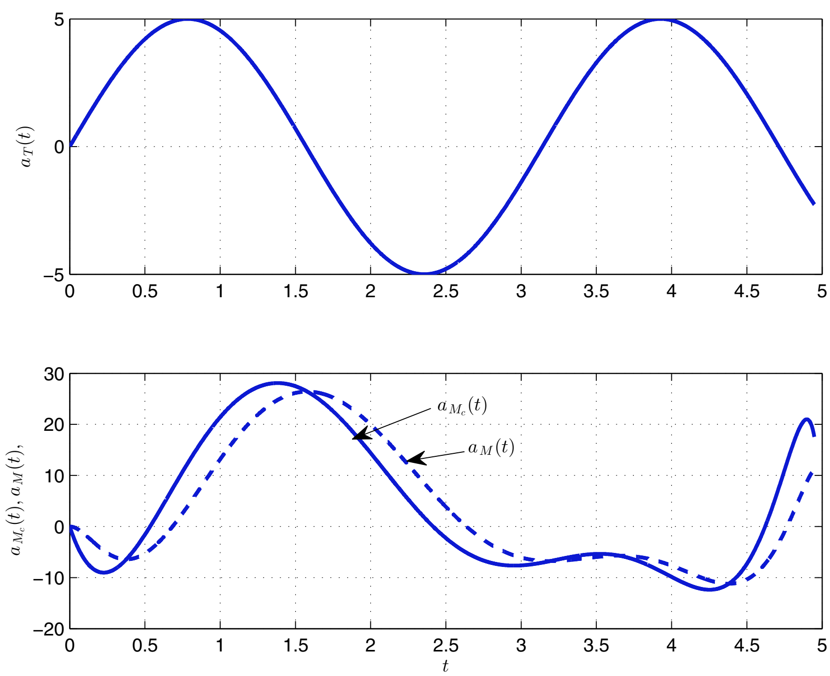

Figure 8.9: Time histories of target and missile acceleration for Example 8.2.

In the previous examples of this chapter, we assumed that the measurement used to estimate the state was perfect. But in realistic tactical missile guidance applications, the measurement will never be perfect, and at a minimum will typically be subjected to some level of noise. Our final example explores the use of FTOFG2 from the previous example but with the addition of pseudo-random white Gaussian measurement noise. Recall that the observer of Chapter 5 used here was not designed to accommodate measurement disturbances, however the observer was still able to perform to some extent in Example 5.3, where this same kind of measurement disturbance was present.

Example 8.3. We repeat Example 8.2 but with the addition of a measurement disturbance according to (5.32) and (5.33), where $\bar{v} = 0$ and $\sigma_v = 5$. The results of the simulation are shown in Figure 8.10–Figure 8.13. Despite the presence of target maneuvering, uncertain autopilot dynamics, and measurement noise, FTOFG2 is able to stabilize y and $\dot{y}$ to within a small neighborhood of the origin relative to initial conditions within the prescribed time $T = 6.5$.

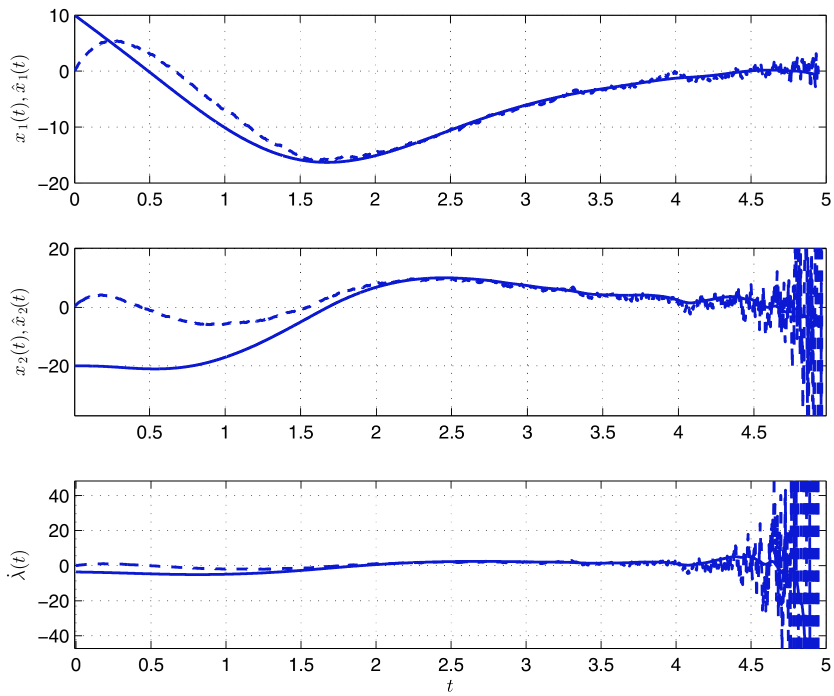

Figure 8.10: Time histories of states and state estimates for Example 8.3. Solid lines denote the states, and dashed lines denote the state estimates.

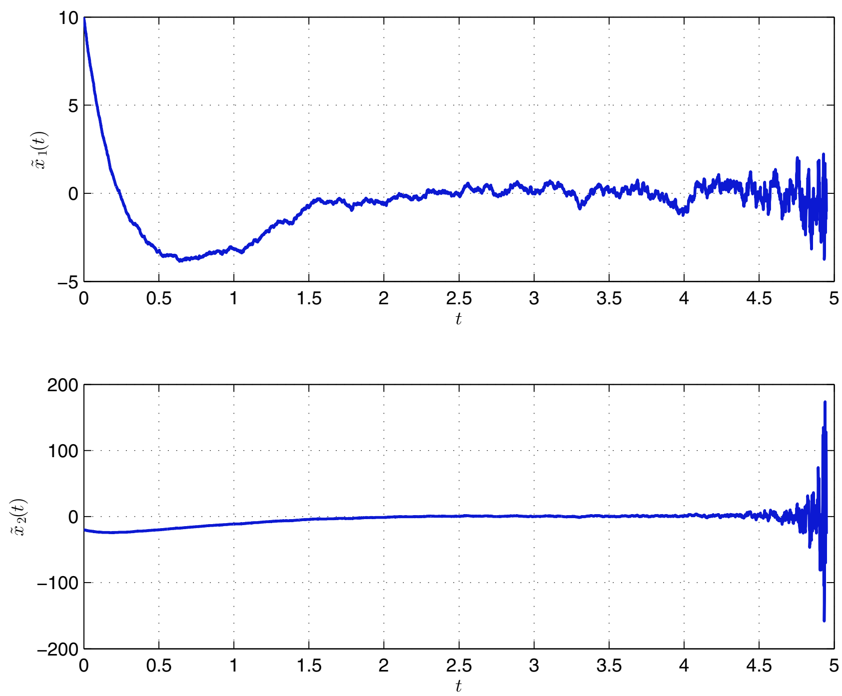

Figure 8.11: Time histories of state estimation errors for Example 8.3.

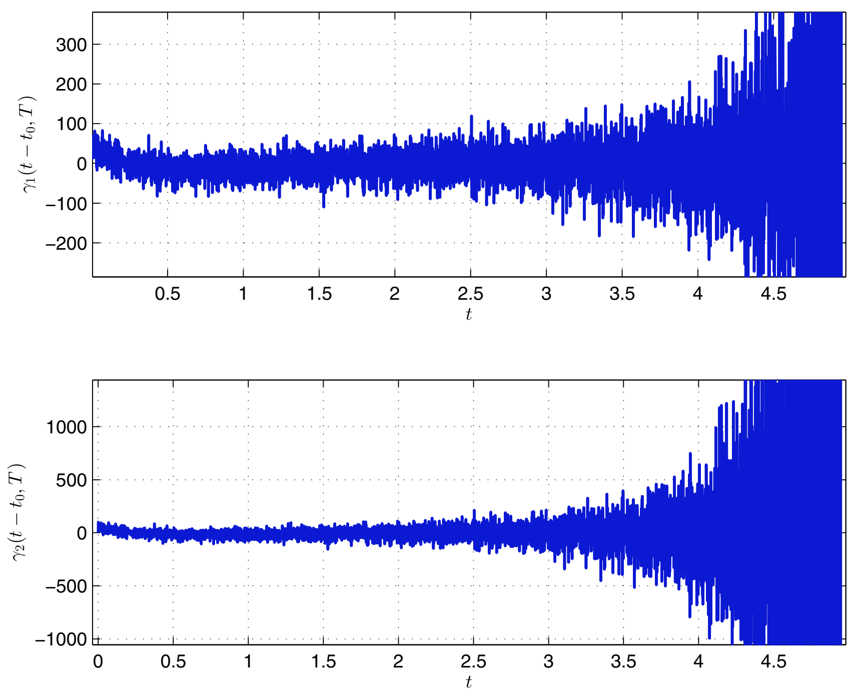

Figure 8.12: Time histories of output estimation error injections for Example 8.3.

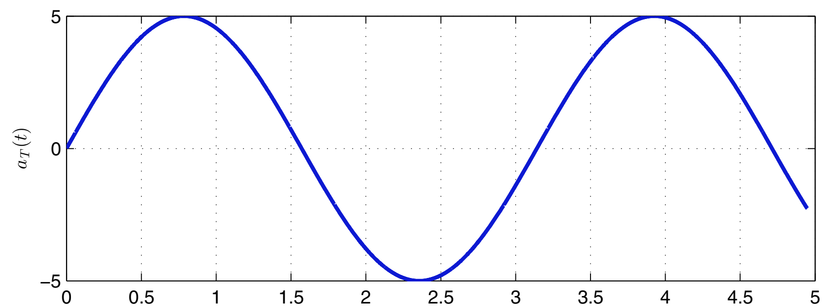

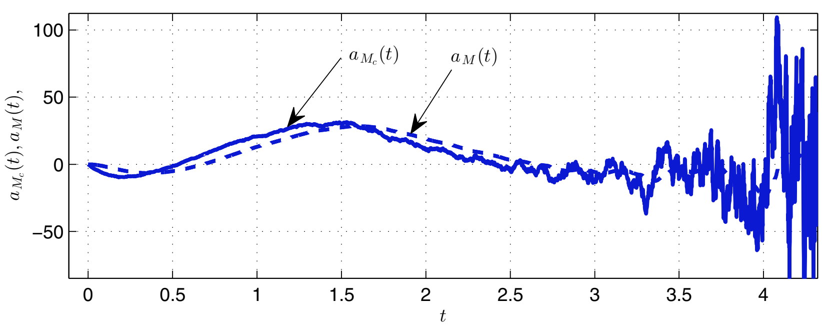

Figure 8.13: Time histories of target and missile acceleration for Example 8.3.

8.3 Discussion

In this chapter we demonstrated that the prescribed-time guidance laws of Chapter 7 and the observer of Chapter 5 can be combined to yield prescribed-time output feedback guidance laws which may be effective in some tactical missile guidance applications. The guidance law of Example 8.1 was more effective at meeting the estimation and stabilization objectives than the guidance law of Example 8.2 and Example 8.3, and this is because the latter exhibit unmodeled plant dynamics and a measurement disturbance which the observer was not designed to accommodate. Although these new guidance laws show promising results, their effectiveness in practice will be limited by both actuator saturation and measurement disturbances, so the missile guidance engineer must take these into account to yield a viable design. Therefore, future work in this area should explore the effects of actuator saturation on the prescribed-time control laws of Chapter 4, and attempt to address the problem of designing a prescribed-time observer similar to the one of Chapter 5 but which can perform with regularity despite the presence of plant and measurement disturbances.

Part IV

Conclusion

Chapter 9

Closing Remarks

In this short chapter, we summarize the main contributions and limitations of the results in this dissertation, and also recommend follow-on tasks which could be of interest to both control theorists and practicing missile guidance and control engineers.

9.1 Summary of contributions

For nonlinear systems in the normal form, which reduces to the controllable canonical form when no nonlinearities or uncertainties are present, we introduced a time-varying coordinate transformation approach to design two controllers that achieve fixed-time stabilization in a time that is freely prescribed by the user and independent of initial conditions. This design framework provides another option for the control designer's toolbox, and we do not claim its superiority with respect to existing designs but highlight the tradeoffs. As in fixed-time optimal control with a terminal penalty, our gains grow unbounded towards the terminal time. Such a high-gain character (near the set point) is similar to sliding mode control (SMC). But unlike SMC and other non-smooth methods, our time-varying approach achieves stabilization in *prescribed time*, and, when the nonlinearity is vanishing, the control also goes to zero as time approaches the prescribed time.

Extensions of the prescribed-time controllers of Chapter 4 to *trajectory tracking* are straightforward. Consider the output $y(t) = x_1(t)$, with a reference $y_r(t)$, and denote the tracking error state components $\varepsilon_i(t) := x_i(t) - y_r^{(i-1)}(t)$, for which $\dot{\varepsilon}_i(t) = \varepsilon_{i+1}(t)$ and $\dot{\varepsilon}_n(t) = f(x,t) + b(x,t)u(t) + y_r^{(i-1)}(t)$. If b is known, then $y_r^{(i-1)}(t)$ is canceled by control, whereas, if only b's lower bound is known, $y_r^{(i-1)}(t)$ is treated in the same fashion as the disturbance $d(t)$ in Chapter 4.

For finite-time linear systems in the observer canonical form, we introduced a state observer that is capable of estimating the state perfectly in a time that is freely prescribed by the user and independent of initial conditions. The attractive features of the observer of Chapter 5 are the simplicity of its design and implementation, and how easily it allows the user to prescribe the convergence time and constructively calculate the observer gains. Because of its simple structure, the prescribed-time observer can be viewed as a time-varying extension of the Luenberger observer, which is widely familiar to practicing controls engineers. This latter point may increase the likelihood of its adoption in practice.

For finite-time linear systems in the controllable canonical form, we showed that by using the nominal controller of Chapter 4 and the observer of Chapter 5, and by selecting observer and controller parameters in simple ways provided, a separation principle holds between the prescribed-time observer and the prescribed-time controller provided the scaling power of the time-varying observer gains exceeds the scaling power of the controller gains by twice the order of the system, i.e., provided the observer is fast enough relative to the controller, irrespective of the constant gains of both. The approach presented allows the user to easily prescribe finite convergence times a priori, independent of initial conditions.

In Chapter 7 and Chapter 8, we showed that the designs of Chapter 4 and Chapter 6, respectively, can be applied to homing missile guidance applications in which the missile and target are in the near-collision course (NCC). In realistic applications, the full state required for guidance is never measured perfectly, so the results of Chapter 7 may be useful for initial guidance law development and parameter tuning, but the results of Chapter 8 will be more useful in practice since they provide an effective means to estimate the state within the guidance law. For engagements having a non-maneuvering target and fast autopilot dynamics, the prescribed-time guidance law of Section 8.2.1 may be effective in realistic applications with minimal tuning of the controller and observer parameters. Then for the more common situation in which the target is maneuvering and autopilot dynamics are not ideal, the prescribed-time guidance law of Section 8.2.2 may be effective in realistic applications, but it will probably require some trial-and-error to tune the parameters of the robust controller of Chapter 4 in a way that yields acceptable performance.

9.2 Limitations and future work

The main shortcoming of the robust prescribed-time controller of Chapter 4 is that its effectiveness is restricted to systems having matched uncertainties. However, this limitation is shared by SMC and is fundamental to the problem of completely rejecting non-vanishing uncertainties—this can be done only when the uncertainties are matched and requires infinite gain. Furthermore, any finite-time feedback, including the existing non-smooth ones and our time-varying one, exhibit a steep deterioration of asymptotic performance under measurement noise. The practicioner's simple solution to this latter problem is to slightly lengthen the control horizon, which prevents the gains from going to infinity but degrades the stabilization slightly (convergence is achieved to within an acceptably small neighborhood of the origin rather than to the origin exactly). A final limitation of the robust controller is that for higher-order systems, trial-and-error through numerical simulation will likely be required to determine acceptable values for the controller parameters. This shortcoming is shared by most existing approaches to finite-time stabilization, however those approaches also make it far more difficult to prescribe the convergence time than our approach presented here.

Considering the prescribed-time observer of Chapter 5, the question of robustness to unmodeled dynamics and/or measurement disturbances is open and left for future research. Future extensions of our approach to prescribed-time estimation should investigate the possibility of designing observers capable of estimating the state to an acceptable level of performance in prescribed time in the presence of both plant and measurement disturbances. Presently, for linear time-invariant systems with piecewise-constant measurement disturbances, the hybrid-system finite-time observer of Li and Sanfelice [54] may be more appropriate than the observer of Chapter 5.

The prescribed-time output feedback guidance laws of Chapter 8 exhibit potential for use in some tactical missile guidance applications. However, missile guidance and control engineers implementing these in real systems will have to account for both actuator saturation and the fact that the observer of Chapter 5 was not designed to accommodate either plant or measurement disturbances. Ideally, these limitations would be explored and overcome with mathematical rigor, but at a minimum, they must be explored through numerical simulation during the design process. Another shortcoming of the guidance laws is the controller parameters must be tuned to optimize performance under the assumption of a particular target maneuver. Some tactical missile systems are designed with particular targets in mind, and the form of target maneuver is known to some extent a priori. But in general, a missile guidance system may have no knowledge of target maneuver capability, and in this case the need for robustness to all possible target maneuvers is clear. Presently, work remains to determine a method capable of obtaining a set of parameters for the guidance law of Section 8.2.2 that will exhibit robustness to a range of possible target maneuvers simultaneously.

References

[1] F. P. Adler. Missile guidance by three-dimensional proportional navigation. *J. Appl. Phys.*, 27(500), 1956.

[2] G. M. Anderson. Comparison of optimal control and differential game intercept missile guidance laws. *Journal of Guidance, Control, and Dynamics*, 4(2):109–115, 1981.

[3] K. Becker. Closed-form solution of pure proportional navigation. *IEEE Trans. on Aerospace and Electron. Syst.*, 26(3), 1990.

[4] J. Z. Ben-Asher and I. Yaesh. *Advances in Missile Guidance Theory*. AIAA, 1998.

[5] S. P. Bhat and D. S. Bernstein. Continuous finite-time stabilization of the translational and rotional double integrators. *IEEE Trans. Automatic Control*, 43(5):678–682, 1998.

[6] S. P. Bhat and D. S. Bernstein. Finite-time stability of continuous autonomous systems. *SIAM Journal on Control and Optimization*, 38(3):751–766, 2000.

[7] N. F. Palumbo, R. A. Blauwkamp, and J. M. Lloyd. Modern homing missile guidance theory and techniques. *Johns Hopkins APL Technical Digest*, 29(1), 2001.

[8] A. Bryson and Y. C. Ho. *Applied Optimal Control: Optimization, Estimation, and Control*. Hemisphere Publishing Corporation, 1975.

[9] E. Garcia, D. Casbeer, and M. Pachter. Active target defense differential game with a fast defender. pages 3752–3757, 2015.

[10] E. Garcia, D. Casbeer, and M. Pachter. Cooperative strategies for optimal aircraft defense from an attacking missile. *Journal of Guidance, Control, and Dynamics*, 38(8), 2015.

[11] G. Chatterji and M. Pachter. A midcourse estimation and guidance law for space based interceptors. 1990.

[12] S. Shi, S. Xu, X. Yu, J. Lu, W. Chen, and Z. Zhang. Robust output-feedback finite-time regulator of systems with mismatched uncertainties bounded by positive functions. *IET Control Theory & Applications*, 11(17):3107–3114, 2017.

[13] C.-K. Ryoo, H. Cho, and M.-J. Tahk. Optimal guidance laws with terminal impact angle constraint. *Journal of Guidance, Control, and Dynamics*, 28(4), 2005.

[14] C.-K. Ryoo, H. Cho, and M.-J. Tahk. Time-to-go weighted optimal guidance with impact angle constraints. *IEEE Transactions on Control Systems Technology*, 14(3):483–492, 2006.

[15] R. G. Cottrell. Optimal intercept guidance for short-range tactical missiles. *AIAA Journal*, 9(7):1414–1415, 1971.

[16] F. Amato, M. Darouach, and G. De Tommasi. Finite-time stabilizability, detectability and dynamic output feedback finite-time stabilization of linear systems. *to appear in IEEE Transactions on Automatic Control*, 2018.

[17] A. Dhar and D. Ghose. Capture region for a realistic TPN guidance law. *IEEE Trans. on Aerospace and Electron. Syst.*, 29(3), 1993.

[18] S. Li, H. Du, and X. Lin. Finite-time consensus algorithm for multi-agent systems with double-integrator dynamics. *Automatica*, 47(8):1706–1712, 2011.

[19] A. Polyakov, D. Efimov, and W. Perruquetti. Finite-time and fixed-time stabilization: Implicit lyapunov function approach. *Automatica*, 51:332–340, 2015.

[20] E. Bernuau, W. Perruquetti, D. Efimov, and E. Moulay. Robust finite-time output feedback stabilisation of the double integrator. *International Journal of Control*, 88(3):451–460, 2015.

[21] F. Lopez-Ramirez, A. Polyakov, D. Efimov, and W. Perruquetti. Finite-time and fixed-time observers design via implicit lyapunov function. pages 289–294, 2016.

[22] R. Engel and G. Kreisselmeier. A continuous-time observer which converges in finite time. *IEEE Transactions on Automatic Control*, 47(7):1202–1204, 2002.

[23] W. Perruquetti, T. Floquet, and E. Moulay. Finite-time observers: application to secure communication. *IEEE Transactions on Automatic Control*, 53(1):356–360, 2008.

[24] R. Fry and S. McManus. Smooth bump functions and the geometry of banach spaces. *Exp. Mathematicae*, 20:143–183, 2002.

[25] D. Ghose. On the generalization of true proportional navigation. *IEEE Trans. on Aerospace and Electron. Syst.*, 30(2), 1994.

[26] D. Ghose. True proportional navigation with maneuvering target. *IEEE Trans. on Aerospace and Electron. Syst.*, 30(1), 1994.

[27] M. Guelman. A qualitative study of proportional navigation. *IEEE Trans. on Aerospace and Electron. Syst.*, 7(4), 1971.

[28] M. Guelman. The closed-form solution of true proportional navigation. *IEEE Trans. on Aerospace and Electron. Syst.*, 12(4), 1976.

[29] S. Gutman. On optimal guidance for homing missiles. *Journal of Guidance, Control, and Dynamics*, 2(4):296–300, 1979.

[30] Q. Hui, W. M. Haddad, and S. P. Bhat. Finite-time semistability and consensus for nonlinear dynamical networks. *IEEE Transactions on Automatic Control*, 53(8):1887–1900, 2008.

[31] V. T. Haimo. Finite time controllers. *SIAM Journal on Control and Optimization*, 24(4):760–770, 1986.

[32] J. Holloway and M. Krstic. Predictor observers for proportional navigation systems subjected to seeker delay. *IEEE Transactions on Control Systems Technology*, 24(6):2002–2015, 2016.

[33] Y. Song, Y. Wang, J. Holloway, and M. Krstic. Time-varying feedback for regulation of normal-form nonlinear systems in prescribed finite time. *Automatica*, 83:243–251, 2017.

[34] Y. Hong. Finite-time stabilization and stabilizability of a class of controllable systems. *System & Control Letters*, 46:231–236, 2002.

[35] Y. Hong and Z. P. Jiang. Finite-time stabilization of nonlinear systems with parametric and dynamic uncertainties. *IEEE Transactions on Automatic Control*, 51(12):1950–1956, 2006.

[36] C. D. Yang, F. B. Hsiao, and F. B. Yeh. Generalized guidance law for homing missiles. *IEEE Trans. on Aerospace and Electron. Syst.*, AES-25(2), 1989.

[37] Y. Hong, J. Huang, and X. Yu. On an output feedback finite-time stabilization problem. *IEEE Trans. Auto. Contr.*, 46:305–309, 2001.

[38] Y. Shen, Y. Huang, and J. Gu. Global finite-time observers for lipschitz nonlinear systems. *IEEE Transactions on Automatic Control*, 56(2):418–424, 2011.

[39] T. Shima, M. Idan, and O. M. Golan. Sliding-mode control for integrated missile autopilot guidance. *Journal of Guidance, Control, and Dynamics*, 29(2):250–260, 2006.

[40] P. Gurfil, M. Jodorkovsky, and M. Guelman. Finite time stability approach to proportional navigation systems analysis. *Journal of Guidance, Control, and Dynamics*, 21(6):853–861, 1998.

[41] M. Krstic, I. Kanellakopoulos, and P. Kokotovic. *Nonlinear and Adaptive Control Design*. John Wiley & Sons, 1995.

[42] H. Khalil. *Nonlinear Systems*. Prentice Hall, 2002.

[43] I. J. Ha, J. S. Hur, M. S. Ko, and T. L. Song. Performance analysis of PNG laws for randomly maneuvering targets. *IEEE Trans. on Aerospace and Electron. Syst.*, 26(5), 1990.

[44] M. Krstic. *Delay Compensation for Nonlinear, Adaptive, and PDE Systems*. Birkhauser, 2009.

[45] Y. Wang, Y. D. Song, M. Krstic, and C. Wen. Fault-tolerant finite time consensus for multiple uncertain nonlinear mechanical systems under single-way directed communication interactions and actuation failures. *Automatica*, 63:374–383, 2016.

[46] B. S. Kim, J. G. Lee, and H. S. Han. Biased PNG law for impact with angular contraint. *IEEE Trans. on Aerospace and Electron. Syst.*, 34(1), 1998.

[47] A. Levant. Robust exact differentiation via sliding mode technique. *Automatica*, 34(3):379–384, 1998.

[48] A. Levant. Higher-order sliding modes, differentiation and output-feedback control. *International Journal of Control*, 76(9/10):924–941, 2003.

[49] A. Levant. Homogeneity approach to high-order sliding mode design. *Automatica*, 41(5):823–830, 2005.

[50] A. Levant. On fixed and finite time stability in sliding mode control. pages 4260–4265, 2013.

[51] C. Y. Li and W. X. Jing. Geometric approach to capture analysis of PN guidance law. *Aerospace Science and Technology*, 12:177–183, 2008.

[52] J. Li and C. Qian. Global finite-time stabilization by dynamic output feedback for a class of continuous nonlinear systems. *IEEE Transactions on Automatic Control*, 51(5):879–884, 2006.

[53] X. Wang, S. Li, and P. Shi. Distributed finite-time containment control for double-integrator multiagent systems. *IEEE Transactions on Cybernetics*, 44(9):1518–1528, 2014.

[54] Y. Li and R. Sanfelice. A finite-time convergent observer with robustness to piecewise-constant measurement noise. *Automatica*, 57:222–230, 2015.

[55] X. Huang, W. Lin, and B. Yang. Global finite-time stabilization of a class of uncertain nonlinear systems. *Automatica*, 41(5):881–888, 2005.

[56] Y. Shen, P. Miao, and Y. Huang. Finite-time stability and its application for solving time-varying sylvester equation by recurrent neural network. *Neur. Proc. Lett.*, 42:763–784, 2015.

[57] M. Monahemi and M. Krstic. Control of wing rock motion using adaptive feedback linearization. *Journal of Guidance on Control Dynamics*, 19(4):905–912, 1996.

[58] E. Cruz-Zavala, J. Moreno, and L. Fridman. Uniform robust exact differentiator. *IEEE Transactions on Automatic Control*, 56(11):2727–2733, 2011.

[59] M. Angulo, J. Moreno, and L. Fridman. Robust exact uniformly convergent arbitrary order differentiator. *Automatica*, 49(11):2489–2495, 2013.

[60] T. Menard, E. Moulay, and W. Perruquetti. A global high-gain finite-time observer. *IEEE Transactions on Automatic Control*, 55(6):1500–1506, 2010.

[61] D. Zhou, C. Mu, and W. Xu. Adaptive sliding-mode guidance of a homing missile. *Journal of Guidance, Control, and Dynamics*, 22(4):589–594, 1999.

[62] S. A. Murtaugh and H. E. Criel. Fundamentals of proportional navigation. *IEEE Spectrum*, 3, 1966.

[63] B. Naveh and A. Lorber. *Theater Ballistic Missile Defense*. AIAA, 2001.

[64] F. Nesline and P. Zarchan. A new look at classical versus modern homing missile guidance. pages 230–242, 1979.

[65] J. H. Oh. Solving a nonlinear output regulation problem: Zero miss distance of pure PNG. *IEEE Trans. on Automatic Control*, 47(1), 2002.

[66] J. H. Oh and I. J. Ha. Capturability of the 3-dimensional pure PNG law. *IEEE Trans. on Aerospace and Electron. Syst.*, 35(2), 1999.

[67] G. Zheng, Y. Orlov, W. Perruquetti, and J. P. Richard. Finite time observer design for nonlinear impulsive systems with impact perturbation. *International Journal of Control*, 87(10):2097–2105, 2014.

[68] A. Polyakov. Nonlinear feedback design for fixed-time stabilization of linear control systems. *IEEE Transactions on Automatic Control*, 57(8):2106–2110, 2012.

[69] A. Polyakov and L. Fridman. Stability notions and lyapunov functions for sliding mode control systems. *J. Franklin Inst.*, 351:1831–1865, 2014.

[70] A. Polyakov and A. Poznyak. Lyapunov function design for finite-time convergence analysis: "twisting" controller for 2nd-order sliding mode realization. *Automatica*, 45:444–448, 2009.

[71] V. Andrieu, L. Praly, and A. Astolfi. Homogeneous approximation, recursive observer design, and output feedback. *SIAM J. Control Optimization*, 47(4):1814–1850, 2008.

[72] C. Qian and J. Li. Global finite-time stabilization by output feedback for planar systems without observable linearization. *IEEE Transactions on Automatic Control*, 50(6):885–890, 2005.

[73] T. Raff and F. Allgower. An impulsive observer that estimates the exact state of a linear continuous-time system in predetermined finite time. pages 1–3, 2007.

[74] K. R. Babu, I. G. Sarma, and K. N. Swamy. Switched bias proportional navigation for homing guidance against highly maneuvering targets. *Journal of Guidance, Control, and Dynamics*, 17(6), 1994.

[75] Y. Shen and Y. Huang. Uniformly observable and globally lipschitzian nonlinear systems admit global finite-time observers. *IEEE Transactions on Automatic Control*, 54(11):2621–2625, 2009.

[76] Y. Shen and Y. Huang. Global finite-time stabilisation for a class of nonlinear systems. *Int. J. Sys. Sci.*, 43:73–78, 2012.

[77] Y. Shen and X. Xia. Semi-global finite-time observers for nonlinear systems. *Automatica*, 44:3152–3156, 2008.

[78] S. Seo, H. Shim, and J. H. Seo. Global finite-time stabilization of a nonlinear system using dynamic exponent scaling. 2008.

[79] J. Shinar and T. Shima. A game theoretical interceptor guidance law for ballistic missile defense. 1996.

[80] N. A. Shneydor. *Missile Guidance and Pursuit: Kinematics, Dynamics and Control*. Woodhead Publishing Limited, 1998.

[81] Y. B. Shtessel and C. H. Tournes. Integrated higher-order sliding mode guidance and autopilot for dual control missiles. *Journal of Guidance, Control, and Dynamics*, 32(1):79–94, 2009.

[82] U. S. Shukla and P. R. Mahapatra. The proportional navigation dilemmna–pure or true? *IEEE Trans. on Aerospace and Electron. Syst.*, 26(2), 1990.

[83] R. Singer. Estimating optimal tracking filter performance for manned maneuvering targets. *IEEE Trans. Aerosp. Electron. Syst.*, 6(4):473–483, 1970.

[84] G. Siouris. *Missile Guidance and Control Systems*. Springer-Verlag, 2004.

[85] S. H. Song and I. J. Ha. A lyapunov-like approach to performance analysis of 3-dimensional pure PNG laws. *IEEE Trans. on Aerospace and Electron. Syst.*, 30(1), 1990.

[86] D. Hull, J. Speyer, and D. Burris. Linear-quadratic guidance law for dual control of homing missiles. *Journal of Guidance, Control, and Dynamics*, 13(1), 1990.

[87] J. Speyer. An adaptive terminal guidance scheme based on an exponential cost criterion with application to homing missile guidance. *IEEE Transactions on Automatic Control*, 21(3), 1976.

[88] R. Chen, J. Speyer, and D. Lianos. Optimal intercept missile guidance strategies with autopilot lag. *Journal of Guidance, Control, and Dynamics*, 33(4), 2010.

[89] D. Zhou, S. Sun, and K. L. Teo. Guidance laws with finite time convergence. *Journal of Guidance, Control, and Dynamics*, 32(6), 2009.

[90] D. Y. Rew, M. J. Tahk, and H. Cho. Short-time stability of proportional navigation guidance loop. *IEEE Trans. Aerosp. Electron. Syst.*, 32(3):1107–1115, 1996.

[91] S. N. Balakrishnan, A. Tsourdos, and B. A. White. *Advances in Missile Guidance, Control, and Estimation*. CRC Press Taylor and Francis Group, 2013.

[92] F. Tyan. Unified approach to missile guidance laws: A 3D extension. *IEEE Trans. on Aerospace and Electron. Syst.*, 41(4), 2005.

[93] S. Vathsal and A. K. Sarkar. Current trends in tactical missile guidance. *Defense Science Journal*, 55(2), 2005.

[94] J. Huang, C. Wen, W. Wang, and Y. D. Song. Adaptive finite-time consensus control of a group of uncertain nonlinear mechanical systems. *Automatica*, 51:292–301, 2015.

[95] L. Wang and F. Xiao. Finite-time consensus problems for networks of dynamic agents. *IEEE Transactions on Automatic Control*, 55(4):950–955, 2010.

[96] Y. Hong, J. Wang, and D. Cheng. Adaptive finite-time control of nonlinear systems with parametric uncertainty. *IEEE Transactions on Automatic Control*, 51(5):858–862, 2006.

[97] G. Willems. Optimal controllers for homing missiles. *U. S. Army Missile Command*, Redstone Arsenal, AL:RE–TR–68–15, 1968.

[98] C. D. Yang and C. C. Yang. Analytical solution of 3D true proportional navigation guidance. *IEEE Trans. on Aerospace and Electron. Syst.*, 32(4), 1996.

[99] C. D. Yang and C. C. Yang. A unified approach to proportional navigation. *IEEE Trans. on Aerospace and Electron. Syst.*, 33(2), 1997.

[100] C. D. Yang and F. B. Yeh. Closed form solution for a class of guidance laws. *Journal of Guidance, Control, and Dynamics*, 10(4), 1987.

[101] H. Du, C. Qian, S. Yang, and S. Li. Recursive design of finite-time convergent observers for a class of time-varying nonlinear systems. *Automatica*, 49:601–609, 2013.

[102] R. Yanushevsky. *Modern Missile Guidance*. CRC Press, 2008.

[103] C. D. Yang, F. B. Yeh, and J. H. Chen. The closed-form solution of generalized proportional navigation. *Journal of Guidance, Control, and Dynamics*, 10(2), 1987.

[104] Y. Feng, X. Yu, and Z. Man. Non-singular terminal sliding mode control of rigid manipulators. *Automatica*, 38(12):2159–2167, 2002.

[105] P. J. Yuan and J. S. Chern. Ideal proportional navigation. *Journal of Guidance*, 15(5), 1992.

[106] P. Zarchan. When bad things happen to good missiles. *AIAA Guidance, Navigation, and Control Conference*, pages 765–773, 1993.

[107] P. Zarchan. Proportional navigation and weaving targets. *Journal of Guidance, Control, and Dynamics*, 18(5):969–974, 1995.

[108] P. Zarchan. *Tactical and Strategic Missile Guidance,* 5th Ed. AIAA, 2007.

[109] S. Sun, D. Zhou, and W. T. Hou. A guidance law with finite time convergence accounting for autopilot lag. *Aerospace Science and Technology*, 25(1):132–137, 2012.